CRANFIELD UNIVERSITY

SCHOOL OF MECHANICAL ENGINEERING

PhD Thesis

Academic Year 1999-2002

Analysis of a 115MW, 3 Shaft, Helium Brayton Cycle

K N Pradeepkumar

Supervisors:
Prof. Pericles Pilidis
Dr. Antonios Tourlidakis

This thesis is submitted in partial fulfilment of the requirements of the degree of Doctor of Philosophy

July 2002

Abstract

This research theme is originated from a development project that is going on in South Africa, for the design and construction of a closed cycle gas turbine plant using gas-cooled reactor as the heat source to generate 115 MW of electricity. South African Power utility company, Eskom, promotes this developmental work through its subsidiary called PBMR (Pebble Bed Modular Reactor). Some of the attractive features of this plant are the inherent and passive safety features, modular geometry, small evacuation area, small infrastructure requirements for the installation and running of the plant, small construction time, quick starting and stopping and also low operational cost.

This exercise is looking at the operational aspects of a closed cycle gas turbine, the finding of which will have a direct input towards the successful development and commissioning of the plant. A thorough understanding of the fluid dynamics in this three-shaft system and its transient performance analysis were the two main objectives of this research work. A computer programme called GTSI, developed by a previous Cranfield University research student, has been used in this as a base programme for the performance analysis. Some modifications were done on this programme to improve its control abilities. The areas covered in the performance analysis are Start-up, Shutdown and Load ramping. A detailed literature survey has been conducted to learn from the helium Turbo machinery experiences, though it is very limited. A critical analysis on the design philosophy of the PBMR is also carried out as part of this research work.

The performance analysis has shown the advantage, disadvantage and impact of various power modulation methods suggested for the PBMR. It has tracked the effect of the operations of the various valves included in the PBMR design. The start-up using a hot gas injection has been analysed in detail and a successful start region has been mapped. A start-up procedure is also written based on this. The analysis on the normal and emergency load rejection using various power modulation devices has been done and it stress the importance of more control facilities during full load rejection due to generator faults.

A computational fluid dynamics (CFD) analysis, using commercial software, has been carried out on some geometry of the PBMR design to find out whether its flow characteristic will have any serious impact on the performance on the cycle during the load control of the plant. The analysis has demonstrated that there will not be much impact on the performance, during load control using pressure level changes, from this geometry. However, some locations in the geometry have been identified as areas where the flow is experiencing comparatively high pressure losses. Recommendations, which include modification in the physical design, were made to improve this.

The CFD analysis has extended to a cascade to compare the flow behaviour of Air and Helium with an objective of using air, being inexpensive, to test the helium flow characteristic in a test rig to simulate the behavioural pattern of helium in the PBMR pressure vessel. The specification of a hypothetical test rig and the necessary scaling parameters has been derived from this exercise. This will be useful for designing test rigs during the developmental and operational stage of the PBMR project.

Acknowledgements

I would like to express my sincere thanks to Prof.P.Pilidis and Dr.A.Tourlidakis of Cranfield University for their invaluable help, support and encouragement during the course of this work.

I am grateful to Eskom-PBMR (South Africa) for giving me the opportunity to conduct this research work. In particular I would like to thank Mr.D.Nicholls and Mr.T.Makubire at PBMR.

I would like to take this opportunity to thank also Prof.R.Singh and Dr.K.W.Ramsden of Cranfield University for their advice and assistance.

Finally I would like to thank my wife Nimisha for her support and encouragement without which this would not have been possible.

K.N.Pradeepkumar
Cranfield, July 2002

Contents

List of Figures

List of Tables

Nomenclature

A	Area
a	Coefficient of thermodynamic properties
CC	Closed Cycle
CCGT	Closed Cycle Gas Turbine
CFD	Computational Fluid Dynamics
CDP	Compressor Discharge Pressure
C_D	Coefficient of discharge
C_p	Specific heat at constant Pressure
D	Diameter
H	Total Enthalpy
H	Static Enthalpy
HP	High Pressure
HPC	High Pressure Compressor
HPS	High Pressure Shaft
I	Mass moment of Inertia
IGV	Inlet Guide Vanes
HPT	High Pressure Turbine
HTGR	High Temperature Gas Reactor
K'	Duct cold pressure loss factor
k	Thermal conductivity
L	Length
LP	Low Pressure
LPC	Low Pressure Compressor
LPS	Low Pressure Shaft
LPT	Low Pressure Turbine
m	Mass flow, kg/sec
M	Mach Number, Molecular Weight
N	Rotational Speed
NGV	Nozzle Guide Vane
N_{stg}	Number of stages
P	Total Pressure
p	Static Pressure, Pressure absolute scale
PBMR	Pebble Bed Modular Reactor
PLF	Pressure Loss Factor
PT	Power Turbine
PW	Power
PWR	Pressurised Water Reactor
Q	Heat flow
R	Gas constant
r	Radius
R_u	Ratio of Velocities
Re	Reynolds number
Rn	Degree of reaction
RNI	Reynolds Number Index
S	Total entropy
sf	Scaling factor

SM	Surge Margin
SOT	Stator Outlet Temperature
SPO	Specific Power Output
T	Total temperature
t	Time
t	Static Temperature
TET	Turbine Entry Temperature
u	Velocity
U	Blade speed
V	Velocity
v, Vol	Volume
W	Mass flow
w	Non Dimensional Specific work
x^i	Mass fraction of component i
x_1, x_2	Flow functions
XN	Shaft speed
XNRT	Corrected speed
Z	Pressure multiplier

α	Variable Stator Angle
β	Compressor map parameter
γ	Ratio of Specific Heats (C_p/C_v)
Δ	Increment
δ	Corrected pressure (P/P_{std}), Differential
ε	Cooling Effectiveness
Φ	Entropy function, Total
ϕ	Entropy function, Static
γ	Ratio of constant specific heats
η	Efficiency
φ	Flow swirl angle
λ_I	Increase in enthalpy
μ	Static Viscosity
σ	Stress level
ν	Kinematic (Dynamic) Viscosity
π	Pressure ratio
θ	Corrected Temperature (T/T_{std}),
τ, θ	Temperature ratios
ρ	Density
ψ	Loading factor
ω	Angular speed

Subscripts / Super scripts

Ax	Axial
b	Bleed
c	Compressor

ds	Design
in	inlet
is	Isentropic
N	Number of variables
n	Number of iteration
out	Outlet
poly	Polytropic
ref	Reference
reg	Regenerator/ Recuperator
sat	Saturation
ss	Steady State
t	Turbine
th	Thermal
tr	Transient
θ	Blading angle
01	Up stream
02	Down stream
2 23 3 33 8	Station numbers, Figure 4.1, [97]

Chapter .1
Introduction

It is almost certain that Nuclear Energy will reappear as a viable option in the Power Generation Industry. Emissions and escalating oil prices are some of the reasons contributing to this resurgence of Nuclear power. However the safety and economic issues, which forced out the Nuclear Power from the field, still exist. The Nuclear Technologists in various countries are working towards a fourth generation reactors and components which can remove or alleviate the safety and economic concerns associated with Nuclear Power Plants. Modular Gas cooled Reactors with an online fuel loading system using Helium turbines are considered as an alternative to the present generation of Nuclear power Technology. The inherent safety features and the economics associated with the modular units make them very attractive.

From a point of commercial viability, these modular HT gas reactors using direct energy conversion offer short construction time, better part load performance, and lesser logistics during the operation. The past activities for the direct conversion using helium could not achieve technical and commercial success. There were issues, which could not be solved with the technology available in those days. Also there were external factors, such as absence of political will, which contributed to the lack of interest towards this technology. With the present day technologies such as magnetic bearings, high performance seals, laser assisted precision manufacturing; inexpensive and powerful computational facilities, technologists are encouraged to look into the potential of gas cooled reactors and closed cycle helium turbines.

Gas cooled Reactors using Helium for the direct conversion of Nuclear energy into electrical energy are considered as one of the possible alternative energy conversion method. The inherent safety features associated with the modular units using this technology make it attractive. From a commercial viability point, these modular HT gas reactors using direct energy conversion offer short construction time, better part load performance, and lesser logistics during the operation. The Figure 1.1 and 1.2 show the evolution of power generation technologies [70].

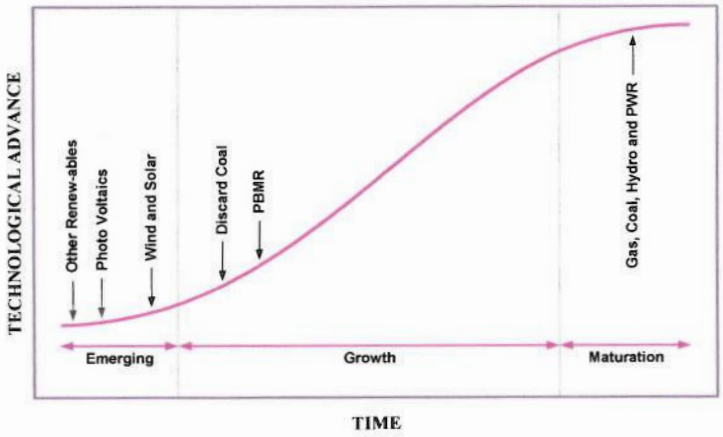

Figure 1.1 Technology Maturation Curve-I

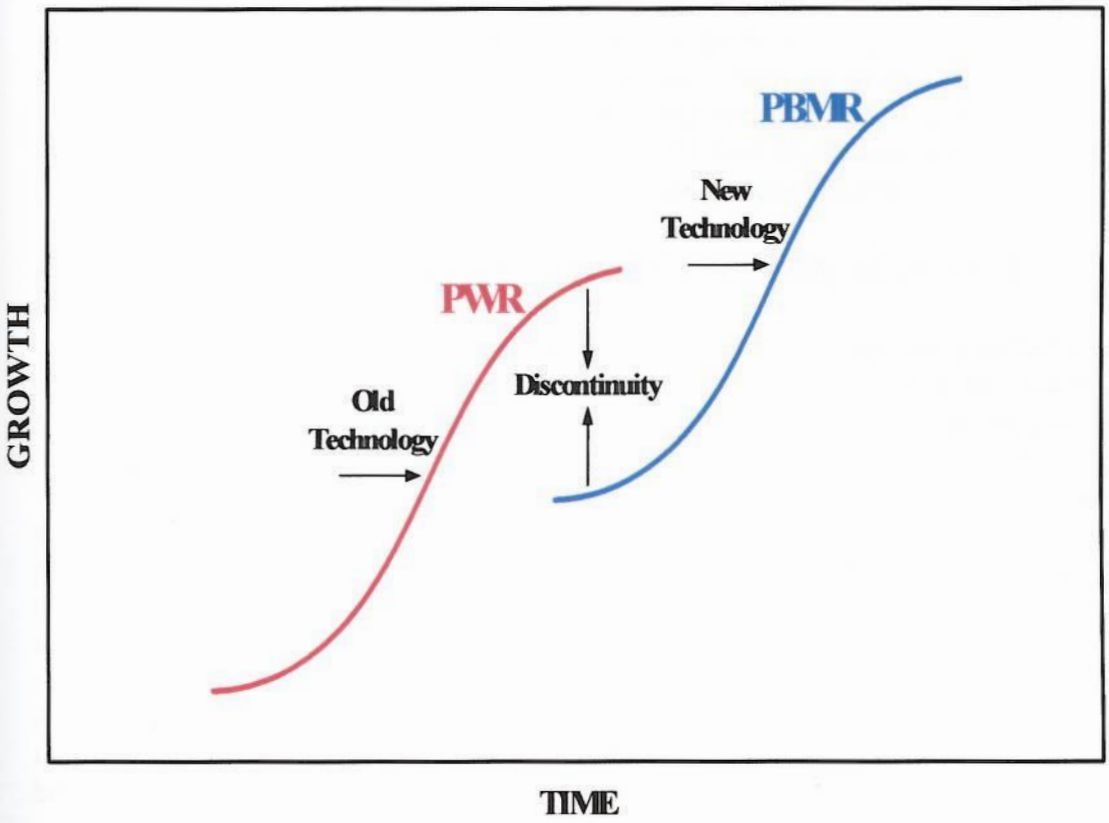

Figure 1.2 Technology Maturation Curve-II

This research topic is originated from a development project that is going on in South Africa, for the design and construction of a closed cycle gas turbine plant using gas-cooled reactor as the heat source to generate 115 MW of electricity. South African Power utility company, Eskom, promotes this developmental work. A separate company called PBMR (Pebble Bed Modular Reactor) has been formed and a conceptual study has been completed. The first prototype is expected to be commissioned in 2006. Some multinational companies are also involved in this project. Some of the attractive features of this plant are the inherent safety due to its negative reactivity to high temperature, modular geometry, small evacuation area, small infrastructure requirements for the installation and running of the plant, small construction time, quick starting and stopping and also low operational cost. This can be used as a base load power plant for small remote load centres and also it can be used as a peak load power plant for larger grids.

The current research project is looking at the operational aspects of a closed cycle gas turbine, the finding of which will have a direct input towards the successful commissioning of the plant. The transient performance and control system requirements are inseparable. The transient behaviour of conventional gas turbine plants are well

understood due to the large effort made by the gas turbine manufactures in that field. But the closed cycle gas turbine field is relatively an unknown field in terms of precise transient behaviour and the methods to predict that. Computational methods have been used to reduce this gap between the theoretical performance and the practical reality. The major engineering challenge of this project is in the operational aspects and hence the performance engineering deserves special attention. A computer simulation model, is used to simulate various operational scenarios such as start-up, shutdown, load ramping etc. The PBMR target is to achieve a load ramping of 10% per minute without grid separation. An exercise using Computational Fluid Dynamics with Fluent has also been carried out to find the flow patterns at various complex locations in the system.

1.1 Pebble Bed Modular Reactor (PBMR) project in South Africa

Eskom is the main power supplier in Southern Africa with an installed capacity of 35 000 MW and catering 95% of the market in the region. Most of the power come from conventional coal fired power stations and also 1800 MW is generated from 2 Nuclear power stations at Koeburg in Cape Town. As per the present estimation, Eskom will have to think of adding more capacity by 2007. Most of the Eskom power stations are high capacity units as in the previous this was good because of the very low percentage of residential load compared to high fraction of industrial load. At present the residential load, which is a fluctuating one, is growing and hence the peak load management is becoming a serious issue for Eskom. Hence Eskom is opting for small units to increase their capacity, which will help them to manage their peak load better. But conventional coal fired power stations of larger capacity are more economical in terms of the initial cost per MW as well as operating cost. The Pebble Bed reactor can be an ideal solution for that issue due to its small size and small construction time etc.

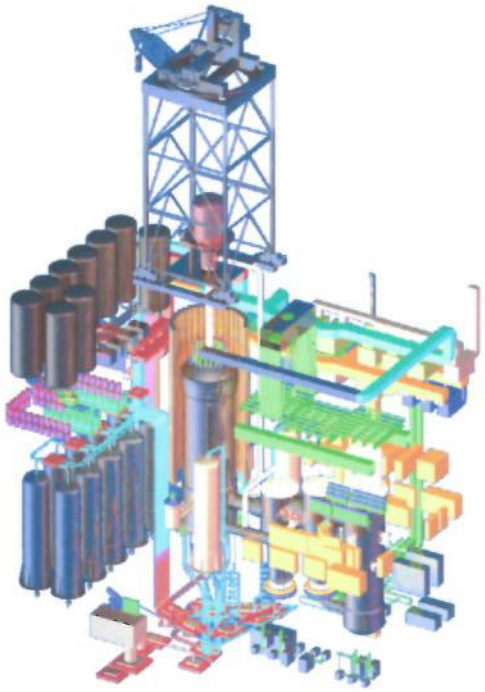

Fig 1.3 PBMR Plant Design

Gas fired power stations can also be a solution but the logistical requirement for PBMR will be far less than the gas-fired power stations. The Figure 1.3 gives the overall three-dimensional view of the plant.

Apart from the role of power producer, Eskom is providing support services to other overseas power companies as well. This comes from Eskom Technical Services International, a division that offers consultancy services in power planning, thermal plant operation, material technology etc. Pebble Bed Modular Reactor (PBMR) is a newly formed company by the South African Power utility Eskom along with two other overseas partners. Eskom is operating and maintaining Thermal, Nuclear and Hydroelectric power plants in Southern Africa. The total installed capacity is 40000MW and catering 95% of the Southern African electricity demand. The first prototype, which is a full-scale version of PBMR, will be installed at Koeburg in Cape Town, the place where the only nuclear power station of South Africa is situated. The first unit is optimised to generate an output of 116 MW electricity, which will be fed into the national grid. The fuel will be in the form of pebbles and an online fuel loading system will be there.

1.2 Objective of the Research

The main objective is to study the project from a system point of view to concentrate on performance engineering. The components in this project, to a large extent, are all established technologies in the market. The system performance is one of the areas where the developers are interested. The control system design is based on the off design and transient behaviour of the plant. The required transient and off design behaviour originate from the user requirements. The difference in actual and required behaviour determines the quality of the project. Hence a proper system simulation during the design stage throws much light onto the final outcome and gives an opportunity for improving it in the design stages.

A thorough literature survey on this technology is quite relevant due to the fact that countries like Germany and UK were actively involved for years in developing this technology commercially. However it was not fully successful with the technology of the day and also various political and commercial reasons caused its end. There is a lot to learn from their experience. Power systems for spacecrafts and submarines using closed cycle gas turbines do have similarity with this project and their experience is also valuable.

Chapter .2
Gas Cooled Reactors and Closed Cycle Gas Turbines

The high – temperature gas cooled reactor is expected to be of prime importance for broadening nuclear energy use in the future because it would supply high temperature heat and have high thermal efficiency, outstanding inherent safety characteristics and high fuel burn up. Design and development of future generation HTGR have been conducted in many countries. Recently conceptual design works have been performed in South Africa, Netherlands and China. In Japan, the High Temperature Engineering Test Reactor at the Oarai Research Establishment of the Japan Atomic Research Institute concluded the final stage of construction.

The HTGRs have several advantages in safety concept. An advanced light water reactor is designed, based on accident management, to prevent or mitigate severe accidents causing core meltdown. On the other hand, HTGR can achieve the same or higher degree of safety by using simpler passive systems to prevent accidents or to minimise the effect of accidents by virtue of inherent safety features.

Gas-cooled reactor history effectively begins with the start-up in November 1943 of the graphite moderated, air cooled 3.5 MW, X-10 reactor in Oak Ridge, Tennessee. The X-10 was the pilot plant for the water-cooled, plutonium production reactors at Hanford, Washington. Commercial gas-cooled nuclear power began in 1953 when the United Kingdom decided to combine plutonium production with electric power generation, and work has started on the four-unit power station at Caldar Hall and became operational in 1956, and continues to produce a combined electrical power of 270MW. The UK's extensive commitment to GCR technology has included construction of 26 magnox reactors and 14 advanced gas-cooled reactors. France's early interest in the GCR aided development in the UK. In 1951, the 2-MW research reactor at Saclay, which began operating with nitrogen coolant and later switched to carbon dioxide, was the first gas-cooled reactor to use closed circuit, pressurized cooling. The first nuclear power in Japan (166MWe), which started commercial operation in July 1966, was the carbon dioxide-cooled Tokai station located 80 miles from Tokyo. [3].

2.1 Operational Experience of HTGRs in Europe and US

Development of the HTGR began in the 1950s to improve upon Gas Cooled Reactor performance. HTGR uses ceramic fuel particles surrounded by coatings and dispersed in a graphite matrix, along with a graphite moderator. Either prismatic type graphite moderator blocks or spherical fuel elements are employed. Helium is used as the coolant to permit an increase in the operating temperature. HTGRs can operate at very high core outlet coolant temperature because of the use of an all-ceramic core.

The initial HTGRs included the Dragon reactor experiment, the Arbeitsgemeinshaft Versuchsreaktor (AVR) and Peach Bottom (No.1). Common among these plants were the utilization of steel vessels to contain the primary system and the attainment of high core outlet temperatures in the AVR achieving extended operation at 950^0 C. More elaborate description of the HTGR development in US and UK can be obtained from these references [3,17,57,64]. The Table 2.1 shows the past and the present activities in the HTGR technology.

Research & Demonstration Reactors			
** DRAGON	1964-77	20MWth	UK
** AVR	1957-89	46MWth	FRG
** Peach Btm	1967-74	115MWth	USA
** HTTR	1998-xx	30MWth	Japan
*+ HTR-10	2000-xx	10MWth	China

Concrete Pressure Vessel
Safety Systems
Economies of Scale by Size

Steel Pressure Vessel
"Walk Away" Safety
Economies of Scale by Numbers

Development Reactors			
Oldbury-on-Severn 2		2x350MWe	UK
** Ft St Vrain	1974-89	300MWe	USA
** THTR	1985-89	330MWe	FRG

"Full Sized HTGRs"			
HTR500	1985+	500MWe	FRG
????	1980+	1000MWe	USA

Modular Reactor Designs (Steam Cycle)			
* MODUL	1980's	80MWe	FRG
HTR-100	1980's	100MWe	FRG
* MHTGR	1980's	150MWe	USA

Modular Reactor Designs (Gas Turbines)			
^ GT-MHR	1996+	300MWe	USA/Russia
^ ACACIA	1998+	17MWe	Netherlands
^ PBMR	1997+	115MWe	RSA

** Built & Operated
*+ Under Construction
* Licensed
^ Active Development

Table 2.1 List of HTGRs

2.2 Past experience with Helium turbines.

In Germany a comprehensive research and development program was initiated in 1966 for a Brayton (closed) cycle power conversion system. The program was for ultimate use with a high temperature, helium cooled reactor heat source for electricity generation using helium as the working fluid. The program continued until 1982 in international cooperation with the United States and Switzerland.

The programme involved two experimental facilities. The first was an experimental cogeneration power plant (district heating and electricity generation) constructed and operated by the municipal utility, Energieversorgung Oberhausen (EVO), at Oberhausen, Germany. It consisted of a fossil fired heater, helium turbines, compressors and related equipments. The second facility was the high temperature helium test plant (HHV) for developing helium turbomachinery and components at the Research Centre Julich (KFA). The heat source for the HHV derived from an electric motor driven helium compressor.

The EVO facility could not reach the design power output of 50MW during the commissioning stage. The reasons for these difficulties were identified (elaborated below) and as far as economically feasible the difficulties were corrected. The research and development programs at both facilities can be judged successful and fully supportive of the feasibility of the use of high temperature helium as a Brayton cycle working fluid for direct power conversion from helium cooled nuclear reactor.

The HHT project was terminated in Germany after a short duration of operation. Except for information on life testing the facilities accomplished their missions. If helium turbomachinery technology is considered for power conversion from a helium-cooled nuclear reactor, no irresolvable problems have been identified in these turbomachinery test facilities.

2.2.1 EVO in Oberhausen, Germany

The design of the EVO test plant provided for an electric power of 50MW and a heating power of 53.5 MW. The inlet temperature into the turbine was limited to 750^0C taking into account the life endurance of the materials for the first turbine stage blades and of the helium heater. During the operation many components and systems showed good performance. However, for some components unexpected problems arose. These are

i) Vibration.

The EVO design had long and slender shafts and the vibration behaviour was carefully pre-calculated in the planning phase. The first resonance frequency of the HP set was originally calculated to be about 2050 rpm assuming stiff bearings and the LP set was calculated to be about 1800 rpm. However at the first start-up, as soon as the pressure and temperature had been increased a sudden rise of the shaft oscillation amplitudes at the rotor of the HP shaft was detected. These oscillation amplitude was so large that the design value of speed and power could not be attained. Moreover severe damages occurred at the sliding surfaces of the bearings including partial tearing the bearing surfaces. The measured first resonance frequency was about 1950 rpm as against 2050rpm in the pre-calculation. The conclusion is that approximately 100 to 200 rpm must be deducted from the theoretical calculations for stiff bearings to meet the realistic conditions. Various modifications were done on the rotor support and the bearings, as a result of these efforts; there was a distinct rise of the stability limit with regard to higher operating pressures and higher speeds. [98].

ii) Non Achievement of the Nominal Power

In the first three years of operation, 28 MW instead of 50MW was the maximum electrical power attained because of the seal gap excited oscillations, the bearing problems, the shaft imbalances and the thermal distortions. After having modified the rotor of the high-pressure stage, nominal values of pressure and temperature could be achieved but the nominal power could not be achieved.

The deficiency of the power production was due to deficiencies inside the turbo-set. The blading efficiencies did not reach the nominal design values and the helium mass flow rates for the cooling and the sealing gas (which are deducted after the compression) were larger than predicted. Since this lost helium flow does not produce power in the turbine, an accordingly large power loss resulted. Additionally, large power losses occurred due to insufficient flow guidance from the inlet diffuser into the

first blade row. In order to overcome the shortfalls, the following modifications were suggested [98].

a) Modification of the inflow and outflow sections of the compressors and turbines after experimental tests.

b) Reduction of the blade gap losses by designing essentially vibration free rotors. The materials for the rotor and the stationary blade carrier should be selected to optimise thermal expansions to achieve minimum gaps at operating conditions. (Eg. Replacement of the non-cooled, austentic stationary blade carrier by a ferritic one, with cooling provided at necessary locations or possibly no cooling at all at 750^0 C, taking into account of the improvements blade and rotor material technology)

c) Optimisation of the applied profiles for the stationary blades by using a reaction ratio of 50% at both compressors instead of 100% resulting in a large number of blade rows.

2.2.2 HHV High Temperature Helium Plant, Germany

The first design proposal was to use a fossil fired heater to replace the nuclear heat source. Because of the desired peak temperatures of 850^0 C (1000^0 C for shorter periods) and the design pressure of 50 bar; there were feasibility concerns about the lifetime capability of such a fossil-fired heater. Thus a test circuit was chosen comparable to a closed cycle gas turbine plant as shown in Appendix I.

In this the compression heat from the compressor is used to heat up the helium to the desired temperature. The required compressor power was 90MW with 45MW generated and regained by the expansion of the gas turbine and 45MW introduced by the electric motor. The selected combination of the turbine and compressor on one shaft resulted in dimensions being comparable with a helium turbine of 300MW capacity (the reference plant size at the time).

The initial difficulties occurring at the commissioning in 1979 were,

i) Oil Ingress

There were two incidents of oil ingress into the main helium circuit, the first one was an operator error and the second one was due to the mechanical defect of a sealing element. In the second incident the quantity of oil was very small and it was removed by cracking at 600^0 C with the use of additives [98].

ii) Excessive Helium Leak rate

The pressure and leak test at ambient temperature showed good leak tightness for the flange joints of the turbo set and of the main and auxiliary helium circuits. But at operating conditions of 850^0 C large helium leaks were detected. Comprehensive counter measures had to be taken. One was to weld the lip seals provided at the flange joints of the main circuits. Another major leak was detected at the front flanges of the turbo set, caused by a non-uniform temperature distribution during operation resulting in thermal stresses forming local gaps of about 0.1 mm. The cooling gas distribution and flow rates within the turbo set housing were modified to improve the temperature distribution to prevent the local gaps.

After overcoming the initial problems, the HHV was successfully operated for about 1100 hours, of which the turbomachinery operated for about 325 hours at 850^0 C. The agreement between pre-calculations and measurements was excellent in spite of the following restrictions

a) Mass flow in the turbomachine cannot be measured directly
b) Mass flows in the stuffing boxes and labyrinth seals can only be estimated
c) Cooling gas flows in the rotor and the stator can only be estimated.

It can be concluded that the thermodynamic design data were achieved and even exceeded. The compressor and the turbine had a better efficiency than assumed at the design. This was derived from the measurement of the electrical drive power and from the direct or indirect measured mass flows, pressures and temperatures at the inlet and exit of the compressor and turbine. [98]

2.3 Current activities on HTGRs in the world

Apart from PBMR, a couple of research and development activities are going on in the world to develop High Temperature Gas Reactors with a Helium turbine for the commercial generation of electricity. The following are these projects [17].

i) Gas Turbine- Modular Helium Reactor (GT-MHR)

Renewed interest in the nuclear powered closed cycle gas turbine system within the US resulted in the present GT-MHR developmental program beginning in early 1993. Subsequent discussions with organizations of Russian Federation resulted in General Atomics (GA) and MINATOM entering into an agreement on the development of GT-MHR to design, develop to construct and test a prototype in Russia. FRAMATOME joined this program in 1996 with Fuji Electric becoming a participant and sponsor in 1997. The conceptual design is completed on this 600MW/293MW(e) plant and the preliminary design of the plant has already started [17].

ii) ECN's ACACIA Plant

ECN Nuclear Research is developing a conceptual design of an HTGR for the combined generation of heat and power for possible industry within the Netherlands as well as for possible export. The ACACIA plant utilizes a pebble bed HTGR to produce 40MW/14MW(e) and 17 tonnes of 10bar, 220^0C steam per hour. The electric generation system utilizes a basic closed cycle gas turbine, which receives helium from the HTGR at 800^0C and 2.3MPa. After the recuperator, a secondary helium loop removes heat from the primary system via an intermediate heat exchanger (pre-cooler), which then transfers energy to the steam/ feed water system for industrial use [17].

iii) Japan's HTGR Gas Turbine Designs

A number of gas turbine plant designs are currently under development within Japan. These plants are primarily under development by the Japanese Atomic Energy Research Institute (JAREI) within the framework of the Japanese HTGR-GT feasibility study

program, and include gas turbine cycle units with reactors of 400MW(t), 300MW(t), and two variations with a power level of 600MW(t)[17].

iv) MIT and INEEL's MPBR Plant

The area of research for this project are aimed at addressing some of these fundamental concerns to determine whether the small, 110MW(e) modular gas- cooled pebble bed plant can become the next generation of Nuclear technology for worldwide deployment. MIT and INEEL have utilized the reference design from the ESKOM PBMR, but with a significantly different balance of plant.

The HTGR design at MIT is of pebble bed with a power level of 250MW(t). Primary coolant helium from the reactor flows through an intermediate heat exchanger to the secondary coolant, air. The secondary loop consists of a high-pressure turbine, which drives three compressors with two stages of intercooling. A second shaft incorporates the low-pressure turbine and electric generator. The MPBR utilizes conventional oil bearings rather than magnetic bearings on its turbomachines.

v) INET's MHTGR-IGT in China

This design features an indirect gas turbine system coupled to a 200MW(t) pebble bed HTGR. Although the HTGR can provide heat at 950^0C with the attributes of outstanding safety and gas turbine cycle efficiency in the range of 47%, the possible radioactivity disposition on the turbine blades and thus the increase in maintenance difficulties suggests that the indirect gas turbine cycle should be applied initially in the development process to help solve these problems.

The whole primary circuit is integrated in a single pressure vessel with the core inlet/outlet temperatures $550/900^0$ C, which can supply heat at around 850^0 C on the secondary side. This heat will be used to drive a nitrogen gas turbine cycle with electric generator.

2.4 Closed Cycle Gas Turbines

The commercial electric power industry has had a continuing interest in the closed cycle gas turbine as the prime movers for the generation of electric. Since the earliest times after the development of combustion turbines, a serious effort by a number of individuals' enterprises has been undertaken to investigate the possibility of using the closed cycle gas turbine as the prime power generator, both with combustion and with nuclear thermal power sources. For a variety of reasons, the closed cycle gas turbine technology has not been developed to the point of a large – scale commercialisation. Further, the successful employment of the closed Brayton cycle requires development of a new class of higher temperature gas cooled reactors (rather than liquid cooled reactors). The reason is that the Brayton cycle demands the highest practical turbine inlet temperature. However the unique capability of a closed cycle to operate with a reduced inventory of working fluid gives it unique flexibility in operating at part load.

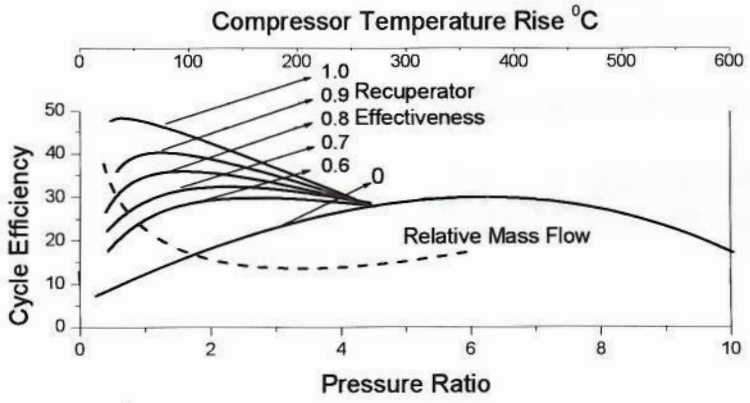

Figure 2.1 Cycle efficiency vs. Pressure Ratio and Recuperator effect. Single compressor, No intercooler.

Figure 2.1, which shows for helium, the cycle efficiency and specific flow rates as a function of expansion ratio and regeneration effectiveness, represents a particularly informative outcome of such work. Top and bottom gas temperatures are fixed, the former by the approximate capability of the HTGR core as presently developed for steam plants, and the latter by the suitability for dry tower heat rejection from an intermediate water cooling loop.

This diagram which relates to the configuration without inter-cooling, has added also a scale of compressor temperature rise, which is important because the number of machine stages required is proportional to this number rather than the compression produced. The important fact brought out is that a highly efficient recuperator is critical to success, not just because it raises peak efficiency, but because it also drastically reduces the number of stages needed at the optimum efficiency point and also results in a volume flow minimum practically coincident with this point. [3]

2.5 Helium as working Fluid

Helium is considered as one of the ideal working fluid in closed cycle gas turbines. It is chemically inert and does not pose a threat to the turbine life by chemical corrosion. It obeys ideal gas state equation and is thermally perfect at all conditions considered so that the mathematical description of the fluid and thus performance is particularly simple. From a nuclear viewpoint, helium is an excellent reactor coolant because it does not undergo absorption reactions with neutrons and thus does not become radioactive. [26]

The desirable properties of the selected gas may be defined roughly as follows: [88]

1. It must not react, to any significant extent, with the materials used in either the reactor or the gas turbine.
2. It should however have a low induced radioactivity and dissociate under irradiation and high temperature.
3. It should have good heat transport properties.
4. Its thermodynamic properties should be suited to simple design of the turbine and compressor.

The properties of some gases, which are considered frequently for reactor cooling, are compared briefly in Table 2.2

The suitability of a gas to simple design of turbines and compressors is governed largely by the value of C_p and to a lesser extent γ. Gases with high specific heat require large numbers of stages in compressors and turbines to achieve the required degree of compression or expansion (number of stages α C_p, approximately). Nitrogen and carbon dioxide present no serious difficulty, but helium compressors and turbines tend to become unwieldy in length and hence complicate the mechanical design.

Gas	Chemical compatibility with reactor and engine materials	Induced radio-activity and dissociation	C_P KJ/Kg. K γ, M	General Remarks
H_2	Generally good, but may embrittle some materials	None	14.68 1.4 2.016	Very good heat transport properties. Difficult to contain at high pressure
He	Very Good	None	5.2 1.66 4.006	Good heat transport properties, but expensive
CO_2	Satisfactory	Negligible radioactivity. Some dissociation at high temperatures	1.09 1.21 44.07	Good heat transport properties. May preclude use of graphite as moderator material at high temperatures (unless both moderator and fuel elements are canned)
N_2	Probably satisfactory	Some induced radioactivity, not of significant level or type	1.09 1.4 28.02	Moderate heat transport properties
Air	Poor, due oxidation of metals at high temperature	Some induced radioactivity in argon and nitrogen	1.006 1.4 28.9	Moderate heat transport properties
Ne	Good	None	1.048 1.64 20.18	Poor heat transport properties

Table 2.2 Reactor coolant gases and its properties [88].

2.6 Thermodynamic consequences of changing from air to helium

Table 2.3 gives the properties of helium, compared at 300 and 1000K where similar cycles might operate. The pressure at the low and high temperature conditions are 1 and 30 atm. respectively. The transport properties such as kinematic viscosity and thermal conductivity vary with temperature, even for helium. [26]

Property	p(atm)	T(K)	Air	Helium
Mol Wt	-	-	28.9	4
γ	1 30	300 1000	1.4 136	1.67 1.67
C_p	1 30	300 1000	1005 1142	5.20kJ/kgK 5.20
k	1 30	300 1000	0028 0068	0.15w/m-K 0.36
ν	1 30	300 1000	16 34	$120\text{x}10^{6}\text{m}^2$/sec 28

Table.2.3 Properties of air and helium at conditions of interest in CCGTs

a) Specific heat

The specific heat of helium is *five* times larger than that for air so that for a chosen temperature increment, helium carries five times the power per unit mass.

b) Pressure Ratio.

A He cycle may be considered to operate between two chosen temperatures (T_2 and T_1). The pressure ratio is given by

$$\frac{p_2}{p_1} = \left(\frac{T_2}{T_1}\right)^{\gamma/(\gamma-1)} \quad \ldots\ldots 2.1$$

where the exponent in Equation. 2.1 equals 3.5 for air and 2.5 for He. This leads to a lower pressure ratio for the helium, which is easier from the point of view of compressor design because the magnitude of the adverse pressure gradient in the compressor tends to be lower.

c) Volume Ratio.

The design of the turbo machinery is simpler when the (geometric) expansion or compression volume ratio is smaller. In the limit of an incompressible fluid, the axial flow machinery may be built with little or no annular contraction. The volume ratio is given by.

$$\frac{v_2}{v_1} = \left(\frac{T_2}{T_1}\right)^{1/(\gamma-1)} \quad \text{.....2.2}$$

which is also smaller for helium compared to air. As an example, consider a temperature change from 300 K to 450 K. The pressure and volume ratios implied by equations 1 and 2 are summarized in Table 2.3

Table 2.4 Characteristics of cycle parameters for a 1.5 temperature ratio in a compression process

	Air	Helium
pressure ratio (p_2/p_1)	4.13	2.747
volume ratio (v_2/v_1)	2.75	1.8316
stage pressure ratio	1.2	1.03
number of compressor stages	8	33
flow velocity	1	2.3
flow area (high pressure side)	1	0.62
flow area (low pressure side)	1	0.37

d) Stage pressure ratio.

The Euler turbine equation relates the work done by the torques exerted with angular speed ω to the change in stagnation enthalpy.

$$C_p(T_{t2} - T_{t1}) = \omega(v_{\theta 2}\, r_2 - v_{\theta 1}\, r_1) \quad \text{.....2.3}$$

For an approximately isentropic flow with a small change in state conditions, the Euler turbine equation may be written for a compressor stage with axial flow ($r_1 = r_2 = r$)

$$\frac{T_{t2}}{T_{t1}} = 1 + \frac{(\omega r)^2}{C_p T_{t1}}\left(\left(\frac{v_\theta}{\omega r}\right)_2 - \left(\frac{v_\theta}{\omega r}\right)_1\right) \quad \text{.....2.4}$$

or, for a reversible process,

$$\frac{p_{t2}}{p_{t1}} = 1 + \frac{(\omega r)^2}{R_u T_1}\frac{T_1}{T_{t1}}(mol.wt)\,fcn(angles) \quad \text{.....2.5}$$

which is developed from first principles. Here the ratios between velocities are grouped to reflect the fact that they are functions of angles in the blading only. The specific heat ratio has been written in terms of the molecular weight, MW. The total to static temperature ratio is a function of Mach number and is close to unity. Thus for air, the pressure ratio is approximately 1.2 for a single axial compression stage, whereas that of the helium compressor is about 1.03 for the same wheel speed *(ωr)* and inlet temperature[26].

e) Number of Compressor Stages

The overall pressure ratio is given by Equation 2.1. This, the stage pressure ratio, Equation 2.5, allows the number of stages, N, for the same temperature rise to be determined.

Overall pressure ratio = (stage pressure ratio)^N

Table 2.4 gives N for air and helium using the numbers quoted above.

f) Pressure Drops in Flow Ducts

Specification of the fractional pressure drop dictates the magnitude of the fluid flow velocity. This has an implication for the compactness of the system. Since the work lost to fluid friction in a duct is at the expense of that obtainable from an adjacent work component, an example of a turbine followed by a heat exchanger where the flow negotiates a tube with a specified L/D can be used to equate the thermodynamic performances of air and helium. Thus ratio of velocity allowable in helium to that in air is found as [26]

$$\frac{Velocity_{He}}{Velocity_{air}} = 2.27 \text{ .....[For equal pressure loss effect]} \quad \text{.....2.6}$$

g) Flow Cross Sectional Area

The flow cross sectional area is given by the steady flow continuity equation

$$A = \frac{m}{\rho u} \quad \text{.....2.7}$$

where the density is given by the state equation and the mass flow rate by an enthalpy flux

$$\dot{m} \approx \frac{power}{C_p T} \quad \text{.....2.8}$$

with the velocity given by the "equal pressure loss effect" equation 2.6 and the pressures on the high pressure side taken as equal for the two cycles one obtains, the flow ratio A(He)/A(air) high and low pressure side. The values are given in Table 2.4. Evidently, the use of helium leads to more compact flow devices compared to air when flow area is used as comparative criterion (for the same pressure loss).

Compared to air, helium has distinct advantages for a closed cycle gas turbine. It is a chemically inert gas. The specific heat of Helium, a measure for the heat capacity and heat transport is five times than that of air, thus requiring smaller heat transfer areas. The sonic velocity is three times as large, resulting in design advantages for the turbo machinery. In particular, the permissible circumferential velocity of the helium compressor is no longer limited by sonic speed consideration but by the centrifugal stresses of the blades. A characteristics of helium's large specific heat is that the enthalpy difference between pre selected temperatures is accordingly large, resulting in a large number of stages for a helium than for air turbine. [26].

h) Effect of Pressure Level on the Helium Closed Cycle Gas Turbine Component Characteristics

In principle the efficiency of the closed cycle using helium depends on pressure ratio and the corresponding temperature ratio and not on the level of the pressure. On the other hand, the mass processed by a duct of a given diameter depends on the density(and therefore for a fixed temperature, on the pressure) of the fluid. Thus the power output of the engine is directly affected by the choice of pressure as are the physical characteristics of several of the engine's components. In this section, the impact of the following is examined:

1. Physical dimensions of the machinery
2. Reynolds number in the flow passages.
3. Physical dimensions of heat exchangers.

When helium is used at varying pressures. The approach is to consider an increase in the pressure of the fluid over some reference level according to

$$p = Zp_0 \quad \text{.....2.9}$$

[Z= Pressure Multiplication factor]

so that the increasing Z determines the sought after effect. The constraints are that the flow velocity (i.e., the Mach number) and the temperatures, which the flow experiences are fixed by consideration of the cycle thermodynamics as, outlined above. Reynolds number effects are ignored except where their influence is specifically examined. Geometric similarity is assumed, and a reference scale is denoted by a zero subscript. The approach and some of the results described here are based on [26]. These are generally used for an examination of processing equipment in power and chemical plants in relation to the choice of fluid and its pressure.

i) Physical Dimensions of the Machinery

FLOW PASSAGE SIZE: The continuity equation gives $\rho uA = constant$, u=*velocity* or, with the state equation,

$$pD^2 = \text{constant} \quad \text{or} \quad \frac{D}{D_0} = \frac{1}{\sqrt{Z}} \qquad \text{.....2.10}$$

ROTATIONAL SPEED: The force balance on an element of the structure yields the fact that the centripetal acceleration acting on the mass of the element is balanced by the stress times an effective area. Thus for a fixed (maximum) stress level, σ, the linear speed of the element is given by:

$$V = \sqrt{\frac{\sigma}{\rho_m}} \qquad \text{.....2.11}$$

where ρ_m is the material density of the blade or wheel disk material. This result could also have been obtained from dimensional analysis. Denoting ω as the angular speed, one obtains

$$\omega D = \text{constant} \quad \text{or} \quad \frac{\omega}{\omega_0} = \sqrt{Z} \qquad \text{.....2.12}$$

using the size scaling result above (eq. 2.10)

SHAFT TORQUE: Torque is given by the power divided by angular speed. Thus

$$Torque = \frac{power}{angularspeed} \propto \frac{1}{\omega} \propto \frac{1}{\sqrt{Z}} \qquad \text{.....2.13}$$

MACHINERY SHAFT DIAMETER: The torsional stress level on the shaft is given by the torque and the polar moment of inertia, J. If the shaft diameter is d, then $J \sim d^4$. For a fixed stress level on the outermost shaft elements where it is largest, d is given by:

$$stress = \frac{d * torque}{J} \quad \text{or} \quad \frac{d}{d_0} = Z^{-1/6} \qquad \text{.....2.14}$$

BLADE STRESS: The individual blades of a compressor or turbine rotor experience "lifting" forces, which tend to deflect them like the bending experienced at the root of the airplane wing. The blade would be designed to operate at the fixed lift coefficient so that the load (force) per unit area of the blade is order

$c_1 \cdot \frac{1}{2}\rho u^2$ varies as [p] for fixed u and T

From the idea of geometric similarity, it follows that the blade length, or span, is proportional to *D*. Combining these notions into a statement concerning the stress at the root due to the bending moment, one has

$$\text{Stress, } \sigma \propto \frac{D * bendingmoment}{I} \propto Z \quad \ldots\ldots\ldots\ldots\ldots\ldots 2.15$$

since the bending moment is proportional to the lift ($\propto ZD^2$) times span (~D). The cross-sectional moment of inertia, *I*, is proportional to D^4. It follows that the stress level is proportional to pressure and thus limits the pressure.

2.7 Complexities associated with closed cycle helium turbines

History of the CCGT shows that few main reasons can be pointed out for the unsuccessful effort to establish gas turbine technology in the sixties and seventies. These are all operational problems manifested in the following forms

1. Heavy leakage of helium through the seals and gaps. This is because of the small molecular size of the helium compared to other gases, for which normal seals are developed. The same as that of the tip leakage in turbo machinery. The blade cooling with helium can be expensive if it is done in a conventional way meant for air. The helium flow rate will be higher compared to air.
2. Welding effect of the high temperature helium, which stopped the functioning of guide vanes, mechanical bearings, control valves etc. When high temperature helium is passing over two moving metallic surfaces, some sort of material transfer takes place between those two surfaces. This is extremely harmful for the sensitive equipments such as mechanical bearings; control valves guide vane support bushes and bearings etc.
3. Rotor vibrations. These were due to the slim and single rotors used in the past with a gear facility at the generator side.

Radical conceptual designs such as electro magnetic bearings, adjustable sealing system, multiple rotors etc have been proposed as an answer to these issues. The success of these theoretical solutions has to be tested with some sort of credible method. A full-scale model as a test facility is expensive and unacceptable considering the financial implications. Computer modelling and simulation is more convenient and economical, but the validation of these models is a challenge.

2.8 Control philosophy of closed cycle gas turbines

In a closed cycle gas turbine of fixed size and volume the gas density, and hence the mass flow and total output power, will vary in proportion to gas pressure, so that power output of a closed cycle turbine might be varied over a vide range without significantly affecting the thermal efficiency, by controlling the level of maximum gas pressure in the cycle. If the reactor has a fairly high negative temperature coefficient of reactivity (reactivity with respect to the temperature) then such a control might be manipulated without adjustment of the reactor control rods, the reactor providing, in effect, an approximate temperature-governing device. However the rate at which the

gas might be pumped in and out of the gas turbine circuit may not be sufficiently fast to meet the rapid changes in power that may be demanded for manoeuvring purposes[88].

Closed cycles present unique issues and opportunities for modulating power output from power systems. Two methods are described and their features are discussed. These systems have been of interest for use in the nuclear power industry.

Power control is achieved by regulating the mass flow of Helium inside the main circuit. This is mainly done by a combination of by-pass and pressure changes. Changing the pressure and therefore the mass flow according to the power level will not change the temperature and pressure ratios. Increasing pressure and subsequent mass flow, increases the heat transfer rate, thus increasing the power extracted from the core. Power reduction is achieved by removing gas from the circuit. The power control system revolves around a series of Helium storage tanks ranging from low pressure to high pressure to maintain the required pressures. The adjustable stator blades on the turbo machinery and bypass flow achieve short-term control.[3]

1. Heat Source Bypass

Figure 2.2 shows a schematic for a regenerated Brayton cycle. Proposed commercial power systems using this cycle offer the advantage of enabling part production with a time variability to match that of the load. To that end, a number of power modulation schemes are available: bypass control, temperature modulation, and inventory control. It is important to be able to produce the part load power at high efficiency and in such a way as to minimize the thermal stress impact on the heat source, especially if the source is a gas-cooled nuclear reactor. For a given machine, the cycle pressure ratio is nominally fixed by the compressor.

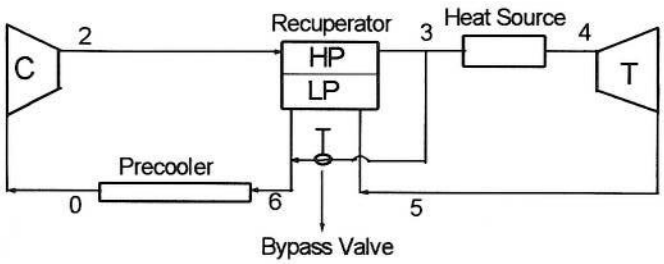

Figure 2.2 Bypass power control of a closed Brayton cycle

The bypass control is exercised through the bleed of high-pressure gas to short-circuit the heat source and the turbine, as shown in Figure 2.2. The throttling process is obviously a source of irreversibility so that use of such a scheme results in reduced part power efficiency. The cycle temperatures can be held constant with just the thermal power input matching that required maintaining the cycle temperatures at the reduced mass flow through the reactor. This has the advantage in that stresses associated with temperature gradients 1 in the metals may be held close to constant.

The impact on performance is readily calculated since the cycle temperature may be taken to remain fixed The regenerator will process equal masses on both sides at all times, which implies that the ideal design situation of $T_3 = T_6$ is maintained at part power. This is due to the fact that with constant T_4 and constant compressor pressure ratio, $T_3 = T_5$. The enthalpy balance on the mixer gives the temperature at state 6, which is, for an ideal and perfect gas, trivial. The cycle analysis is merely a work accounting with the full mass flow processed by the compressor and less in the heater and turbine. An ideal cycle analysis yields [26]

$$\eta_{th} = \left[1 + \frac{w}{w_{\max}}\left(\frac{\theta_4}{\tau_c} - 1\right)\right]^{-1} \quad \text{.....2.16}$$

$$w_{\max} = \left(\frac{\theta_4}{\tau_c} - 1\right)(\tau_c - 1) \quad \text{.....2.17}$$

For values of these parameters of 4 and 1.5, respectively, the efficiency is as shown in Figure. 2.3

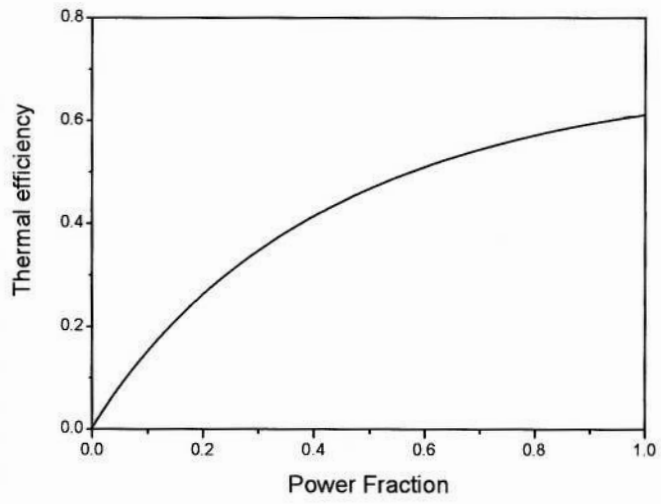

Figure 2.3 Thermal efficiency of a regenerated Brayton cycle as a function of power fraction with a bypass power control with ideal components. PR=1.5, TR =4

The modulation of T_4 in an ideal cycle gives efficiency results that are identical to those of bypass control. The implication is that bypass and peak temperature reduction have the same thermodynamic merit. Temperature modulation and bypass may therefore be used together if the resulting performance is acceptable. In practice, accurate part power performances are evaluated with significantly greater consideration of the irreversibilities.

2. Inventory Control

A good method of producing part-load power is available to closed cycle engines where the pressure and thus the density of the working fluid may be controlled by connecting the cycle fluid to a storage vessel, as shown in Figure 2.4

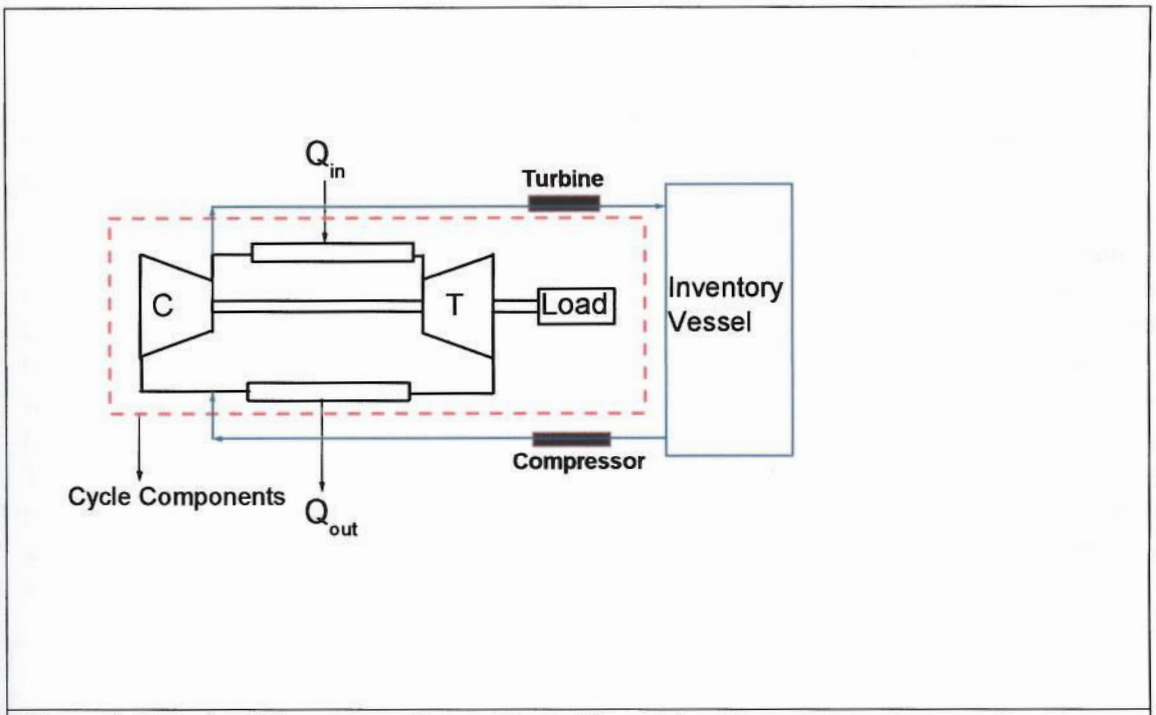

Figure 2.4 Basic of Inventory Control in a Closed Cycle

The compressor shown in the figure is used to pump the working fluid out of the system of working components. The reduced mass of the circulating fluid results in a smaller mass flow rate, which, in turn, reduces power output from the system. Means are also provided to allow the return of the fluid to the cycle when power is to be increased. In order to minimize heat transfer in the storage component, the fluid is removed from the lowest temperature point in the cycle with appropriate means for cooling. The operation of the cycle at reduced mass flow rate allows operation with the same temperatures and pressure ratio This means that the heat engine operates with the same thermodynamic cycle, resulting in approximately constant efficiency and specific work

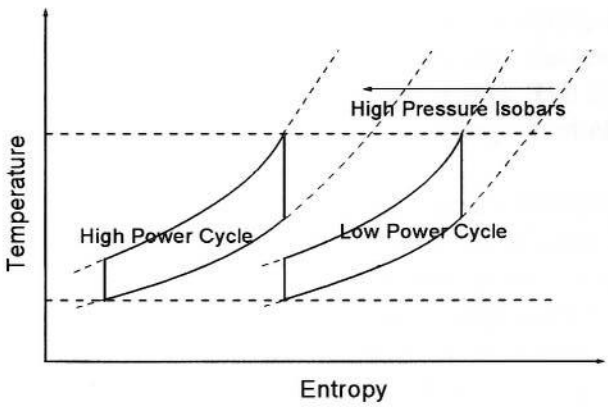

Figure 2.5 Temperature- Entropy diagram for part and full power for the inventory controlled closed Brayton cycle.

The fact that the temperatures remain invariant as the mass flow rate is reduced implies that the local sound speeds are constant. Blading and flow-passage geometric design fix the local Mach numbers so that local flow velocities are everywhere constant to first order. With velocities constant, the mass flow rate is proportional to the density, which, for constant temperature, is also proportional to the absolute pressure. The thermodynamic cycle operating at various pressure levels can be shown as in Figure 2.5 The variation of cycle performance is a function of the working fluid properties. These properties are insensitive to absolute pressure when the gas is monatomic. For other gases, the effect of changing pressure may be significant in affecting specific work and efficiency.[26]

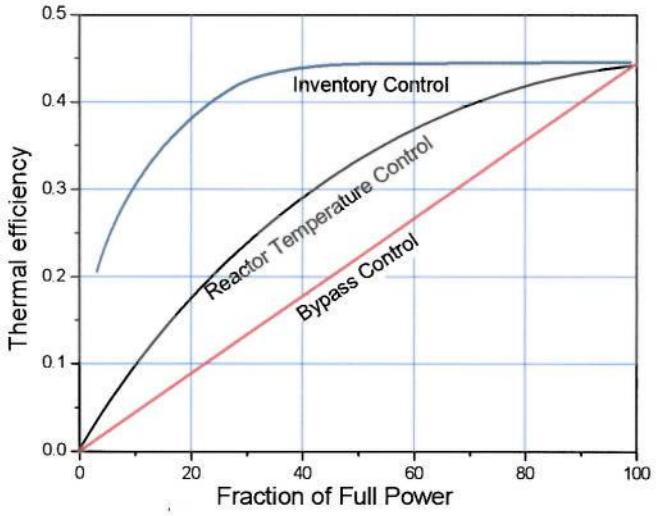

Figure 2.6 Performance of the cycle with various control types.

It is expected, therefore, that the relation between efficiency and fractional power is relatively flat (Figure 2.6) and a small fractional power output can be obtained by operating at low absolute pressure. In practice, the fluid frictional losses are slightly altered because the decreased density also decreases the flow Reynolds numbers. This increases the importance of viscous losses. The effect is to reduce efficiency slightly as the power output is reduced because component efficiencies are reduced.

The peak and part-power cycle efficiency noted for bypass and temperature modulation control on a realistic analysis (Figure 2.6) are about half the value noted for an idealized analysis for the same temperature extremes, showing the importance of the irreversibilities. Further, the serious degradation of efficiency with bypass control is noted as a disadvantage in relation to inventory control. It should be noted, however, that the severity is important only if the fraction of time spent at less than full power is significant.

Chapter .3
PBMR Plant Description

The plant typically consists of a single building approximately 50 x 26 m in plan and 42m in height, with 21m below ground level. Fig 3.1 shows the 3D view of the plant. The only other facilities envisaged would be the cooling water supply, access control and security systems, maintenance and APU buildings, the control room and the high voltage switchyard. Depending on the specific site, the main building may be constructed as little as half the height protruding above the ground surface level. The building layout will be designed to facilitate easy access for all components and for easy handling of these components within the building. The layout also makes provision for the storage of spent fuel for the 40 years of operating life cycle of the system and after shutdown of the plant, for an additional 40 years of interim spent fuel storage. This implies that no radioactive waste will be removed from the site during the lifetime of the plant. The systems will be designed to withstand specific predicted seismic conditions. The structure will also be designed to withstand the direct impact of specific high-speed aircraft as laid down in the stringent German aircraft crash specifications [65].

Figure 3.1 Reactor and the Power Conversion Unit[70]

3.1 How the PBMR works

The PBMR consists of a vertical steel pressure vessel, 6m in diameter and about 20m high, which is lined with 100cm thick graphite bricks. It uses silicon carbide coated particles of enriched uranium oxide encased in graphite to form a fuel sphere or pebble about the size of a tennis ball. Helium is used as the coolant and energy transfer medium to a closed cycle gas turbine and generator system. During normal operation, the pressure vessel contains a load of 440 000 spheres, 310 000 of which are fuel spheres. The rest are pure graphite spheres, which serve the function of an additional nuclear moderator. One fuel sphere contains some 15 000 uranium dioxide particles, each a millimetre in size. A fuel sphere contains 9 grams of uranium, which means that the total uranium in one fuel load is 2,79 tons.

A reactor will use 10 to 15 total fuel loads in its design lifetime (the actual calculated figure for continuous operation at full power is 13,8 fuel loads).To remove the heat generated by the nuclear reaction, helium gas at ~500°C enters the pressure vessel at the top. It then moves down between the hot fuel balls, after which it leaves the bottom of the vessel having been heated to a temperature of 900°C. The hot gas then passes through a closed cycle gas turbine system to drive an electrical generator before being returned to the reactor[70]. Fig 3.2 shows the process diagram of PBMR.

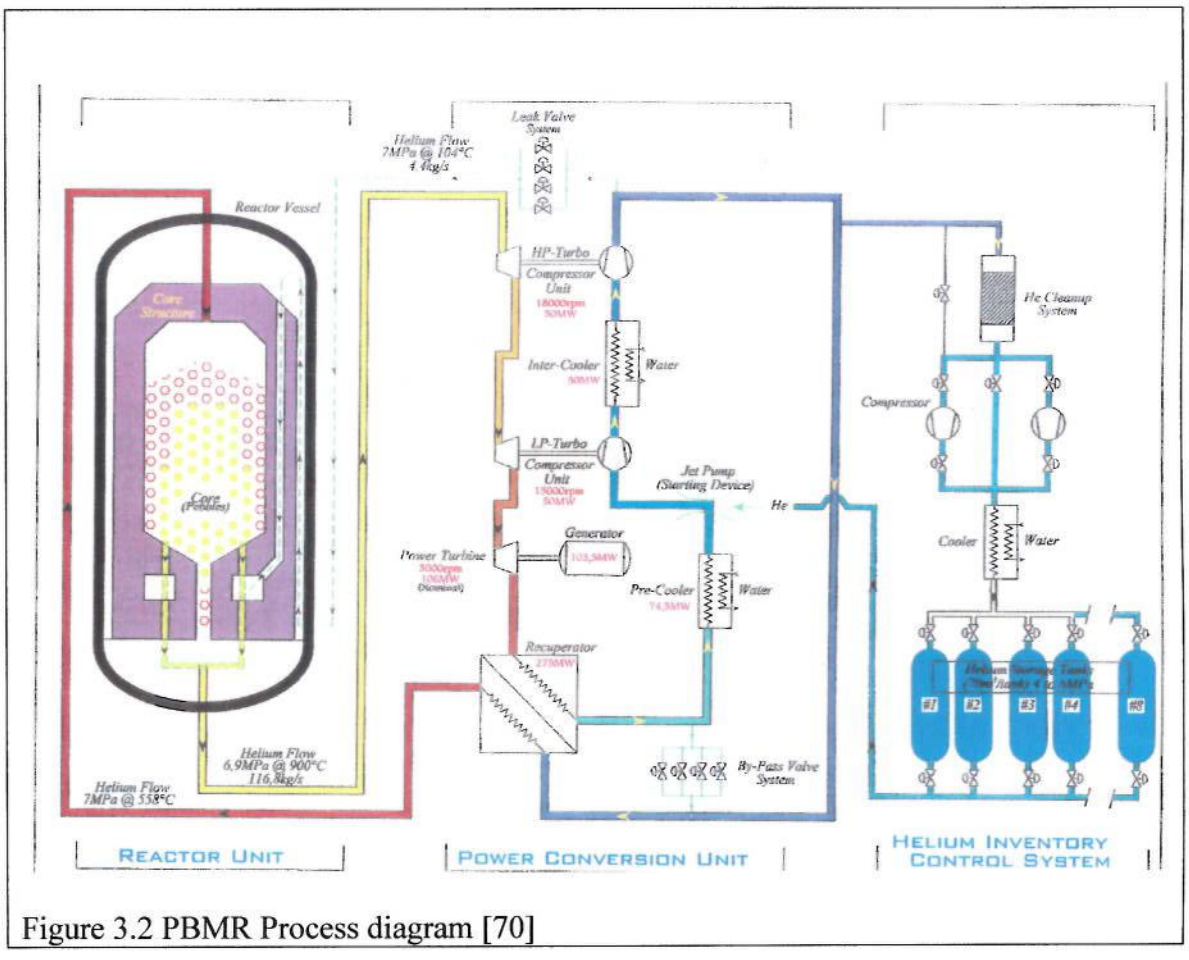

Figure 3.2 PBMR Process diagram [70]

3.1.1 How the PBMR fuel works

The enriched uranium oxide fuel is formed into tiny particles, coated with successive layers of porous carbon, pyrolytic carbon and silicon carbide. Fig 3.3 shows the detail of a pebble. The porous carbon accommodates any mechanical deformation that the uranium oxide particle may undergo during the lifetime of the fuel. The pyrolytic carbon and silicon carbide layers provide an impenetrable barrier designed to contain the fuel and the radioactive decay products resulting from the nuclear reactions.

Each pebble passes through the reactor about 10 times. They are extracted, measured electronically to determine the amount of fissionable material left, and then either returned to the reactor or stored. The extent to which the enriched uranium is used to depletion (called the extent of 'burn-up') is much greater in the PBMR than in conventional power reactors. There is therefore minimal fissile material that could be extracted from depleted PBMR fuel. This, coupled with the level of technology and cost required to break down the barriers surrounding the spent fuel particles, protects the PBMR fuel against the possibility of nuclear proliferation or other covert use[70].

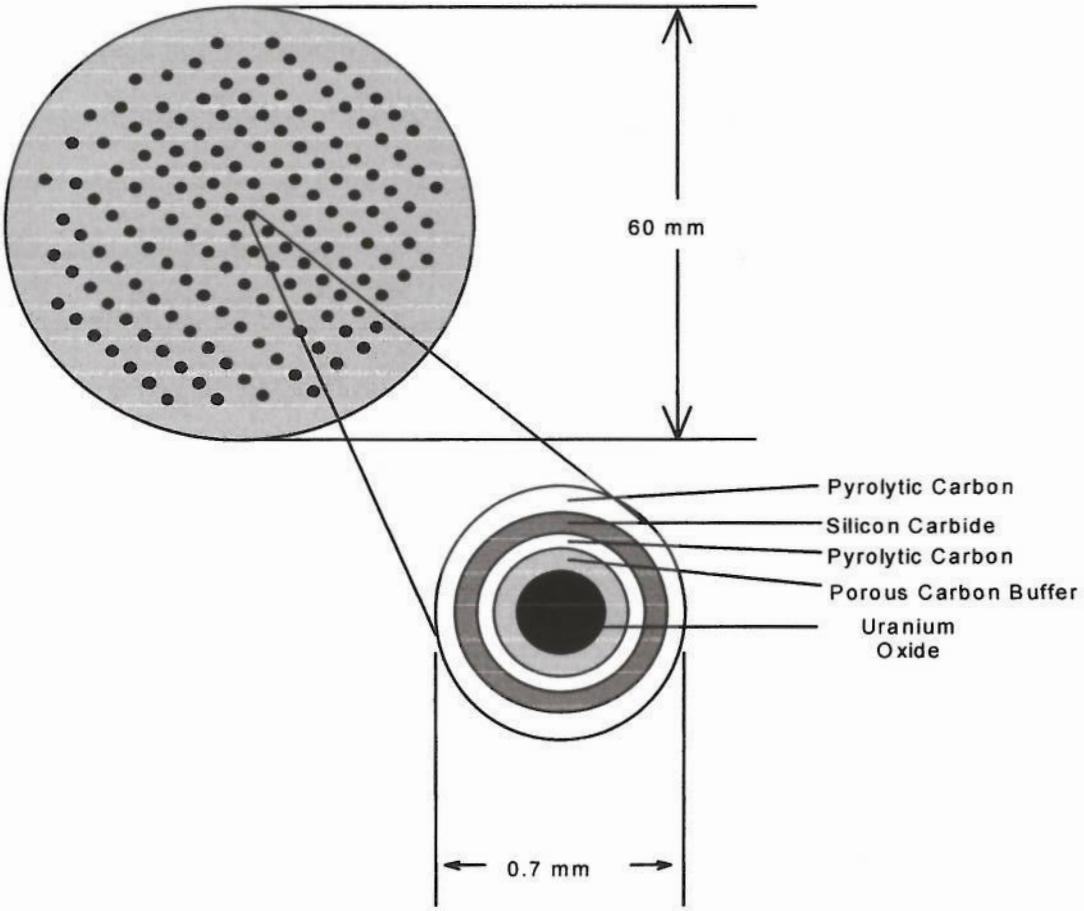

Figure 3.3. The detail of a Pebble [70]

3.1.2 Design Parameters

The PBMR project is in the conceptual stage and hence only a technical specification of broad nature is available at the moment. A detailed specification will only be available when the manufacturers input after their part of developmental work is completed. The specification currently available is as follows[65].

Table 3.1 Process Parameters

Parameter	Value
Cycle Core mass-flow	145 kg/s
Reactor thermal power	265 MW
Reactor inlet temperature	536 °C
Reactor outlet temperature	900 °C
Generator electrical output	116.3 MW
Overall pressure ratio	2.7
Cooling water temperature to heat exchangers	22 °C
Generator efficiency	98.5 %
Cycle efficiency (Generator excluded)	45.3 %
System efficiency (Generator included)	44.1 %
Plant net efficiency	42.7 %

Table 3.2 Cycle Temperatures and Pressure

System Position	Pressure MPa abs.	Temperature °C
1	2.59	27.9
2A	4.24	104.4
2a	4.23	27.6
2	7.00	104
2	6.952	105.4
3	6.955	536
4	6.72	900
5A	5.46	812
5a	4.34	721
5	2.61	553
6	2.59	138

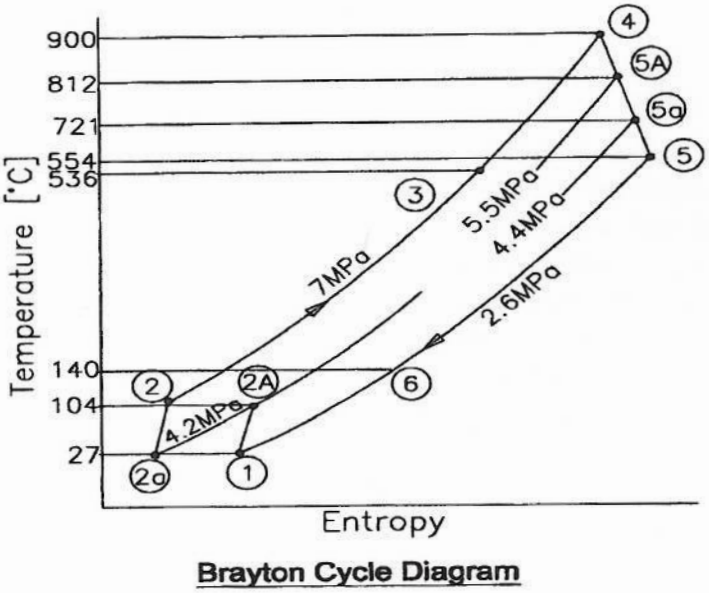

Figure 3.4 PBMR Brayton cycle

Characteristic	Unit	HPC	LPC	HPT	LPT
Shaft speed	Rev/min	15200	14200	15200	14200
Isentropic efficiency	%	89	89	89	89
Inlet diameter	mm	551	630	678	704
Blade length, inlet	mm	74.4	119.4	32.6	38
Load coefficient		0.306	0.306	1.6	1.7
Flow coefficient		0.50	0.50	0.75	0.75
No. stages		9	9	1+1	1+1
No. rotor blades		43	43	330x2	330x2
No. stator blades		50	50	36	36
Power	MW	58.4	58.4	58.4	58.4
Cooling flow	Kg/sec	0	0	2.1	3.0

Table 3.3 Turbo-Machinery Design Detail

HPC = High Pressure Compressor, LPC = Low Pressure Compressor, HPT = High Pressure Compressor Turbine, LPT = Low Pressure Compressor Turbine

3.2 PBMR Design Criteria

3.2.1 Direct/ Indirect arrangement

High temperature gas cooled reactors would appear to be particularly well suited to nuclear- powered closed cycle gas turbines, particularly if the working gas in the gas turbine circuit may be passed through and heated directly in the reactor core. This gives the most compact and efficient system possible. A possible disadvantage to such an arrangement is that accidental escape of fission products from the reactor core into the gas stream may contaminate the machinery, and further problems are introduced if the gas used is of a type which can acquire induced radioactivity in passing through the reactor. This may demand light shielding around the turbo-machinery, a safety containment vessel enclosing the entire reactor and turbo-machinery, and will introduce some problems in machinery maintenance if the machinery becomes mildly radioactive. Such problem may not be particularly troublesome, however, except in the event of a major mishap in the reactor core.

In the indirect arrangement an intermediate heat exchanger is introduced between the reactor and the power conversion system. The problems of radioactive contaminations as explained above can be minimized in this by separating the reactor coolant circuit and the gas turbine circuit each other. However, with such an arrangement the intermediary high temperature heat exchanger would be bulky, heavy and expensive and the potential advantage of compactness might be lost. The inclusion of a heat exchanger between the reactor gas coolant and the turbine gas inevitably necessitates that the maximum turbine gas temperature is depressed to a value 50-100^{0}C lower than the maximum gas coolant temperature at outlet from the reactor, leading to some sacrifice in the gas turbine thermal efficiency.

A separate and independently driven compressor must be inserted in the reactor gas coolant circuit in order to circulate the coolant gas, resulting in additional overall mechanical complexity and further loss of net overall thermal efficiency. Therefore a dual circuit arrangement of reactor and gas turbine of the above form might show little or no advantage over the more conventional reactor-steam turbine systems. Such dual arrangements might only prove attractive if high temperature liquid cooled reactor systems become practical [64,88].

3.2.2 Multiple shafts arrangement

The PBMR design consists of a three-shaft arrangement. The HP and LP shafts are driving the HP and LP compressors. The third shaft is for the free power turbine. All the 3 shafts are physically apart and placed in 3 different chambers with no mechanical link between them. This allows a free selection of the speed of the compressors and its turbines, which improve the efficiencies of these machines. The speed of these is no more restricted by the synchronous speed of the turbo generator. This will help to have short shafts and lesser number of stages. This will improve the shaft dynamic stability as well. The disadvantage of the independent shaft system, compared to the single shaft is that the multiple shafts need a separate drive to start-up the compressor. Also it will be difficult to control its over speed for various assumed accidents. The full load rejection by the generator can cause overrunning of the power turbine shaft due to the lack of compressor resistance on the power shaft [64].

The single shaft arrangement will have long and slender shaft running at generator synchronous speed. Because of the low speed turbines and compressors, this will be less efficient compared to multiple shafts. The advantage is that the start-up will not need extra equipment as the generator can be used a starting motor. Also during a full load rejection, the shaft overrunning can be easily controlled due to the high inertia and the resistance from the compressors. The multiple shaft system provides better part load performance compared to the single shaft. These various mechanical arrangements in no way affect the design point performance such as thermal efficiency, specific power etc, their use only leading to more stable and convenient operation at speeds and powers much less than the maximum values

A study on the performance of single or multiple shaft arrangement was done by Korakianitis et al [52] and shows that variable compressor or turbine geometry for part load performance has a beneficial but less pronounced effect than from going from the single shaft to multiple shaft arrangement.

3.2.3 Selection Criteria for TET

The PBMR has a negative reactivity coefficient as the temperature increases. This means as the temperature increases, the reactivity comes down causing the thermal output being reduced by several percent of the design value.

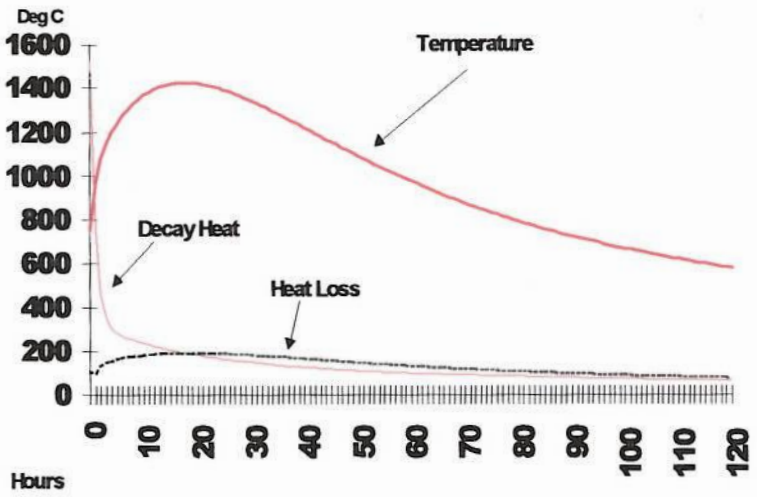

Figure 3.5 Reactor post failure cooling

This is one of the basis of the so-called inherent and passive safety features of the PBMR. The outlet temperature of the reactor has been set at 900^0 C so that the maximum temperature of the fuel during an accident can always be maintained below 1400^0C. This maximum reactor outlet temperature is still far below the technological limit for the cooled turbine blade [70].

3.2.4 Vertical shaft arrangement

The vertical shaft arrangement is good for heavy-duty magnetic bearings. This will help to have more lateral magnetic surface to carry the weight by adding disks or simply by increasing the diameter of the existing one. In a horizontal shaft design, the magnetic area depends on the shaft diameter and length. The Figure 3.6 shows the effect of horizontal and vertical design in the magnetic bearings.

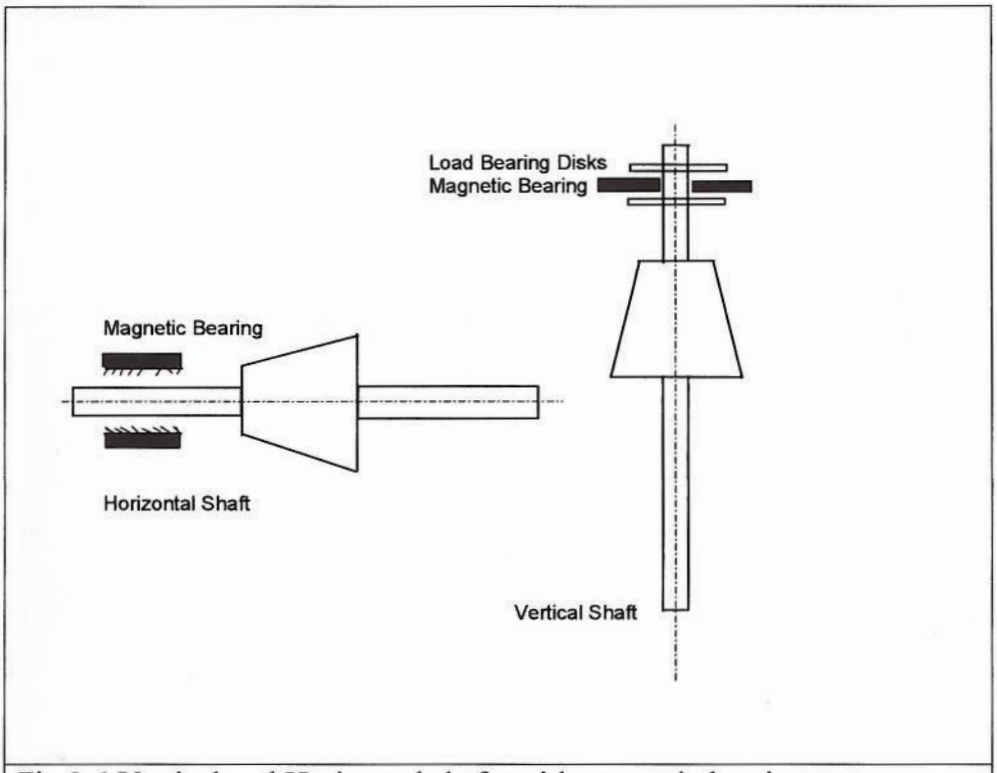

Fig 3.6 Vertical and Horizontal shafts with magnetic bearings

3.2.5 Pressure Ratio Selection

The thermal efficiency and specific power output of a gas turbine are dependent upon a) the compressor pressure ratio b) the maximum and minimum gas temperatures in the cycle c) the compressor and turbine component efficiencies d) effectiveness of the heat exchangers and coolers e) the thermodynamic constants of the gas such as specific heats, gas constants etc. [88]

In the relationship between thermal efficiency, pressure ratio and turbine entry temperature for various gases in the PBMR design, for any pre-selected maximum gas temperature, there is an optimum value for the pressure ratio to give maximum thermal efficiency. This optimum thermal efficiency increases if the TET is increased and so, also, does the optimum pressure ratio. The actual values of the optimum pressure ratios depend upon the type of gas used in the cycle. This way the PBMR pressure ratio has been optimised at 2.77 with helium.

3.2.6 Practical limitations to gas pressure

The absolute magnitude of the maximum gas pressure in a closed cycle gas turbine does not influence significantly the thermal efficiency or the specific power

output (power output kg of mass flow per sec) of the engine. However, higher pressures lead to higher gas densities and smaller plant volume for a given power output, thus providing an incentive to use the highest possible levels of pressure. The upper limit will depend on the maximum practicable thickness and permissible stress levels in easily constructed and reliable casings, ducts, pressure vessels, etc. These may be expected to increase in the course of long-term development. It will also depend very largely upon the required output power, since these will determine approximately the mass of gas to be contained in the circuit. Obviously, a large plant of high output power will necessarily be constrained to operate at very much lower levels of pressure than a smaller plant of lower output power. Indeed it may be anticipated that plant volume will increase with design power output at a rate rather greater than the simple linear proportion normally associated with geometrically similar machines operating at fixed pressure levels [88].

Figure.3.7 Pressure Vessel in which the turbomachineries are enclosed.

The gas pressure in the system determines the thickness of this pressure vessel. PBMR is a modular design and very little site work is catered in the physical design. Hence there is a need to optimise the size and weight of the pressure vessel.

3.3 Power Conversion Unit (PCU) Valves

There are 3 sets of valves will be pivotal in the operation of the PBMR. The bypass valves which bypass the high pressure compressor outlet gas from the reactor, the interrupt valves which cuts-off the gas path and the inventory valves which supply the gas in and out of the system. The Bypass and Inventory valves do have control characteristics meant to be used frequently whereas the interrupt valves are isolation valves, which will be rarely used. The bypass allows for load rejection and fast acting load reduction.

The interrupt valve consists of four 300mm diameter butterfly valves, assembled in parallel in the cold inlet of the recuperator. The interrupt valves will act as the ultimate over speed protection of the power turbine generator and also to stop the reverse flow of decay heat removal system when in service. Therefore the valves will see no significant sustained differential pressures, and are not designed to be fully leak-tight.

3.4 Recuperator.

The recuperator helps to keep the pressure ratio low for the same TET to get the same cycle efficiency. Alternate solution is to provide another low pressure turbine to extract that heat which necessitate high pressure ratio. Since helium needs more stages compared to air for the same pressure ratio, it would be more advantageous to have recuperation than having more stages in the turbine to extract the heat from the downstream [65].

Parameter	Quantity	Unit
Cold Mass flow	139.	Kg/sec
Hot side Mass flow	145	Kg/sec
Cold side inlet temperature	105	^{0}C
Cold side outlet temperature	536	^{0}C
Hot side inlet temperature	554	^{0}C
Hot side outlet temperature	140	^{0}C
Heat Transfer	313	MW
Effectiveness	96	%
Mean Cold flow velocity	2.1	m/sec
Mean Hot flow velocity	2.4	m/sec
Cold side pressure Drop	1.280	Kpa
Hot side pressure Drop	3.500	Kpa

Table 3.4 Recuperator Process Parameters

3.5 Heat Exchangers

There are two heat exchangers other than the recuperator in the system. Both pre-cooler and intercooler use water-cooling system. Both the coolers are positioned at the lowest elevations of the PCU to decrease the likelihood of water ingress into the rest of the system. Water ingress into the main gas circuit is unlikely as the helium pressure is always higher than the water pressure [65]. Pre-cooler and Intercooler process parameters are given in Table 3.5

Parameter	Pre-cooler	Intercooler	Unit
Mass flow	145	146.5	Kg/sec
Gas inlet temperature	140.5	104.4	^{0}C
Gas outlet temperature	27.9	27.6	^{0}C
Water Inlet temperature	22	22	^{0}C
Water outlet temperature	54	44.4	^{0}C
Heat Transfer capacity	85	58	MW
Water Mass flow	628	628	Kg/sec
Gas pressure drop	152	76	Pa
Heat Conduction	8.1	7.2	KW/m^2

Table 3.5 Pre-cooler and Intercooler Process Parameters [65]

3.6 Potential application of the latest technologies

Though it was promising, high temperature helium turbines never had a successful operational history in the past. To a large extent, the reasons were external and institutional than technical. The availability of certain technology of the present day can help the high temperature helium turbines to gain the attention it deserves. Some of these are

a) Magnetic Bearings

The magnetic bearing is provided with the following features

i) No lubricant is needed.
ii) Small energy loss.
iii) The shaft vibration is controllable.
iv) The load capacity does not depend on the rotational speed.

The non-lubricant magnetic bearing can be identified as candidate bearings for closed cycles to avoid ingress of the lubricant to the working fluid. They are better than gas bearings, which poses problems of the cooling method and small deformations of the bearing and the shaft because the gas bearing has a small load capacity and a large loss. The thrust bearing of the magnetic bearing can support a large load because it has a small loss and provides a large support area. In journal bearing, control of the shaft vibration from the low to high modes is available. This is the best bearing system for the

vertical shafting arrangement of an extended shaft length where the thrust bearing supports an overall weight of the rotor.[64]

However the magnetic bearing is supposedly needed to be provided with conventional bearings as the backup bearings at the shaft ends in order to avoid contacts at start-up and a large clearance must be provided to avoid the contact of this bearing with the shaft during the normal operation. Accordingly, it becomes necessary to provide large clearances for turbine and compressor tips, which may affect their performance.

b) Recuperator

In order to be competitive, the thermal efficiency of nuclear power had to be markedly improved to compete with modern high efficiency fossil plants. Recuperators play a vital role in the development of direct helium Brayton cycles with nuclear heat. This demands high heat transfer efficiency and large heat transfer. The new developments in the recuperators are the highly effective plate-fin recuperators, which are much smaller than equivalent tube and shell heat exchangers, provides substantially less complexity and capital cost.

c) Magnetic Sealing System

Magnetic bearings have inherent clearances due to the principle of working. The electromagnets of the magnetic bearing attract the disk on the vertical shaft from both sides and a control system keep it centred by measuring the displacement and controlling the magnetic force because magnetic bearing do have stiffness and damping and will be displaced if forces are impinged on the shaft. Due to the large clearances, a conventional static seal will have large gaps and will have large leakage. The principle of magnetic seal is same as that of the magnetic bearing. The losses in the magnetic seal is minimised by making the seal to follow the shaft with the help of magnetic force and a spring type base for the seal system.

b) Process Automation

The process plant automation has advanced drastically in the last 25 years. An example of this is the manual synchronisation of the electricity generators to the grid. This has been replaced by the automatic system which is much more quick, efficient and reliable. Similarly the PLCs (Programmable Logic Control) used in the process plant now can observe several process parameters same time and it can take online remedial actions at any number of locations to maintain the plant output. The process control hardware also had significant improvement. The remote controlled variable speed electric actuators for the valve operation is an example of this. One of the remarks in the past about closed cycle gas turbine plant was that it was ahead of the time. It may not be true anymore with the level of technology today.

3.7 Performance Targets

The following performance characteristics are given as design goals for the first reference module[65].

Parameter	Target
Maximum sent out power	116 MW
Load following range, without losses	100-40-100%
Continuous Stable Power Range	0 to 100%
Ramp Rate	10MW/min
Step Change	10% of current electrical output
Load Rejection without trip	100%
Plant Life	35 full power years
Net Plant efficiency	43%
General Overhauls	30 days /72 months (excl. shutdown)
Planned outage rate	2%
Forced outage rate	3%
Module availability	95%
Spent Fuel Storage	35 full power years
Emergency Planning radius	400 metres

Table 3.6 Performance Targets

Chapter 4
The Computer Model (GTSI)

This computer model is originally developed by Dr Inaki Ulizar [94]. The programme is used to run the basic aspects of the simulation and was modified to suit Eskom PBMR model. The modifications are elaborated later in this report. This is capable of testing the steady state and transient operations. This model carries the elementary features at present, but more features will be added to it as more detailed design of the project becomes available. The various leakages flows and pressure losses are based on empirical approximations due to the lack of specific information on the physical design. Hence the transient results are of more of a qualitative, in order to find the trend during transient operation. The method of inter component volume (ICV) is used in this model. The ICV method is more realistic, than Constant Mass Flow (CMF) method since it includes allowance for gas mass storage, which is ignored in the Constant Mass Flow (CMF) method [97]. For each time interval in the segmented transient period, the calculation of the thermodynamic parameters of the gas path has been carried out. Once these parameters have been found, the power input and output of each component can be calculated. Then a power balance has been carried for each shaft and thus accelerating torque can be calculated. This accelerating torque is then integrated over the time interval, and the change in shaft speed is obtained. This process is repeated over several time intervals as required [23,74].

The structure of the programme
The code was written in Fortran by Dr Inaki Ulizar and is structured in the following way.

GTSIT -> CMATH01->	
LECT00-> LECT001->	[Conventional maps or LPC, HPC, HPT,
LECT02 ->LECT03	LPT and Power Turbine are read]
THERMO00	
COINL00	[Inlet of the LPC]
COLPCVS2	[LPC with variable stators]
COHEX01	[Intercooler]
COHPCVS2	[HPC with variable stators]
COSMGVS2	[Calculation of the surge margin for LPC & HPC]
COCOHTB00	[HPT cooling bleed extraction]
COREG00	[Cold side of the regenerator]
COMHE00	[Main heat Exchanger, Reactor]
COHPTVS2	[HPT with variable stators]
COHPLPD	[HPT-LPT inter turbine duct]
COLPTVS2	[LPT with variable stators]
COLPFPD	[LPT-FPT inter turbine duct]
COFPTVS2	[FPT with variable stators]
COFPRGD	[FPT-Recuperator Duct]
COREG10	[Recuperator Hot side]
COHEX06	[Pre-cooler]
CONOZ00	[Diffuser/ Nozzle]
CMATH02	[Calculation of the deviations from the targets]

CMATH03	[Jacobian calculation]
OUT	
THERMO01 to THERMO16	[Thermodynamic subroutines that give the properties and solve the compressors and turbines]
CMINT01, CMINT02	[Curve fitting subroutines]

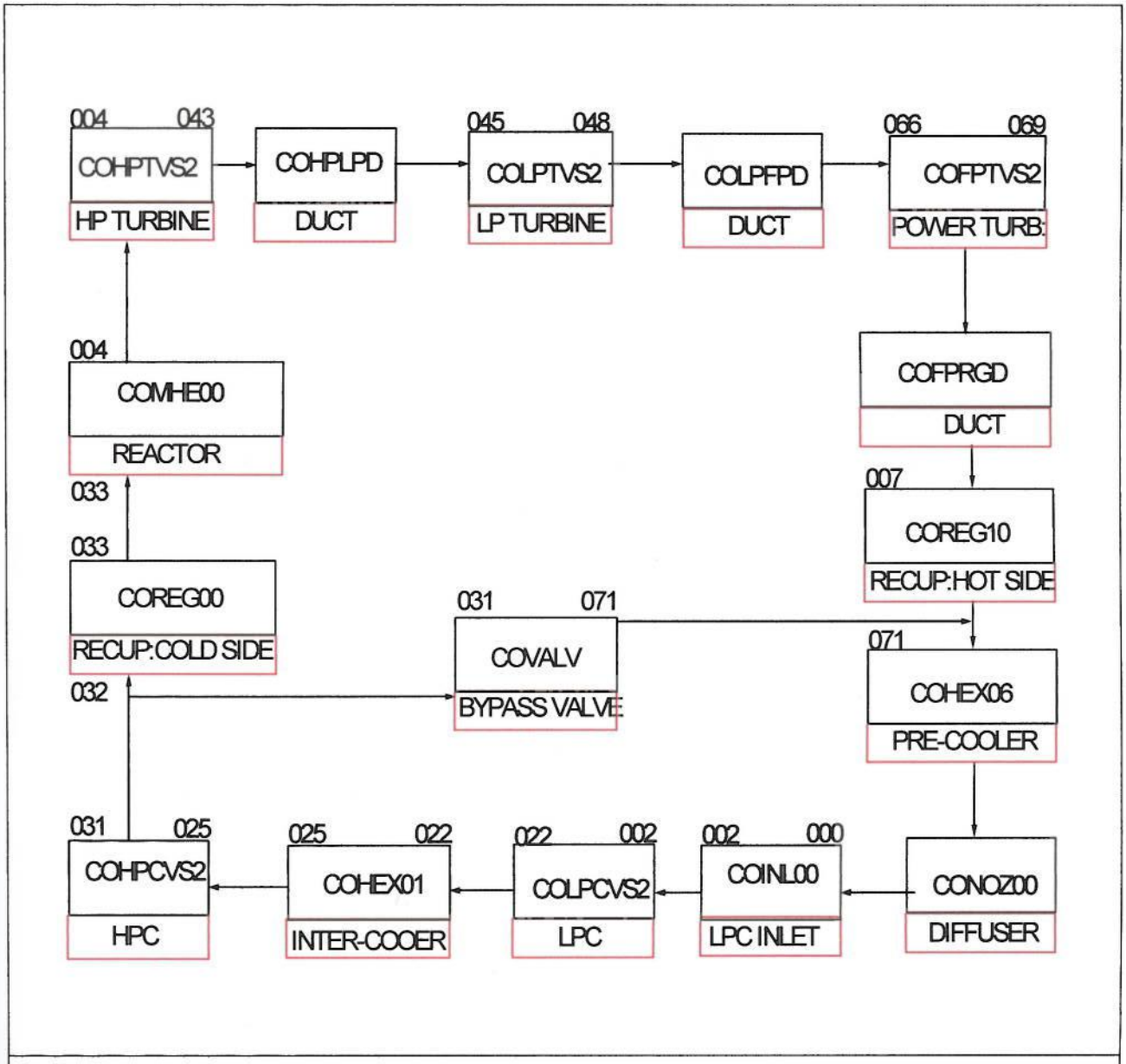

Fig.4.1The structure of the simulation programme

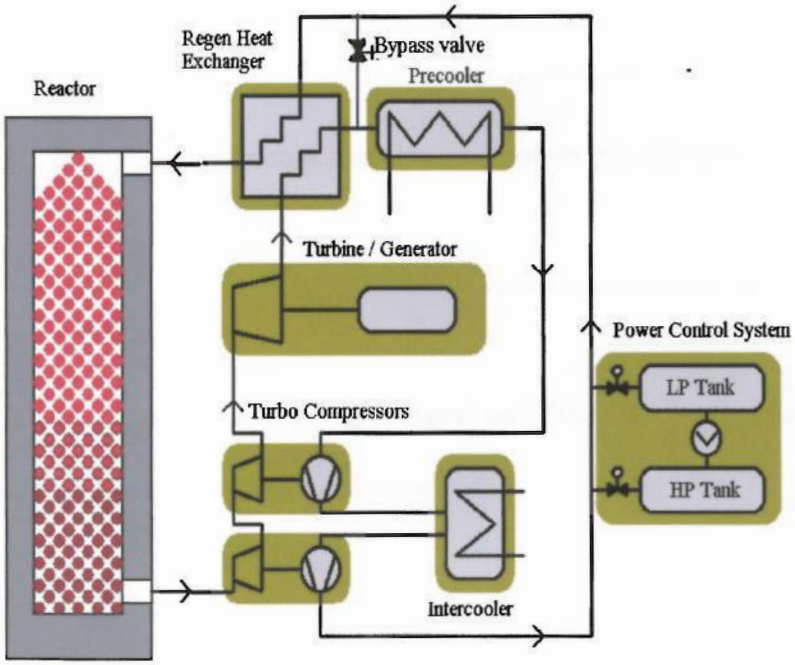

Figure 4.2 Process diagram of PBMR

4.1 Component Simulations

4.1.1. Compressors

Low, intermediate and high pressure compressors are simulated using the same equations, with the only difference being the cooling bleeds, extracted typically from the high pressure compressor.
The four possibilities of giving the input data are

1. Pressure ratio and Isentropic efficiency data.

$$r_{HPC} = \frac{P_3}{P_{25}} \qquad \text{.....4.1}$$

$$\eta_{isHPC} = \eta_{is25-3}$$

2. Pressure ratio and Polytropic efficiency data

$$r_{HPC} = \frac{P_3}{P_{25}} \qquad \text{.....4.2}$$

$$\eta_{polyHPC} = \eta_{poly25-3}$$

3. Increase in corrected enthalpy and isentropic efficiency data.

$$\frac{\Delta H_{HPC}}{(\gamma R\theta)_{HPC}} = \frac{\Delta H_{25-3}}{\gamma_{25} R_{25} \theta_{25}}$$

$$\eta_{isHPC} = \eta_{is25-3} \quad \text{.....4.3}$$

4. Increase in corrected enthalpy and polytropic efficiency data.

$$\frac{\Delta H_{HPC}}{(\gamma R\theta)_{HPC}} = \frac{\Delta H_{25-3}}{\gamma_{25} R_{25} \theta_{25}} \quad \text{.....4.4}$$

$$\eta_{polyHPC} = \eta_{ploy25-3}$$

i.) Compressor delivery Temperature and Pressure from η_{is} *and* Pressure ratio.

The definition of isentropic efficiency is

$$\eta_{25-3} = \frac{\Delta H_{25-3}^{IS}}{\Delta H_{25-3}} = \frac{\int_{T_{25}}^{T_3^{IS}} C_p dT}{\int_{T_{25}}^{T_3} CpdT}$$

$$\int_{T_{25}}^{T_3} CpdT = \frac{1}{\eta_{25-3}} \int_{T_{25}}^{T_3^{IS}} C_p dT \quad \text{.....4.5}$$

If the isentropic exit temperature is determined, the real exit temperature will be found using an alternative procedure.

The Gibbs equation:

$$TdS = dH - \frac{1}{\rho} dP \quad \text{.....4.6}$$

For the compression process from 25 –3

$$\int_{T_{25}}^{T_3} dS = \int_{T_{25}}^{T_3} \frac{1}{T} dH - \int_{P_{25}}^{P_3} \frac{1}{T\rho} dP \quad \text{.....4.7}$$

Expressing dH as a function of T and ρ as a function of P, T and R

$$s_3 - s_{25} = \int_{T_{25}}^{T_3} C_p \frac{dT}{T} - \int_{P_{25}}^{P_3} \frac{R}{P} dP \quad \text{.....4.8}$$

If R is constant the following expression is finally obtained

$$s_3 - s_{25} = \int_{T_{25}}^{T_3} C_p \frac{dT}{T} - R_{25} L_n \frac{P_3}{P_{25}} = (\phi_3 - \varphi_{25}) - R_{25} L_n \frac{P_3}{P_{25}} \quad \text{.....4.8}$$

In the case of an isentropic process the equation will be

$$s_3^{IS} - s_{25} = 0 = \int_{T_{25}}^{T_3^{IS}} C_p \frac{dT}{T} - R_{25} L_n \frac{P_3^{IS}}{P_{25}} = (\phi_3 - \varphi_{25}) - R_{25} L_n \frac{P_3^{IS}}{P_{25}} \quad \text{.....4.9}$$

The final pressure will be the same in the real and isentropic processes

$$\int_{T_{25}}^{T_3^{IS}} C_p \frac{dT}{T} - R_{25} L_n \frac{P_3}{P_{25}} = (\phi_3^{IS} - \varphi_{25}) - R_{25} L_n \frac{P_3}{P_{25}} \quad \text{.....4.10}$$

Using this equation, the compressor isentropic temperature can be easily calculated employing an iterative method. The first value of the isentropic temperature, to start the iterative process, is given by;

$$T_3^{IS} = T_{25} \left(\frac{P_3}{P_{25}} \right)^{\frac{\gamma_{25}-1}{\gamma_{25}}} \quad \text{.....4.11}$$

ii.) Compressor delivery Temperature and Pressure from η_{poly} *and* Pressure ratio.

The definition of polytropic efficiency is

$$\eta_{25-3}^{poly} = \frac{dH^{is}}{dH} \quad \text{.....4.12}$$

Employing the Gibbs equation in its differential form for an isentropic process

$$dH^{is} = \frac{1}{\rho} dP \quad \text{.....4.13}$$

$$\eta_{25-3}^{poly} = \frac{\frac{1}{\rho} dP}{C_p dT} = \frac{R}{C_p} \frac{\frac{dP}{P}}{\frac{dT}{T}} \quad \text{.....4.14}$$

The resultant equation will be

$$\eta_{25-3}^{poly}\int_{T_{25}}^{T_3} C_p\frac{dT}{T}=\int_{P_{25}}^{P_3} R\frac{dP}{P} \quad \text{.....4.15}$$

If the gas constant does not change, the final expression relating the exit temperature with the polytropic efficiency and pressure ratio will be:

$$\eta_{25-3}^{poly}\int_{T_{25}}^{T_3} C_p\frac{dT}{T}=\eta_{25-3}^{poly}(\phi_3-\phi_{25})=R_{25}Ln\frac{P_3}{P_{25}} \quad \text{.....4.16}$$

The exit temperature from this equation will be determined with an iterative procedure.
The first estimation of its value can be done by assuming constant C_p during the compression processes, resulting

$$T_3=T_{25}\left[\frac{P_3}{P_{25}}\right]^{\frac{\gamma_{25}-1}{\eta_{25}^{poly}\gamma_{25}}} \quad \text{.....4.17}$$

iii.) Compressor delivery Temperature and Pressure from η_{is} *and* increase in corrected enthalpy

The equation 4.8 obtained above gives the relation between isentropic temperature and pressure ratio.

From the isentropic efficiency definition the expression below can be determined.

$$\int_{T_{25}}^{T_3^{is}} CpdT=\eta_{25-3}\gamma_{25}R_{25}\theta_{25}\left(\frac{\Delta H_{25-3}}{\gamma_{25}R_{25}\theta_{25}}\right) \quad \text{.....4.18}$$

iv.) Compressor delivery Temperature and Pressure from η_{poly} *and* increase in corrected enthalpy

The equation 4.16 gives a relation between exit temperature, polytropic efficiency and pressure ratio. Hence, if the compressor discharge temperature is found, the pressure ratio can be obtained.
The corrected enthalpy is obtained as

$$\left(\frac{\Delta H_{25-3}}{\gamma_{25}R_{25}\theta_{25}}\right)=\frac{1}{\gamma_{25}R_{25}\theta_{25}}\int_{T_{25}}^{T_3} CpdT \quad \text{.....4.19}$$

where everything but the exit temperature is known. Once T_3 is found, the pressure ratio can be calculated as described above. The four scenarios can happen at

the design stage, while at off design and transient, cases 1 and 3 are the only possibilities. The situation of having polytropic efficiency maps is not considered, as the result of compressor testing is adiabatic efficiency. However, its use would be easy, changing from one efficiency map to the other with the functions already described. [95]

4.1.2 Compressor Work

At Design point, the relative position of the flow extraction points for bleeds for cooling and surge control are given in terms of enthalpy rise ratio.

Enthalpy Rise Ratio for bleed $25i$ is given by

$$\lambda_{25i} = \left(\frac{\Delta H_{25-25i}}{\Delta H_{25-3}} \right) \quad \text{.....4.20}$$

The pressure will be calculated using the polytropic efficiency, assuming that all the compressor rows have the same one. The method described in 4.1.1 (iii) is used and the resulting pressure will be decreased for the total pressure drop close to the walls, where the flow is extracted from, additional pipe losses, restrictors etc. [94]

Once the compressor bleed flows have been calculated the required work can be obtained from the following equation

$$PW_{25} = W_3 \Delta H_{25-3} + \sum_{\forall} W_{25i} \Delta H_{25-25i} = W_3 \Delta H_{25-3} + \sum_{\forall} W_{25i} \lambda_{25i} \Delta H_{25-3} = \Delta H_{25-3} \left(W_3 + \sum_{\forall} W_{25i} \Delta H_{25i} \right)$$

.....4.21

4.1.3 Off Design performance of the Compressor.

In the off design, the compressor maps are used. These are pressure ratio vs corrected mass flow and isentropic efficiency vs. corrected mass flow. The requirement and positioning of variable geometry, the bleed valves to avoid surge, the possibility of moving the operating point to increase the efficiency are available from these maps.

The compressor maps are functions that relate mass flow, rotational speed, pressure ratio or corrected enthalpy and adiabatic (isentropic) efficiency.

$$\left(\frac{\Delta H_{25-3}}{\gamma_{25}R_{25}\theta_{25}}\right) = f\left(\frac{W_{25}\sqrt{\theta_{25}}}{\delta_{25}}\sqrt{\frac{R_{25}}{\gamma_{25}}}, \frac{N_{HPS}}{\sqrt{\gamma_{25}R_{25}\theta_{25}}}\right) \quad \text{.....4.22}$$

$$\frac{P_3}{P_{25}} = f\left(\frac{W_{25}\sqrt{\theta_{25}}}{\delta_{25}}\sqrt{\frac{R_{25}}{\gamma_{25}}}, \frac{N_{HPS}}{\sqrt{\gamma_{25}R_{25}\theta_{25}}}\right) \quad \text{.....4.23}$$

$$\eta_{25-3} = f\left(\frac{W_{25}\sqrt{\theta_{25}}}{\delta_{25}}\sqrt{\frac{R_{25}}{\gamma_{25}}}, \frac{N_{HPS}}{\sqrt{\gamma_{25}R_{25}\theta_{25}}}\right) \quad \text{.....4.24}$$

The gas properties are considered to use the same component with different working fluids or with the same fluid but different thermodynamic conditions. The term $\sqrt{\gamma_{25}R_{25}\theta_{25}}$ is closely related with the sonic velocity at the compressor entry. The use of these functions will be limited when the corrected speed lines are vertical at high speed (close to choke) and horizontal at low speed (close to surge). In the first case there will be several values of pressure, corrected enthalpy or efficiency for the same mass flow rate and in the second case, there will be several mass flow rates for the same pressure ratio, efficiency or corrected enthalpy. These problems are solved by introducing the additional parameter, called β. There is no physical meaning behind it, but allows the user to compute the compressor characteristic easily.

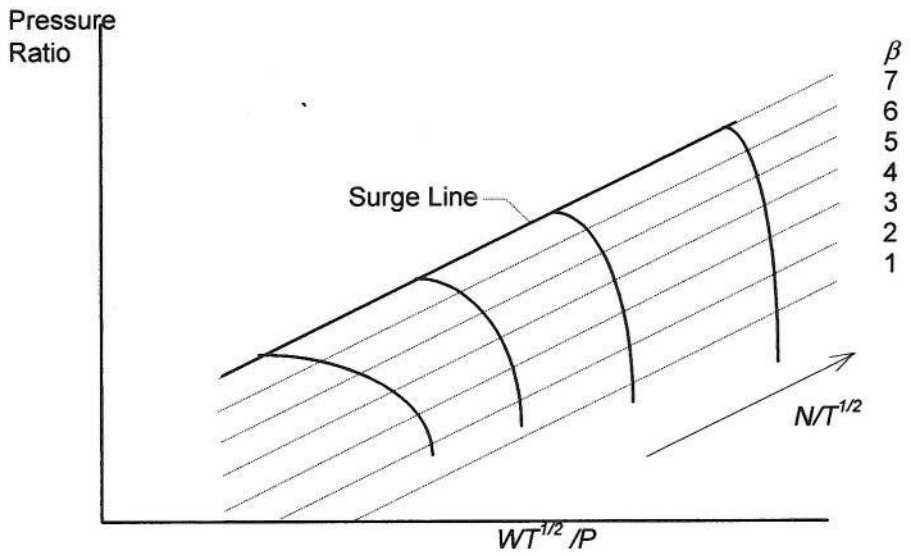

Figure 4.3 The β lines in the compressor map

Here the new functions are as follows,

$$\left(\frac{\Delta H_{25-3}}{\gamma_{25}R_{25}\theta_{25}}\right) = f_1\left(\beta_{HPC}, \frac{N_{HPS}}{\sqrt{\gamma_{25}R_{25}\theta_{25}}}\right) \quad \text{.....4.25}$$

$$\frac{P_3}{P_{25}} = f_2\left(\beta_{HPC}, \frac{N_{HPS}}{\sqrt{\gamma_{25}R_{25}\theta_{25}}}\right) \quad \text{.....4.26}$$

$$\eta_{25-3} = f_3\left(\beta_{HPC}, \frac{N_{HPS}}{\sqrt{\gamma_{25}R_{25}\theta_{25}}}\right) \quad \text{.....4.27}$$

$$\frac{W_{25}\sqrt{\theta_{25}}}{\delta_{25}}\sqrt{\frac{R_{25}}{\gamma_{25}}} = f_4\left(\beta_{HPC}, \frac{N_{HPS}}{\sqrt{\gamma_{25}R_{25}\theta_{25}}}\right) \quad \text{.....4.28}$$

Instead of using the approximated expressions, which neglect the Mach Number term, it is possible to employ the complete equations using the design compressor inlet Mach number.

$$\left(\frac{\Delta H_{25-3}\left(1+\frac{\gamma_{25}-1}{2}M_{25DS}^2\right)}{\gamma_{25}R_{25}\theta_{25}}\right) = f_1\left(\beta_{HPC}, \frac{N_{HPS}\sqrt{\left(1+\frac{\gamma_{25}-1}{2}M_{25DS}^2\right)}}{\sqrt{\gamma_{25}R_{25}\theta_{25}}}\right) \quad \text{.....4.29}$$

$$\frac{P_3}{P_{25}} = f_2\left(\beta_{HPC}, \frac{N_{HPS}\sqrt{\left(1+\frac{\gamma_{25}-1}{2}M_{25DS}^2\right)}}{\sqrt{\gamma_{25}R_{25}\theta_{25}}}\right) \quad \text{.....4.30}$$

$$\eta_{25-3} = f_3\left(\beta_{HPC}, \frac{N_{HPS}\sqrt{\left(1+\frac{\gamma_{25}-1}{2}M_{25DS}^2\right)}}{\sqrt{\gamma_{25}R_{25}\theta_{25}}}\right) \quad \text{.....4.31}$$

$$\frac{W_{25}\sqrt{\theta_{25}}}{\delta_{25}}\sqrt{\frac{R_{25}}{\gamma_{25}}} = f_4\left(\beta_{HPC}, \frac{N_{HPS}\sqrt{\left(1+\frac{\gamma_{25}-1}{2}M_{25DS}^2\right)}}{\sqrt{\gamma_{25}R_{25}\theta_{25}}}\right) \quad \text{.....4.32}$$

4.1.4 Scaling Factors.

Scaling factors are used to adapt an available map to the real compressor because the pressure ratio, efficiency etc may not be the same, although its general behaviour can be very similar

$$\left(\frac{\Delta H_{25-3}}{\gamma_{25}R_{25}\theta_{25}}\right)_{Design} = sf_{H_{HPC}}\left(\frac{\Delta H_{25-3}}{\gamma_{25}R_{25}\theta_{25}}\right)_{Map} \quad \text{.....4.33}$$

$$\left(\frac{P_3}{P_{25}}-1\right)_{Design} = sf_{PR_{HPC}}\left(\frac{P_3}{P_{25}}-1\right)_{Map} \quad \text{.....4.34}$$

$$(\eta_{25-3})_{Design} = sf_{\eta_{HPC}}(\eta_{25-3})_{Map} \quad \text{.....4.35}$$

$$\left(\frac{W_{25}\sqrt{\theta_{25}}}{\delta_{25}}\sqrt{\frac{R_{25}}{\gamma_{25}}}\right)_{Design} = sf_{W_{HPC}}\left(\frac{W_{25}\sqrt{\theta_{25}}}{\delta_{25}}\sqrt{\frac{R_{25}}{\gamma_{25}}}\right)_{Map} \quad \text{.....4.36}$$

The scaling factors are calculated at the deign, and assumed that the value will not change at off-design or transient conditions. If the full expressions are used, including the Mach number terms, the enthalpy and mass flow scaling factors will be,

$$sf_{H_{HPC}} = \frac{\left(\dfrac{\Delta H_{25-3}\left(1+\dfrac{\gamma_{25}-1}{2}M_{25DS}^2\right)}{\gamma_{25}R_{25}\theta_{25}}\right)_{Design}}{\left(\dfrac{\Delta H_{25-3}\left(1+\dfrac{\gamma_{25}-1}{2}M_{25DS}^2\right)}{\gamma_{25}R_{25}\theta_{25}}\right)_{Map}} \quad \text{.....4.37}$$

$$sf_{W_{HPC}} = \frac{\left(\frac{W_{25}\sqrt{\theta_{25}}}{\delta_{25}} \sqrt{\frac{R_{25}}{\gamma_{25}}} \left(1 + \frac{\gamma_{25}-1}{2} M_{25DS}^2 \right)^{\frac{\gamma_{25}+1}{2(\gamma_{25}-1)}} \right)_{Design}}{\left(\frac{W_{25}\sqrt{\theta_{25}}}{\delta_{25}} \sqrt{\frac{R_{25}}{\gamma_{25}}} \left(1 + \frac{\gamma_{25}-1}{2} M_{25DS}^2 \right)^{\frac{\gamma_{25}+1}{2(\gamma_{25}-1)}} \right)_{Map}} \quad \text{.....4.38}$$

4.1.5 Variable Geometry in the Compressor.

There are two approaches to consider the variable stators in the performance simulation.

- The variables as a function of the stator angle, having performance maps for several angles.

Or

- A single parametric curve, which is a function of the stator angle, to be used in a 'look-up form' for each performance variable.

The second approach was employed in the code by the developer, while the first one can be easily implemented

4.1.6 Reynolds Number Correction

Compressor maps are given for a certain Reynolds number and changes in its value can widely modify the performance. Instead of using the absolute Reynolds number, a Reynolds Number Index (RNI) is frequently employed, which can be expressed, using thermodynamic properties at compressor inlet face as [95, 94]

$$RNI = \frac{\mathrm{Re}}{\mathrm{Re}_{ref}} = \frac{\rho V L}{(\rho V L)_{ref}} \frac{\mu_{ref}}{\mu} \quad \text{.....4.39}$$

For the same compressor the characteristic length can be cancelled. Therefore the expression will be

$$RNI = \frac{pM\sqrt{\frac{\gamma}{Rt}}}{p_{ref} M_{ref} \sqrt{\left(\frac{\gamma}{Rt}\right)_{ref}}} \frac{\mu_{ref}}{\mu} \quad \text{.....4.40}$$

In some cases the static pressure and temperature are not available and the total magnitude should be employed. A more simple approach is done using the mass flow definition

$$RNI = \frac{\rho VA}{(\rho VA)_{ref}} \frac{A_{ref}}{A} \frac{L}{L_{ref}} \frac{\mu_{ref}}{\mu} = \frac{W}{W_{ref}} \frac{A_{ref}}{A} \frac{L}{L_{ref}} \frac{\mu_{ref}}{\mu} \quad \text{.....4.41}$$

where the only unknown will be the dynamic viscosity. When the correction is applied to the same hardware the geometric parameters disappear

$$RNI = \frac{W}{W_{ref}} \frac{\mu_{ref}}{\mu} \quad \text{.....4.42}$$

The whole map, including the surge line, is modified with the Reynolds effect. However all these are considering the properties at the compressor inlet face, with no rotating effect. For rotating turbomachinery, the Reynolds correction should include an additional term

$$\mathrm{Re}_{correction} = f\left(\frac{pM\sqrt{\frac{\gamma}{Rt}}}{p_{ref} M_{ref} \sqrt{\left(\frac{\gamma}{Rt}\right)_{ref}}} \frac{L}{L_{ref}} \frac{\mu_{ref}}{\mu} \Bigg|_{\substack{Compressor \\ Inlet}} , \frac{N\sqrt{(\gamma Rt)_{ref}}}{N_{ref}\sqrt{\gamma Rt}} \frac{D}{D_{ref}} \right) \quad \text{.....4.43}$$

4.1.7 Compressor Transient Operation

For a simplified transient simulation, the compressor effects such as heat storage, blade tip clearance changes, surge, distortion internal gas variations etc can be introduced as time dependant scaling factors.

4.1.8 Intercooler

The intercooler increases the specific power output by decreasing the temperature between the compressors. No mass or working fluid composition variation takes place, only the total pressure and temperature change. Assuming that the inlet conditions are known from the compressor discharge and the flow has no swirl component, the equations describing this system are equivalent to

$$H_2 = h_2 + \frac{1}{2}V_2^2 = h_2 + \frac{1}{2}\gamma_2 R_2 t_2 M_2^2 \quad \text{.....4.44}$$

$$W_2 = \rho_2 V_2 A_2 = \frac{p_2}{R_2 t_2}\sqrt{\gamma_2 R_2 t_2} M_2 A_2 \quad \text{.....4.45}$$

In this H_{out}, T_{out} or *Power extracted* is known. The design equations are valid for off design, the only unknown being the total pressure losses. The exit temperature will be obtained from the energy equation and will constitute the control of the machine.

4.1.9 Recuperator

The parameter, which describes the performance of the recuperator, is the effectiveness.

$$\eta_{\mathrm{Rec}} = \frac{T_{Exit}^{Cold} - T_{Inlet}^{Cold}}{T_{Inlet}^{Hot} - T_{Exit}^{Hot}} \quad \text{.....4.48}$$

The equations of mass, momentum and energy conservation are

$$\begin{aligned} W_{out}^{Cold} &= W_{in}^{Cold} + W_{Leakage}^{Cold} \\ W_{out}^{Hot} &= W_{in}^{Hot} + W_{Leakage}^{Hot} \end{aligned} \quad \text{.....4.49}$$

$$W_{out}^{cold} H_{out}^{cold} - W_{in}^{cold} H_{in}^{cold} + WQ_{Losses} = W_{in}^{hot} H_{in}^{hot} - W_{out}^{hot} H_{out}^{hot} \quad \text{.....4.50}$$

$$P_{out}^{cold} = P_{in}^{cold} \left(1 - K_{in}^{cold} \left(\frac{W_{in}^{cold} \sqrt{T_{in}^{cold}}}{A_{in}^{cold} P_{in}^{cold}} \right)^2 \right) \quad \text{.....4.51}$$

$$P_{out}^{hot} = P_{in}^{hot} \left(1 - K_{in}^{hot} \left(\frac{W_{in}^{hot} \sqrt{T_{in}^{hot}}}{A_{in}^{hot} P_{in}^{hot}} \right)^2 \right) \quad \text{.....4.52}$$

$$H_{out}^{cold} = h_{out}^{cold} + \frac{1}{2} V_{out}^2 = h_{out}^{cold} + \frac{1}{2} \gamma_{out}^{cold} R_{out}^{cold} t_{out}^{cold} M_{out}^2 \quad \text{.....4.53}$$

$$H_{out}^{hot} = h_{out}^{hot} + \frac{1}{2} V_{out}^2 = h_{out}^{hot} + \frac{1}{2} \gamma_{out}^{hot} R_{out}^{hot} t_{out}^{hot} M_{out}^2 \quad \text{.....4.54}$$

$$0 = \left(\Phi_{T_{out}}^{cold} - \Phi_{t_{out}}^{cold} \right) - R_{out}^{cold} \ln \frac{P_{out}^{cold}}{p_{out}^{cold}} \quad \text{.....4.55}$$

$$0 = \left(\Phi_{T_{out}}^{hot} - \Phi_{t_{out}}^{hot} \right) - R_{out}^{hot} \ln \frac{P_{out}^{hot}}{p_{out}^{hot}} \quad \text{.....4.56}$$

$$W_{out}^{cold} = \rho_{out}^{cold} V_{out}^{cold} A_{out}^{cold} = \frac{p_{out}^{cold}}{R_{out}^{cold} t_{out}^{cold}} \sqrt{\gamma_{out}^{cold} R_{out}^{cold} t_{out}^{cold}} M_{out}^{cold} A_{out}^{cold} \quad \text{.....4.57}$$

$$W_{out}^{hot} = \rho_{out}^{hot} V_{out}^{hot} A_{out}^{hot} = \frac{p_{out}^{hot}}{R_{out}^{hot} t_{out}^{hot}} \sqrt{\gamma_{out}^{hot} R_{out}^{hot} t_{out}^{hot}} M_{out}^{hot} A_{out}^{hot} \quad \text{.....4.58}$$

If the Mach number is too low, a simplified system could be employed. Also if the area is not given, only the total magnitudes will be calculated [95].

4.1.10 Reactor

The conventional combustor is replaced with a heat exchanger in Dr. Inaki's code. This heat exchanger has been replaced with an elaborate but one dimensional model of the reactor from PBMR project.

A pebble bed reactor core can be represented either by the internal one-dimensional model or by coupling the code with other commercial programmes, which allows two- or three-dimensional core models. The modelling in all of the reactor models is essentially the same with the only differences being in the way in which the coolant gas temperatures are calculated.

All of the core models require a prescription of the thermal power distribution within the core. At the moment the core power distribution is specified through the core power map file. The core power map only specifies the shape of the power distribution based on geometry. The total thermal power output of the core is either specified by the user in a steady state calculation or is determined by model in a transient [65]. The total thermal power output is used to scale the core power map so that the power density at the centre of each computational cell of the core is obtained.

If the local scaled power density at a given location, j, in the core is $\dot{q}_C'''\left(z_j, r_j, \theta_j\right)$, the heat input into the computational cell, of volume vol_j centered on that location is;

$$\dot{q}_{Cj} = Vol_j \dot{q}_C'''\left(z_j, r_j, \theta_j\right) \qquad \text{.....4.59}$$

The number of fuel spheres in the computational cell is;

$$N_{Sj} = \frac{Vol_j\left(1-\varepsilon\right)}{Vol_S} \qquad \text{.....4.60}$$

where ε is the average void fraction of the pebble bed and vol_S is the volume of one sphere.

The average power generated by a sphere in the computational cell is;

$$\dot{q}_{Sj} = \dot{q}_{Cj} / N_{Sj} \qquad \text{.....4.61}$$

If the average number of particles in a fuel sphere is N_P and it is assumed that all particles in a sphere generate the same power, then the power generated by a fuel particle is;

$$\dot{q}_f = \dot{q}_{Sj} / N_P \qquad \text{.....4.62}$$

The energy equation is solved for one representative fuel sphere in each computational cell. This solution yields the average sphere surface temperature within a computational cell. The coolant velocity within the computational cell is used to determine a convective heat transfer coefficient. This heat transfer coefficient together

with the number of spheres in the cell and the mean surface-to-gas temperature difference are used to determine the heat transferred to the coolant flowing through the cell.

Assuming that, within a fuel sphere, the only significant temperature gradients occur in the radial direction allows the heat transfer to be modelled by a one-dimensional transient conduction equation with a distributed heat source. A fuel particle has a thermal inertia but it is considered to be too small for significant radial temperature gradient. A zero-dimensional transient conduction model is therefore used for the particles. The resulting differential energy equations for the graphite matrix and fuel particles respectively are;[65]

Graphite;

$$\rho_g c_{Vg} \frac{\partial T_g}{\partial t} = r \frac{\partial}{\partial r}\left(r k_g \frac{\partial T_g}{\partial r} \right) + n_f h_{fc} A_f \left(T_f - T_g \right) \qquad \text{.....4.63}$$

Fuel particle;

$$\rho_f Vol_f c_{Vf} \frac{dT_f}{dt} = \dot{q}_f + h_{fc} A_f \left(T_g - T_f \right) \text{.....4.64}$$

where;

T_g, T_f	graphite and fuel particle temperatures respectively (K)
r	radial distance from the centre of a sphere (m)
n_f	number density of fuel particles within graphite (m^{-3})
h_{fc}	effective fuel particle/graphite heat transfer coefficient ($W/m^2/K$)
A_f	effective surface area of a fuel particle (m^2)
ρ_g, ρ_f	densities of graphite and fuel particle respectively (kg/m^3)
k_g	thermal conductivity of graphite (W/m/K)
c_{Vg}, c_{Vf}	specific heat capacities of graphite and fuel particle (J/kg/K)
Vol_f	volume of a fuel particle (m^3)
Vol_s	volume of a sphere (m^3)

A finite difference scheme is used to solve this pair of equations. The fuel sphere is divided into a number of layers (currently 6) each with the same radial thickness. Each layer contains the number of fuel particles, which is proportional to the volume of the layer - except for the outer layer, which is designed to not contain any fuel particles. The temperature of one particle is evaluated in a given layer and this is taken as being representative of all of the particles in the layer. The discretised energy equation for layer i in the graphite matrix is;

$$\rho_{gi} Vol_{gi} c_{Vgi} \frac{T_{gi}^{\,t+\Delta t} - T_{gi}^{\,t}}{\Delta t} = \frac{4\pi r_{i-1}^2 k_{gni}}{\Delta r}\left(T_{gi-1}^{t+\Delta t} - T_{gi}^{t+\Delta t} \right) + \frac{4\pi r_{i+1}^2 k_{gsi}}{\Delta r}\left(T_{gi+1}^{t+\Delta t} - T_{gi}^{t+\Delta t} \right) + Vol_{gi} n_f h_{fci} A_f \left(T_{fi}^{t+\Delta t} - T_{gi}^{t+\Delta t} \right)$$

.....4.65

This equation is re-arranged to give the resulting matrix a structure,

$$A_i T_{gi-1}^{t+\Delta t} + B_i T_{gi}^{t+\Delta t} + C_i T_{gi+1}^{t+\Delta t} = D_i \quad \text{.....4.66}$$

The discretised energy equation for the a fuel particle is;

$$\rho_f Vol_f c_{Vfi} \frac{T_{fi}^{t+\Delta t} - T_{fi}^{t}}{\Delta t} = \dot{q}_f + h_{fci} A_f \left(T_{gi}^{t} - T_{fi}^{t+\Delta t} \right) \quad \text{.....4.67}$$

The 'old' graphite layer temperature in the particle/graphite heat transfer term was chosen to allow an explicit coupling between the two equations. The boundary condition on the surface of the sphere differs depending on whether the solution forms part of the one-dimensional reactor model or whether it part of multi-dimensional model. In the one dimensional model, the coolant gas temperature is used in conjunction with a continuity of heat flux condition that requires all of the heat leaving a sphere to enter the coolant. In the multi-dimensional models, only fraction the heat leaving a sphere enters the coolant, with the remainder being transferred to the neighbouring spheres.

The fuel particle and graphite temperatures are first averaged over each layer and subsequently averaged over the whole pebble bed. This double averaging gives the mean fuel particle temperature and the mean moderator temperature for whole reactor. These values are passed back to the point kinetics model to enable the total thermal power on the next time step to be calculated.

The convective heat transfer coefficient between surface of the sphere and the coolant is obtained as;[65]

$$h = \frac{k}{d}\left(1.27 \frac{\mathrm{Pr}^{0.33}}{\varepsilon^{1.18}} \mathrm{Re}^{0.36} + 0.033 \frac{\mathrm{Pr}^{0.5}}{\varepsilon^{1.07}} \mathrm{Re}^{0.86} \right) \quad \text{.....4.68}$$

where

Re	Reynolds number based upon the sphere diameter and the local superficial fluid velocity
Pr	Prandtl number
k	thermal conductivity of the coolant (W/m/K)
d	sphere diameter (m)

The pressure drop incurred by the flow on passage through a computational cell, of length Δx, within the pebble bed is given by [65];

$$\Delta p = \psi \frac{1-\varepsilon}{\varepsilon^3} \frac{\Delta x}{d} \frac{\rho v_S^{\,2}}{2} \quad \text{.....4.69}$$

where;

$$\psi = \frac{320}{\left(\frac{\mathrm{Re}}{1-\varepsilon}\right)} + \frac{6}{\left(\frac{\mathrm{Re}}{1-\varepsilon}\right)^{0.1}} \quad \text{.....4.70}$$

and

v_S	superficial velocity (local velocity multiplied by the void fraction) (m/s)
ρ	coolant density (kg/m^3)
Δx	length of a computational cell (m)
ε	average void fraction

4.1.11 Turbine

i) Turbine delivery temperature and pressure from isentropic efficiency and pressure ratio.

From the adiabatic efficiency equation,

$$\int_{T_{41}}^{T_{42}} C_p dT = \frac{1}{\eta_{41-42}} \int_{T_{41}}^{T_{42}^{IS}} C_p dT \quad \text{.....4.71}$$

The isentropic exit temperature will be obtained using the Gibbs equation

$$0 = \int_{T_{41}}^{T_{42}^{IS}} C_p dT - R_{41} Ln \frac{P_{42}}{P_{41}} = (\Phi_{42}^{IS} - \Phi_{41}) - R_{41} ln \frac{P_{42}}{P_{41}} \quad \text{.....4.72}$$

The isentropic and actual exit temperatures will be determined using iteration. The first value of the isentropic temperature will be obtained with the conventional relation between pressure and temperature as shown for the compressor simulation.

ii) Turbine delivery temperature and pressure from polytropic efficiency and pressure ratio.

The definition of the poytropic efficiency for a turbine will be

$$\eta_{41-42}^{POLY} = \frac{dH}{dH_{IS}} \quad \text{.....4.73}$$

Using Gibbs equation and the definition of polytropic efficiency is

$$\frac{1}{\eta_{41-42}^{POLY}} \int_{T_{41}}^{T_{42}} C_P \frac{dT}{T} = \frac{1}{\eta_{41-42}^{POLY}} (\Phi_{42} - \Phi_{41}) = R_{41} Ln \frac{P_{42}}{P_{41}} \quad \text{.....4.74}$$

The exit temperature will be determined by iteration. The first estimation of its value is done by assuming constant C_p during expansion process,

$$T_{42} = T_{41}\left(\frac{P_{42}}{P_{41}}\right)^{\frac{\eta_{41}^{poly}(\gamma_{41}-1)}{\gamma_{41}}} \quad \text{.....4.75}$$

iii) Turbine delivery temperature and pressure from isentropic efficiency and reduction in corrected enthalpy.

Equation 4.72 obtained in 4.1.11 gives the relation between isentropic temperature and pressure ratio. The pressure ratio can be obtained if the isentropic temperature is known. Using the Isentropic efficiency definition,

$$\int_{T_{41}}^{T_{42}^{IS}} C_p dT = \eta_{41-42}\gamma 41 R_{41}\theta_{41}\left(\frac{\Delta H_{41-42}}{\gamma_{41}R_{41}\theta_{41}}\right) \text{.....4.76}$$

iv) Turbine Delivery Temperature and Pressure from Polytropic efficiency and reduction in corrected Enthalpy.

$$\left(\frac{\Delta H_{41-42}}{\gamma_{41}R_{41}\theta_{41}}\right) = \frac{1}{\gamma_{41}R_{41}\theta_{41}}\int_{T_{41}}^{T_{42}} CpdT \text{.....4.77}$$

The unknown in the equation, T_{42} can be found using iteration.

v) Exit of the Turbine.

This is introduced with a last cooling flow, which takes into account the rotor cooling flow and others do not contribute to the turbine work.

The mass flow and energy describe the flow evolution between the exit of the rotor and exit of the turbine, with no pressure loss being considered

$$W_{43} = W_{42} + W_3^{Bleed} \text{.....4.78}$$

$$P_{43} = P_{42} \text{.....4.79}$$

$$H_{43} = \frac{\left(W_{42}H_{42} + W_3^{Bleed}H_3^{Bleed}\right)}{W_{42} + W_3^{Bleed}} \text{.....4.80}$$

$$x_{i43} = \frac{\left(W_{42}x_{i42} + W_3^{Bleed}x_{i3}^{Bleed}\right)}{W_{42} + W_3^{Bleed}} \text{.....4.81}$$

vi) Turbine off - design behaviour.

As in the case of the compressor, the turbine characteristics can be corrected using the mass flow, enthalpy drop or pressure ratio, shaft speed and efficiency.

$$\left(\frac{W_{405}\sqrt{\theta_{405}}}{A_{405}\delta_{405}}\sqrt{\frac{R_{405}}{\gamma_{405}}}\right)=f\left(\frac{\Delta H_{41-42}}{\gamma_{405}R_{405}\theta_{405}},\frac{N_{HPS}}{\sqrt{\gamma_{405}R_{405}\theta_{405}}}\right) \quad \text{.....4.82}$$

$$\eta_{41}=f\left(\frac{\Delta H_{41-42}}{\gamma_{41}R_{41}\theta_{41}},\frac{N_{HPS}}{\sqrt{\gamma_{41}R_{41}\theta_{41}}}\right) \quad \text{.....4.83}$$

$$\left(\frac{W_{405}\sqrt{\theta_{405}}}{A_{405}\delta_{405}}\sqrt{\frac{R_{405}}{\gamma_{405}}}\right)=f\left(\frac{P_{41}}{P_{42}},\frac{N_{HPS}}{\sqrt{\gamma_{405}R_{405}\theta_{405}}}\right) \quad \text{.....4.84}$$

$$\eta_{41}=f\left(\frac{P_{41}}{P_{42}},\frac{N_{HPS}}{\sqrt{\gamma_{405}R_{405}\theta_{405}}}\right) \quad \text{.....4.85}$$

When the Mach number is included,

$$\frac{W_{405}\sqrt{\theta_{405}}}{A_{405}\delta_{405}}\sqrt{\frac{R_{405}}{\gamma_{405}}}\left(1+\frac{\gamma_{405}-1}{2}M^2_{405_{Ds}}\right)^{\frac{\gamma_{405}+1}{2(\gamma_{405}-1)}}=f_1\left(\frac{\Delta H_{41-42}\left(1+\frac{\gamma_{405}-1}{2}M^2_{405_{DS}}\right)}{\gamma_{405}R_{405}\theta_{405}},\frac{N_{HPS}\sqrt{1+\frac{\gamma_{405}-1}{2}M^2_{405_{DS}}}}{\gamma_{405}R_{405}\theta_{405}}\right)$$

.....4.86

$$\eta_{41-42}=f_2\left(\frac{\Delta H_{41-42}\left(1+\frac{\gamma_{405}-1}{2}M^2_{405_{DS}}\right)}{\gamma_{405}R_{405}\theta_{405}},\frac{N_{HPS}\sqrt{1+\frac{\gamma_{405}-1}{2}M^2_{405_{DS}}}}{\gamma_{405}R_{405}\theta_{405}}\right) \quad \text{.....4.87}$$

Generic Turbine maps can also be scaled to simulate particular cases

$$\left(\frac{\Delta H_{41-42}}{\gamma_{405}R_{405}\theta_{405}}\right)_{DESIGN}=sf_{\Delta H_{HPT}}\left(\frac{\Delta H_{41-42}}{\gamma_{405}R_{405}\theta_{405}}\right)_{MAP} \quad \text{.....4.88}$$

$$\left(\frac{P_{41}}{P_{42}}-1\right)_{DESIGN}=sf_{PR_{HPT}}\left(\frac{P_{41}}{P_{42}}-1\right)_{MAP} \quad \text{.....4.89}$$

$$(\eta_{41-42})_{DESIGN}=sf_{\eta_{HPT}}(\eta_{41-42})_{MAP} \quad \text{.....4.90}$$

$$\left(\frac{W_{405}\sqrt{\theta_{405}}}{\delta_{405}}\sqrt{\frac{R_{405}}{\gamma_{405}}}\right)_{DESIGN}=sf_{W_{HPT}}\left(\frac{W_{405}\sqrt{\theta_{405}}}{\delta_{405}}\sqrt{\frac{R_{405}}{\gamma_{405}}}\right)_{MAP} \quad \text{.....4.91}$$

If a more accurate definition of the non-dimensional parameters were employed, the enthalpy and mass flow scaling factors would be

$$sf_{\Delta H_{HPT}}=\frac{\left(\dfrac{\Delta H_{41-42}\left(1+\dfrac{\gamma_{405}-1}{2}M^2_{405_{DS}}\right)}{\gamma_{405}R_{405}\theta_{405}}\right)_{DESIGN}}{\left(\dfrac{\Delta H_{41-42}\left(1+\dfrac{\gamma_{405}-1}{2}M^2_{405_{DS}}\right)}{\gamma_{405}R_{405}\theta_{405}}\right)_{MAP}} \quad \text{.....4.92}$$

$$sf_{W_{HPT}}=\frac{\left(\dfrac{W_{405}\sqrt{\theta_{405}}}{A_{405}\delta_{405}}\sqrt{\dfrac{R_{405}}{\gamma_{405}}}\left(1+\dfrac{\gamma_{405}-1}{2}M^2_{405_{Ds}}\right)^{\frac{\gamma_{405}+1}{2(\gamma_{405}-1)}}\right)_{DESIGN}}{\left(\dfrac{W_{405}\sqrt{\theta_{405}}}{A_{405}\delta_{405}}\sqrt{\dfrac{R_{405}}{\gamma_{405}}}\left(1+\dfrac{\gamma_{405}-1}{2}M^2_{405_{Ds}}\right)^{\frac{\gamma_{405}+1}{2(\gamma_{405}-1)}}\right)_{MAP}} \quad \text{.....4.93}$$

4.1.12 Multi-Stage Turbine

The turbine is characterised by two maps for all the performance purposes. When the turbine has more than one stage and the mass flow through the turbine changes, due to the cooling and sealing flows, the links between the power supplied, the efficiency and

the exit temperature may not be clear. The typical way to solve the problem is to have the following [94]

a) An efficiency map, which does not correspond with the aerodynamic efficiency, but produces the exit temperature (enthalpy) for a given speed.
b) A corrected mass flow map which produces the work for the enthalpy drop and speed

The target is to find an inlet mass flow and enthalpy that give the exit temperature and power with an efficiency that has some aerodynamic meaning, having information of the first NGV corrected mass flow.

4.1.13 Reynolds Number Correction

The generic equation derived for the compressors is applied here as well.

For open cycles, using assumptions similar to the ones made for the compressor, the expression of the Reynolds number correction will be

$$\mathrm{Re}_{correction} = f\left(\frac{p}{p_{ref}} \left(\frac{t_{ref}}{t} \right)^{1.15}, \frac{N\sqrt{T_{ref}}}{N_{ref}\sqrt{T}} \right) \quad \text{.....4.94}$$

The full expression, which includes gas properties and scale corrections is

$$\mathrm{Re}_{correction} = f\left(\frac{pM\sqrt{\frac{\gamma}{Rt}}}{p_{ref}M_{ref}\sqrt{\left(\frac{\gamma}{Rt}\right)_{ref}}} \frac{L}{L_{ref}} \frac{\mu_{ref}}{\mu}\Bigg|_{\substack{Turbine \\ Inlet}}, \frac{N\sqrt{(\gamma Rt)_{ref}}}{N_{ref}\sqrt{\gamma Rt}} \frac{D}{D_{ref}} \right) \text{.....4.95}$$

4.1.14 Exhaust Diffuser

In industrial gas turbine engines, the exhaust kinetic energy should be minimised to improve the performance. The compromise between final area (or Mach Number) and Diffuser length. Long diffuser can give a low exit Mach number but the frictional loss will be high whereas the short diffuser will have low friction loss but the exit Mach number can be high. The equation that solve the exhaust diffuser are the following

$$W_8 = W_{72}$$

$$T_8 = T_{72}$$

$$H_8 = H_{72}$$

$$P_8 = P_{72}\left(1 - \frac{\Delta P_{Friction}}{P_{72}} - \frac{\Delta P_{Swirl}}{P_{72}}\right) = P_{72}\left(1 - K'_{72}\left(\frac{W_{72}\sqrt{T_{72}}}{A_{72}P_{72}}\right) - \frac{\Delta P_{Swirl}}{P_{72}}\right) \text{.....4.96}$$

$$\frac{\Delta P_{Swirl}}{P_{72}} = f\left(M_{72}, \varphi_{72}\right) \text{.....4.97}$$

$$\frac{\Delta P_{Swirl}}{P_{72}} = f\left(M_8, \varphi_8\right) \text{.....4.98}$$

$$H_8 = h_8 + \frac{1}{2}v_8^2 = h_8 + \frac{1}{2}\gamma_8 R_8 t_8 M_8^2 \text{.....4.99}$$

$$\Delta S_8 = 0 = \left(\Phi_{T_8} - \varphi_{t_8}\right) - R_8 \ln\frac{P_8}{p_8} \text{.....4.100}$$

$$W_8 = \rho_8 V_{8ax} A_8 = \frac{p_8}{R_8 t_8}\sqrt{\gamma_8 R_8 t_8} M_{8ax} A_8 \text{.....4.101}$$

These expressions together with the thermodynamic model is used to solve the exhaust system.

4.1.15 Orifices and valves

The PBMR will be heavily relying on the Bypass and Inventory control system to modulate the power. Hence these features are added to the GTSI programme (subroutine COVALV). Some hypothetical valves were created for the simulation of start-up and shutdown.

The valve can be modelled as a flow restriction devices. Some of the flow restriction devices are orifices, bursting discs, control valves, non-return valves and pressure relief valves. All of these devices use the same equation to determine the mass flow rate through the device as a function of the upstream and downstream pressures;

$$\dot{m}_C = C_D A \sqrt{\frac{2\gamma}{(\gamma-1)}\rho_{01}P_{01}\left[\left(\frac{p_2}{P_{01}}\right)^{2/\gamma} - \left(\frac{p_2}{P_{01}}\right)^{(\gamma+1)/\gamma}\right]} \text{.....4.102}$$

where;

P_{01}	upstream total pressure (Pa)
p_2	downstream static pressure (Pa)
ρ_{01}	upstream total density (kg/m^3)
C_D	discharge coefficient
A	flow area (m^2)

The differences between the modelling of the different devices lie in the way in which the discharge coefficient C_D is obtained and what value is assumed for the flow area A.

For an orifice the discharge coefficient can either be specified as a single value, two values, or as a tabular function of Reynolds number. If a single value is specified, it is assumed that the discharge coefficient does not vary with the Reynolds number and the same value applies regardless of the flow direction. If two values are specified the second value is applied when the flow reverses through the orifice. Either combined discharge coefficients for both flow directions or for each direction individually can be given as functions of Reynolds number, where the Reynolds number is based upon the hydraulic diameter and velocity in the pipe upstream of the orifice. The upstream side is taken as the actual upstream side, which is dictated by the instantaneous flow direction. The flow area used in the above equation is taken as being the orifice area.

A bursting disc is treated as a closed valve before failure and as an orifice after failure. The static pressure differential at which the disc fails is set by the user. After failure the treatment is identical to that for an orifice with the same options available for the specification of the discharge coefficients.

Valves are modelled using the same equation, but with the discharge coefficient varying with valve position and, optionally, with Reynolds number for control valves. The flow area is taken as being the passage area on the upstream side of the valve, with the upstream side being defined strictly by the flow direction and not by the orientation of the valve.

For a control valve, the discharge coefficients are obtained from a tabular function, which, as a minimum, prescribes the discharge coefficients as a function of position. Optionally, a two-dimensional function can be specified in which the Reynolds number of the approach flow is also taken into account. To simplify the specification of the discharge coefficients it is assumed that the discharge coefficients are independent of the flow direction.

The modelling for non-return valves and pressure relief valves is similar. In both cases, the valve is assumed to be closed until a prescribed threshold pressure differential is exceeded. In addition to the opening pressure, the user also prescribes the static pressure differential at which the valve is fully open and the corresponding discharge coefficient. For pressure differentials, which lie between the threshold and the fully open values, the discharge coefficient is linearly interpolated between zero and the fully open value. A non-return valve is assumed to close when the pressure differential falls below the opening threshold value. A pressure relief is assumed to re-seat when the pressure differential falls below the user defined re-seat pressure - which is usually slightly lower than the opening pressure. Some pressure relief valves work with a pop-action, in that they jump to the fully open position almost immediately once the opening threshold pressure differential has been exceeded. In this case the discharge coefficient is simply set to the fully open value without using the aforementioned linear interpolation.

All of the devices can choke if the pressure ratio falls below the critical pressure ratio, which is;

$$\left(\frac{p_2}{P_{01}}\right)_{CRIT} = \left(\frac{2}{\gamma+1}\right)^{\frac{\gamma}{\gamma+1}} \quad \text{.....4.103}$$

To predict the choking condition correctly, the pressure ratio used is taken as the maximum of either the applied pressure ratio or the critical pressure ratio.

The flow through the flow restriction devices is assumed to be adiabatic, therefore, there is no change in total enthalpy on passage through the device.

4.2 Thermodynamic and physical properties of Helium

In principle, GTSI can handle any gas as the working fluid. However, to optimise the code for use with helium-cooled reactors, the current fluid property subroutines within the program determine the properties for helium[13]. The specific heat capacities at constant pressure and constant volume are both essentially constant over the temperature range of 0 to 2750°C and over the pressure range of 1 to 100bar. As such, the thermodynamic behaviour of helium closely follows the perfect gas equation;

$$p = \rho RT \quad \text{.....4.104}$$

where;

p	absolute pressure (Pa),	ρ	density (kg/m^3)
R	specific gas constant for helium, with the value 2077.3 J/kg/K		
T	absolute temperature (K)		

The ratio of specific heat capacities γ is essentially constant and has the value 1.6667. The specific heat capacity at constant pressure is also constant and has the value 5.195kJ/kg/K.

The dynamic viscosity, υ, of helium is calculated using the following formula;

$$\upsilon = \frac{10^{-6}\sqrt{T}}{0.45217235 + \left(3.5591461\left(\frac{100}{T}\right)\right) + \left(-15.376631\left(\frac{100}{T}\right)^2\right) + \left(36.663014\left(\frac{100}{T}\right)^3\right) + \left(-33.851656\left(\frac{100}{T}\right)^4\right)} \quad \text{.....4.105}$$

where;

υ	dynamic viscosity (Pa.s)

The thermal conductivity of helium is calculated using;

$$k = 2.682 \times 10^{-3}\left(1 + 1.123 \times 10^{-8} p\right) T^{\left(0.71\left(1-2\times10^{-9}p\right)\right)} \quad \text{...4.106}$$

where;

k thermal conductivity (W/m/K)

The local sonic velocity is calculated from;

$$c = \sqrt{\gamma RT} \qquad \text{.....4.107}$$

It is assumed that helium is thermally perfect so that enthalpy and temperature are related through;

$$h = c_p T \qquad \text{.....4.108}$$

4.3 Component Integration

Based on the component models described above various configurations of plant models can be simulated. This can be from single shaft simple open cycle to complex cycles with multiple shaft, intercooler, recuperator etc. The two simulation cases, design point and off design will be treated separately.

i) Design Point Simulation

The variables required to solve each component and a summary for the complete system will be given. The first requirement is the plant arrangement such as open or closed cycle, number of spools, presence or absence or intercoolers, regenerator, free power turbine etc. A file called Motor.dat will be created each time a design point run. Four files will be necessary to run the design point simulation

i) Control.dat: Contain the control of the gas turbine and the name of the other files. The name of the following files such as Control, Engine and Outdat can be found in this file.
ii) Design.dat: Contain the design point values for the variables
iii) Engine.dat: Contain the component maps
iv) Contain the output variables.

A sample of the above files are given in the Appendix II

ii) Off-Design Simulation and control

The off-design is carried out, once the design point has been run and the files containing all the gas turbine information such as component maps, pressure losses, cooling flows etc are available. There are provisions for keeping the lower and upper limit of some parameters such as compressor surge margin and various temperatures. The output can be formatted according to the requirement. Most of the information related to all equipments can be requested. The time duration of the run in seconds can be specified in the input file. The following is a list of characteristic map available in the input file.

1.	Intercooler Heat, PWX22	vs.	Time
2.	Pre-cooler Heat, PWX71	vs.	Time
3.	Reactor output, PWX33	vs.	Time
4.	Power output, PWX67	vs.	Time
5.	LPC Guide vane angle, ANGVS2	vs.	LP Speed
6.	HPC Guide vane angle, ANGVS25	vs.	HP Speed
7.	Compressor and Turbine maps can be loaded separately in the programme.		

Table 4.1 List of characteristic maps in the input file.

There is a capability to change certain design parameters of some components in the off design mode. This parameters are efficiency, pressure loss, flow capacity etc. This capability is to carry out studies such as the effect of replacing a component or the deterioration of the gas turbine etc. However this feature has not been used in the PBMR simulation as it was not necessary at this stage.

Off – Design limiting values

The gas turbine components have certain values that must not be exceeded during off-design operation. Some of these are

1. Compressor minimum surge margin.
2. Compressor and Turbine minimum and maximum corrected speed
3. Maximum compressor discharge temperature and pressure.
4. Maximum turbine stator outlet temperature
5. Maximum shaft speeds
6. Maximum power output

If the value exceed the limit the code will either runs normally with the exceeding value but a warning message will appear in the output file or some control of the gas turbine to limit the parameter from exceeding. Some of the control variables were introduced specifically for PBMR purpose such as the Bypass valve.

Chapter .5
Performance Analysis.

The PBMR plant will be used as a peak load power station as well as base load station. Hence its capability of load manoeuvring is an important parameter. Because of its complex design with multiple shafts, its part-load performances are expected to be better than single shaft. However, managing the transients with multiple shafts can be a reliability issue. The performance analysis examines these aspects. The various complexities associated with this project can be generally categorized as complexity in Design, Manufacturing, Installation and Operational. Out of these, the operational complexity is the most severe and costly. Solutions of the problems during commissioning and operations can be very costly and will be pivotal for the success of the project.

5.1 Design point

The Brayton cycle is optimised for the parameters given in Chapter 4. The theory and the reasons for the parameter selection are also given in previous chapters. The LP and HP compressors are identical but will be running at 14000rpm and 15000 rpm respectively. The LP compressor mass flow rate at design point is 146.5 kg/sec at a pressure ratio of 1.66 and the estimated efficiency is 88%. LPC and HPC maps are given in Fig 5.1. and Fig 5.2 respectively.

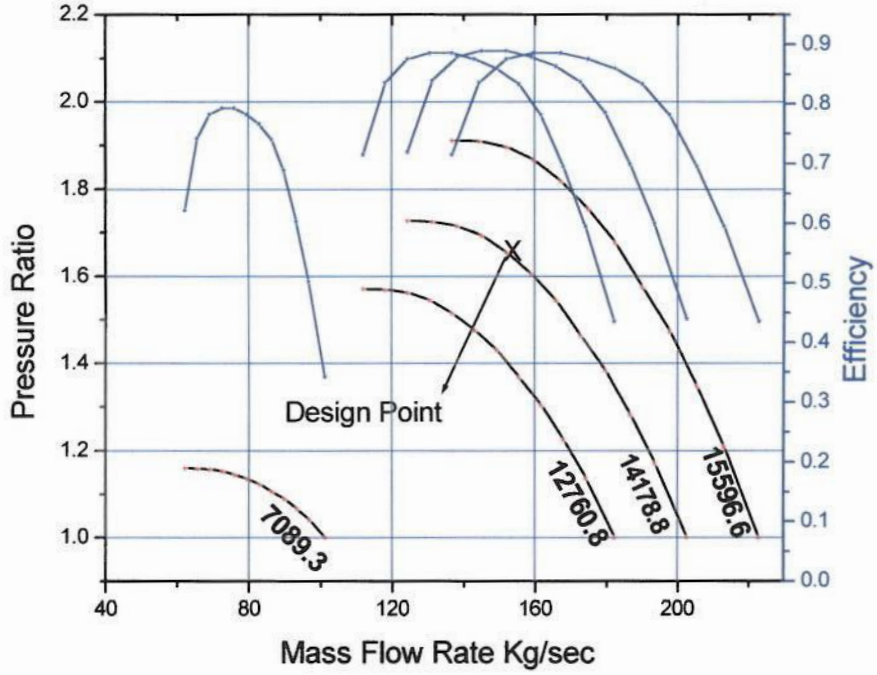

Figure 5.1 LP Compressor Map for the full opening of the IGV at 23 C and 29 bar. [65]

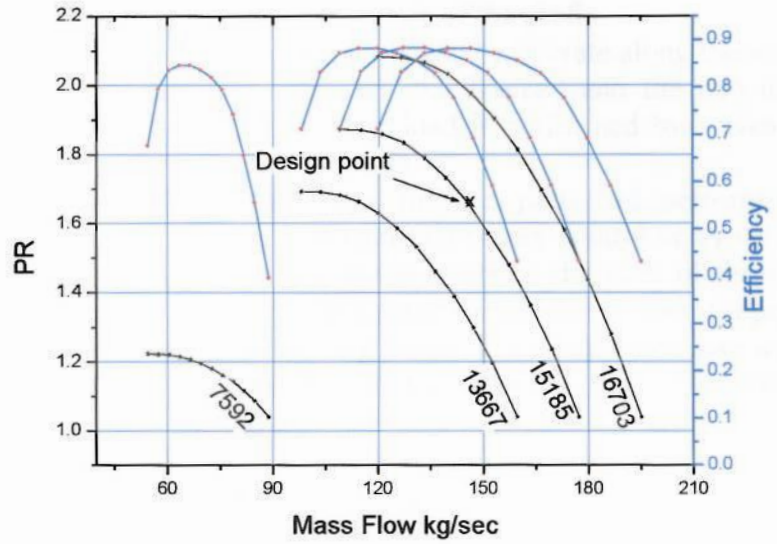

Figure 5.2 HP Compressor Map for the full opening of the IGV at 23^0 C and 42.3 bar[65]

5.2 Steady State Operation

The steady state operation is designed at 20% surge margin for both compressors. The house load (in plant load) is 2.5MWe and the maximum output at generator is 116.3MW. The system pressure at the LP compressor inlet will be 29 bar.

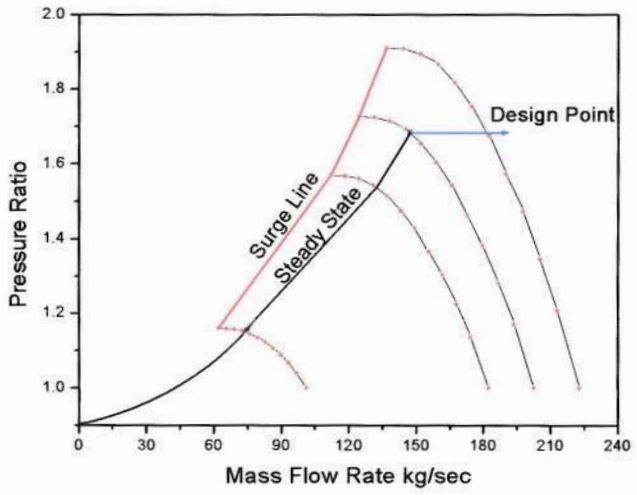

Figure 5.3 LP Compressor Steady State operating line.[65]

The operating line below 40% of the speed is obtained by extrapolating it to origin (zero). However that region is not of much significant in the normal operation. This is significant only during the start-up and shutdown. Even during the start-up, usually gas turbines are designed to attain 50% speed in few seconds to avoid the unstable regions and critical speeds of the shafts.

The gas turbine engines normally operate along the steady state line. During this process, the pressure ratio, corrected speed and the non dimensional speed will be changing. However, if the part load is performed by variable guide vanes, it will be following a separate map or maps.

In a closed cycle gas turbine, part load performance can be achieved by changing the pressure level using inventory control or by using the bypass valve to tap the HP gas from HP compressor outlet to the inlet of the pre-cooler or by using the reactor power control. In the case of the inventory control operation, the operating point will not necessarily be moving down. The compressor map will remain same with same non-dimensional parameters and rotational speed. The absolute mass flow and the density will be changing.

5.3 Operational Transients.

Transient operations happen during the start-up, load ramping and shutdown. The transient operation can be caused by the pull from the demand side (change in the load demand), by the push from the heat supply side (change in the TET etc.) or due to rapid operational changes created by auxiliary equipments (rapid flow of helium inventory etc.) or a combination of some or all of the above.

The PBMR target is to achieve a loading rate of 10% load per minute, which is approximately 11MW per minute. This target will help the PBMR to be successfully used as a peak load power station. This has to be achieved mainly with the Helium inventory control. The load shedding target is 10% per second and this has to be achieved using helium bypass valves alone. However load shedding and loading at a moderate speed can be achieved by either inventory control or bypass alone. Maintaining high efficiency during high speed ramping will not be a priority as the emphasis will be to maintain the reliability of the supply by avoiding a grid separation.

Depending on the speed, the operational transients can be categorised as follows

1. **Normal Loading**. The target is 10% per minute. Inability to attain this will cause problem in load management. Not much of a safety issue. This normal loading can be done by increase of the inventory level. The reactor should be able to maintain the TET, when the flow through the reactor increases rapidly.

2. **Load ramping.** This is done when the demand from the grid fluctuates. The bypass valve operation is the rapid way and the inventory control is the efficient way. In this process the operators have time to respond and depending on the urgency they can plan their action. The risk is to prevent the shafts over-running causes isolation of the unit from the grid.

3. **Normal Load rejection.** This is very similar to ramping except the reloading is not intended. This allows the operators some time. However automatic load rejection may be required in some cases. The rejection should be gradual and shafts overrun should be avoided.

4. **Full load rejection.** In this case, the unit is isolated from the grid from a full load situation. This will be a fast transient with a time gap of a fraction of a second. The risk of over speeding and overheating are the main concerns. In single shaft configuration, this is more manageable due to the high inertia and the resistance load from the compressor attached to the same shaft. In multiple shafts with free power turbine arrangement, this is a critical issue.

   The full load rejection has to be managed with fast bypass operation. Another way is to give a resistance load to the generator to face the full load rejection from the grid. However, providing the hardware for a full load rejection is not practical and normally a percentage of the maximum load will be specified as resistance load. The capacity of the resistance load depends on the duration in which it is exposed. For a very short duration it will be able to take very high current similar to an electric motor starting current.

   In conventional steam power plants, the governors are closed to the turbines and hence a full load rejection is more manageable. In the PBMR design a hot bypass instead of a cold bypass will be an ideal way to manage the full load rejection. But valves operating at that temperature may not be practical in terms of long term plant reliability. Hence hot bypass is is not recommended for PBMR.

5.3.1 Managing the Operational Transients.

Transient stability has traditionally been the performance issue most limiting on power systems. Transient stability refers to the ability of all machines in the system to remain synchronised following a disturbance such as transmission system fault, a generator or transmission line trip or a sudden loss of load. Transient stability is a fast phenomenon, with loss of synchronism typically occurring within two seconds of a major disturbance. If the speed of any machine does not return toward an acceptable steady state value within one to three seconds after a power system disturbance, the machine is said to have lost synchronism with the system. The loss of synchronism will typically result in the generator being tripped off-line by a protective relay.

The control hardware available for managing the transients are listed below

1. **Reactor temperature control.** This controls the reactivity in the reactor, which will be manifested as TET. This is a slow and steady process. Not meant for any rapid change. Good for pre planned load modulation.

2. **Inventory control.** Medium to high speed. Good for planned and unplanned load modulation. Not good for any situation which needs rapid response like full load rejection. One of the efficient ways to modulate.

3. **Bypass control Valves.** Good for fast responses. But considered as an inefficient method of control due to the low efficiency. Not meant for any pre planned load modulation.

4. **Compressor guide vanes.** Useful during the start up. Mainly to manage the compressor instabilities. Not much of a help for the direct control of the load.

5. **Interrupt valves.** This is provided at the recuperator cold side inlet. This has very limited control characteristic and not meant to use as a control valve. Useful to manage the full load rejection. Its use at full load may cause instability in the turbo compressors, which has to be solved with other control hardware.

6. **Resistor bank.** This is to prevent the power turbine shaft from over speeding. Not much of a help during normal load ramping.

7. **Start up Motors / System.** Though they are meant to be operated during the start up, some cases it can be useful to solve stability problems in the turbomachineries. Can be helpful for the fine adjustment of the power output. Mostly depends on what type of start up facility will be used.

The transients have to be managed from a safety, reliability and long-term plant health point of view. PBMR relies on mainly two control hardware to manage the transients. These are Inventory, Bypass and interrupt valves. Others include compressor guide vanes and reactor fuel control etc. The shortest time span available for correcting a synchronous speed disturbance in the generator shaft will be in the order of few seconds. This is the time available to sense the change, decide the corrective action, send the signal for corrective measure, time for the corrective action, process inertia (shaft and gas), verification of the result to adjust it further if required etc. Considering the fact that valves takes few second to operate, managing the transient becomes a critical issue.

As mentioned above, pressure level and bypass control are the major players for the operational reliability. The interrupt valve is meant to stop the flow completely for an emergency shutdown. The pressure level is proportional to the density and hence if the machine inlet temperatures remain constant, the velocities of the flow remain unchanged so that the turbo machines work in their design point. Several storage vessels with different pressure levels are an efficient way of changing the pressure level in the system.

The total distance the gas has to travel from the HP compressor to the inlet of the LP compressor, through the reactor, is around 60m of which 40 m will be through the pipes and 20 m will be through the pressure vessel. Considering the maximum velocity of helium of 80m/sec in the circuit, the normal gas response time will be less than 1 sec. The mechanical, thermal and gas mass flow inertia are adding more delay and complexity to the gas response time .

5.3.2 The Scientific background of the Transients

One of the root cause of the transients becoming an issue is the time delay between the cause and the effect of it.

The following major time delays are categorised as follows

1. The first relates to mass inertia due to pressure changes caused by gas oscillation. This amounts to few deciseconds. Sudden opening and closing of a valve can create gas oscillation.

2. The time delay due to the energy storing (inertia) of the rotating shafts, which cause time delay in rotor speed change and mass storing of the volumes, which cause delay in flow change. The calculation shows in normally in the range of few seconds.

3. Heat storage or thermal inertia in the heat exchangers cause time delay during temperature changes. This will be 10 times higher than the delay mentioned above in the second group.

The above categorisation, based on their velocity, is done by estimating the time delay using e-functions, periods of oscillation, running times, transport times etc.

5.4 Temperature Transient

The performance during temperature transients is simulated by running the programme at different Turbine Entry Temperature. Fig 5.4 shows its effect of rising TET on the LP Compressor. As the TET increases the output power and mass flow also increases. The programme stopped when the surge margin reaches zero. This simulation was done at a particular guide vane setting.

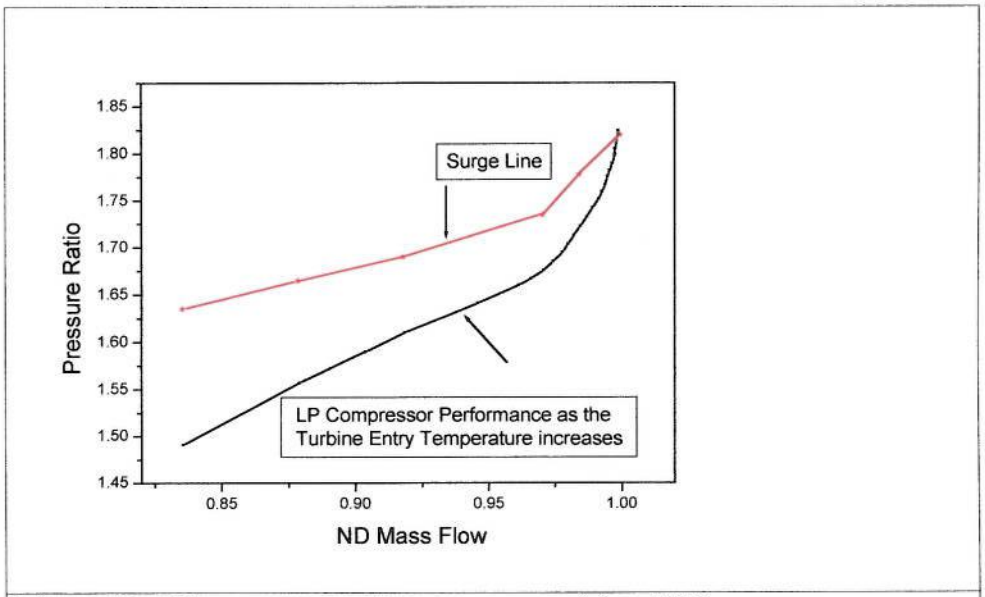

Figure. 5.4 Compressor performance on a rising TET

A rise in Temperature will increase the speed of the Turbine, which increases the pressure ratio and pushes the operating line towards the surge line. This has to be adjusted by the compressor guide vanes.

In the actual situation the Reactor outlet temperature will be controlled by the fuel supply and this is not considered in this programme. Also the graphite in the Reactors is having high thermal storage capacities and this feature will influence the Temperature transients as well.

The temperature transients at the turbine inlet originate from the following actions.

1. When the fuel input increases rapidly. The fuel loading changes will be according to the demand and hence this is an unlikely source of temperature transient. The fuel rate control is meant for steady and pre planned load changes.

2. When the Bypass valve opens. This means less flow through the reactor for the same heat output. This can be retarded by reducing the fuel supply and also by the negative reactivity. (Producing less heat when the temperature rises).

3. When the Inventory flows out of the system to effect a load reduction. This will also reduce the flow through the reactor.

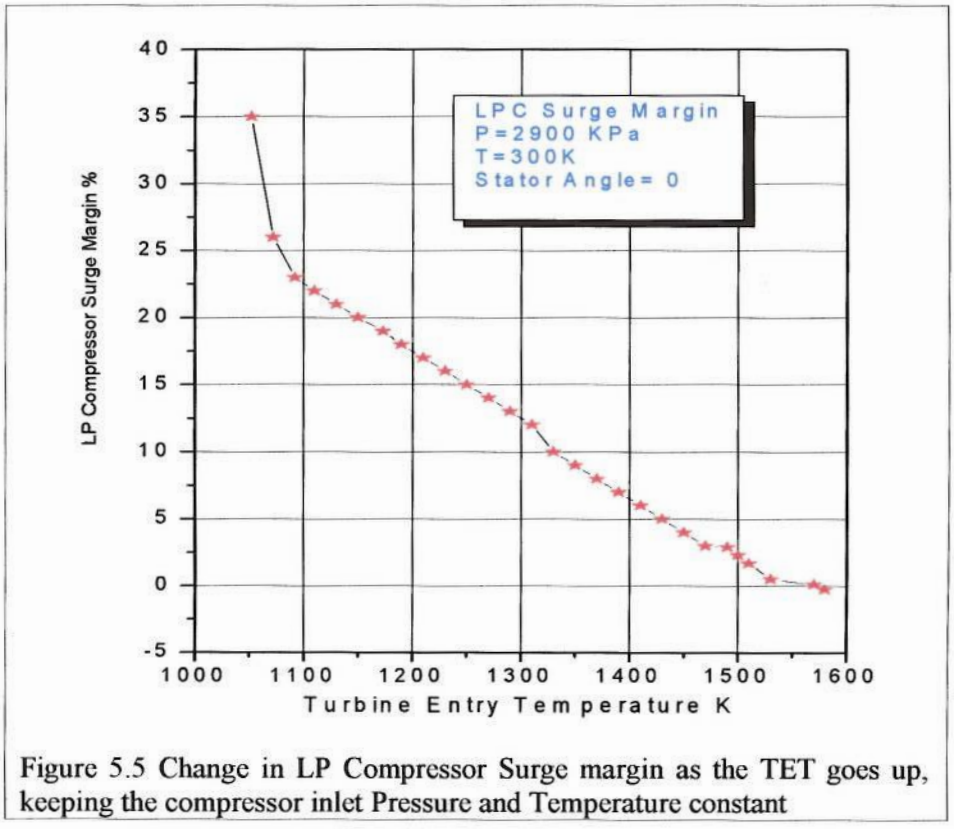

Figure 5.5 Change in LP Compressor Surge margin as the TET goes up, keeping the compressor inlet Pressure and Temperature constant

As the TET goes up, the turbine speed and efficiency will increase which will allow the compressor to increase its mass flow rate as well. This moves the operating line towards the right and eventually to the surge region (Figure 5.5). During a temperature transient, the surge can be avoided by opening the bypass, which will reduce the power input into the turbine to compensate for the rise in the TET.

Figure 5.7 shows the IGV angles required to maintain the surge margin at various TETs. This reveals that a slight change in the compressor IGV angles can make drastic change in the surge margin and hence it will be an effective tool in protecting compressors from the consequence of temperature transient.

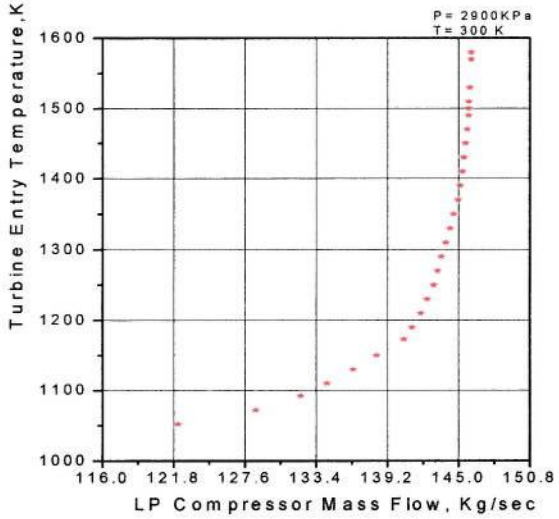

Figure 5.6 Mass flow through the compressor at various TET

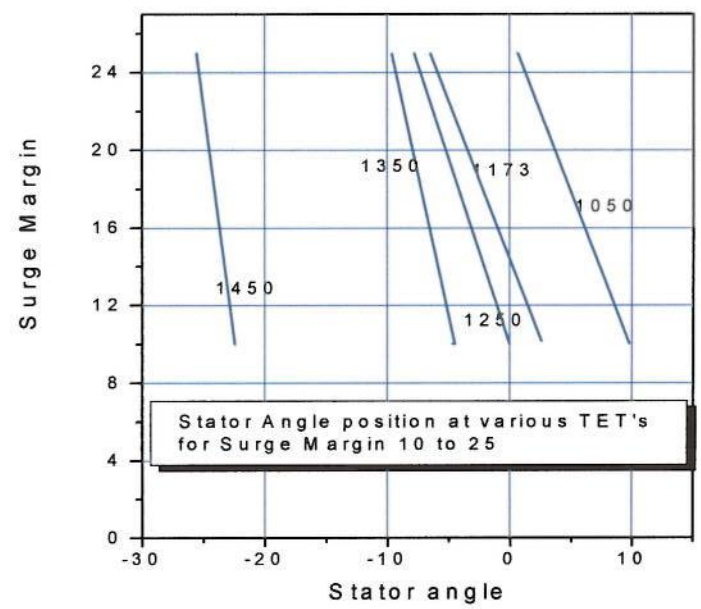

Figure 5.7 LP Compressor Stator Angles at different TET's for maintaining the Surge Margin between 10% and 25%

5.5 Load Transients

Load transients occur at start up, shut down and during grid following. Smooth transition from one load to another is important for the reliability and safety of the system. The acceleration and the deceleration of the shafts should pass through critical speeds without delay and also without causing a grid separation. Grid separation mainly happens when the frequency of the electricity generated does not match with the frequency of the grid. The frequency of the grid is the synchronised frequency of all the generators connected to the grid at that time. The frequency difference on the individual generator occur when it can not maintain the speed either due to the mismatch in the energy supplied to the prime mover such as the turbine and the load demanded by the grid. This mismatch in demand and supply can be due to the slow response from the turbine governing system to the grid load or it can be genuine lack of capacity at the power source.

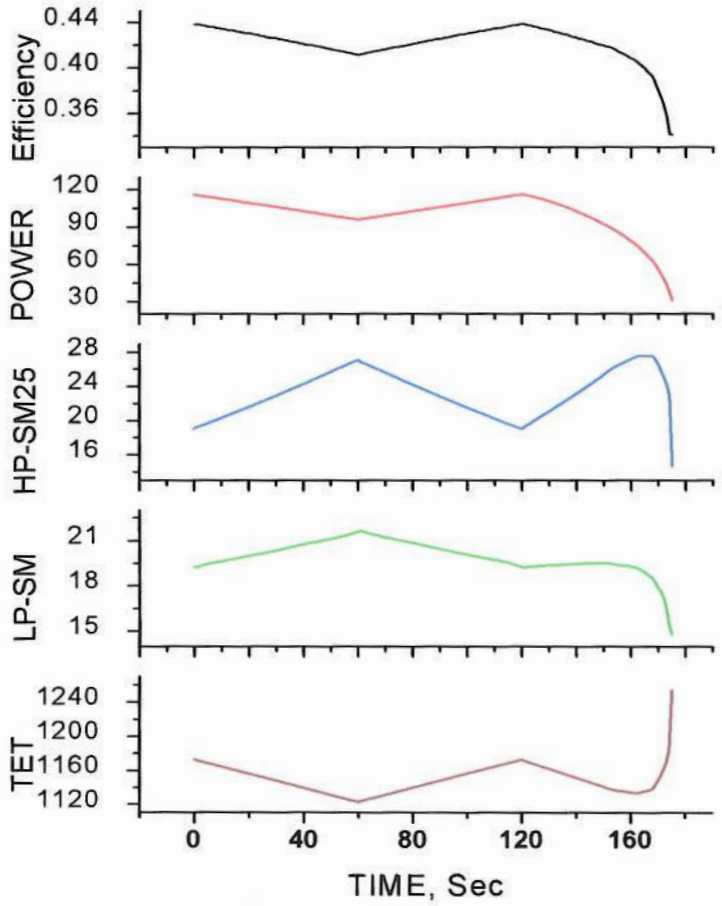

Figure 5.8 The TET, LP and HP Surge Margin and Efficiency during a load ramp scenario where power is reduced by 20% and brought back to normal before reduced to 50% in 180 sec.

Grid separation during start up or its ascending to full load normally due to the control system failure. Similarly during planned shut down the load has to be reduced from full to without causing a grid separation. The emergency tripping of the units always follows an automatic grid separation. In this case the load jumps from full load to no load in a fraction of second. However the turbine speed has to be controlled to remain in the mechanical design limit.

The Figure 5.8 shows the effect of a load ramping, where the generator power is reduced by 20% and brought back to normal before reduced to 50% in 180 sec. The entire operation is done using the reactor power control. As expected, the surge margin of the HP and LP compressors improved as the load decreases during the normal reduction. But during the final load rejection, which is 50% in 60 seconds, the LP compressor was slowly moving towards the surge line whereas the HP compressor moved towards the choke line before jumping towards the surge line. The final rise in TET is due to the reduction in mass flow through the reactor, when the compressors are moving close to the surge line.

The efficiency of the system is also behaving as expected. The initial gradual reduction in the load gives the corresponding part load efficiency and then as the load regained, the efficiency also regained its design value. When the final load rejection happened, the efficiency again slips to less than 30%.

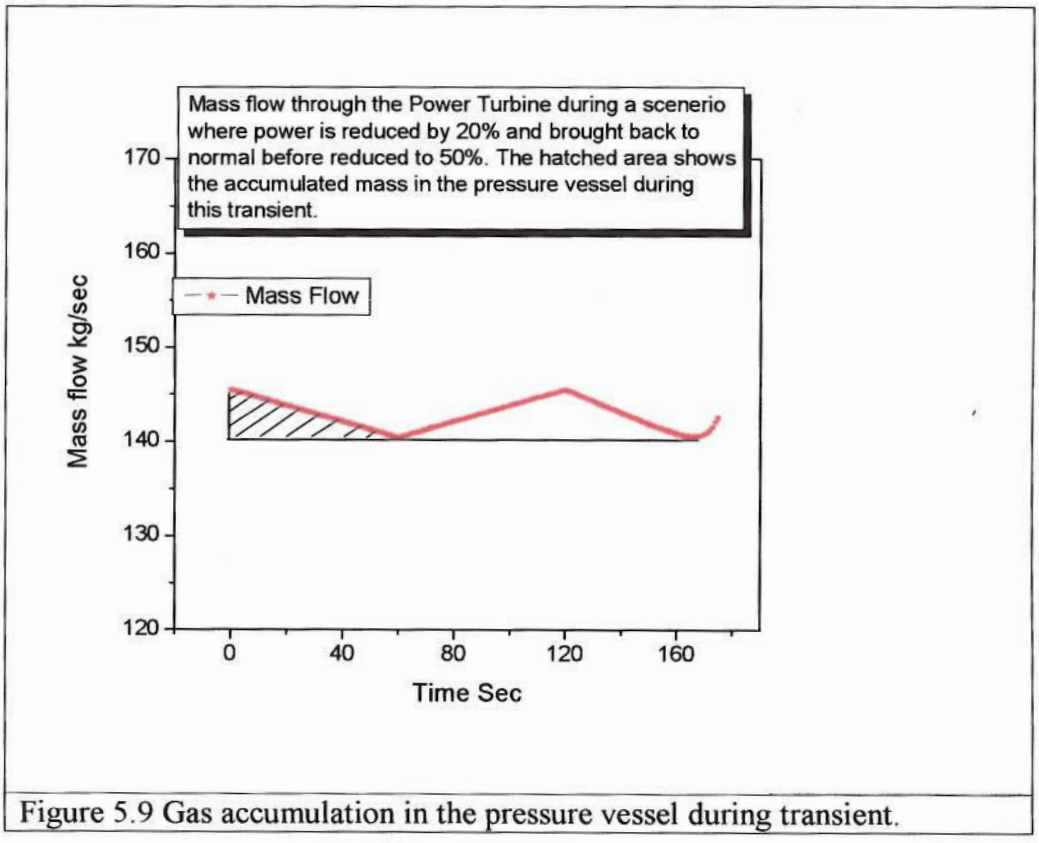

Figure 5.9 Gas accumulation in the pressure vessel during transient.

The Figure 5.9 shows the load rejection from 116MW to 50 MW in 60 second. The mass flow through the turbine had been reduced initially due to the mass storage in the pressure vessel, but it started regain the mass losses after some time. The efficiency as expected dropped quite linearly in proportion to the generator power output. The LP surge margin reduces linearly to the power output and the LPC is moving towards surge. The HP Compressor operating line was moving away from the surge line initially but later it jumped towards the surge line. These are due to the reduction of flow velocity towards the reactor.

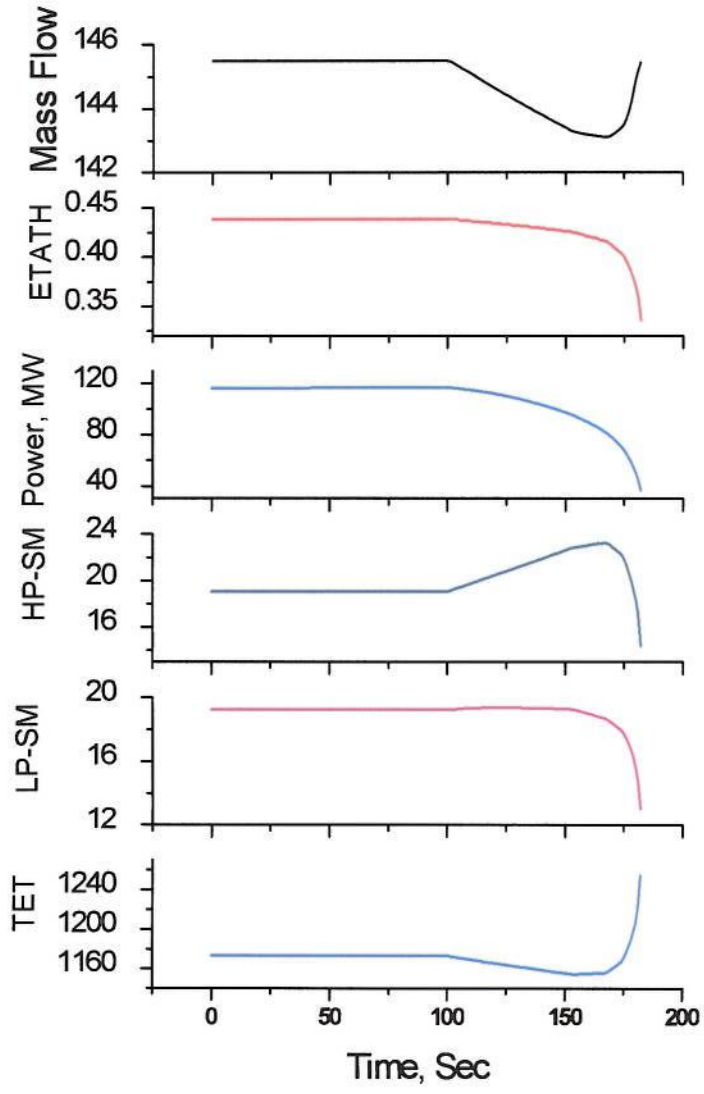

Figure 5.10 A load rejection scenario. The TET, LP and HP Surge Margin and Efficiency during a load ramp when power is reduced to 50 MW in 80 Sec.

Figure 5.11 gives the pre-cooler response to a load dip. As expected, the response is proportional to the power output. The pre-cooler is designed with a variable cooling water flow arrangement to make sure the LP compressor inlet temperature of the gas remain same. This is designed for 300K.

The Brayton cycle efficiency is inversely proportional to the compressor inlet temperature and hence theoretically it would be beneficial to bring down the pre-cooler inlet temperature further down. This will be possible with extra cooling modules in the cooler and more pumping power. Again its success depends on the ambient temperature. However the extra arrangement may not be economically worth-while more bulky and expensive. However when the unit operates in an environment, where the ambient temperature is lower than the designed value of the PBMR, the extra cooling of the compressor inlet gas can increase the efficiency.

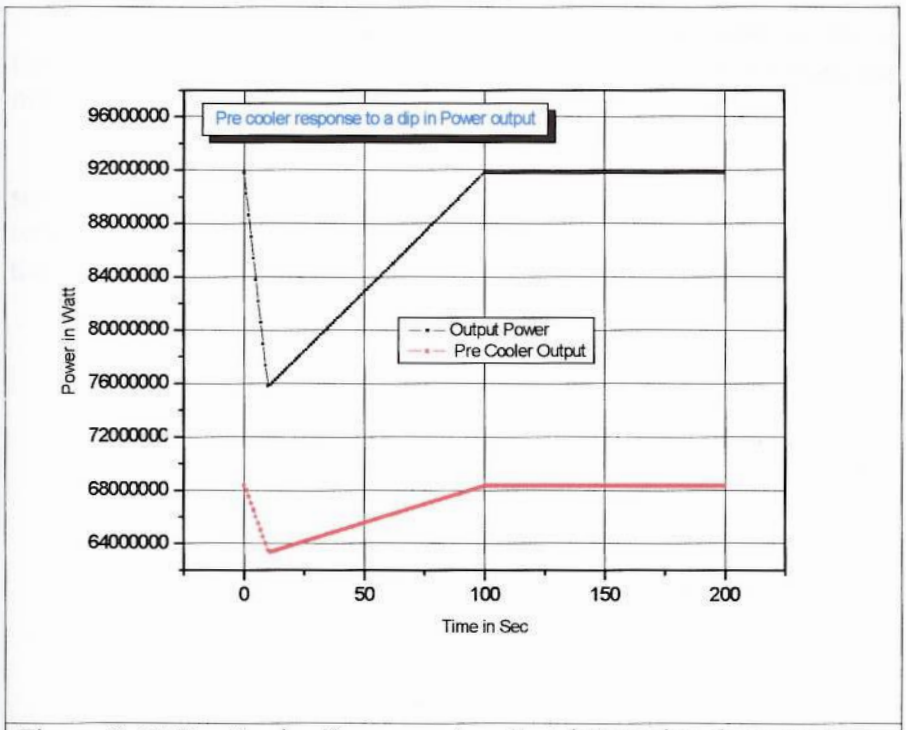

Figure 5.11 Pre Cooler Response to a Load Ramping from 92 MW to 76 MW and back in 100 sec.

5.6 Speed Transients

The PBMR has three independent rotating shafts. The speed control of the LP and HP shafts are achieved by the compressor inlet guide vanes, inventory control valves and bypass valves. The power turbine speed control is done by the bypass, inventory, and interrupt valves and electric resistor banks. The issue of overrun of the LP and HP shafts are not that critical because these are short in length with low moment of inertia and also the compressor resistance load will always try to limit its overrun.

When using the bypass, the turbine power will be reduced and the compressor load will remain the same. This will slow down the shaft. The inventory valves can also be used to prevent the shaft overrun by doing loading and unloading of the gas at the

same time. The supply gas will be given at the LP compressor inlet and gas will be taken out from the HP compressor outlet back into the inventory storage. This process will have the same effect as the bypass valve and it will reduce the shaft speed. This process can be used when the unit is already running at low inventory in order to use the bypass valve for speed control.

The issue of the power turbine overrun is more critical than the others as it has more diameter, mass and moment of inertia. Over and above, there is no compressor resistance load attached to the shaft. The degree of power turbine overrun depends on the load from which it tripped. The full load rejection is the maximum situation. The operation of the Bypass and the inventory will stop further supply of energy to the turbine. However it will not be able to act as a break for the overrun due to the energy stored in the shaft at the time of overrun. The interrupt valve will act as a complete stop for the gas circulation, which will give some resistance to the shaft. The electric resistance load (this is an electrical load connected to the generator output, the energy will be dissipated through cooling water) will be used in the event of a full load rejection. However in the event of a trip due to generator failure the resistance load will not be used.

The Power Turbine can be simulated for a speed transient only when it is separated from the grid. This is to know the extent of overrun of the PT shaft after a grid separation. In reality it will not be loaded if it is not at the synchronous speed. However the speed transient simulations can be applied to other turbo compressor shafts.

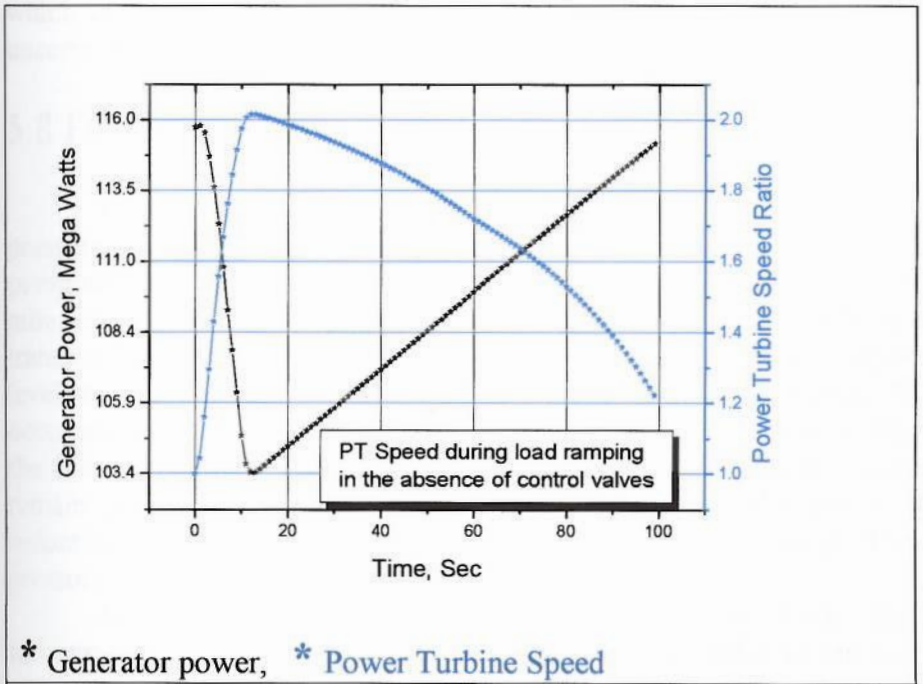

Figure 5.12 Power turbine speed in the absence of control facility during load ramp.

Figure 5.12 shows that the power turbine speed has been doubled during a load ramping as shown. In reality this will be prevented by flow control valves. The power turbine shaft speed is critical for the frequency of the electricity produced and hence it will be maintained constant when it is connected to the grid.

5.7 Pressure transients

Different valves used in the PBMR system are mainly responsible for the pressure transients. Pressure transients can happen due to the following actions.

1. When the interrupt valve operates, it can create a reverse or an oscillating flow. This will produce pressure excursions for a very short duration with high intensity.

2. When the Bypass valve opens to redirect some of the high-pressure gas from the Reactor to the inlet of the pre-cooler for load reduction or during the reverse, a pressure transient can happen. This is due to the high differential pressure between the Bypass valve and Pre-cooler. The Bypass valve inlet pressure is 7MPa and the pre-cooler inlet pressure is 2.6Mpa.

3. When the inventory control system supply high pressure helium at the LP side to increase the pressure level or when it is being taken out from the HP side to reduce it, the possibility of a pressure transient occur.

The exact cause and effect depends on the geometry of the components and the way in which they acts. Hence analysis based on the final geometry is useful to reduce the uncertainty, such as CFD.

5.8 Flow transients

The compressor operating point remains the same for different loads at different pressure levels in a closed cycle system. However the pressure level changes by pumping more gas in to the system or out of it. This may take few seconds to few minutes. During this time the compressor operation will be far from steady. This flow transient has to be analysed separately. Once the system pressure level reached a steady level the compressors will again be in the design point operation. The flow transients occur mainly from the inventory valves and bypass valves. During the bypass operation, the flow through the reactor and the turbines will be reduced. However pressure will remain same, because the compressor pressure ratio will come down, due to the reduction in speed, which will keep the outlet pressure constant. The compressor inlet pressure goes up when the bypass is in operation.

Another source of flow transient will be from the leakages. The turbomachineries are enclosed in the pressure vessel and it is surrounded by gas at the maximum operating pressure. Hence the gas leak will be into the turbomachines except the final stages of the HP compressor, where the differential pressure between the stages and the outside pressure will be very low. The leak into the turbines can be equated and simulated as a cooling flow for all the practical purposes. The compressor leak can be simulated as a surge bypass because the effect is same.

5.9 Effect of Compressor Surge in PBMR Design

Surge is part of the inherent operating characteristics of centrifugal and axial compressors. The impact and severity of the surge depends on the sensitivity of the equipment, duration of the surge and the layout of the system. Based on this, a comparative analysis is done on the effect of surge on a conventional compressor-combustor-turbine layout and PBMR layout.

COMPRESSOR-COMBUSTOR-TURBINE	PBMR
1. **Temperature-** During the back flow, gas at discharge temperature is introduced to the inlet. If more than one cycle occurs, the same gas is reheated and returned, getting hotter with each cycle. The effect is damaging as the compressor components are not designed for high temperature.	1. **Temperature-** The recuperator is placed at the opposite end of the pressure vessel and reverse flow does not bring any heat other than the heat generated during compression. The gas quantity and inertia in the pressure vessel is quite high for the recuperator to have an effect on the HP compressor. Hence even the Nuclear reactor, which serves the purpose of a combustor here, will not have any effect due to a back flow in the HP compressor.
2. **Load on the shaft.-** During the back flow the shaft torque is reduced, then restored with feed forward giving a torsional pulse with each cycle. An axial movement of the shaft can be expected in this process. Overall the effect is not that severe, but can cause vibration.	2. **Load on the shaft.-** The PBMR design consists of vertical shafts running on magnetic bearings. There will be a torsional pulse with each cycle. The axial movement will be in vertical direction and can be accommodated by the magnetic bearing without causing any mechanical stress. The axial thrust due to the reverse flow will be accommodated by the thrust bearings compared to the journal bearings in the horizontal shaft. However there is a possibility of the shaft speed rising due to the fact that the turbine is getting an uninterrupted energy input even when the compressor torque is reduced.

3. **Component Stress.-** During the back and forward reversals, all the components involved with the gas propulsion are loaded and unloaded, placing blading in a cyclic loading. This can cause severe vibration to the extent of breaking the blade, if the duration of the surge is long.	3. **Component stress.-** The blades will be experiencing similar cyclic loading during a flow reversal. However the helium compressors have shorter blades, which will be helpful in this regard.
4. **Effect on the process.-** Lack of air in the combustor can cause flame out. Also unburned gas and combustion products can enter the compressor	4. **Effect on the process.-** the HP compressor is delivering the gas into a chamber, in which all the rotating equipments are stationed . Any flow reversal for a short duration will not be affected due to the size of this vessel. The recupertaor cold side inlet will be the first region to be affected and then the nuclear reactor afterwards. An oscillating flow in the pressure vessel will not have much impact in the process.

5.10 Effect of Bypass Valve operation

As mentioned earlier, bypass valve control is for the fast response to output changes. During bypass valve operation, the turbine will have less gas and the compressor mass will remain unchanged. Bypass operation has the same thermodynamic effect as the reactor power control. The shaft speed will decrease accordingly because of the reduction in enthalpy available in the turbines.

Since the bypassed valve is discharging the gas to the pre-cooler inlet, the compressor inlet temperature will remain same. The compressor inlet pressure will go up in the beginning but stabilise. As the shaft speed reduces, the pressure ratio reduces. The compressor inlet pressure will be a sum of the low pressure discharge from the Recuperator hot side outlet and the high pressure from the HP bypass.

The Fig 5.13 gives the flow distribution during the bypass valve operation. The new turbine power will be $(m-\Delta m).Cp.\Delta T$, which is the reduced one whereas the compressor power remains same. This will reduce the speed of the shaft. Once the compressor power has reached the same level as turbine power, the shaft speed will stabilise and remain constant. In this situation the compressor will be running at reduced speed and pressure ratio but the compressor outlet pressure will same as that of the normal load operation. This is because of the rise in compressor inlet pressure.

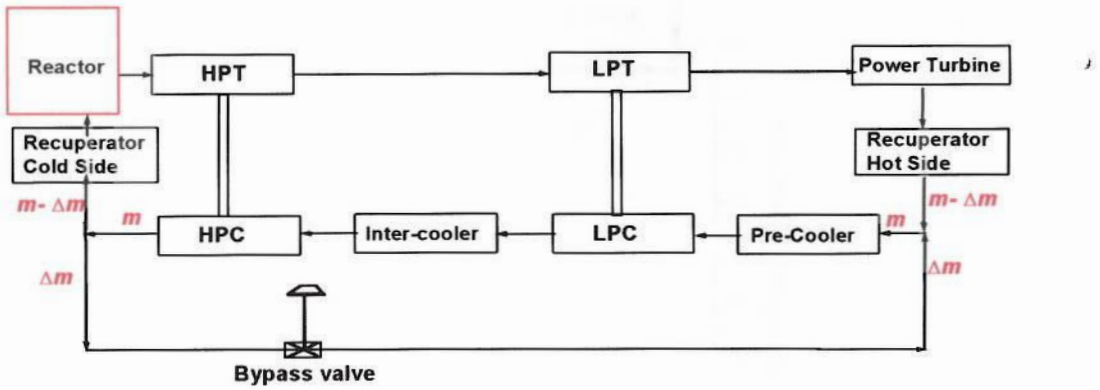

Figure 5.13 General layout of PBMR with Bypass flow details.

The LP compressor is more vulnerable for surges than HP compressor during the bypass operation. Figure 5.14 shows the result of the bypass valve operation simulation. This is due to the fact that the bypass opening after the HP compressor will increase the axial velocity, which will improve its surge situation. The first effect of the bypass operation is the reduced flow in the turbine and the rise in LP inlet pressure. This will push the LP operating line towards the surge.

The Table 5.1 summarise the compressor behaviour found from the analysis.

LPC	EFFECT	HPC	EFFECT
Pressure, P	⇑	Pressure, P	⇒
Speed, N	⇓	Speed, N	⇓
Mass Flow, W	⇒	Mass Flow, W	⇒
Temperature, T	⇒	Temperature, T	⇒
Pressure Ratio	⇓	Pressure Ratio	⇓
$WT^{1/2}/P$	⇓	$WT^{1/2}/P$	⇒
$N/ T^{1/2}$	⇓	$N/ T^{1/2}$	⇓

Table 5.1 Compressor performance during bypass valve operation

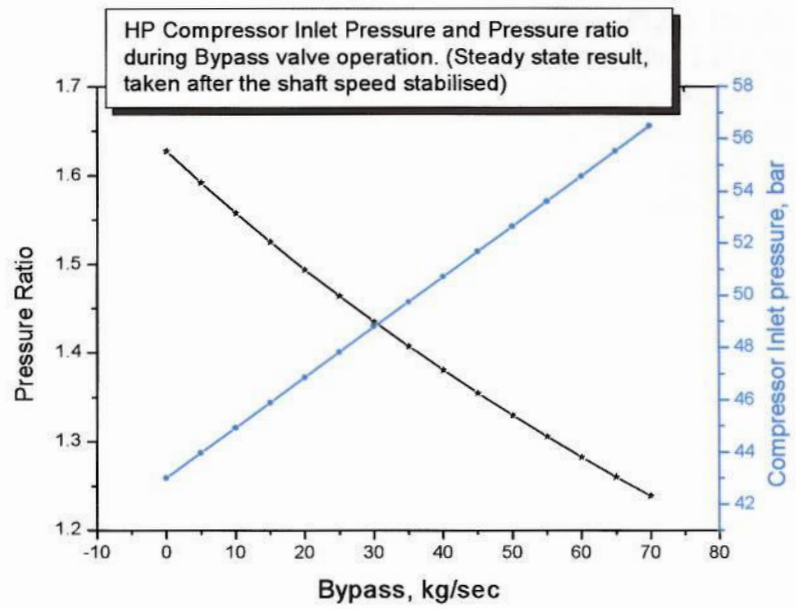

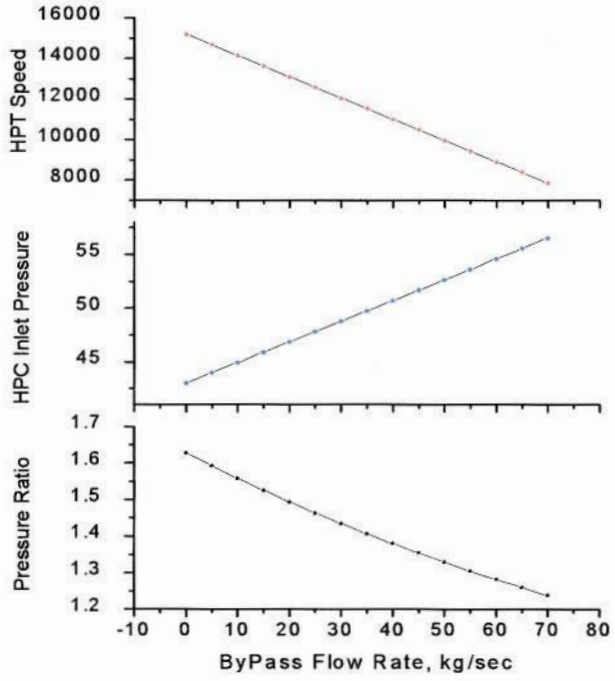

Figure 5.14 HP Compressor Pressure Ratio, Inlet Pressure and HP Turbine speed during Bypass operation.

From the above analysis, the LP and HP compressor behaviour during the bypass operation can be represented in the map. Fig 5.15 shows the movement of the operating lines for the LP and HP compressors. The LP compressor is moving down along the operating line but coming closer to the surge line. The HP compressor operating line is moving down and also moving towards the choking line. Theoretically this is suppose to move downward without any increase in the non dimensional mass flow. In reality it is experiencing a high inlet pressure and hence it moves to the choking line.

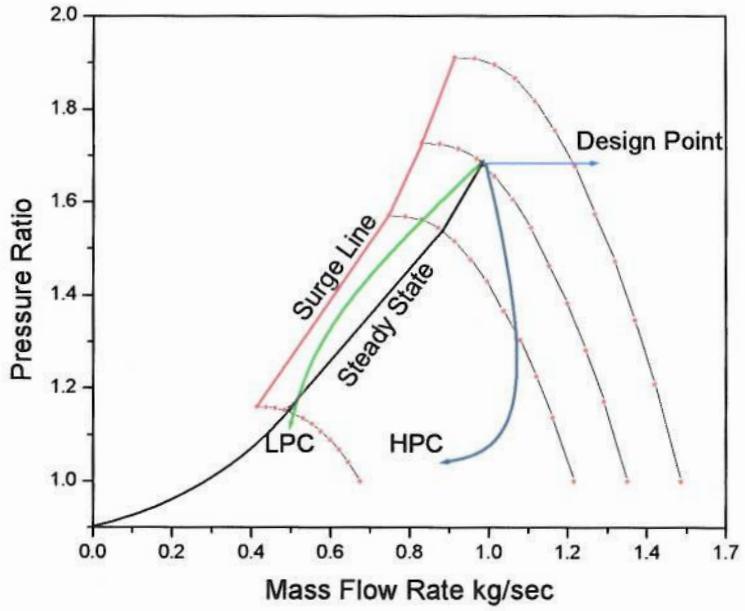

Figure 5.15 The LP and HP compressor operating line during a bypass operation in the map.

The type of bypass valve and its operation also plays a role in protecting the compressors getting into instability. As shown in the Figure 5.15, the LP compressor moving towards the surge due to the reduction in speed and high inlet pressure which decreases the non-dimensional mass flow. If the LP compressor is given enough time for the gradual reduction in pressure ratio, then the instability in the HP compressor can be avoided.

Figure 5.16 shows the HP shaft speed during different type of valve operation. (valves with different actuation characteristics). The resulting shaft speed shows the importance of the type and mode of the valve operation. However this has to be optimised as this will be a contradicting requirement to the load rejection requirement, in which the load has to be reduced as rapid as possible.

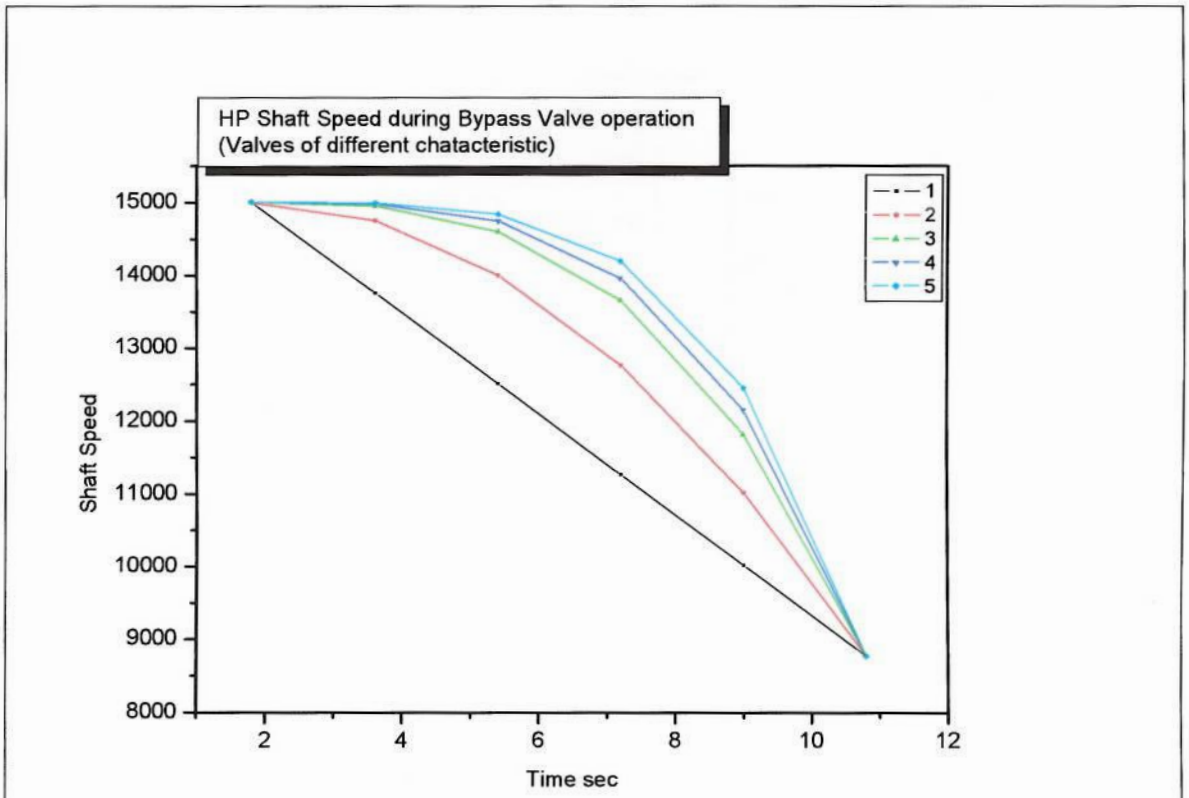

Fig 5.16 HP Turbo shaft speed during the Bypass valve operation. The characteristic of the Valves 1 to 5 is given in the appendix 4

This situation of synchronous idling (*Synchronous idling*- in which the generator is running at 3000rpm and producing no electric power but ready to start and raise the load) occurs at the start up as well as after a load rejection. During the start up, synchronous idling is achieved with low inventory, which is an efficient way of achieving this. However there are situations in which the system will have a full inventory and has to be in the synchronous idling mode. The bypass can be used to bring the system to synchronous idle running.

The Figure 5.17 shows how the generator output and system efficiency is affected by the bypass operation. The efficiency is inversely proportional to the bypass operation and hence the generator power output as well. At around 30% bypass the generator power output ceases. This shows that a 30% opening of the bypass is necessary to achieve the synchronous idling. Though this is not an efficient way, especially if the reloading of the unit is very gradual, by gradually reducing the bypass flow, the system will be running at low efficiency for a prolonged time till it achieve the full load and maximum efficiency. However this way of idling the plant is useful for the rapid load rejection and reloading. The effect of synchronous idling on the reactor is not considered here. The pre-cooler and the inter cooler will not be affected

much though the cooling load will increase slightly during the synchronous idling with 30% bypass opening.

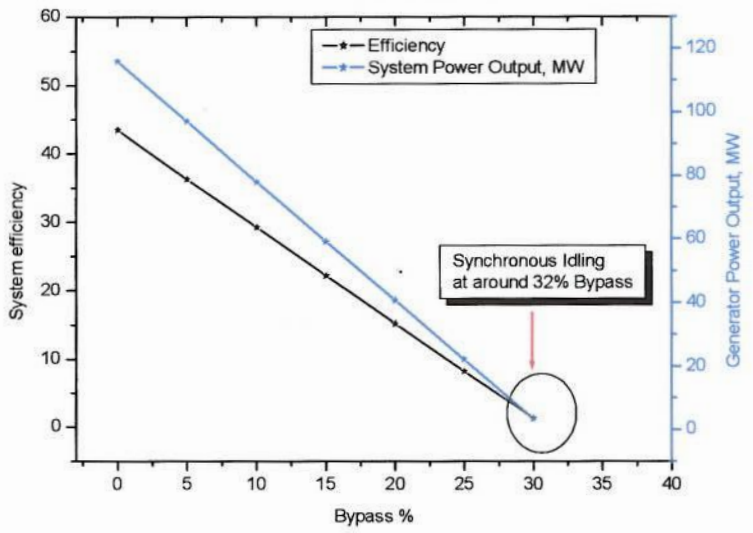

Figure 5.17 Synchronous Idling With Bypass valve

The bypass operation will result in less flow through the reactor. This can create a temperature excursion. The value of this excursion is very low as shown in the Fig 5.18, so that it is considered as constant in this simulation.

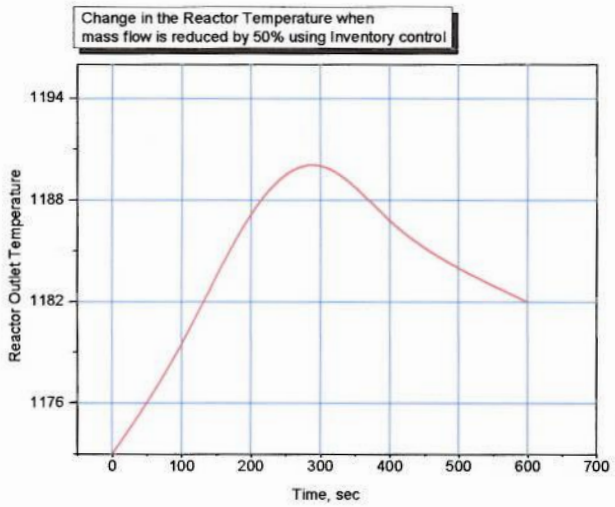

Figure 5. 18 Change in the Reactor outlet temperature when mass flow is reduced by 50%

5.11 Effect of Interrupt Valve Operation.

The interrupt valves are placed at the inlet of the cold side of the recuperator. These are isolation valves without any control characteristics. The operation of this is to stop the Brayton cycle. During the full load rejection, these valves will be used to stop the energy supply to the turbines and thus the shaft overrun can be prevented. This valve is placed in the pressure vessel without any inlet piping, rather it takes the gas from the vessel itself. Upstream gas oscillation will be in the vessel itself and the down stream gas oscillation will be in the recuperator.

The consequence of this valve operation will affect the HP compressor only when the pressure in the vessel increases. If the axial gas velocity reduces, then it may push the operating line of the HP compressor towards surge. During water hammering (fluid oscillations) situations the pressure can be as high as the double the design pressure. Though this experience for very short time, it can create enough damage to the system. The HP shaft speed will reduce immediately and if a sudden pressure in the vessel is experienced due to the back flow, then it can create surge situation.

The LP compressor performance will mainly depend on the HP compressor. The speed of the LPC will also come down and if the gas flow through the HP compressor is restricted in the HP compressor as mentioned earlier, the LP compressor can also be get into the surge situation.

The reverse flow through the turbines back to the reactor is not expected during interrupt valve operation, because the pressure vessel will act as a mass storage to prevent any reverse flow.

5.12 Effect of Inventory Change.

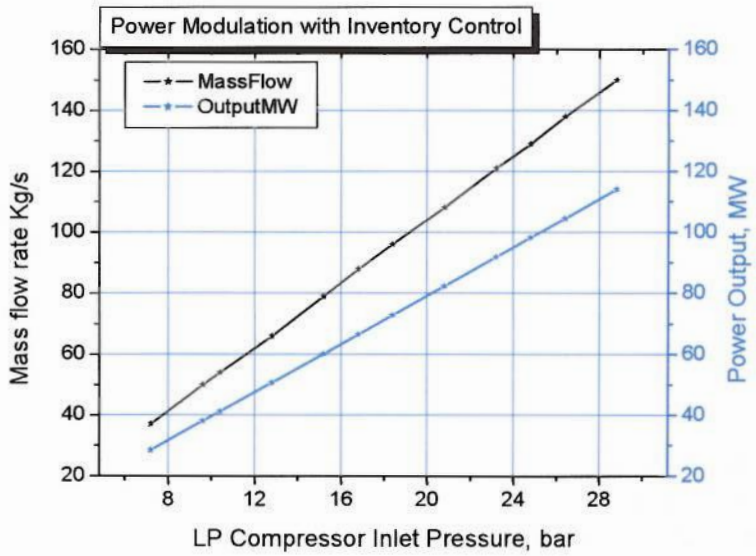

Figure 5.19 Effect of change in the system pressure (LPC inlet Pressure shown) on the plant output. The efficiency, Pressure Ratio, TET are theoretically constant for the whole range.

Fig 5.19 gives the relationship between the mass flow and the generator output at various system pressure. This is the behaviour of the system during a load ramping using inventory control. The PBMR plan to use the inventory control system to do the load variation at the rate of 10MW/min. The Figure 5.19 shows that, in order to achieve that target the pressure (absolute) change required is around 2.5 bar/min (calculated from the slope). Also the change in mass flow rate is 12.23 kg/sec/min.

Another use of the inventory control is its use for the load rejection when the inventory level in the system is only a fraction of the full load level. In this operation, the gas will be given into the LP inlet and taken out from the HP out let at the same time. This way it is possible to overload the turbines to reduce its speed.

During the inventory supply, the LPC inlet mass flow rate and pressure will increase. This will take the operating line from surge to the choke region and the HP compressor will not be affected. During the inventory discharge, the HP compressor exit velocity will increase which will improve its surge situation. When both supply and discharge are used, it will be similar to the bypass operation as explained earlier.

5.13 Conclusion on Performance Analysis

Closed cycle gas turbine plant offers some of the unique opportunities in performance and control. Some of the conclusions derived from this exercise are

1. Different loads can be attained without moving from the compressor characteristic design point. This is done by changing the pressure level in the system. For a power reduction to 40% of full load the efficiency remains the same.

2. The TET is not supposed to go up in the PBMR design. This is due to the negative reactivity, which reduces the release of heat in the event of a temperature rise. This neutronic action is instantaneous. However the fuel particles are coated and surrounded by other low conducting materials like graphite. Hence there will be a time delay in the response to a rise in TET. In the event of a rising TET, the power available to the turbine will go up provided the mass flow remains same or higher. The possibility of a rise in temperature can happen only when there is a reduction in the mass flow rate through the reactor. This means, a temperature rise will be accompanied by a fall in mass flow. This may keep the turbine power constant.

3. The only practical possibility of turbine power going up is when the mass flow rate goes up. When the mass flow rate goes up, the reactor will release more heat to keep the temperature constant because the reactivity is a function of temperature and not the total heat. This will give more energy into the turbine, which will increase the speed and can take the compressor to surge. The possibility of high mass flow through the turbine is when the bypass valve closes or when the pressure level in the system increases.

The bypass valve operation has to be optimised to keep the shaft speed constant. A slow operating valve will give enough time for the compressor to increase its resistance against a rising turbine power.

Chapter 6

Start-up and Shutdown

The design of power plants focuses on steady-state operation and high efficiency at full load. However the start-up and shutdown procedures in a plant are events that occur quite frequently. Even large power plants that have been designed originally for base load operation are reported to go through several start-ups in a year. The control of these start-up procedures is important because the life span of power plants is severely affected by thermal stresses caused by temperature gradients in turbines. A start-up design based on thermal stress alone will result in a slow start-up procedure that takes long time to reach the desired load. On the other hand the start-up should be accomplished in the shortest time for economic and other operational reasons.
Gas turbines are self-starting, it being necessary to rotate the turbo-compressor unit to a minimum idling speed by means of an external support. It would be necessary to bring the turbo-compressor unit up to idling speed, thus circulating a low flow of gas through the core, heating the gas, and ultimately bringing the gas turbine into a self-running condition. On shut down it would also be necessary to rotate the gas turbine from an external power source for a few hours in order to maintain a small gas through the reactor core to remove the radioactive decay heat from the core.

6.1 Start-up

6.1.1. Start-up using Electric Motor

A variable speed electric motor can be used to drive the Turbocompressor shaft to the self-sustaining speed to initiate the Brayton cycle as shown in Figure 6.1. The electric motor can be attached to the cold end of the shaft. The advantage of this system is its speed control ability. A very linear speed control of different slope can be achieved in this case and this will prevent the possibility of low speed surge in the compressor.

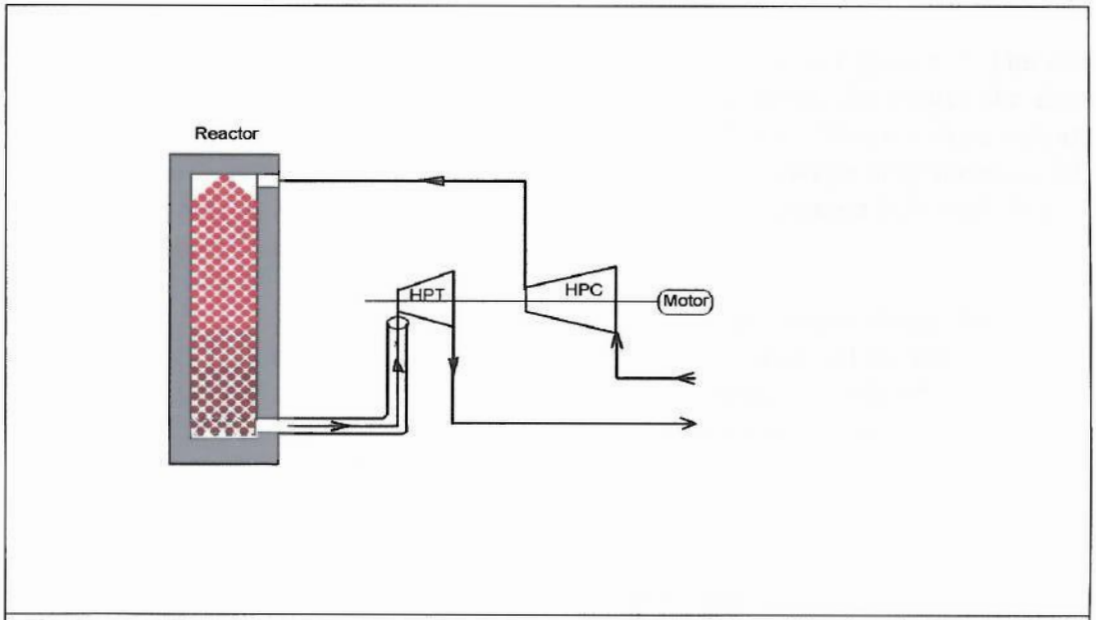

Figure 6.1 Conceptual Design of a Start-up arrangement with Electric Motor

The disadvantage is that this additional electrical system will be a redundant hardware during normal operation. This arrangement can also increase the required shaft length and hence the possibility of shaft vibration. In a helium environment the additional bearings required for the electric motor may cause problems due to the cold welding of helium. However a start-up motor without additional bearings (by placing the rotor windings on the existing shaft) can be a possibility, which is to be explored. For large industrial closed cycle units, the start-up motor capacity can be substantial. This will make the plant a load centre, which has to be catered by other generating stations, which may not be practical.

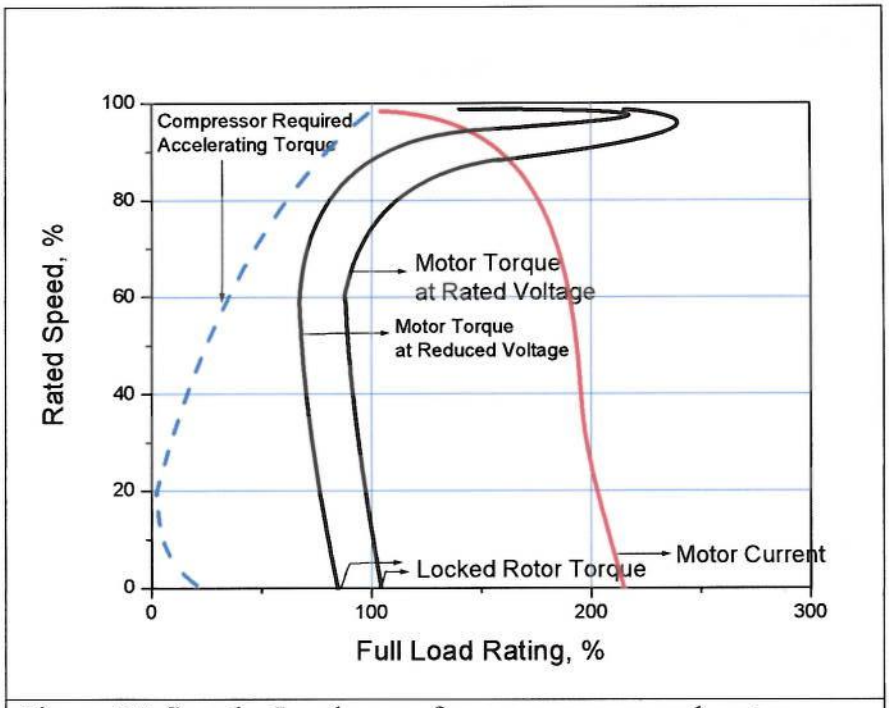

Figure 6.2 Speed – Load curve for a compressor and motor.

i) Starting Characteristics of the motor

Load curve for a compressor and motor are given in Figure 6.2. The closer the motor and compressor speed-load curves are to each other, the longer the driver will take to reach full speed, and the hotter the motor will get. Motor torque output varies approximately as the square of applied voltage. A 10 % voltage drop means a 20% drop in torque, which is enough to keep the drives from ever reaching full load. A lower than required voltage may appear as an overloaded compressor.

ii) Starting Time

If a motor has sufficient torque available at all points along the speed torque curve, the starting time can be calculated. An approximation of motor starting time can be obtained by summation of starting time increments calculated for several speed intervals. Small intervals are used when accelerating torque changes are large and large intervals when torque changes are small.

$$\Delta t = \frac{2\pi \Delta N}{\Delta T.g} WR^2 \quad \text{.....6.1}$$

where Δt =incremental starting time, ΔN =Speed Interval, ΔT = Average accelerating torque over the speed interval (difference between motor and load torque)

g= gravitational constant, WR^2=Torsional moment of inertia

An early appraisal of motor and compressor speed-torque characteristics, particularly at the reduced voltage occurring during starting is necessary. It is summarised below

Motor	Turbo-Compressor
1. Speed-torque curve 2. Speed –current curve 3. Moment of Inertia 4. Locked rotor power factor 5. Time constant for open circuit voltage. (when motor control will use delayed transfer to alternate sources on voltage loss).	1. Unloaded speed-torque curve (no flow) 2. Design point speed-torque curve 3. Moment of Inertia

6.1.2. Generator as Starting Motor.

In this arrangement, the electric generator (alternator) will run as a motor to initiate the flow. The compressor will have to achieve the self sustained flow before the electric power can be cut off. This is one of the most convenient ways to start the system. However this is not applicable on free power turbine arrangement without a compressor attached to it. Heavy-duty electricity generators may take substantial amount of power to reach the necessary speed to initiate the gas flow. In the PBMR design this is not possible due to the free power shaft arrangement.

6.1.3. Cold gas injection

In this arrangement, compressed helium is injected to the high pressure turbine to initiate the flow. The compressed helium can be obtained from the high pressure inventory tank or by using additional helium compressors or from pre-pressurized helium gas cylinders.

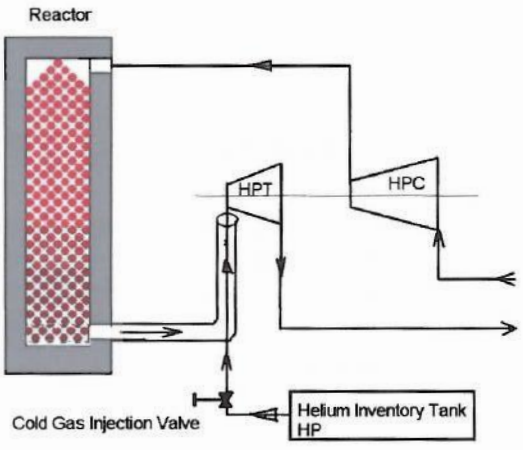

Figure 6.3 Suggested Start-up Arrangement with Cold Helium Injection

This is not an efficient way though it is simple compared to hot gas injection. For large closed power plants, the quantity of gas required can be substantial and also unsuccessful start-up attempts will empty the reserves quickly. Also it will increase the gas level in the system, which may not be necessary at low loads. In addition, it has to be pumped out to control the load. The acceleration rate is purely reliant on the quantity of the gas for a given system. If different acceleration rate has to be tried without increasing the pressure level in the system, some of the gas injected will have to be taken out.

The momentum of the gas is the driving source and hence the high momentum can create a gas bending stress on the blade, which may not be designed to take that type of load. This will require the need of a separate pony turbine attached to the shaft, which will complicate the design further.

6.1.4 Hot Gas Injection

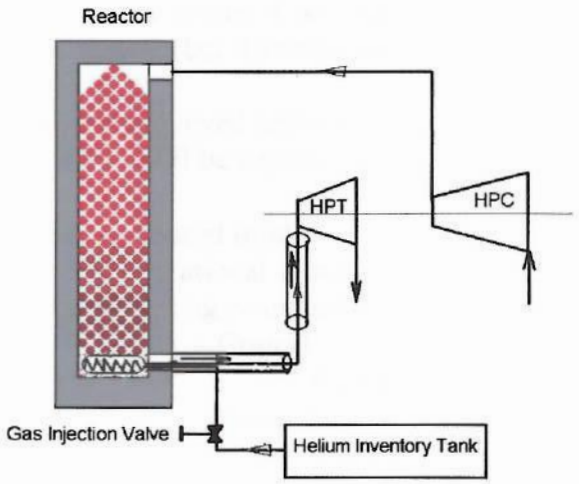

Figure 6.4 Suggested Start-up Arrangement with Hot Gas Injection

This system uses pressurized gas from a storage facility. The Brayton cycle heat source will heat up the gas. The hot gas will drive the gas turbines to attain the required speed. The advantage is that this system normally does not require much additional logistics. In some cases it may be required to introduce another heat exchanger in the main heat source to heat the injection gas. The disadvantage is that speed controls characteristics of a gas injection system are not as good as a motor start-up system. This is due to the delay and inaccuracies in the valve operation and heat addition.

i) Start-up arrangement

Out of various options for the start-up as mentioned above, a hot gas injection is suggested as given in Figure 6.4. In this a separate heat exchanger is suggested to heat the injection gas from the Helium Inventory vessel.

The philosophy is to get the best out of the limited amount of injection gas available for start-up. Since the volume of the Power conversion Unit and the Reactor are quite substantial for the quantity of injection gas, the injection pressure will be reduced drastically, if the high-pressure gas is released to the vessel. The system pressure is maintained at a low level (5bar) during start up, to keep the compressor load minimum. The injection pressure is 6 times than that of the system pressure.

An extra heat exchanger within the reactor will prevent the injection gas pressure loss. This will also reduce the distance required for the injection gas to reach the HP turbine. Once the system is self-sustained, the system pressure can be raised gradually.

ii) Description of Start

The start scenario depends on the current shutdown mode of the unit. The different modes are

1) Islanding. (Disconnected from grid, generation for station use only.)
2) Standby. Stable operation of thermodynamic cycle. Core critical. Plant is ready for ascension or shutdown.
3) Cold shutdown mode. Core sub-critical. Brayton cycle not operational. System pressure less than 1.1bar. Core temperature less than 250^0 C.

Once the system achieved self-sustaining speed, the start up gas injection will be closed and the inventory will be adjusted to the required level.

ii) Standby operational mode

Standby operational mode is one of the shutdown modes in which the plant is ready for power loading or unloading. The main system parameters during standby are

Core : Critical
Brayton Cycle : Operational
Heat Removal :Pre-cooler and Inter-cooler
Grid` : Not connected to grid
Generator electrical output : 0 MW
Core outlet temperature : 250^0 C $\leq$ T $\leq$ 900^0 C
System Pressure : 1.1 bar $\leq$ P $\leq$ 10 bar

A start-up from other modes such as cold or sub critical mode is not discussed here because of its irrelevance to the Brayton Cycle.

6.1.4.1 Start-up procedure with Hot Gas Injection

A brief start-up procedure is written based on the simulation results and findings.

1) Attain the standby mode. (As described above)
2) Open the Bypass valves. This will be bypassing much of the gas from the Reactor. This is to prevent any over speeding or early activation of the Brayton cycle.
3) Pressurize the system to 5bar using Helium Inventory System.

4) Helium from the inventory can be passed through the reactor to heat up the system to 300^0 C
5) The circulation of the hot gas is achieved by using the He inventory start up system to flow through the reactor, turbine, heat exchangers, and compressors and will be back to the inventory vessel. This way all the hardware will achieve the necessary thermal soaking.
6) Close the Bypass valve
7) Keep the compressor inlet guide vanes at its minimum (closed position)
8) Open the Gas Injection valve
9) Open the compressor inlet guide vanes
10) Once the self-sustaining speed, (based on the reactor outlet temperature) is reached, the injection valve start closing and the compressor IGVs will still be opening further.
11) Once the injection valves are fully closed and the IGVs are fully opened, the shaft will stop accelerating further.
12) Further acceleration from the self-sustained stage to the design speed can be achieved by raising the Turbine entry temperature to the designed value.
13) Any shortfall can be adjusted by raising the level of inventory by passing more gas into the low-pressure compressor inlet. This will create a dip in the speed for a short duration because the compressor will be processing more gas for the same turbine power until that added gas reaches the reactor and turbine.
14) Any unwanted acceleration at any stage can be stopped by opening the bypass valve.
15) Further loading to raise the power turbine shaft to the idling speed is achieved by raising the inventory only.
16) The compressor guide vanes will be adjusted to keep the surge margin during the inventory addition.

i) Self-sustaining speed

There is a minimum speed at which the Turbine output, without gas injection support, would be more than the compressor output and losses added together. At this point the gas injection can be stopped. This speed is the self-sustaining speed. The self-sustaining speed is a function of turbine entry temperature. The time and amount of gas required for successful start depends on the pressure level of the system, Turbine entry temperature and self-sustaining speed.

ii) Simulation of Performance at low speed

It is extremely hard to simulate an actual start-up scenario due to the unavailability of compressor and turbine characteristics at low speed and low flow. In addition to that, Helium, having low molecular weight, will cause high-pressure losses at low Reynolds number. Since PBMR is still in its design stage, the approach here was to dictate and design the final performance based on normal industrial practice and available information on control hardware. This simulation has used the compressor and turbine map supplied by PBMR.

This exercise is based on the following:-

1. An extrapolation of operating line, which will be safe rather than efficient.
2. The characteristic of the Gas Injection Valve

3. Normal practice for the acceleration of turbomachinery shafts in the Power Generation Industry.
4. An assumed value of mass moment of Inertia
5. The compressor guide vanes are assumed to be able to control the flow as required in the process.
6. The assumptions in simulation attempt are to take the turbomachinery equipment to the speed from where detailed maps are available. These assumptions are based on normal practice and certain output requirements.

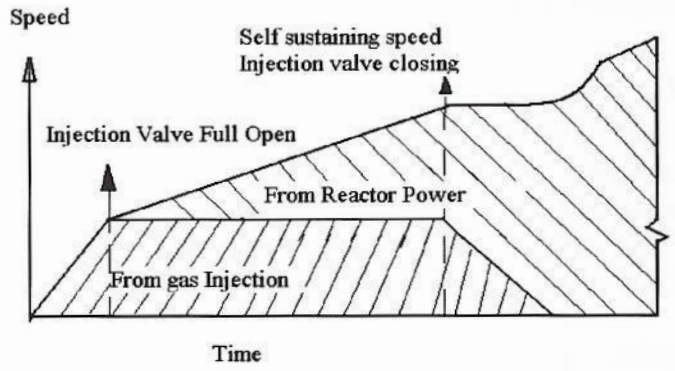

Figure 6.5 Philosophy of the gas Injection

iii) Theory

The Pressurized (30bar) gas from the Helium Inventory tank is passed through the heat exchanger placed in the reactor. The characteristic curve of a typical gas injection valve is given in Figure 6.6. The maximum capacity of the valve is chosen to be 15kg/s. The gas outlet temperature begins at 525K. The system pressure is 5 bar when the shafts are at zero speed.

1) A value for shaft acceleration is chosen based on the normal industrial practice. Acceleration from zero speed to 7000 rpm in 15 sec. has been chosen based on the industry practice.
2) The actuator's (on gas injection valve) acting time and the flow rate (based on the characteristic curve) is scaled to match the shaft acceleration requirement. A final characteristic based on time is extracted (Figure 6.6).
3) The Compressor flow is the extrapolated flow on the safe side. This is equated to the shaft acceleration requirement to obtain the curve in the (Figure.6.7)
4) The required starting speed (as shown in Figure 6.10 and Figure 6.12) is calculated by converting required Compressor work and losses into acceleration.

$$m.Cp.\Delta T + Losses = \frac{1}{2} I\omega^2 \quad \ldots\ldots\ldots\ldots 6.2$$

5) The Turbine flow at the start is same as the flow through the valve with a time delay and the turbine work is calculated for a particular TET
6) The guide vanes are assumed to throttle the flow. The difference in the turbine and compressor flow is accumulated in the Pressure Vessel as given in the Figure 6.8

$$Quantity\ of\ gas = \int_0^t f(x_2) - \int_0^t f(x_1) \quad \ldots\ldots\ldots\ldots 6.3$$

The pressure rise in the vessel can be calculated. This is negligible for large units. The total quantity of gas accumulated in this simulation is 45.69 kg, which is not significant, compared to the full load inventory of 2500kg in the system.

7) The turbine flow in the new time step will be the flow through the valve and the compressor flow. This is obtained from Figure 6.6 and Figure 6.7

$$m_{Turbine} = m_{Compressor} + m_{GasInjection} \quad \ldots\ldots\ldots\ldots 6.4$$

$$Turbine\ Work = (m_{Compressor} + m_{GasInjection}).C_p.\Delta T_T \quad \ldots\ldots\ldots 6.5$$

8) The new turbine work is calculated. The difference between the works is converted to acceleration as shown in Figure.6.12 for various TETs. As the TET increases, the speed reaches the required target quickly.
9) Self-sustaining speed is the speed at which the Turbine work by the gas in the system (without the external injection) will be more than the compressor work and the losses.
10) This can be found by calculating the turbine work without injection mass flow using the normal maps This is again based on an assumption that self-sustaining speed will be in a region where maps are available.
11) Once the shaft speed reaches the required speed as given in Figure 6.5, the injection valve can be closed gradually. The shaft speed will reduce for a while due to the reduction in the turbine flow. However, this can be compensated by increasing the compressor flow until it becomes equal to the turbine flow. In this simulation, the gas injection valve is assumed to be closing at the same rate as it was for opening.

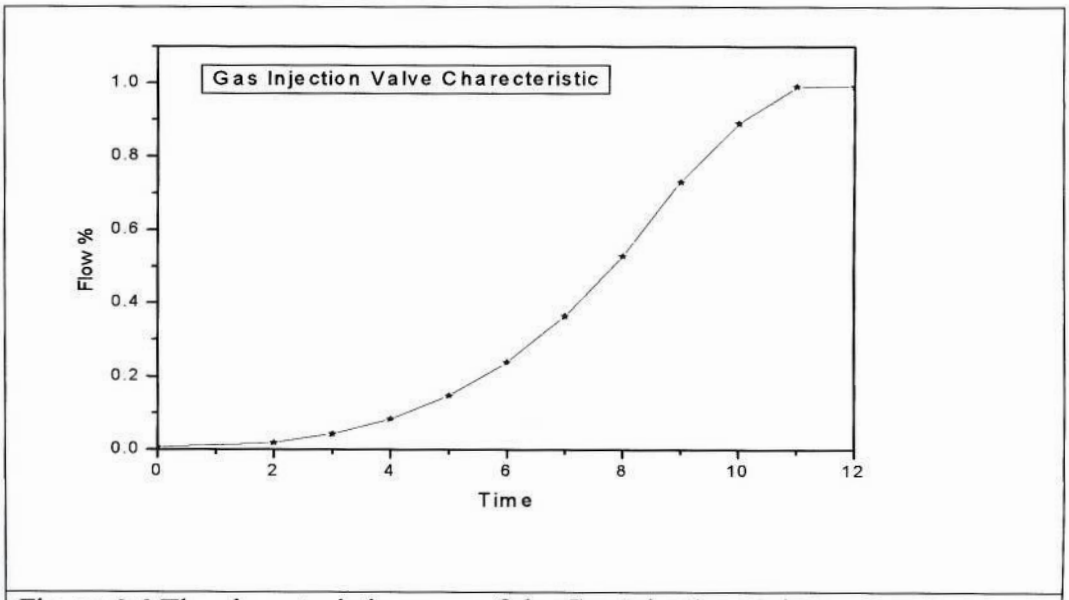

Figure 6.6 The characteristic curve of the Gas Injection Valve

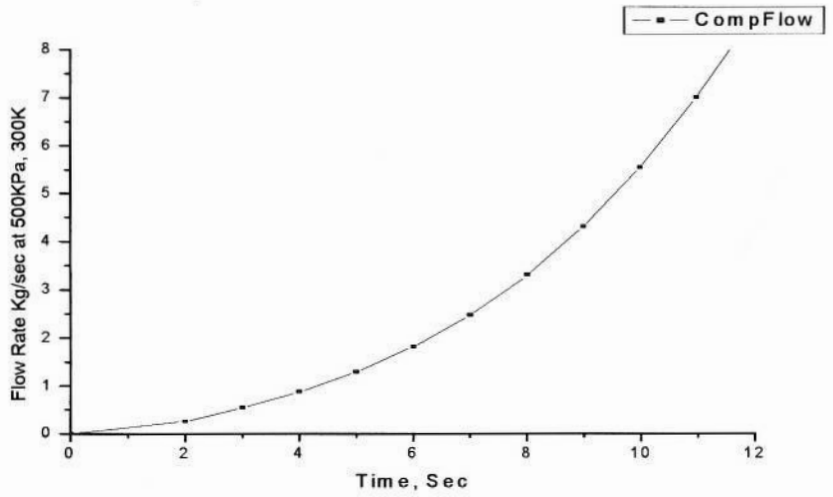

Figure 6.7 Compressor flow during start-up. Extrapolated from the map

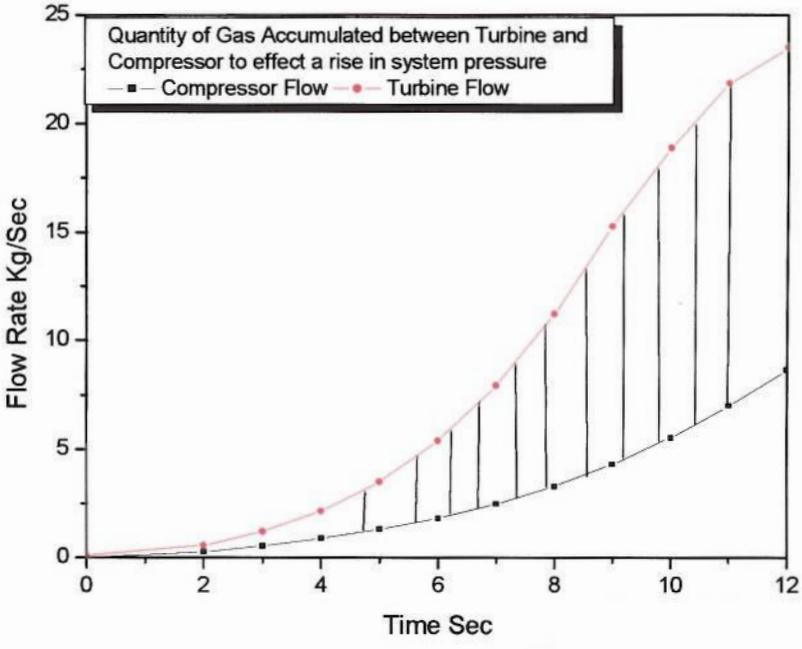

Figure 6.8 Gas accumulation in the Pressure Vessel during start-up

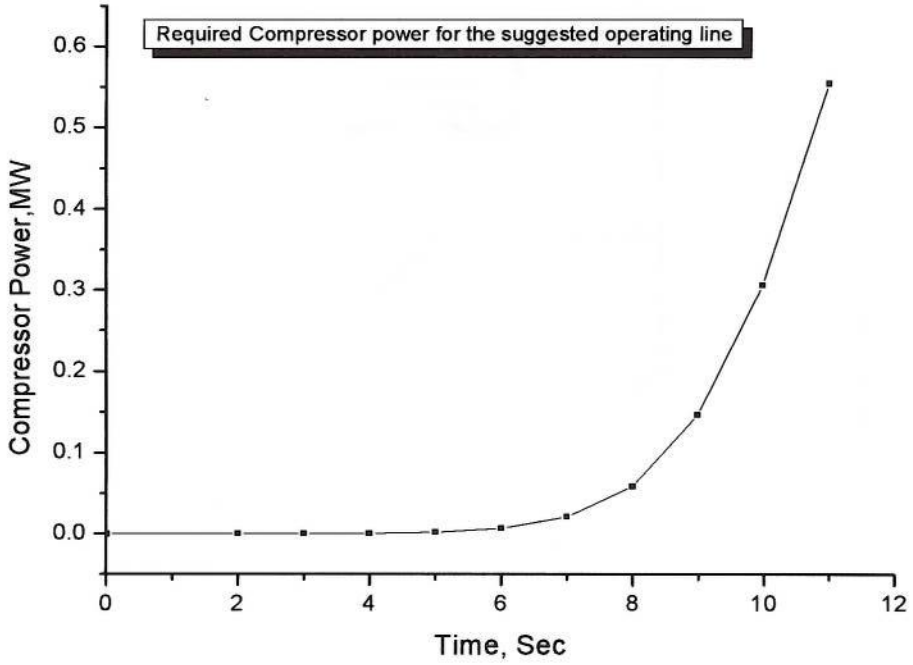

Figure 6.9 Required Compressor Power

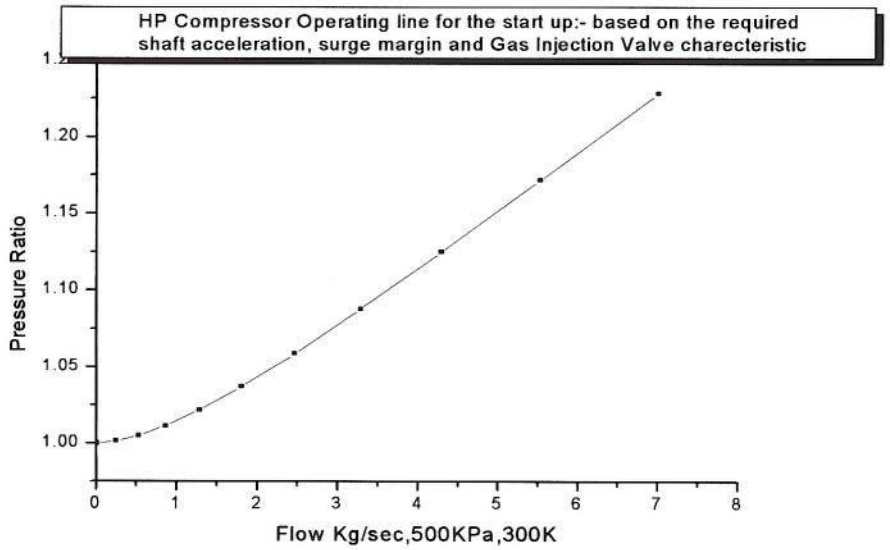

Figure 6.10 Extrapolated operating line of HP Compressor

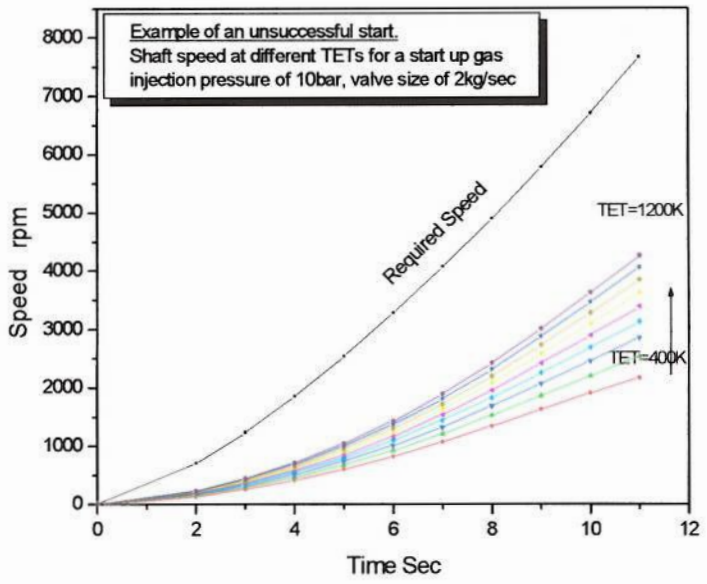

Figure 6.11 An Unsuccessful Start

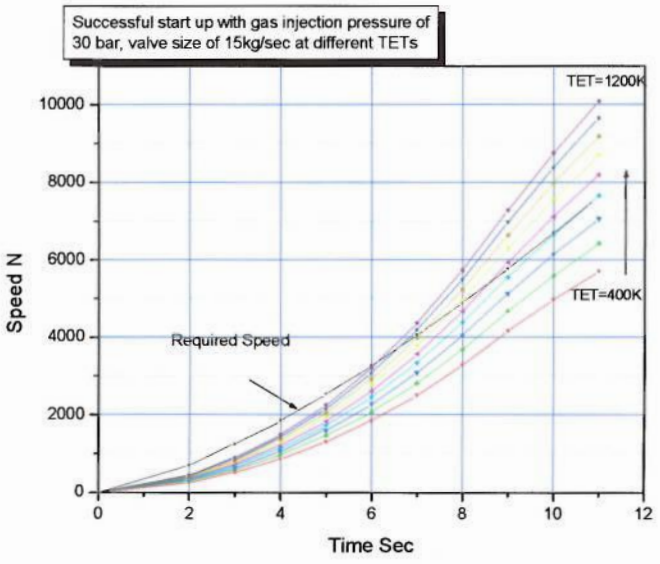

Figure 6.12 Successful Start-up

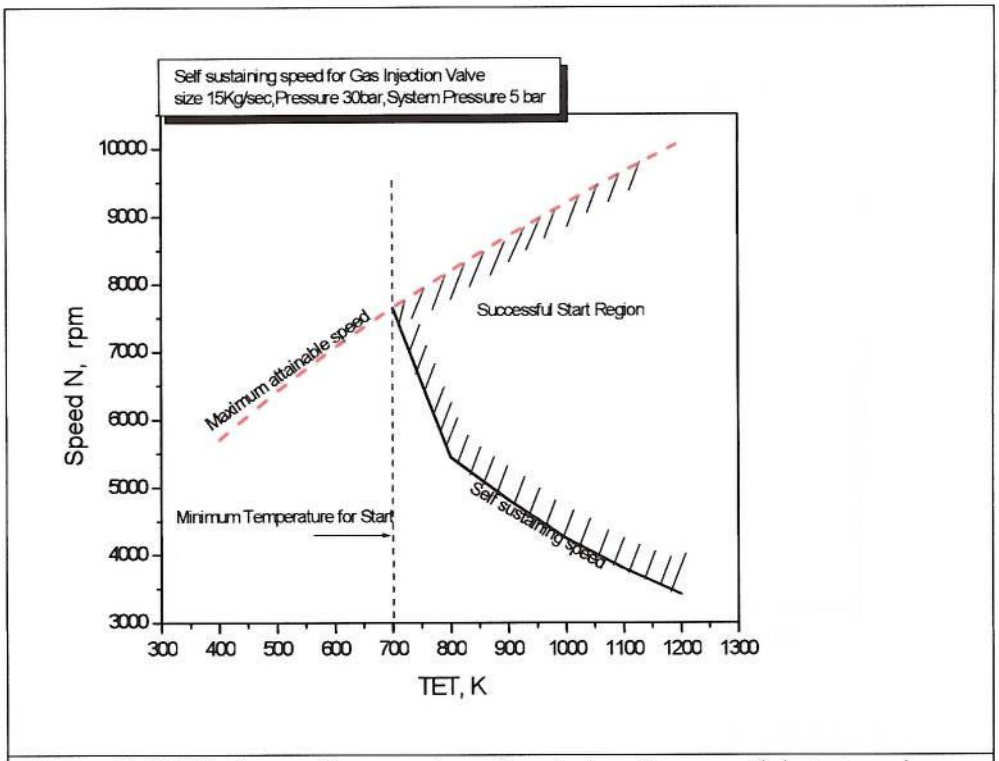

Figure 6.13 Minimum Temperature for start and successful start region.

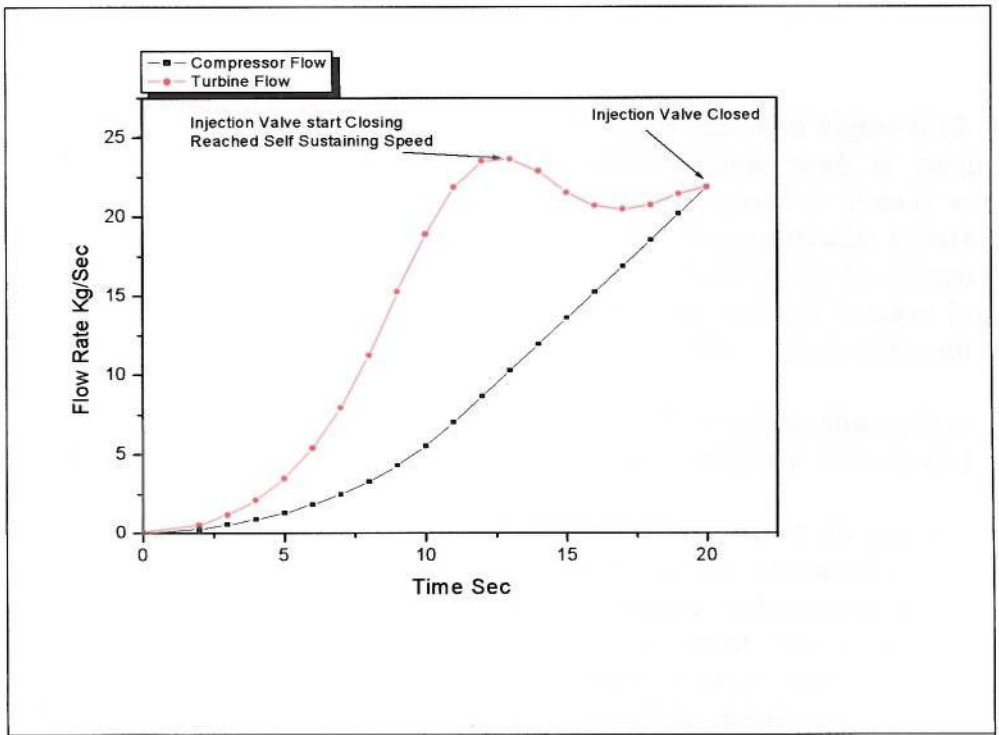

Figure 6.14 Turbine and compressor mass flow during the start-up

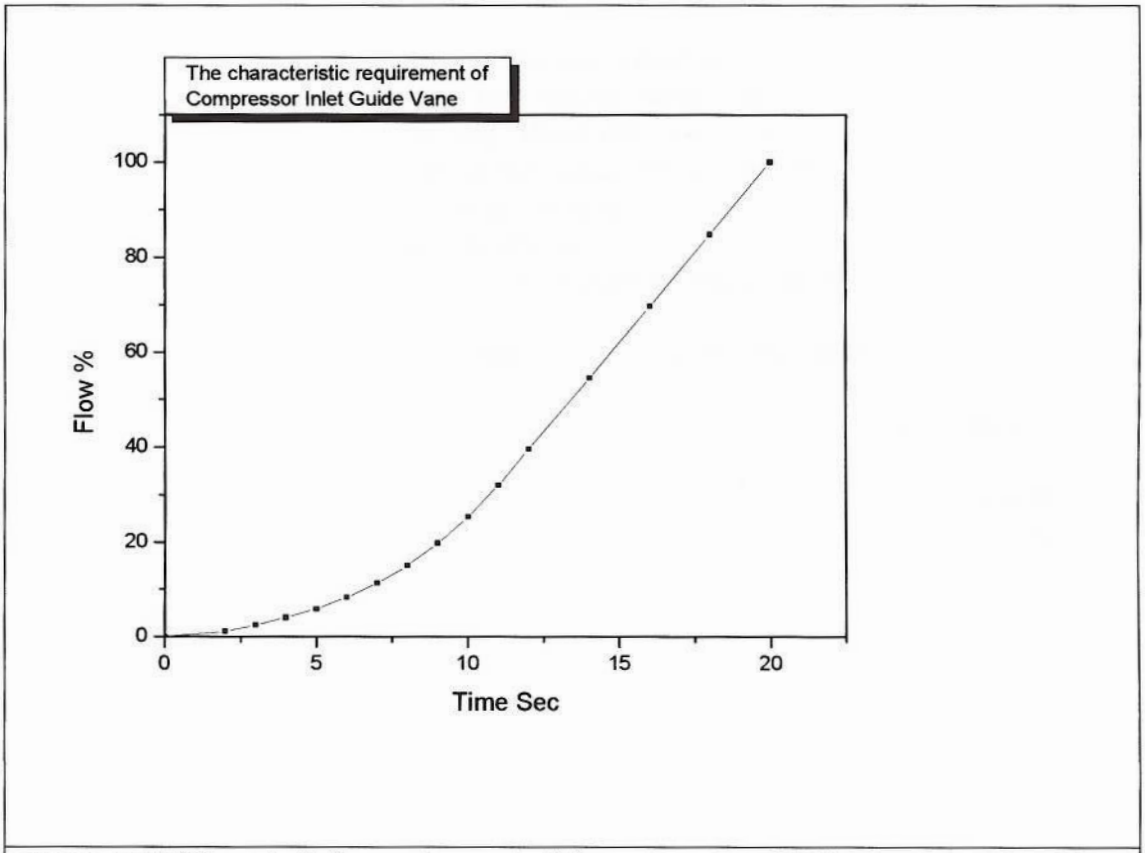

Figure 6.15 Characteristic requirement of the compressor IGV.

iv) Successful Start Region

A successful start region can be drawn as shown in Figure 6.12. The maximum attainable speed is the one when the whole turbine work is being used for the acceleration of the shaft only. The self-sustaining speed is already explained above. There is a minimum required temperature to start for a particular injection pressure and valve size. An attempt below this temperature will not bring the system to the required speed because the system pressure level will keep rising if it takes long to close the injection valve. As the pressure level and density rises, the compressor work will also increase proportionate to the turbine work.

It is advisable to start the injection with a temperature close to the design temperature. A start-up with high TET will be an efficient start-up and it requires less amount of gas.

The additional heat exchanger suggested will be of no use during the normal operation. However, the possibility of using it as an additional device to control the speed during sudden load variation can be explored. A hot gas injection during normal running will have a significant impact on the speed. The overheating of this heat exchanger can be prevented by keeping a small flow of high pressure gas through the heat exchanger throughout the whole duration of the speed variation.

6.2 Shutdown

There are different modes of shutdown which exist in a PBMR design. However these are all the sub divisions of two major modes such as Normal Shutdown and Emergency Shutdown. The normal shutdown mode would be used for planned shutdown and the emergency shut down would be used to shut the system down in the event of a failure, which might damage the system.
Some of the challenges of the shut down are

1. Over speeding of the power turbine shaft during a load shedding and subsequent grid separation.
2. Slow deceleration of the shafts, which causes the shafts to pass through the critical velocity very slowly.
3. Thermal stress in the system due to the sudden decrease in temperature.

The PBMR closed cycle system carries 2400kg of gas in the system and the inventory system carries another 2600kg outside the pressure vessel system. A hypothetical inventory valve is studied to simulate the response of the shaft speed and shutdown.

6.2.1 Normal Planned Shutdown

The generator power output, during a normal shutdown, can be reduced by controlling either the reactor temperature or by reducing the pressure level in the system by tapping the inventory out of the vessel or a combination of both. The reactor outlet temperature can be reduced by reducing the reactivity or by bypassing the cold side of the recuperator. The recuperator bypass will prevent the gas from taking heat from the outgoing gas from the power turbine. Then extra cooling has to be done in the pre-cooler to bring the exhaust gas to design temperature. Bypassing the recuperator can be critical to the reactor as well.

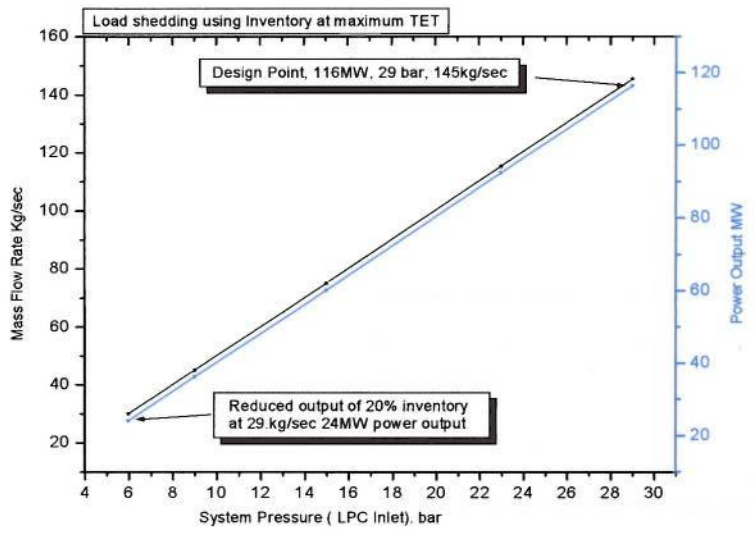

Figure 6. 16 Load shedding using pressure level control in the Brayton Cycle at constant Turbine Entry Temperature.

Figure 6.16 is the result of the simulation of a load shedding from full to 20% load. This is done by reducing pressure level in the Brayton cycle from a full load pressure of 29 bar to 6 bar. The designed mass flow rate will be reduced from 145kg/sec to 29kg/sec and the generator output will be reduced from 116MW to 24MW. This simulation is done at constant turbine entry temperature. All the 3 shafts will be running at the designed speed and the system will be performing at a scaled down manner. The Reynolds number losses below 20% inventory will be severe and hence an inventory alone load shedding is not performed for below 20% pressure level.

In this process the energy is being taken away from the system through the tapping of compressed gas into the inventory system. Hence, even in this load shedding process, turbine power output remains equal to the compressor power input and hence the shaft speeds remain constant.

The above mentioned load reduction is only the first stage and the next step is to reduce the generator output from 24MW to 0 MW without reducing the power turbine shaft speed to be in the synchronous idling mode. The generator shaft will be running at 3000rpm and producing no electricity. The power turbine is delivering power just to overcome the frictional losses of the shaft.

This is achieved by reducing the turbine entry temperature continuously until the electric output becomes zero and the alternator is disconnected from the grid. This will bring the shaft to idle running.

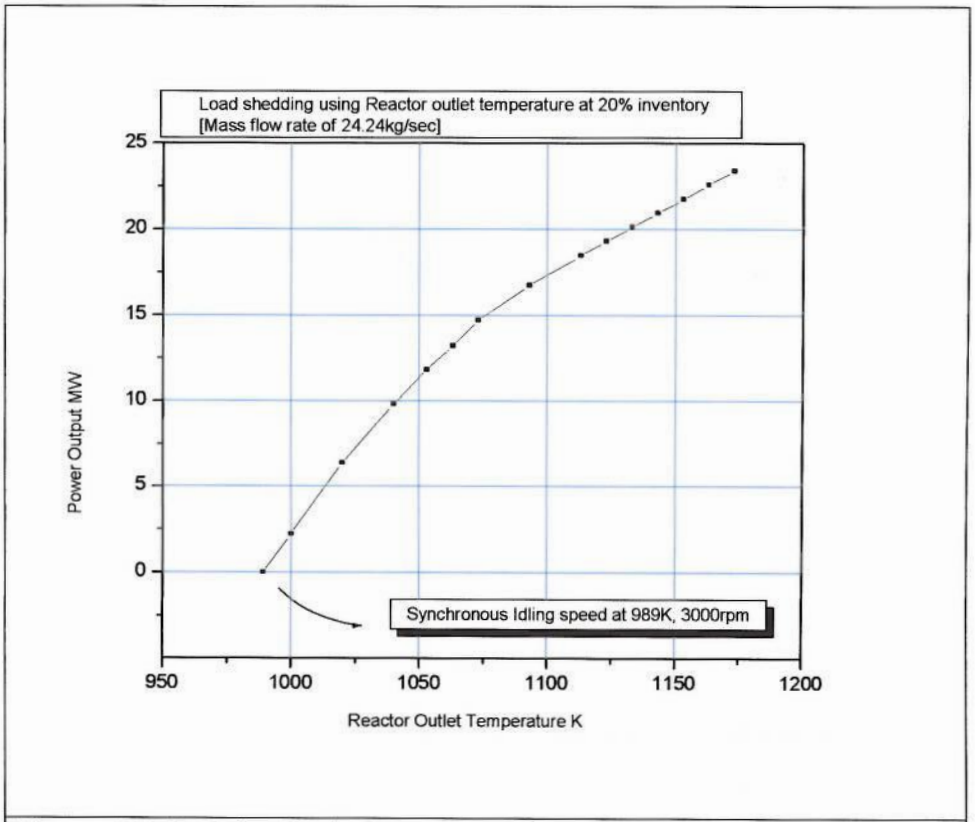

Figure 6.17 Load reduction from 20% to synchronous idling using Reactor temperature control

Figure 6.17 shows the reactor outlet temperature at which the generator is idling at synchronous speed for a pressure level of 20%. The low Reynolds number pressure losses are ignored in this run.

As the TET reduces, the compressor power input would be more than the turbine power output, which causes the speed to fall with continuously growing gradient. The bypass valves, which help the gas to bypass the reactor, can be opened to prevent the speed passing through critical speeds too slowly. The gas bypass valves helps to overload the compressor to decelerate further.

During normal shutdown, heat recovery from the recuperator can also be bypassed. This sudden response on the reactor outlet temperature The PBMR design does not have a recuperator cold side bypass at present.

6.2.1.1 Three Stages of Normal Shutdown

i) Stage I- Load reduction from 100% to 20% using Helium Inventory Control.

The total gas in the system during normal operation is 2400kg and 20% is 480 kg of gas. The difference of 1920kg of gas has to be driven out during the normal shutdown process.

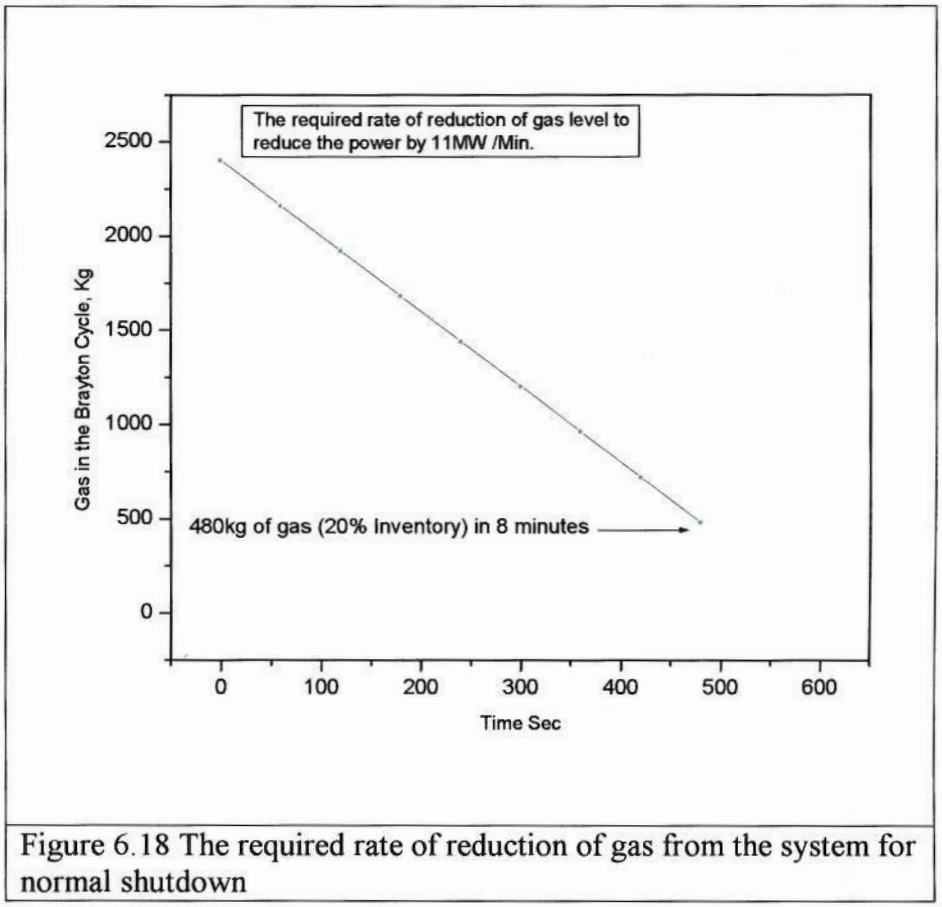

Figure 6.18 The required rate of reduction of gas from the system for normal shutdown

A control valve is specified here to achieve the targeted normal load shedding. Figure 6.18 shows the required characteristic of a control valve for achieving a normal shutdown of 10% per minute. This valve will be discharging 1920kg of gas in 8 minutes. The maximum flow capacity should be 4.125kg/sec and will be operating at a differential pressure of 70/40 bar.

Figure 6.19 shows the valve operation during the normal shutdown. The valve takes 9 sec from full closed position to full open. It takes same time for the closing also. The area under the curve shows the total quantity of gas discharged during the process.

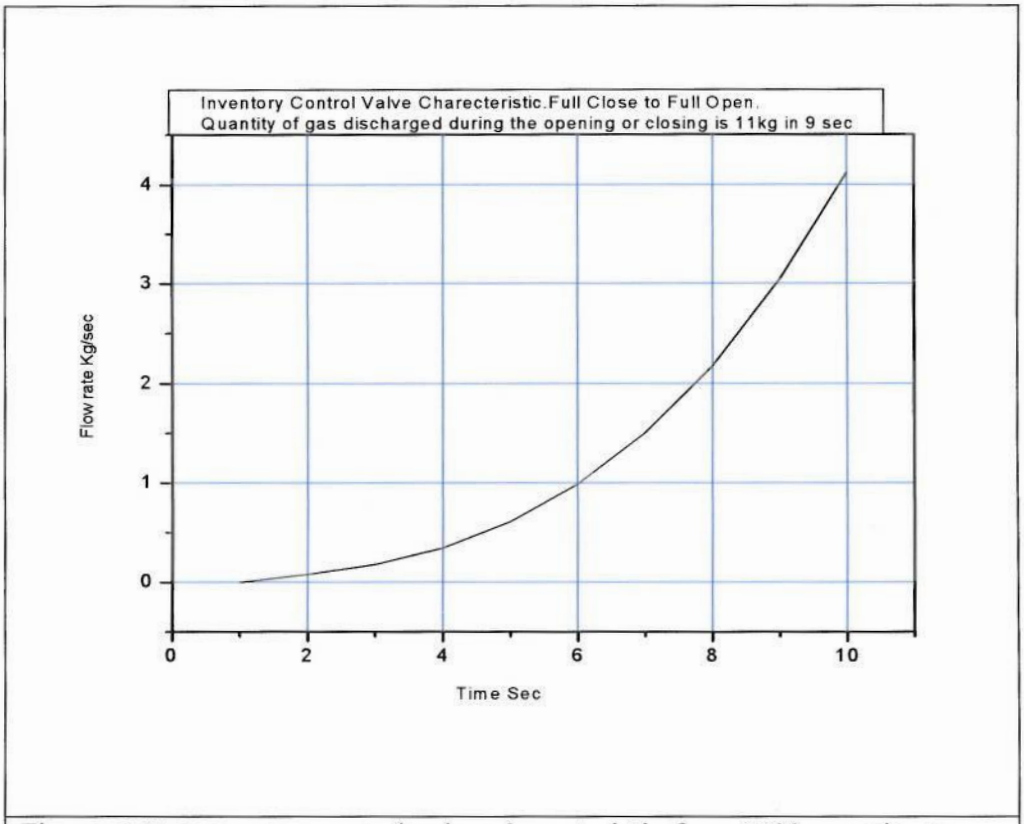

Figure 6.19 Inventory control valve characteristic for a 10% per minute normal shutdown.

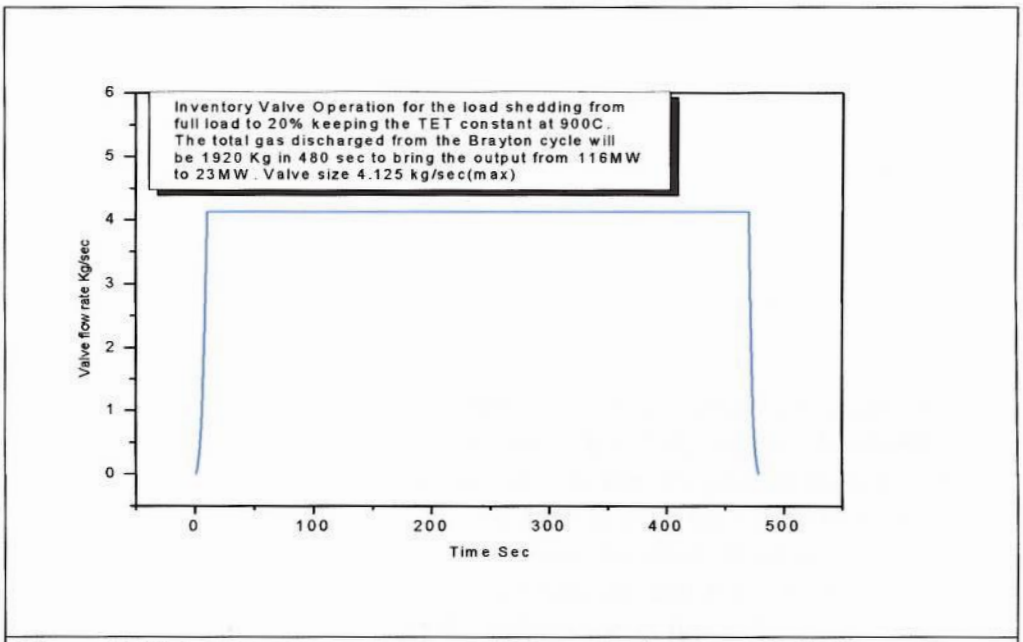

Figure 6.20 Inventory valve operation to bring the Brayton Cycle pressure level to 20%.

ii) Stage II- Load reduction from 20% to Synchronous Idling

Once the pressure level reaches 20%, further reduction in load should be accompanied by reduction in temperature as well. This will prevent the overheating of any component in the absence of necessary heat transfer due to the lack of gas flow. Figure 6.17 estimate the point at which the system reaches synchronous idling with 20% pressure level.

During reactor temperature control, the system components will be more dynamic compared to inventory control. The LP and HP compressors are identical and the compressor inlet gas temperature will always be maintained at 300K using the intercooler and pre-cooler irrespective of the dynamics of other components. However, as the reactor outlet temperature changes the two turbomachineries will show different rate of response. The surge margins will be different. Figure 6.21 shows the turbocompressor speed during the temperature control. As we can see the HP shaft is steadier against a drop in temperature because the efficiency is proportional to temperature and hence LP shaft will be less efficient.

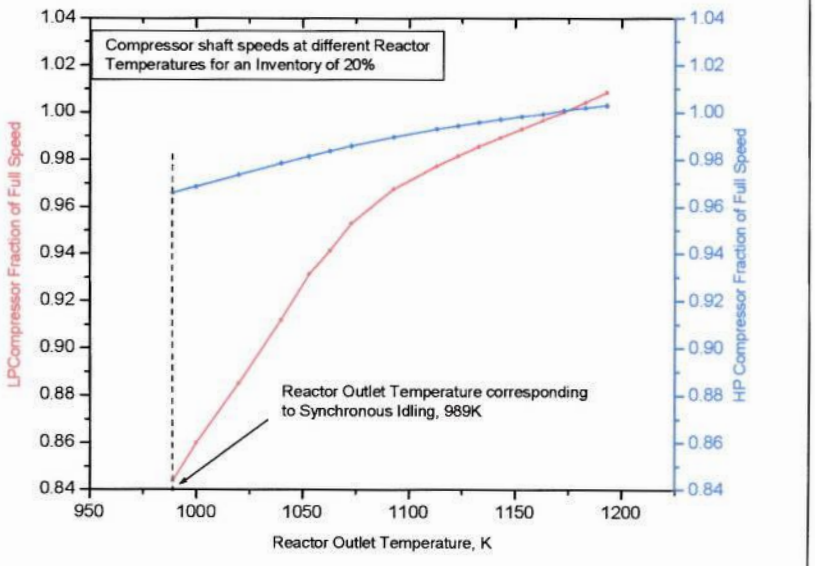

Figure 6.21 LP and HP shaft speed during the load shedding from 20% to idling using Temperature control.

As mentioned earlier, the reduction in temperature is achieved by reducing the reactivity or by bypassing the gas from the recuperator. A normal speed reduction happens when the turbine power is less than the compressor power. When the TET goes down the Turbine work reduces and technically, the compressor power will be more than the turbine input. This will slow down the shaft to settle at a lower level. Since the gas velocity in the PBMR design is 100m/sec and the total length of the gas route is small the time taken to adjust the imbalance is ignored in this. Hence Figure 6.22 is obtained with the LP compressor and Turbine powers matching on the same line but the speed is reducing. The shaft speed is following the trend.

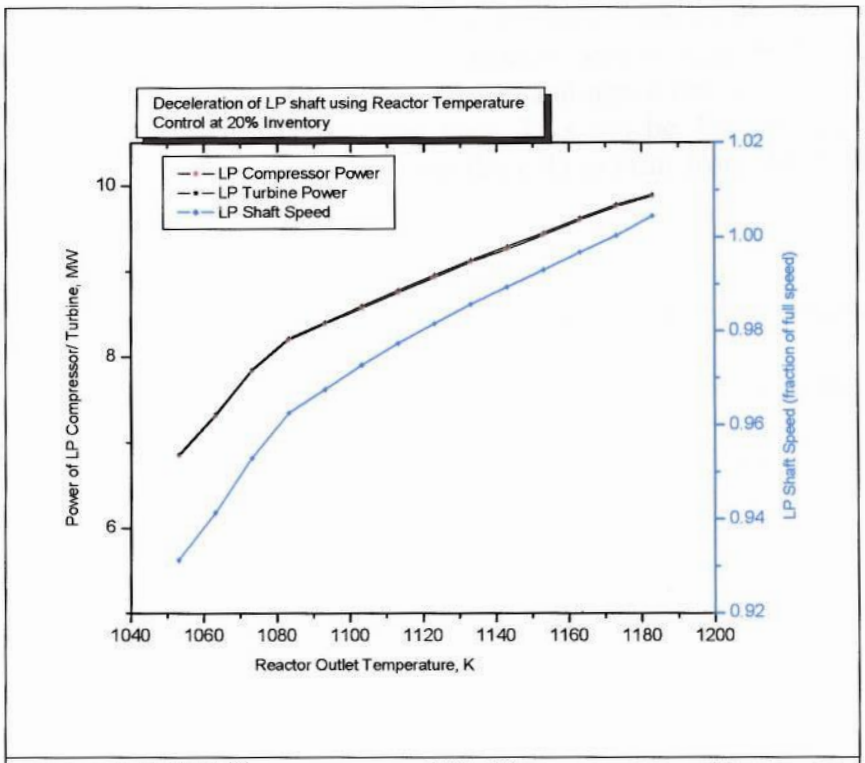

Figure 6.22 LP Compressor and Turbine power matching

iii) Stage - III Speed Reduction from Synchronous Idling to Full stop.

This can be achieved by either

1. Reducing the reactor outlet temperature
2. Reducing the inventory
3. Overloading the compressors by opening the bypass at the HP outlet
4. Overloading the compressor by opening the Inventory inlet and exit valves together.
5. Overloading the turbo generator shaft with a resistor bank to stop that particular shaft.
6. A combination of some or all of the above.

A slow speed reduction can be harmful if the shaft speed is going through the critical speeds slowly. This can happen if the speed reduction is by temperature control alone. Reactor temperature control is slow compared to other measures. Also a sudden reduction in the temperature may not be advisable due to potential thermal stresses.

Overloading the turbo-generator shaft to stop it from idling stage has to be done only when the temperature has reached low enough to prevent the formation of hot spots due to the lack of flow. Once the shaft become stationary, the turbine and compressor will act as mere pressure drops and a high temperature gas circulation may not be advisable.

iv) Stage - IV Barring of the Shafts

This is to prevent the shafts from bending or buckling when it comes to stationary at high temperatures. This is done by running the shaft at low speed (typically 30rpm) for several hours until it becomes cold enough. In the PBMR design all the 3 shafts are exposed to high temperatures and hence barring has to be done on all of them at the end of a shutdown from load. This can be done by separate electrical motors attached to the shafts or by using the cold helium from the inventory tank to turn the turbines.

6.2.2 Procedure for a normal shutdown

A procedure is written for a normal shutdown from the finding of the simulation model.

1. Open the inventory valve from the HP compressor outlet to the inventory tank. The normal opening time is 9sec. The maximum flow rate will be 4.125kg/sec.
2. Reduce the power output from the generator at the rate of 10%MW/min (or at a rate specified by the user) by reducing the Helium inventory.
3. Any temperature excursion has to be arrested by adjusting the reactivity. The precision control of the power turbine has to be done by cold bypass valve.
4. At 20% inventory or at a system pressure of 5.8bar, shut the inventory valve and the power output will be stabilised at 23.5MW.
5. Start reducing the reactor outlet temperature. At 989K, the power turbine will be running at synchronous idling. This means the power shaft is running at 3000 rpm and disconnected from the grid hence producing no electrical output. The energy available is just to overcome the frictional losses. The LP turbocompressor shaft will be running at a lower speed than the HP turbocompressor shaft. Here also, the precise speed maintenance of the power shaft can be done by cold bypass valves. The Brayton cycle is still fully operational and hence it is possible to reload the system if necessary.
6. The complete shutdown is achieved by further reducing the Turbine Entry Temperature to reduce the speed from synchronous idling to full stop. During this process, below certain TET, the turbocompressors gets into the unstable region. This happens typically below 40% of the design speed. To pass through this region quickly and to bring the shafts to rest, bypass valves can be opened to reduce the power input to the turbine and keep the compressor flow constant.
7. The turbogenerator can be overloaded with the help of resistor banks to reduce the generator shaft speed.
8. The turbocompressor and power turbine shafts are to be kept running at low rpm (barring) until the shafts are cooled enough to avoid any bending or buckling. This can be done by small electric motors attached to the shafts or by using cold or hot gas injection.

6.2.3 Possibility and Effect of Temperature Excursion

The reactor gas outlet temperature remains almost same due to negative reactivity. An excursion of temperature may happen for a very short period of time (less than a minute as per PBMR spec) due to the thermal properties of graphite around the fuel. The system pressure will be coming down as the inventory reduces. This will not have much adverse effect on the compressor operating lines because the gas will be taken out of the system from the outlet of the compressor, which will push the operating line further away from the surge line. The quantity of cooling water circulating through

the pre-cooler has to be adjusted to balance with the higher temperature at the hot gas outlet temperature. This will be a momentary effect due to the sudden reduction in the gas through the cold side of the recuperator.

6.2.4 Factors Affecting the Rate of Deceleration.

The main concern during the slow down will be to maintain the compressor surge margin and escaping from the critical speeds. The possibility of the surge is low due to the presence of inventory valves and bypass valves, which reduces the resistance at the compressor exit. However quick opening of the inventory valve can increase the speed of the compressor and can push the operating line towards the surge line. This is due to the excess Turbine work available for a short period of time, which drives the turbocompressor shafts. This can be avoided by optimising the rate of opening of the Inventory valves.

During the deceleration the turbocompressor shafts can pass through the critical velocity by opening the bypass as mentioned earlier. Another way to solve this problem is to bring down the power output to the possible minimum by reducing the pressure level, using inventory and then overload the compressor with fresh supply of gas from the inventory system. However the gas has to be channelled back to the inventory vessel from the exit of the HP compressor otherwise the Brayton Cycle will re-energized due to high amount of gas going through the reactor. This overloading of the compressor can increase the deceleration rate drastically. The power turbine shaft speed from idling to full stop can be achieved by loading the alternator with resistor load.

6.2.5 Efficiency during the Shutdown process.

Efficiency, during the normal shutdown process, can be maintained, if it is done by reducing the pressure level gradually. If the power is reduced using bypass valve, the efficiency will be reduced linearly to the power output. Even with the inventory controlled power reduction, efficiency at low load will be linear to the power output. Compared to other challenges and complexities involved during shutdown, maintaining efficiency will be a low priority. However, a very slow shutdown due to any specific grid requirement requires an efficient process.

Assumptions made in the simulation

1. The unloading rate is 10%/min. Hence the inventory is reduced from 2400 kg at 29 bar system inlet pressure to 5.8 bar at the rate of 4.125kg/sec to match that unloading requirement.
2. The bypass valve which bypasses gas from the reactor remains closed during normal shutdown simulation
3. All the three shafts are maintaining design speed when the load is brought down from full load to synchronous idling.
4. The required inventory for the synchronous idling is calculated at the maximum TET (1173K).
5. The TET is being brought down once the minimum required inventory level for the synchronous idling is reached.
6. An inventory of 20% is selected and found the corresponding TET to keep the plant running at synchronous idling.

6.2.6 Unplanned Shutdown with or without grid separation

Unplanned shutdown happen when there is sudden reduction in load demand from the grid. The challenge is that the system should be able to prevent the shafts from overrunning also it should keep the Brayton Cycle operational to be ready for any load recovery. The grid separation happens when the generator frequency does not match with the grid frequency. This can happen either due to the overloading of the generator or due to low demand from the grid.

The PBMR cold bypass helps to keep the generator speed constant. A resistor bank connected to the generator output prevents the shaft from over speeding. The resistor bank can act as a load centre (10- 20MW) for a short duration to compensate the time delay caused by the control hardware.

6.3 Conclusion on Start-up and Shutdown

A detailed analysis of various start-up and shutdown methods for a closed cycle multiple shaft arrangement has been carried out. The electrical motor starting will be simple and convenient, but extra hardware will not be useful for normal operation. Cold gas injection is simple but inefficient. Unsuccessful start-ups can increase the inventory, which will have to be pumped back.

A hot gas injection method has been suggested here. In this the gas will be heated before injecting into the HP turbine. This is an efficient way and also obviates the need of any extra hardware on the shaft such as pony turbines. The drawback is to have a heating system for the start-up. If the reactor is not ready for it, a separate heating may not be practical. The starting time depends on the flow rate of valve and the gas temperature. A successful start region is mapped using a specific control valve and it gives certain temperature as the minimum required temperature to attain self-sustaining speed. A procedure is written based on the analysis.

Different mode of shutdown is also analysed. Normal shut down can be done by lowering the inventory level. The turbo-shaft speed can be reduced by overloading it using the bypass or by using the inventory inlet and exit together. The valve characteristics were derived for various type of shutdown. From the performance analysis it is found that around 30% of the bypass will be sufficient to bring the system to synchronous idling. Synchronous idling using bypass, is not recommended for long duration, as it is not efficient. An emergency shutdown will have to use interrupt valves to stop the Brayton cycle completely.

Chapter 7
CFD Model of the flow in the Pressure Vessel

A CFD analysis of the flow of the pressure vessel (Figure 7.1) has been carried out with the following objectives.

1. The pressure vessel of the PBMR is a unique arrangement for a power plant. The nature of flow between the HP compressor and the recuperator cold inlet through this vessel is not well understood because of its complex geometry. Hence a CFD analysis would contribute into a better understanding and could highlight whether any negative aspect in the flow here, which can affect the Brayton cycle. This will manifest as high total pressure loss, high velocity pockets or uneven velocity distribution. The incremental pressure loss from one end to the other can also be calculated which will help to redesign the vessel if necessary.

2. The PBMR will be relying on the inventory control system for its load operation. The efficiency down to 40% of the load will not be affected by the low inventory. But further down, the effect of low Reynolds number will play a role to bring the system efficiency down. Since the pressure vessel is carrying a substantial amount of gas at any moment in time, the low inventory flow through the vessel has to be analysed. A CFD analysis is carried out at various inventory level to find the absolute and percentile pressure losses.

7.1 Commercial CFD Programme Fluent / Gambit.

The CFD analysis has been carried out using the commercial CFD programme Fluent. Fluent is one of the most popular CFD package for modelling fluid flow, heat transfer and chemical reaction. It models this wide range of phenomena by solving the conservation equations for mass, momentum, energy and chemical species using a control volume approach. The governing equations are descretized on a curvilinear grid to enable computations to be performed in complex geometries. The equations are solved using the SIMPLE algorithm.

Each iteration of Fluent's basic solution procedure consists of the following steps.

1. The u, v and w momentum equations are solved in turn using an estimated pressure field to update the velocity field.
2. The pressure connection equation is then solved to update the pressure field. Corresponding adjustments to the velocity components are also made so that the mass continuity equation is satisfied locally.
3. For turbulent flows the relevant equations for the turbulence model are solved using the updated velocity field to obtain the distribution of the effective viscosity.
4. Fluid properties are updated.

These steps are continued until the error or residual in each conservation equation within each volume and hence over the global domain have increased to a prescribed

value. Fluent can solve the governing equations in a time dependent form. The spatial descretization remains the same as for the steady state case. Descretization in time involves the integration of every term in the differential equations over a time step Δt. This integration uses a fully implicit scheme giving unconditional stability. One of the main requirements for the computational solver is the ability to handle high Reynolds number flows. This is done through the use of turbulence models and wall functions.

In turbulent flows the velocity at a point is taken to be the sum of a mean, of time averaged, component and a fluctuating component. The subject of turbulence modelling is still unresolved and further advances are required for direct solutions of the Reynolds averaged equations to be feasible.

Within Fluent, three different turbulence models are included – Reynolds Stress model (RSM), k-ε and RNG k-ε. The Reynolds Stress Model involves seven equations and thus is computationally demanding. With just two equations required for closure the standard k-ε model is most commonly used. However, in regions of high streamline curvature, it can over predict the levels of turbulence energy, thus increasing local turbulence viscosity. This tends to over predict mixing and suppresses separation and fluctuations such as vortex shedding. Since the computational constraint was a factor due to the size of the model, the standard k-ε model was used.

Wall functions are empirical functions used at the near wall grid point to estimate the effect of the wall boundaries on the flow and are required to close the turbulence models in a boundary layer. The wall functions are based on the assumption that a fully developed equilibrium turbulent boundary layer exists and therefore all the flow properties can be obtained from the log law. This removes the need to place a lot of grid points in a boundary layer, thus reducing computational effort. For high Reynolds numbers a two layer based non equilibrium wall function is used which assumes wall neighbouring cells consists of a viscous sub layer and a fully turbulent layer.

7.2 Geometry

The geometry of the flow to be analysed is given in the Figure 7.1. It is the volumetric space between these two vessels when it is assembled as shown. The length of the vessel from left to right is around 20 m and the largest diameter is 5m. The pre cooler and the inter cooler will be placed at the bottom and the generator will be at the top of the vessel on the right hand side. All the 3 shafts are vertical.

The HP Compressor outlet is considered as inlet of the helium flow into the vessel. The inlet consists of 300 mm diameter ports around the inner chamber. The direction of the inlet flow is in the XZ plane. The recuperator cold side inlet is taken as outlet of the gas flow. The direction of the outlet flow is in the –Y direction. The connecting duct between the pressure vessel and the reactor (extreme left) is also taken, though the flow there is irrelevant in this analysis.

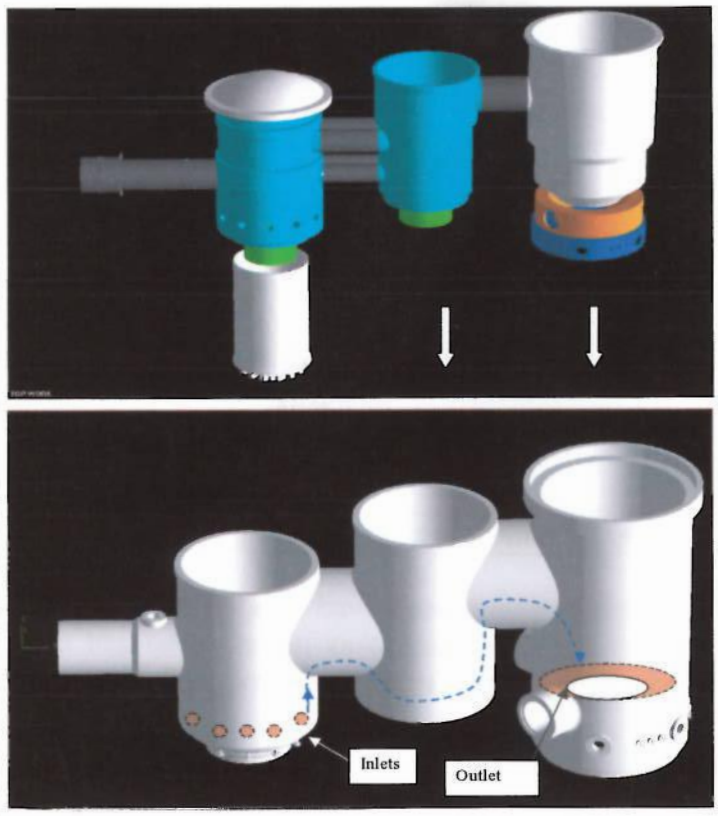

Figure 7.1 The Pressure Vessel assembly. The flow geometry is the volume created in the gap when these two vessels are assembled as shown.

7.3 Geometry creation using Gambit

The geometry was created using the dimensions taken from the Unigraphics model of the vessel supplied by Eskom-PBMR in South Africa. The first step was to create component volumes and then the final geometry was created by uniting component volumes together. The component volumes were created using the ready made three dimensional shapes available in the Gambit program. All the components are in the form of cylindrical shapes. Hence it was not necessary to start creating the geometry with points, lines, faces etc. Attempts were made to import the Unigraphics file directly into the mesh generation software called *Ideas*. However the attempt was not successful due to the lack of flexibility with the imported geometry. It was practically impossible to do any alteration on the imported file.

A volume was created in the beginning, which is the inner side profile of the outer vessel shown in the Fig 8.1. Another volume is created inside the first one, which has the outer side profile of the internal casing as shown in the Figure 8.1. Then the second volume was deducted from the first one in order to obtain the gap between these two vessels, which is the flow geometry.

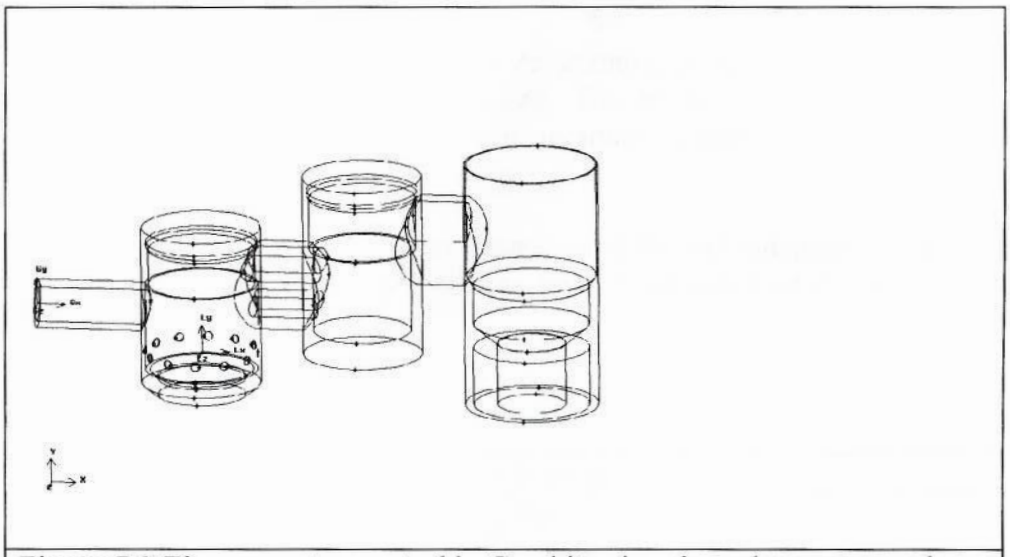

Figure 7.2 The geometry created in Gambit using the volume approach.

Twelve circular faces have been drawn to represent the inlet ports and a circular ring face has been chosen as output (Figure 7.1). The fluid is helium with default wall properties. The flow direction is perpendicular to the surface.

7.4 Mesh Generation.

Since the volume of the geometry is quite high, a cell size of 170mm has been taken for meshing. The total number of cells were exceeding the computational limit when lower sizes were tried. The surfaces were covered with triangular elements and the volume was filled with tetrahedral. The total number of cells were 230000. All the individual volumes were united to create a single one. This is done before meshing.

A smaller cell size was used for the inlet faces due to its own small sizes and to get a clear picture of the flow in those areas. The mesh size of 170mm for the geometry is at the expense of the accuracy and at a later stage a finer mesh generation has to be used to improve the credibility of the whole analysis. The created mesh was then exported as .msh file to be read in Fluent 3d.

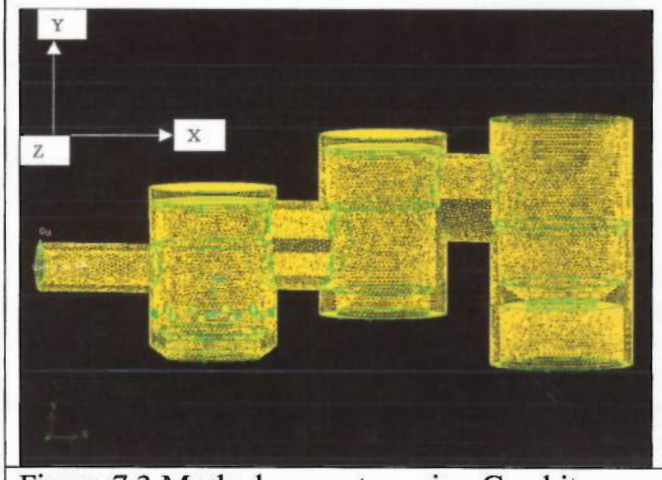

Figure 7.3 Meshed geometry using Gambit

7.5 Boundary Conditions.

After reading it into Fluent 3d programme as an .msh file the following settings and boundary conditions were applied. The model is simulated for the full load conditions. After 3000 iterations the programme converged when the residual reached below the default values.

The density of Helium is given as constant and the value depends on the pressure level. The model is run for various pressure level from full load (70 bar pressure) to 10% (7bar).

Model	Settings
Space	3D
Time	Steady
Viscous	Standard k-epsilon turbulence model
Wall Treatment	Standard Wall Functions
Heat Transfer	Enabled
Melting-Freezing	Disabled
Radiation	None

Table 7.1 Model Settings

Zones name	Type
fluid.4	fluid
main-outlet	pressure-outlet
inlets	mass-flow-inlet
boundary	wall
default-interior	interior

Table 7.2 Boundary Conditions

Property	Method	Value	Units
Density	Constant	0.16249999	kg/m3
Cp (Specific Heat)	Constant	5193	j/kg-k
Thermal Conductivity	Constant	0.152	w/m-k
Viscosity	Constant	1.9900001e-05	kg/m-s
Molecular Weight	Constant	4.0026	kg/kgmol
Thermal Expansion Coefficient	Constant	0	1/k

Table 7.3 Input details of fluid, Helium

Condition	Value
Gauge Pressure	6800000
Radial Equilibrium Pressure Distribution	no
Backflow Total Temperature	360
Turbulence Specification Method	0
Backflow Turb. Kinetic Energy	1
Backflow Turb. Dissipation Rate	1
Backflow Turbulence intensity	0.1
Backflow Turbulence Length Scale	1
Backflow Turbulent Viscosity Ratio	10
Backflow Hydraulic Diameter	1

Table 7.4 Outlet

Condition	Value
Mass Flow-Rate	140
Mass Flux	1
Total Temperature	370
Supersonic/Initial Gauge Pressure	1000000
Direction Specification Method	1
Turbulence Specification Method	0
Turb. Kinetic Energy	1
Turb. Dissipation Rate	1
Turbulence intensity	0.1
Turbulent Viscosity Ratio	10
Hydraulic Diameter	1

Table 7.5 Inlets

7.6 Test sections and Planes of interest

Due to the complex geometry of the fluid flow through the vessel, it is difficult to visualize the flow path from outside. Few sections were made as shown in the Fig 8.4 and 8.5. These sections were in XY and YZ planes. The Fig 8.5 shows the XY section of the entire vessel. A flow analysis with this plane can reveal the bottleneck situations where the flow is experiencing much pressure loss due to high velocity. This will be the main sectional view on which the model will be analysed.

The cross sectional planes 1 to 6 as shown in Figure 8.4 was quite useful in monitoring the flow along the X direction. The main locations responsible for significant pressure drop were found using these sectional views. The inlet and outlet planes are also analysed for the pressure and velocity distribution. The inlets are twelve circular ports of 300mm diameter each and around a vertical cylinder in the Y direction. The initial inlet flows are in the X and Z directions and then the fluid takes a vertical path. The outlet is a circular ring with an inner diameter of 2400mm and outer diameter of 4100mm. This is in the XZ plane. Hence the final flow to the outlet will be in –Y direction.

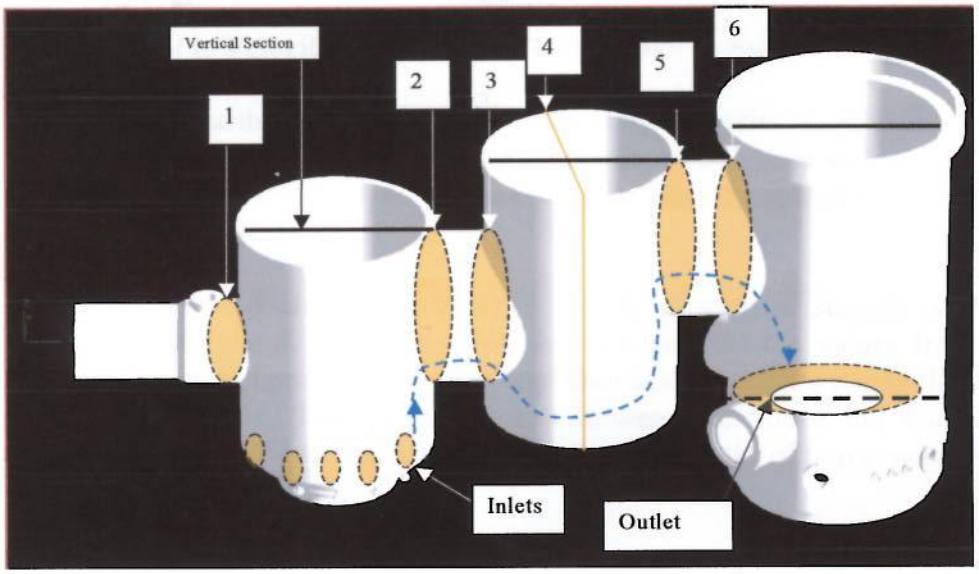

Fig 7.4 Sections and Faces subjected to analysis

Fig 7.5 Sectional view of the geometry. A vertical section on XY plane as given in the Fig 7.4

7.7 Results and Discussion

7.7.1 Case I: Velocity and Pressure loss profile at Full Load.

i) Velocity Distribution

The distribution of the magnitude of the velocity profile along the XY plane shows the velocity ranges from less than 1m/sec to 20 m/sec and an average of 6m/sec. The velocities at the inlet ports are relatively high compared to the rest of the flow except for few pockets.

Figure 7.6 shows the velocity profile of vertical section plotted against its position along the X direction. This shows a peak in the values from location 4 to location 8 which represents the inlets and then again a sudden rise in the values between location 15 and 16. The rise in velocity between location 4 and 8 is also due to the regions where the flow is passing through the narrow gap of two concentric vessels.

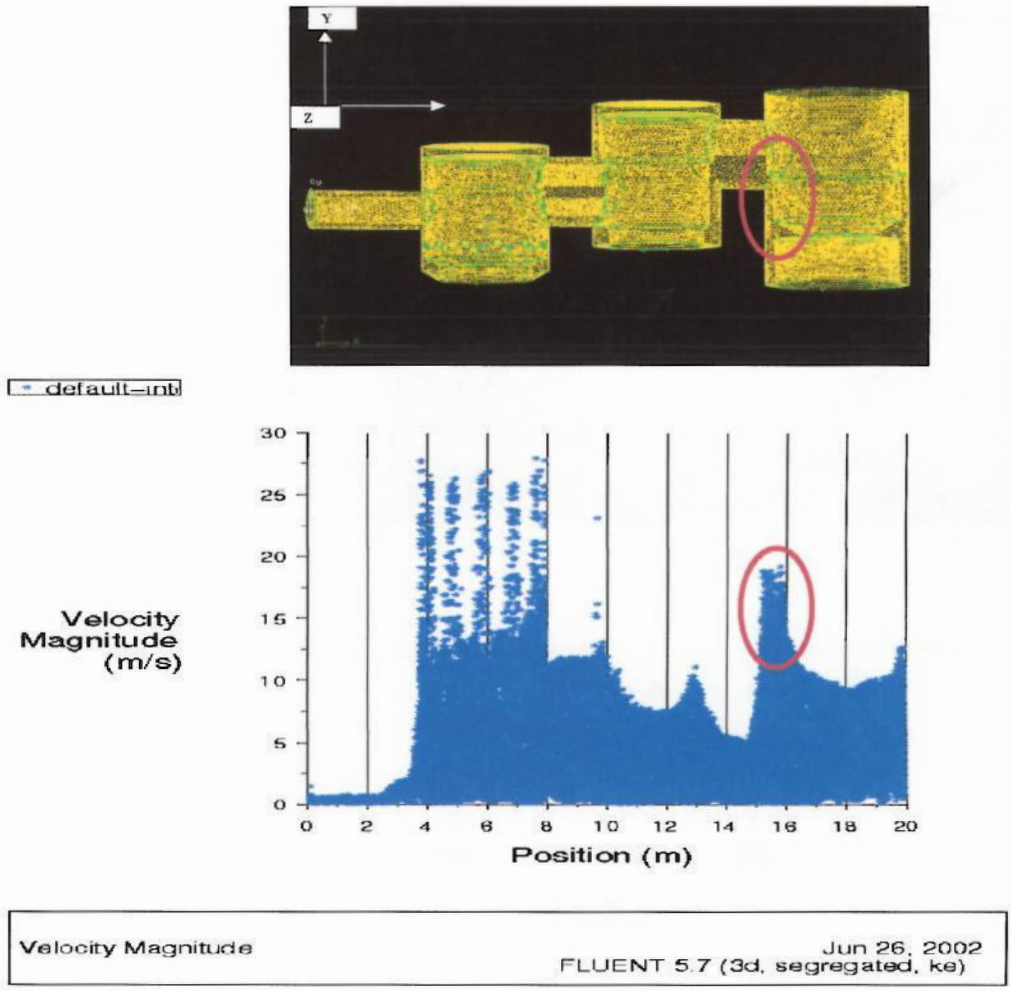

Figure 7.6 Velocity Magnitude at XY Plane along X direction. The position is in the X direction as shown above. The length of the vessel 20m from left to right.

The second velocity excursion between 15 and 16 as given (the regions are circled) in the Figure 7.6 reveals a velocity increase in the region where the horizontal connection between the LP turbo compressor vessel and PT vessel. The flow is taking a 90^0 path through the narrow space. These pressure losses due to these bottleneck shapes are avoidable because there is some flexibility in the shape of the pressure vessel design. It may not be necessary to sacrifice the pressure in these regions, as it is not adding much value in the overall design or performance.

ii) Pressure Loss Profile at Full load.

The velocity profile shows that only a very small percentage of the whole region is experiencing high velocity values. However if majority of the flow has to pass through that region then there will be significant pressure loss due to these small regions. Figure7.7 shows the total pressure level at various section of interest. As expected there is a gradual decline from inlet to outlet.

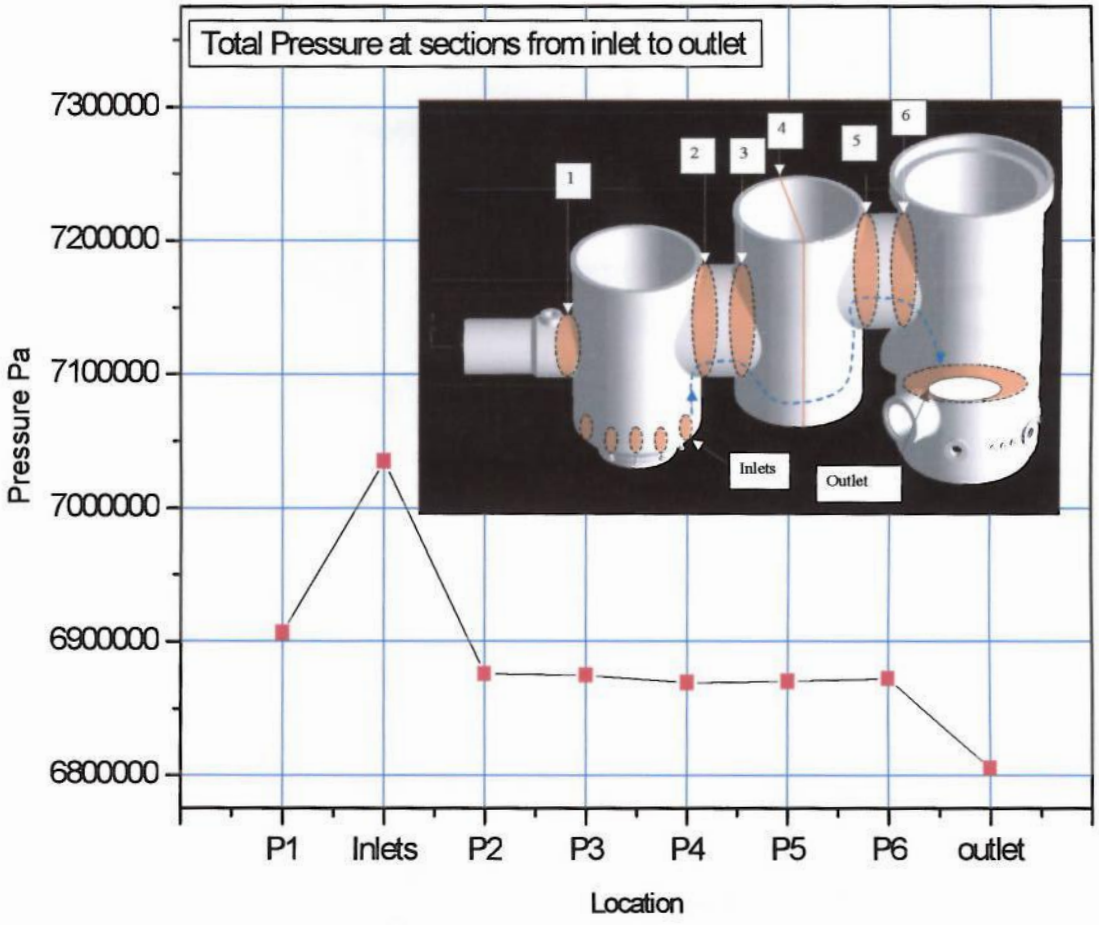

Figure 7.7 Pressure drop along the flow in X- direction

Point P1 can be ignored as it is in the opposite direction of the flow. There are two locations where pressure drop is clear and significant. The drop from inlet to point P2 then again at P6 and outlet. As revealed in the velocity profile, the gas is experiencing a pressure loss due to its radial flow from the inner cylinder and onward flow upward through the gap between the concentric cylinders. This is the cause of the pressure loss from inlet to point P2.

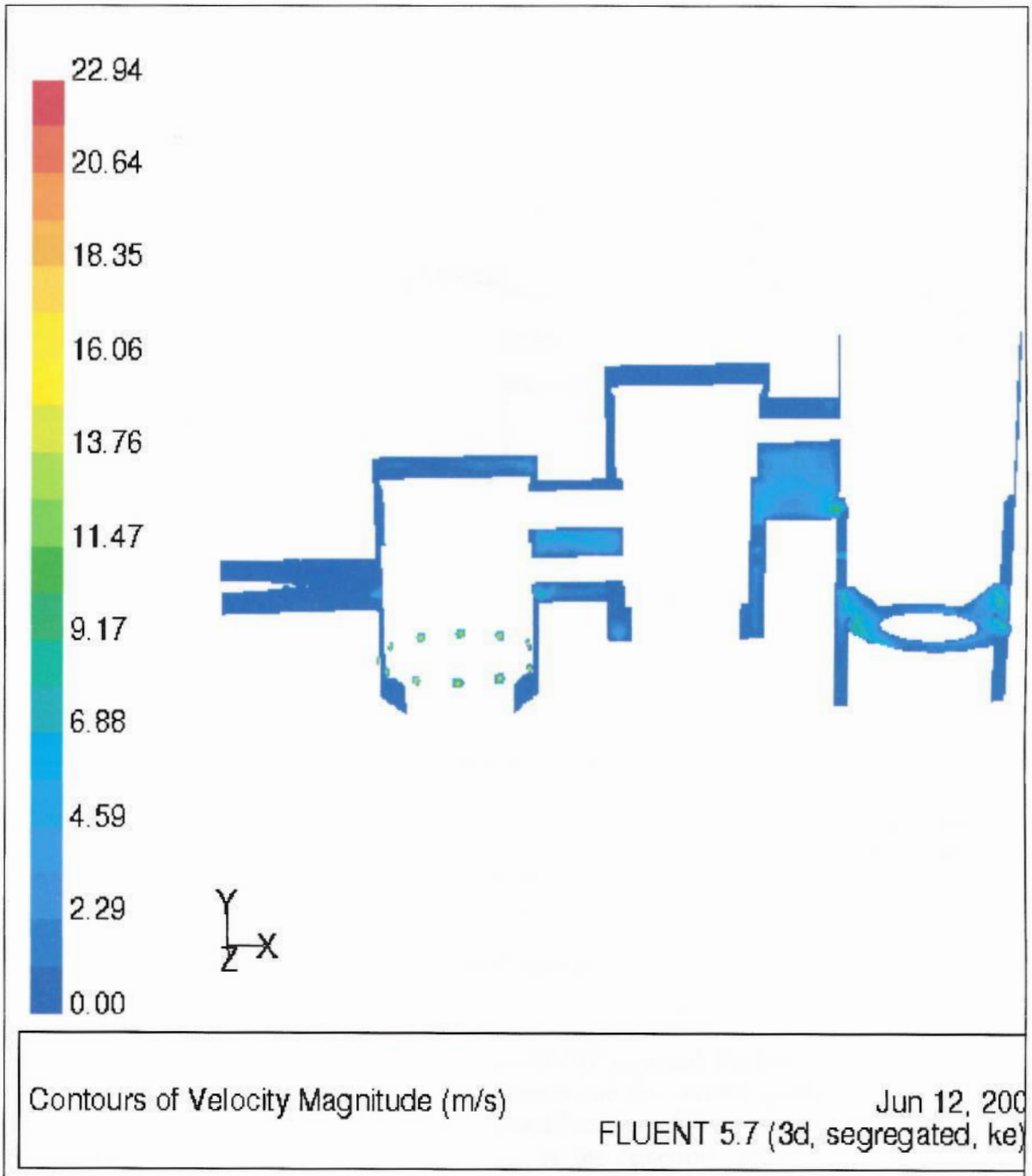

Figure 7.8 Velocity contours in vertical section

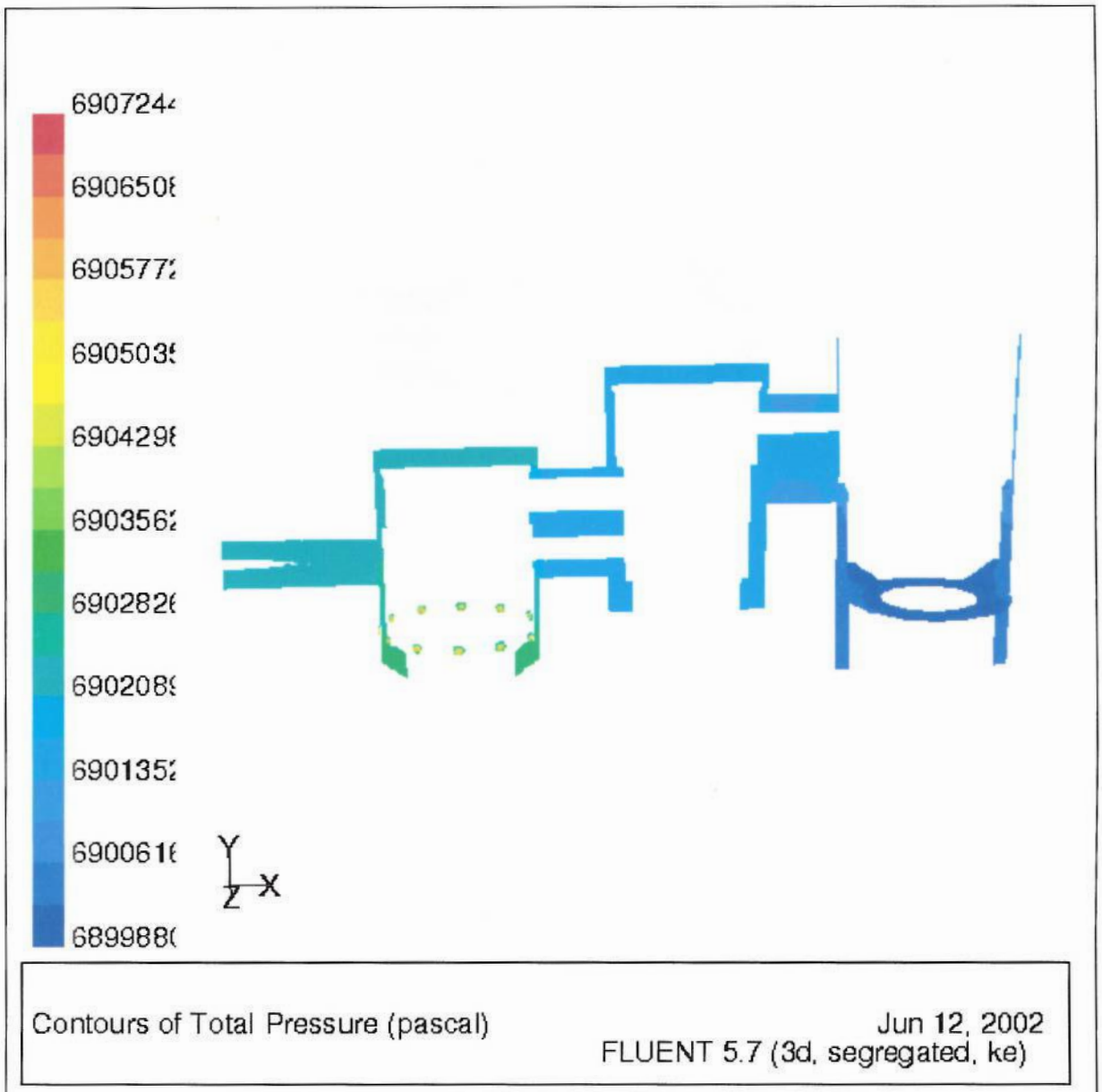

Figure 7.9 Total pressure contours in vertical section

The second significant drop is due to the 90^0 turn and the downward flow at the junction between the horizontal part of the vessel and the vertical generator vessel. The XY view of the picture does not show the exact location of the problem in this pressure loss. Figure 7.10 shows the high velocity at the junction. There are two similar locations close to the inlet, which is already explained. The rest of the outlet ring is experiencing low velocity. The overall velocity and pressure distribution in this area needs to be improved.

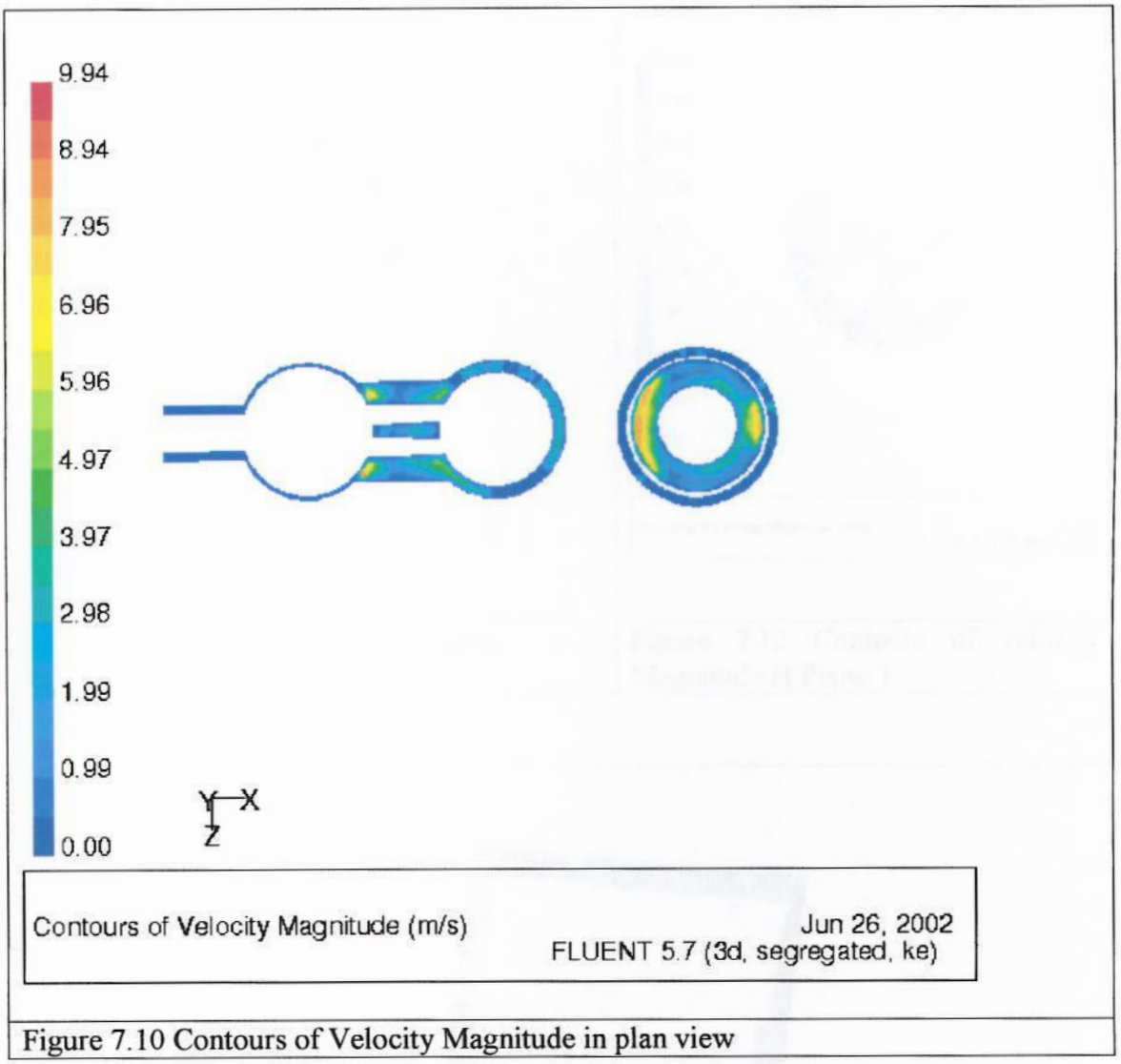

Figure 7.10 Contours of Velocity Magnitude in plan view

Pressure Drop at Sections

Some other sectional planes in ZY were analysed in order to find out the regions where significant drops are experienced. The high pressure helium gas is coming out of the 12 circular ports at the compressor exit at a pressure of 7Mpa and moving towards the outlet at the right side. The Figure 7.11 shows cross section of the four pipes between the HP and LP compressor region and there is not much of a problem there.

The Figure 7.12 is a vertical section around the LP compressor and not much of a pressure loss or velocity excursion can be seen here. Unlike the HP vessel, it seems there is enough space for the flow. In Figure 7.13, it can be seen that the velocity excursion start from the LP vessel and by the time it reaches the Plane 6, it becomes severe. The sectional view again confirms that, not all of the cross sectional area is experiencing this.

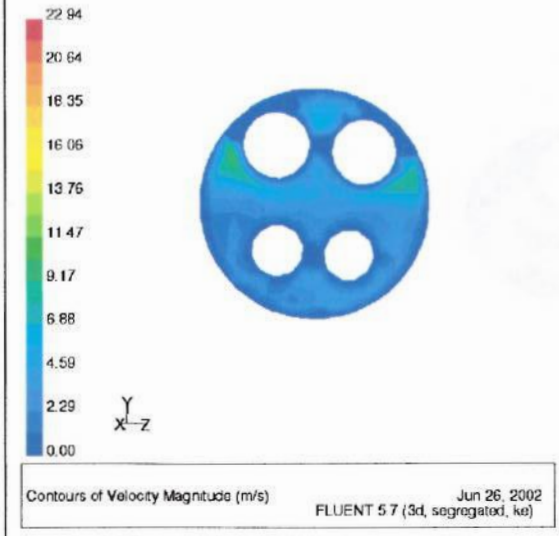

Figure 7.11 Contours of Velocity Magnitude at Plane 2

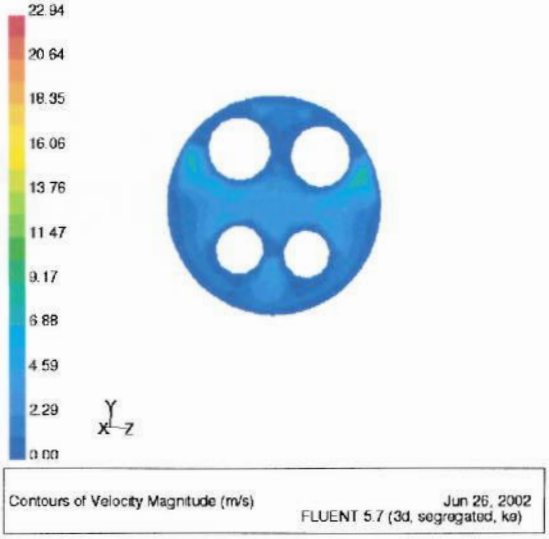

Figure 7.12 Contours of velocity Magnitude at Plane 3

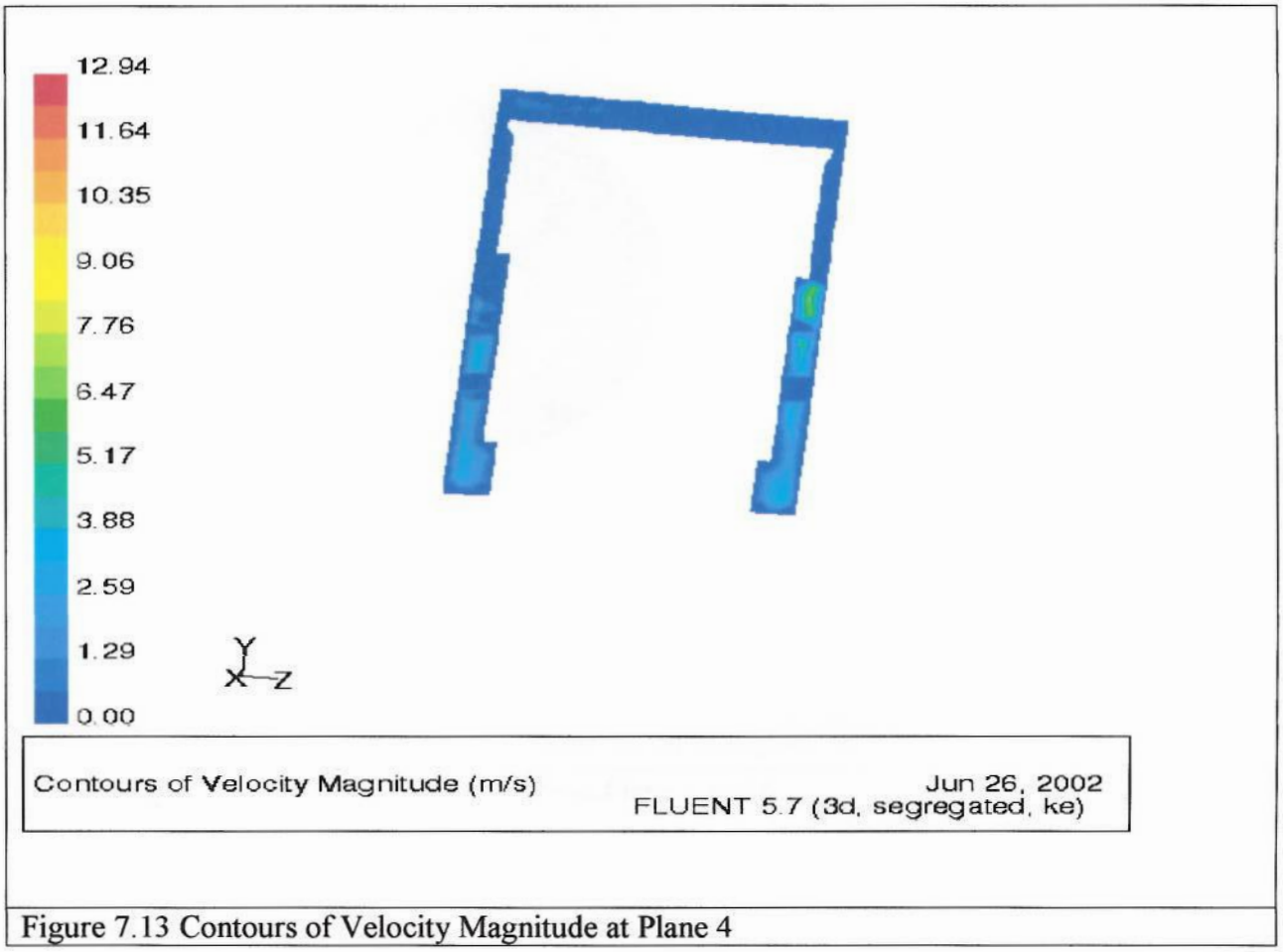

Figure 7.13 Contours of Velocity Magnitude at Plane 4

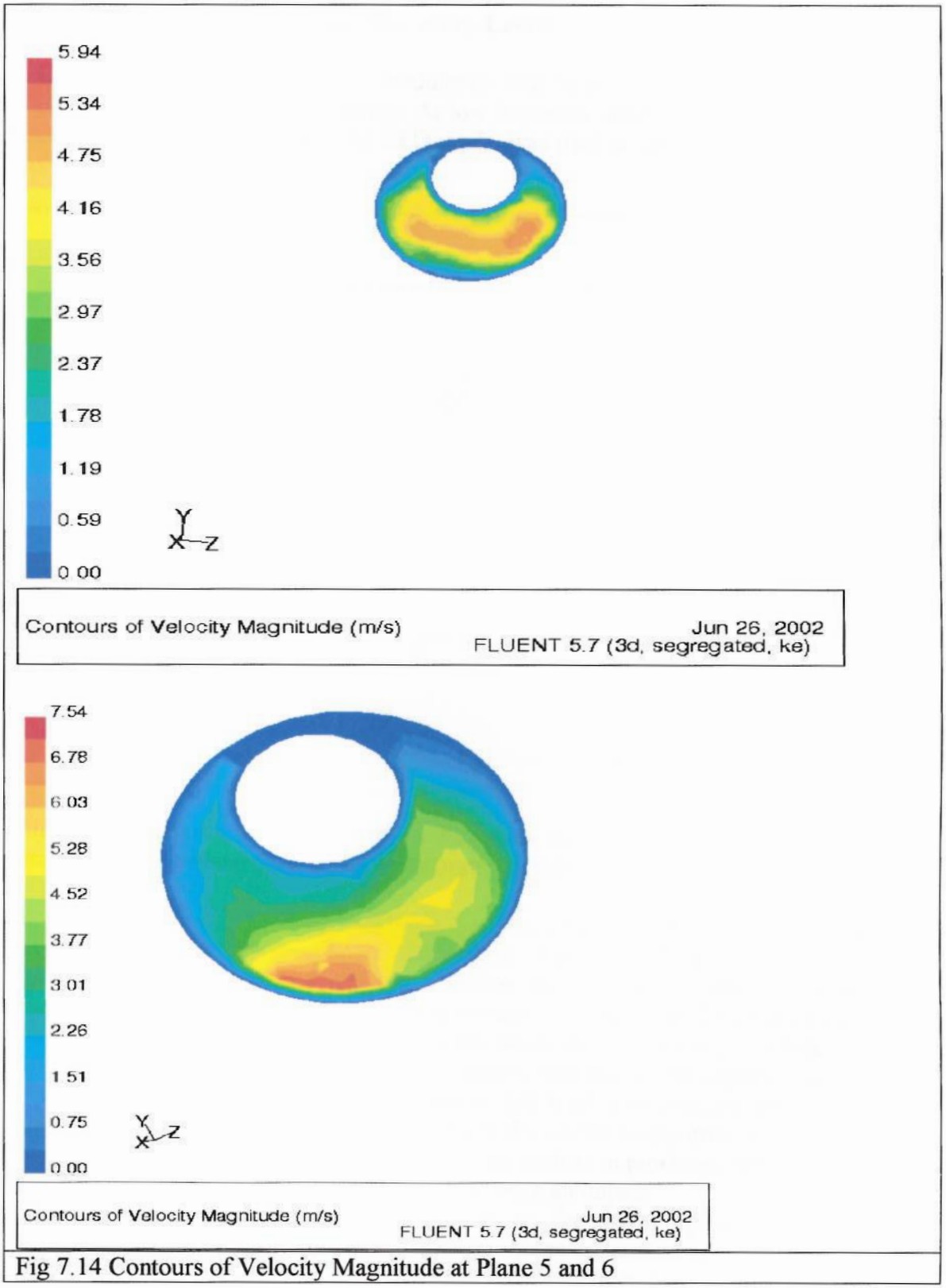

Fig 7.14 Contours of Velocity Magnitude at Plane 5 and 6

7.7.2 Pressure Loss at Various Inventory Levels

As mentioned earlier, the power modulation will be performed by the inventory level, which is proportional to the density. At low Reynolds numbers the losses will be much more due to flow separation. The CFD model was tried at various densities to check the effect of low inventory.

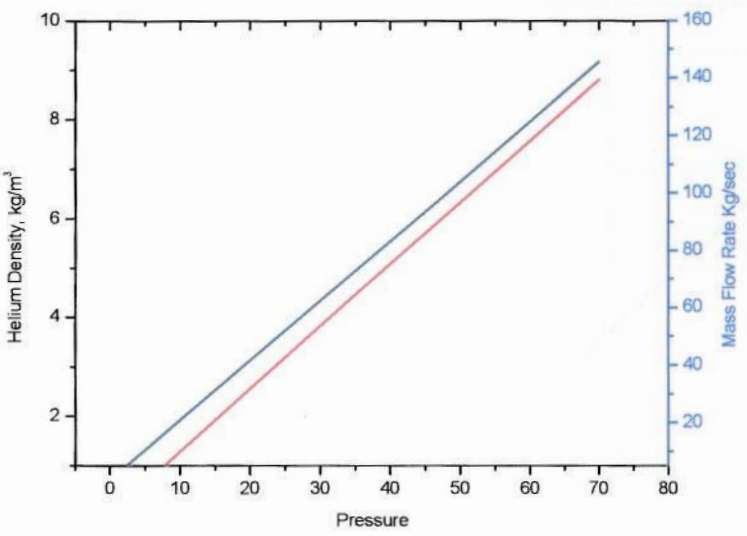

Figure 7.15, Helium Density at T=373K

The helium density and the corresponding flow rate are given in Figure 7.15. The various run for several load situations is based on this.

The pressure loss at various loads is given in Figure 7.16. The total pressure loss is proportional to gas density in the system. This was different from what was anticipated. The expectation was for a sudden drop in the pressure due to the flow separation losses. The reason for this may be due to the fact that the velocity of the gas during a normal operation is around 10m/sec, when the sonic velocity of helium at that temperature is more than 1000m/sec. This means that the system experiences very low Mach number and Reynolds number even at full load. The pressure loss at full load itself is very low. A reduction in the density in the vessel hardly affects the losses. This may not be the cases in other parts of the system such as in pipelines, where the velocity is around 100m/sec; the low-density flow may have an impact.

The percentage of loss with respect to the system pressure is the same throughout the pressure level changes. This comes to around 0.1 % of the system pressure. This shows that the pressure vessel flow characteristic will not have much impact on the overall performance during the inventory changes. The deciding factor will come from other parts of the plant such as piping, heat exchangers, reactor etc.

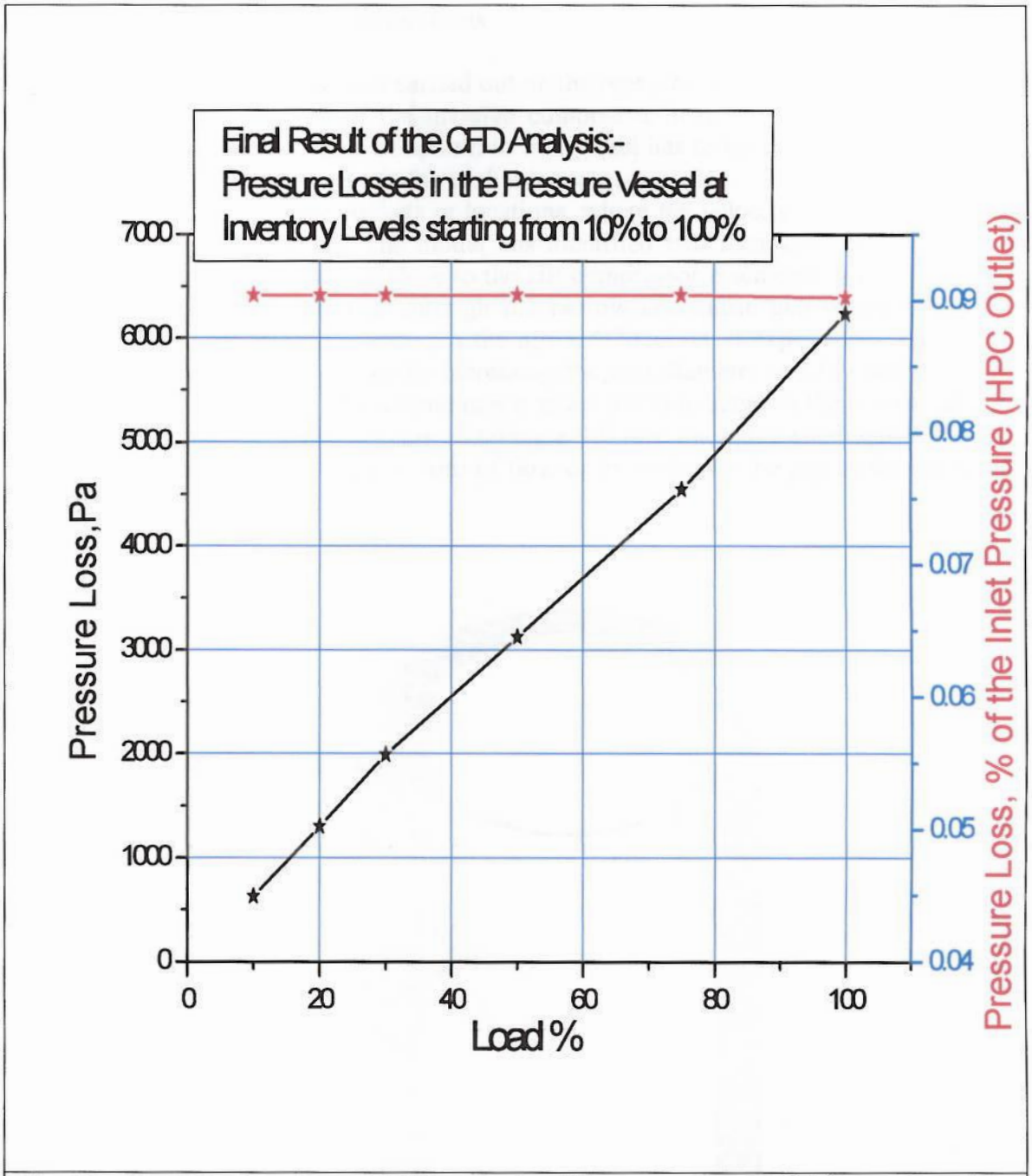

Figure 7.16 Final result of the CFD analysis of the pressure vessel. The pressure loss (absolute and percentile) in the pressure vessel at various inventory level starting from 10% to 100%.

7.8 Conclusions and Recommendations

A CFD analysis has been carried out on the pressure vessel of the PBMR design. The pressure vessel is one of the massive component in the design with a complex geometry. The flow behaviour of helium in this vessel has to be understood prior to its manufacturing. The CFD analysis focused at two aspects.

One was to identify pockets or locations, where the velocity is high or a source of significant pressure drop. The model has identified two locations with significant pressure losses. The first one is close to the HP compressor discharge. When the gas if flowing from the HP discharge through the narrow concentric gap between the HP compressor and the pressure vessel, in the upward direction, it experiences significant pressure loss. This can be solved by increasing the port diameter and / or widening the gap available for the flow. The second one is at the junction between the horizontal part and the power turbine. Here the flow is taking a 90^0 turn through a small gap. This can be solved by reducing the angle of turn of flow or by widening the gap as shown in the picture below.

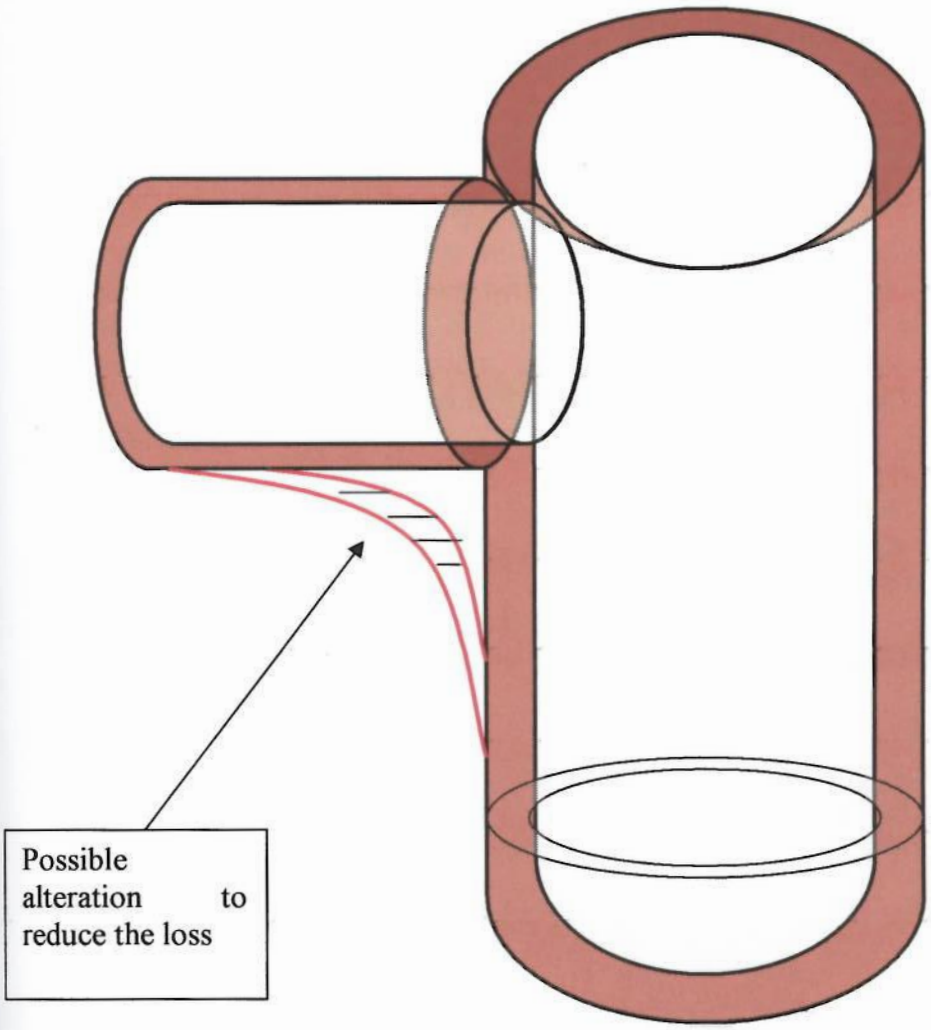

Figure 7.17 Possible alteration to reduce the loss in the Pressure Vessel.

The second objective was to study the flow behaviour during various inventory level. The percentile flow loss with respect to the system pressure was found to be very much the same. The relation between pressure loss and density is quite linear and no sudden increase in the pressure loss was noticed as the density decreased. The reason is that the system inherently has a very low Mach number and Reynolds number even during full load. This shows that the pressure vessel will not be contributing much to the low efficiency during low inventory operation.

7.9 Recommendations for further work

a) Pressure Drop estimation.

The current exercise is carried out with a mesh size of 170mm due to the computational limitations. The dimensional detail of the geometry is taken from a conceptual design. As more details become available, the geometry has to be remodelled with more dimensional details and to be meshed in fine grids to improve the accuracy.

b) Unsteady Flow during Valve Operations and the Response Time Evaluation.

An attempt was made to carry out a time dependant, user defined flow condition. However due to the complexity and massiveness of the model and due to the computational limitations, the programme was crashing and the attempt was unsuccessful. This activity is recommended for the future work.

The pressure vessel is acting as a pipe connecting HP Compressor and the Recuperator inlet. The Bypass valve will be opening for branching the flow to the pre-cooler inlet where the pressure will be one of the lowest in the system. Hence a sudden opening of the Bypass valve is a source of unsteady flow. This can be modelled in CFD. As a next step, a time dependant, unsteady flow solution can be done. This will give an idea of the response time required by the valves to change the flow through the reactor for load control.

The Interrupt valves are for the Emergency shut down. These are stop valves placed between the HP compressor outlet and the pre cooler inlet to stop the flow completely through the reactor. This flow should be modelled to see the possibility of any reverse flow or any other oscillatory flow in the pressure vessel due to the operation of Interrupt valves. This should be done with a time dependant user defined input

Chapter .8
Comparison of Helium and Air flow in a cascade using CFD analysis

A CFD analysis was carried out to compare the flow characteristic of Air and Helium around an axial compressor cascade blade. This was carried out with the objective of doing some preliminary work for the design and development of a test rig for helium turbomachinery development. Since helium is expensive, the possibility of using air, wherever possible, to perform the task was explored. This CFD simulation was based on an experimental work done by Rhoden [81] using air. The same geometry was used here in CFD. After the successful validation of this in air, a comparative study was done with helium for Mach number similarity, Reynolds number similarity and also for both Mach and Reynolds numbers by scaling the geometry. This gave the scaling required for using a test rig to study helium flow behaviour by using air instead.

8.1 Experimental Results

The experimental work consisted of the separate testing of 3 cascades of axial flow compressor blades of camber angles 20, 30 and 40 deg. Measurements were made of the distribution of static pressure over the central cross section of the middle blade of each cascade, together with traverses of static pressure, total head and angle of flow at inlet and outlet to each cascade in the plane of the central cross-section. The experimental test carried out by Rhoden covered a range of actual Reynolds number from $3x10^4$ to $5x10^5$, based on the inlet air velocity and the blade chord, and also a range of inlet air angle, from 35deg to 60deg.

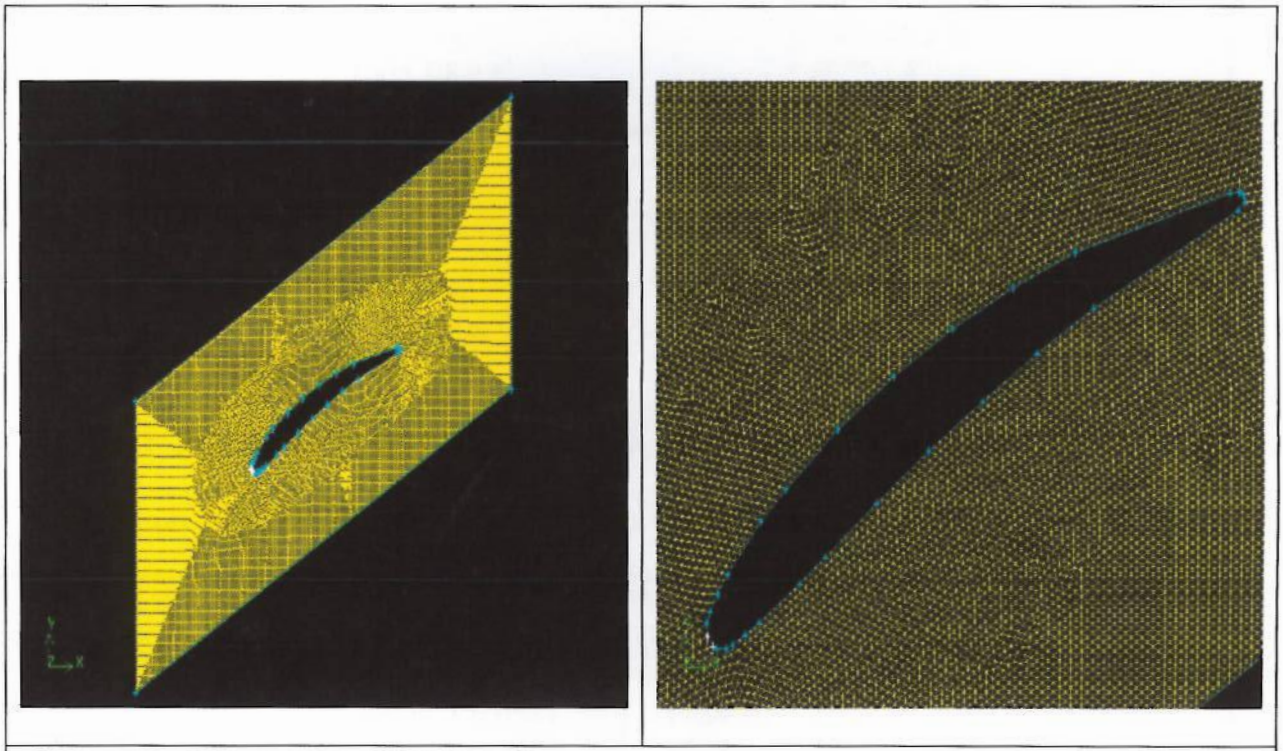

Figure 8.1 The mesh around the cascade

8.2 CFD Model

The geometry was created using the pre processor Gambit. The aerofoil profile is the same as that was used by Rhoden [81] in the experiment. A camber angle of 30 deg and a Stagger Angle of 36 deg were chosen. The aerofoil is placed between a pair of periodic boundaries at half pitch length on each side. Two vertical faces are assigned as inlet and outlet.

A mesh size of 1mm was used. The Convex and Concave faces are assigned as separate walls to extract the results separately. The mesh was then exported to two-dimensional Fluent solver. The inlet wall has been given as a 'velocity inlet' and the outlet wall is given as 'outflow'. The convex and concave faces of the aerofoil are given as walls.

8.2.1 Input Boundary Conditions.

1. Velocity Magnitude at Inlet for Air and Helium

a) Constant Reynolds Number

Re= Reynolds number, μ = Viscosity, ρ =Density ,D=Hydraulic Diameter

$$Velocity, V = \frac{\mathrm{Re}.\mu.}{\rho.D}$$

Property	Air	Helium
1. Density	1.225 kg/m^3	0.1625 kg/m^3
2. Viscosity	1.789 x 10^{-5}kg/m.s	1.99 x 10^{-5}kg/m.s
3. γ	1.4	1.667
4.R	287 J/Kg K	2078 J/Kg K
5.C_p	1005 J/Kg K	5277 J/Kg K
6. Temperature	300 K	300K

Reynolds Number	Air		Helium	
	Velocity	**Mach Number**	**Velocity**	**Mach Number**
1. 1x10^5	9.58 m/sec	0.0290	80.35 m/s	0.0787
2. 2x10^5	19.16 m/sec	0.0581	160.7 m/s	0.1575
3. 3x10^5	28.74 m/sec	0.0870	241.05m/s	0.2361

Table 8.1 Input- Boundary conditions at constant Reynolds number

b) Constant Reynolds Number and Mach Number

Reynolds Number	Air velocity	Mach number	Diameter (For Air), m	Helium velocity	Diameter (For Helium), m
1. 1x10^5	9.58 m/sec	0.0290	0.1524	29.58	0.138
2. 2x10^5	19.16 m/sec	0.0581	0.1524	59.26	0.276
3. 3x10^5	28.74 m/sec	0.0870	0.1524	88.74	0.414

Table 8.2 Input- Boundary conditions at constant Reynolds number and Mach number

2. Velocity Angle at Inlet

The following Camber angle, Stagger angle and Air inlet angles were used in the simulation.

Camber angle	Stagger angle	Inlet blade angle	Air Inlet Angle	Angle of Incidence
30	36	51	60	9
			55	4
			51	0
			45	-6
			40	-11
			30	-21

Table 8.3 Velocity angle at inlet

3. Other Fluent properties Input

Property	Value
1. Model	k-epsilon
2. Material	Air, helium
3. Density	Constant
4. Geometry Units	Meter
5. Operating condition,	
P	101325 Pa
T	288.15 K

Table 8.4 Input properties list

8.3 Output

1. Pressure distribution

Pressure distribution on the blade surface = Local Static Pressure – Average outlet static pressure /[0.5.Density. (Average outlet velocity magnitude)^2]

2. Loss Coefficient

Loss coefficient = (Total Pressure at inlet – Total Pressure at outlet / Total Pressure at Inlet)

3. Blading efficiency

Efficiency = 1- total head loss / reduction of velocity head

8.4 Result Analysis

8.4.1 Validation of the simulation with the experimental result

The results of the air and helium in the Fluent model are compared and the results are very close enough with the experimental results in which air was used.

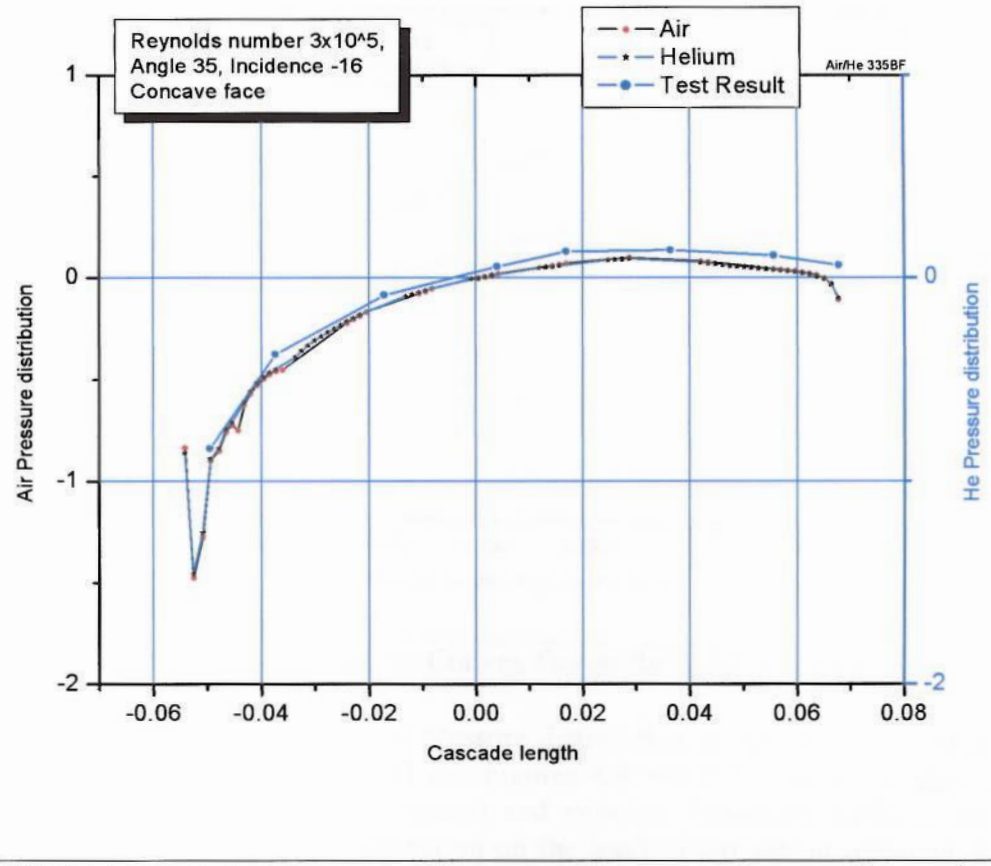

Fig 8.2. Matching between experimental and CFD results at constant Re number and fix geometry.

Figure 8.2 shows the result in terms of pressure distribution along the concave surface of the blade at Reynolds number $3x10^5$ and an inlet angle of 35 deg. There is a matching of approximately 98% between the test result and the CFD simulation result. The two CFD results of air and Helium are matching fully. In this run, the Re and the geometry remain constant and hence the velocity of helium and air is different.

8.4.2 Comparative performance of Helium and Air

i) At constant Reynolds number on a fixed geometry.

Separation from the blade surface increases the losses seriously reducing the efficiency of the cascades. The effect of separation can be detected on the curves of static pressure distribution over the blade surfaces as a reduction in the positive pressure gradient. When separation is complete the curves are horizontal with no further rise in static pressure. The experimental tests by Rhoden [81] have also had the same results.

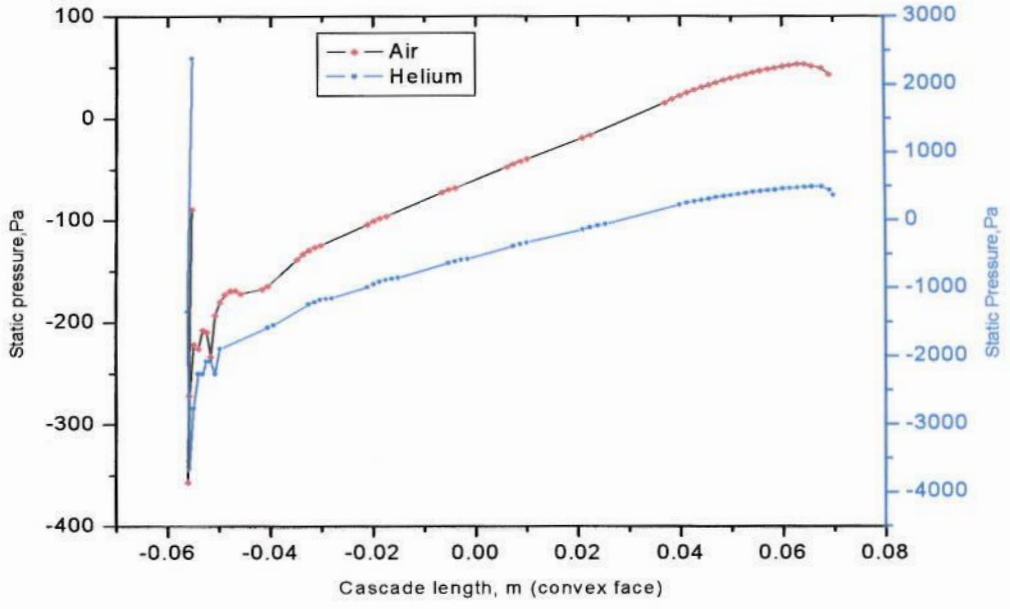

Figure 8.3 Static Pressure along the Convex face at Re $2x10^5$ and angle 50deg.

Figure 8.3 shows the static pressure distribution along the convex face (suction side) of the airfoil for helium and air. Figures 8.4 and 8.5 present the static pressure distribution along the convex (suction) and concave (pressure) surfaces for air and helium. This provides a good indication on the level of agreement obtained during the analysis.

Figure 8.6A and 8.6B compare the results for different Reynolds Number for the same inlet angle. At low Reynolds Number, the losses due to flow separation are slightly higher. A significant reduction in the pressure loss due to flow separation occurs when the angle changes from 50^0 to 35^0 as shown in Figures 8.6C and 8.6D. This is for a constant Reynolds Number of $2x\ 10^5$. A similar result is shown in Figure 8.6E and 8.6F for a high Reynolds Number of $3x\ 10^5$. Figure 8.6G and 8.6H compares the total pressure distributions of helium at Reynolds Numbers of $1x10^5$ and $2x10^5$ for an inlet angle of 50^0. At higher Reynolds number the thickness of the boundary layer reduces. These plots can be used to demonstrate the areas and the level of losses in the flow region.

Pressure distribution along the concave (pressure) and convex (suction) surface for air and helium (at constant Mach Number and Reynolds number) is shown in Figures 8.7 and 8.8. This is achieved by scaling the geometry for helium in order to maintain the same Reynolds Number as in the case with air. The results are very identical for air with original geometry and helium with modified geometry.

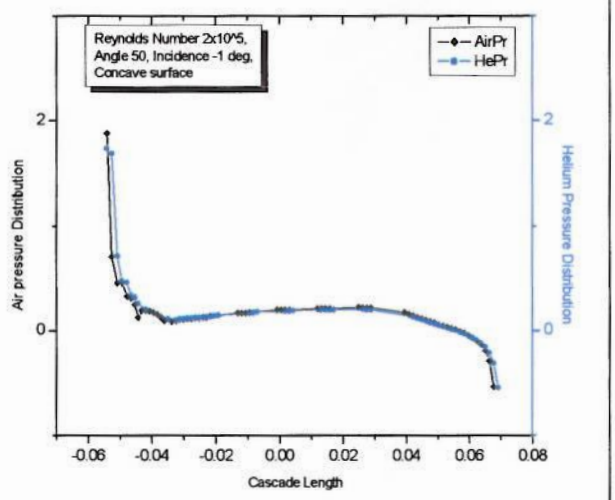

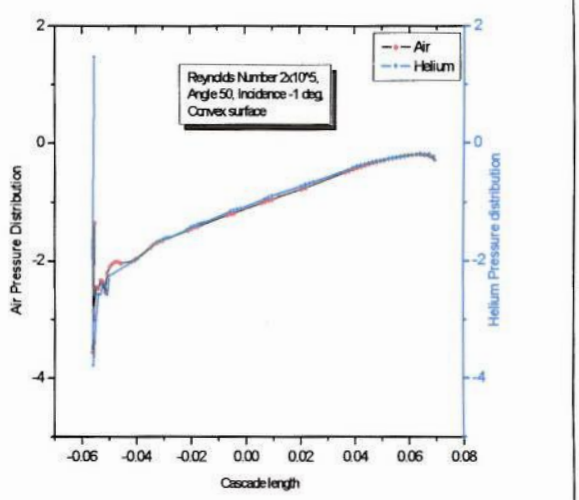

Figure 8.4 Static Pressure distribution along concave (pressure) and convex (suction) surfaces of the blade at Re $2x10^5$ for Helium and Air.

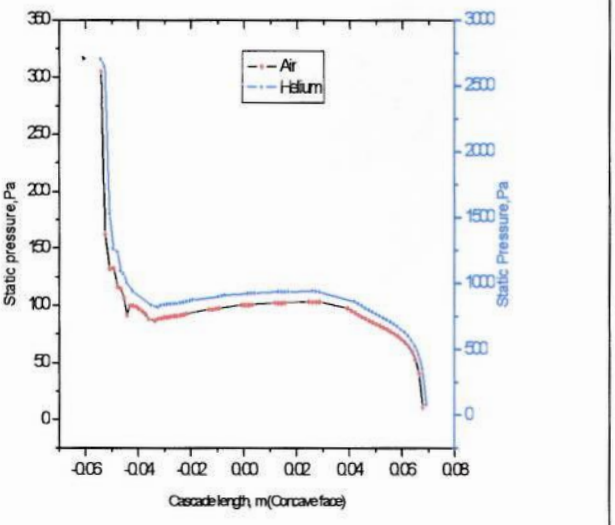

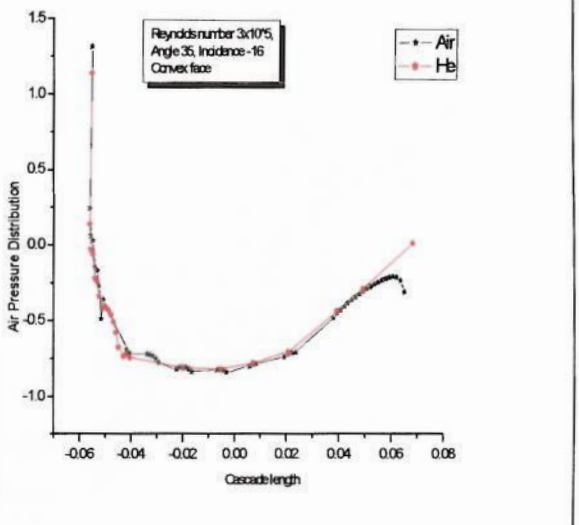

Figure 8.5 Static Pressure distribution along concave (pressure) and convex (suction) surfaces of the blade at Re $3x10^5$ for Helium and Air. Inlet angle 35^0.

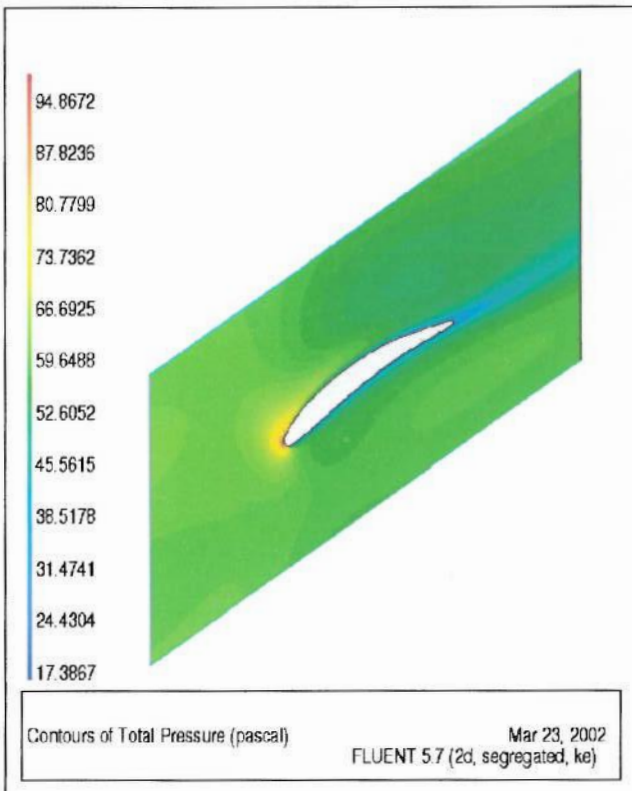

Figure.8.6A Air, Re=1x10^5, Angle= 35

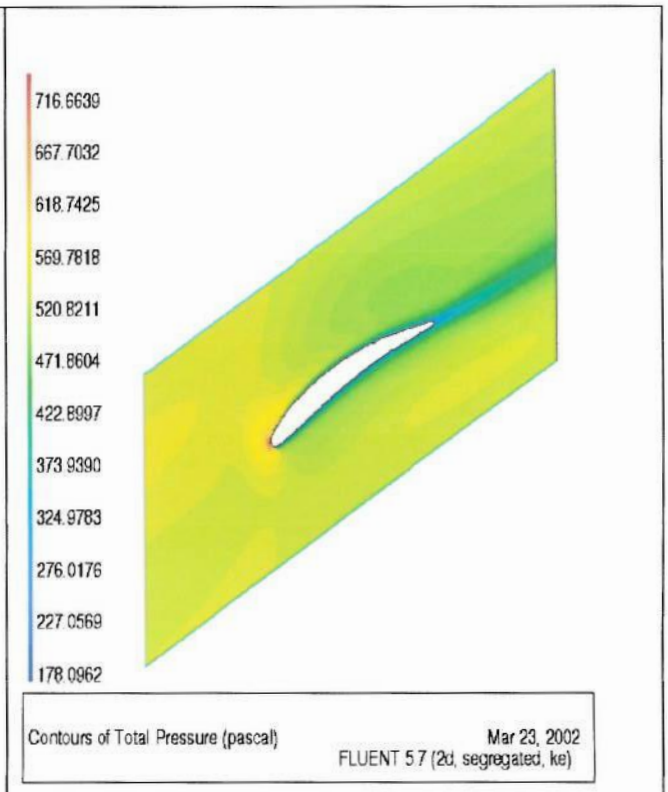

Figure.8.6B Air, Re=3x10^5, Angle= 35

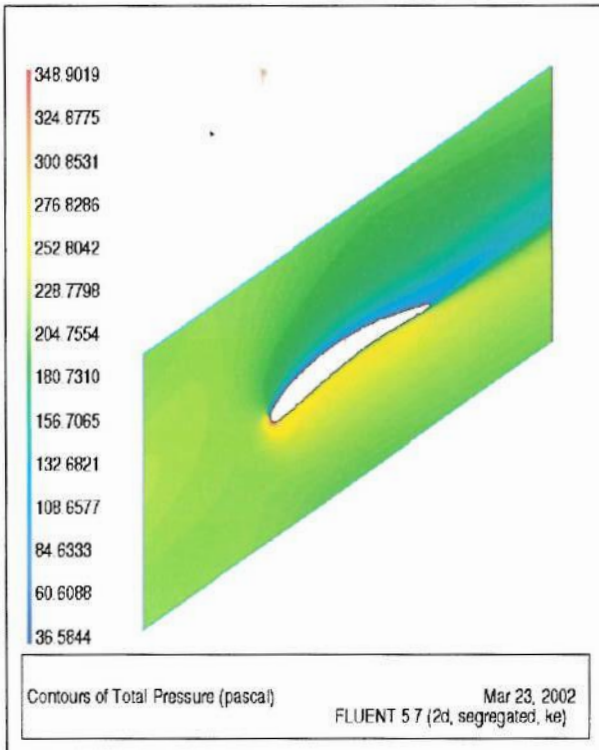

Figure.8.6C Air, Re=2x10^5, Angle= 50

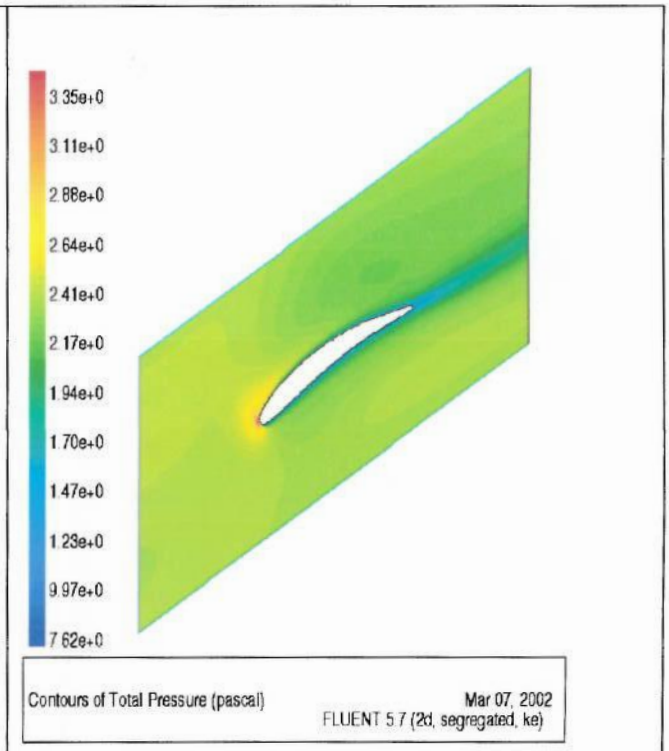

Figure.8.6D Air, Re=2x10^5, Angle= 35

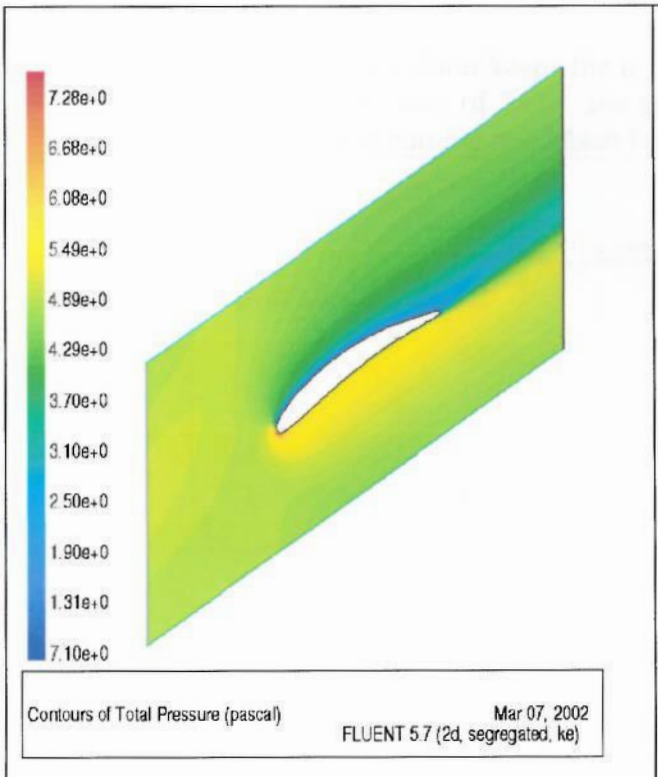

Figure.8.6E Air, Re = 3 x 10^5, Angle= 50

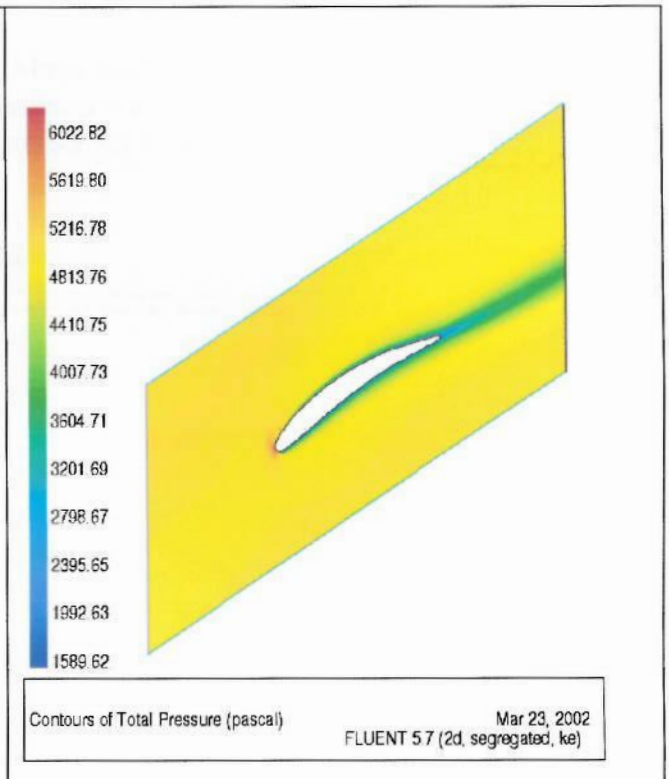

Figure.8.6F Air, Re=3x10^5, Angle= 35

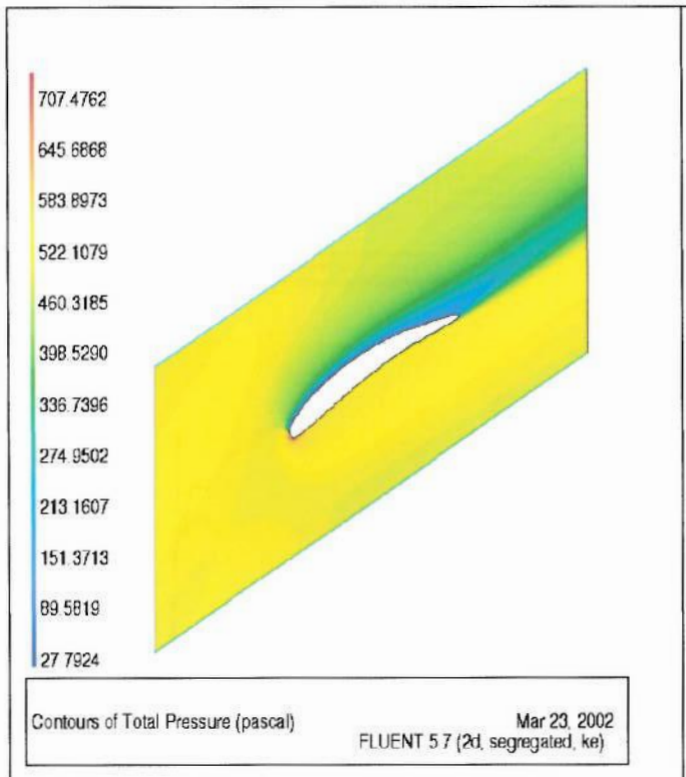

Figure.8.6G. He, Re=1x10^5, Angle= 50

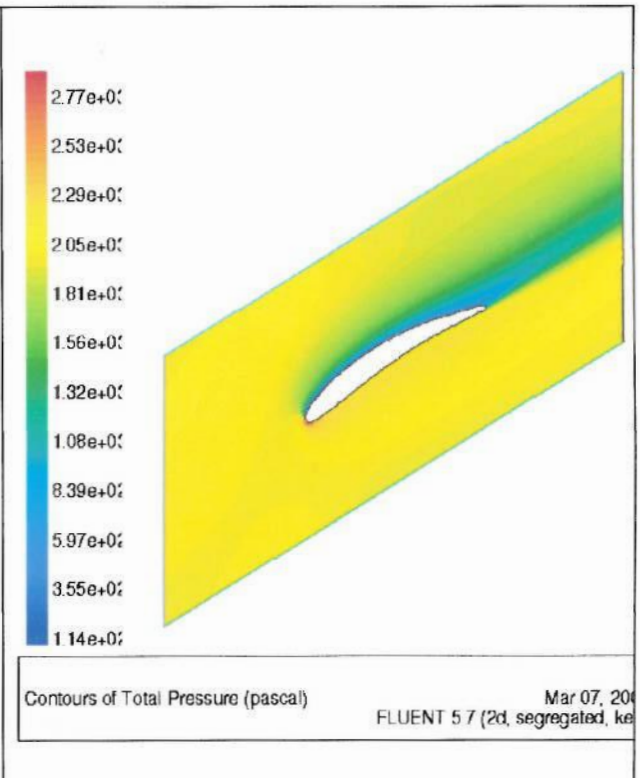

Figure.8.6H. He, Re=2x10^5, Angle= 50

ii) At constant Reynolds number and Constant Mach number.

The high sonic velocity of helium keeps the its Mach number low for the same velocity in air. For a Reynolds number of $3x10^5$ the geometry has to be enlarged by a factor 2.713 to have the same Re number and Mach Number for helium.

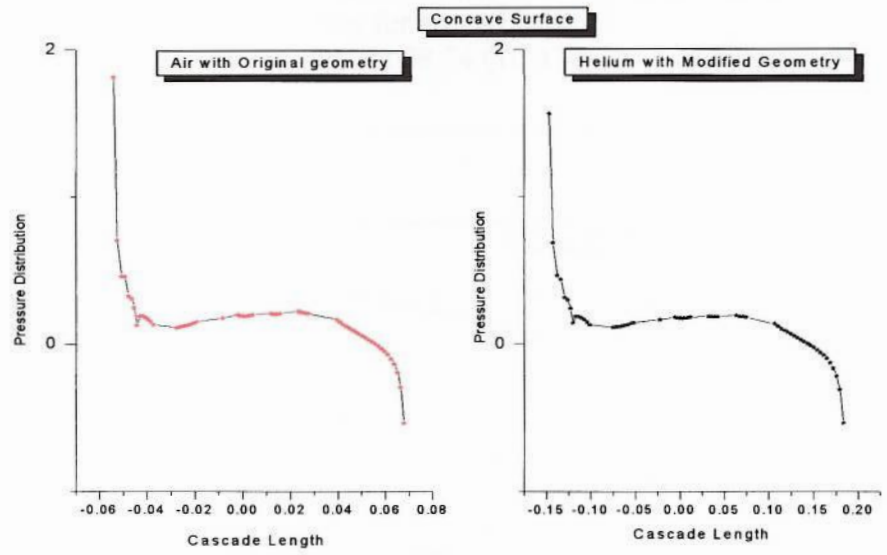

Figure 8.7 Pressure distribution along concave face on different geometry for the same Re and Mach Number.

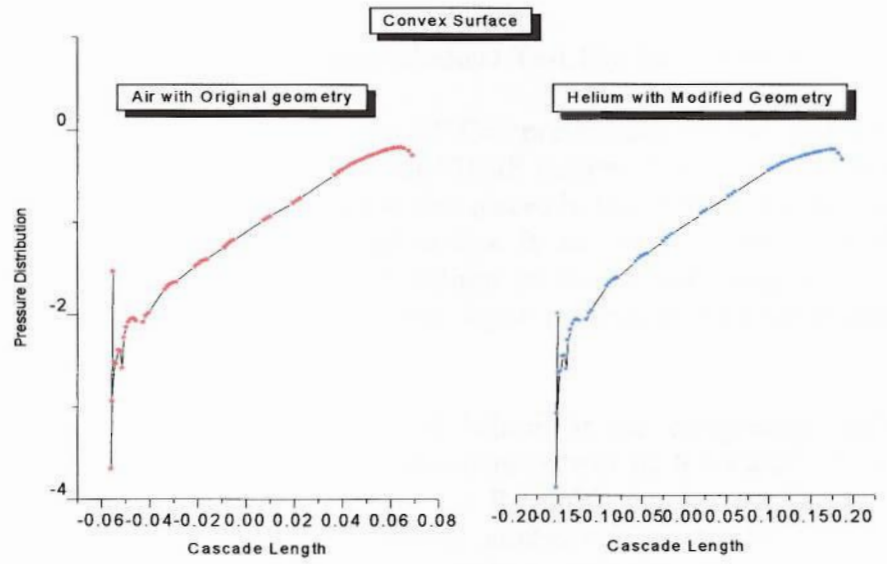

Figure 8.8 Pressure distribution along convex face on different geometry for the same Re and Mach Number.

The non-dimensional pressure distribution for constant Re and Mach numbers are exactly the same for air and helium as shown in the Fig 8.8

8.4.3 Pressure loss

The difference in total pressure between inlet and outlet is calculated and the percentile loss to the inlet pressure is found to be same. Figure 8.9 compares the Total Pressure loss between the inlet and outlet for air and helium.
Average pressure loss in helium is 58.24 (10.47 %) and in Air is 52.635 (9.15%)

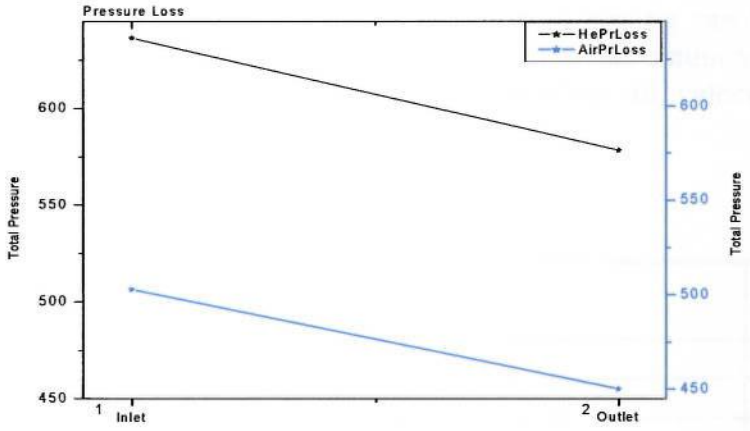

Fig 8.9 Total Pressure loss between the inlet and outlet for air and helium at constant Reynolds number and Mach number.

8.5 Design Philosophy of a Hypothetical Test Rig for Helium using Air

The flow path between the HP Compressor and the Recuperator inlet (cold side) is a chamber of oblique shape, in the PBMR design. This vessel is called pressure vessel and all the turbomachineries are in fact placed in this. The flow is taking a complex path around all the equipments placed in that. It may be possible to establish a test rig to study the flow characteristic of helium in the vessel using air. The proportionate difference in the geometry and the input parameters can be established from this cascade tests conducted here.

The maximum flow rate of helium at the compressor outlet in PBMR is 140kg/sec at 70 bar and 120 C. The density will be 8.4 kg/m^3. A simulation for the above scenario can be done either for Reynolds number similarity or Mach number similarity. Analysis based on Reynolds number can be used for pressure loss estimation and the analysis based on Mach number similarity can be used for the transient performance studies.

i) Reynolds Number similarity

	Helium Re = 1x 10^5	Air Re = 1x 10^5
Pressure	70 bar	70 bar
Temperature	393 K	393 K
Density	8.4 kg/m^3	48.5kg/m^3
Viscosity	1.99 x 10^{-5}kg/m.s	1.789 x 10^{-5}kg/m.s
Velocity	6.42 m/sec for a unit diameter.	1 m/sec for a unit diameter.

Table 8.5 Test rig operating parameters for Reynolds number similarity.

From the above table it is clear that helium test rig can be tested for pressure drop characteristics using air at a low velocity. The maximum velocity of helium in PBMR design is around 100m/sec and corresponding air velocity for the same Reynolds number will be 15.6m/sec.

ii) Mach Number similarity

	Helium Mach = 1	Air Mach =1
Pressure	70 bar	70 bar
Temperature	393 K	393 K
Density	8.4 kg/m^3	48.5kg/m^3
Viscosity	1.99 x 10^{-5}kg/m.s	1.789 x 10^{-5}kg/m.s
Velocity	1167 m/sec for a unit diameter.	404.41 m/sec for a unit diameter.
Reynolds Number	4.93 x 10^8	10.96 x 10^8
Diameter	1 unit	1 unit

Table 8.6 Test rig operating parameters for Mach number similarity.

Mach number similarity will be useful for the transient performance analysis and the above table shows that air can be used in the test rig at a low velocity to match the Mach number of helium. In the above two comparisons, it is assumed that the geometry remains the same and the diameter is taken as unity.

iii) Mach Number and Reynolds Number similarity

	Helium Mach = 0.1	Air Mach =0.1
Pressure	70 bar	70 bar
Temperature	393 K	393 K
Density	8.4 kg/m^3	48.5kg/m^3
Viscosity	1.99 x 10^{-5}kg/m.s	1.789 x 10^{-5}kg/m.s
Velocity	116.7 m/sec for a unit diameter.	40.441 m/sec for a unit diameter.
Reynolds Number	4.93 x 10^7	4.93 x 10^7
Diameter	1 Unit	0.45 unit

Table 8.7 Test rig operating parameters for Mach number and Reynolds number similarity.

A comparison of different geometry for air and helium is considered here to keep the same Mach number and Reynolds number. A ratio of 1: 0.45 in diameter is given here for a particular Re and Mach. This shows that the test rig will be small in size and also the required velocity will be low if air is used to test the flow characteristics of helium at a particular Mach number and Reynolds number.
However when heat transfer is considered, helium test rig will be small in size because of its high enthalpy.

	Enthalpy 120 C	200 C	700 C	900 C
Air	3.94×10^5 J / kg	4.76×10^5 J / kg	10.15×10^5 J / kg	12.46×10^5 J / kg
Helium	6.47×10^5 J / kg	10.061×10^5 J / kg	36.56×10^5 J / kg	46.94×10^5 J / kg

Table 8.8 Enthalpy changes of Air and Helium

8.6 Conclusion on the Comparison of Helium and Air flow in a cascade

A CFD analysis was carried out to compare the flow characteristic of Air and Helium inside an axial flow compressor cascade. This was carried out with the objective of performing some preliminary work for the design and development of a test rig for helium turbomachinery development, which can be run with air.

The CFD analysis was based on an experimental test carried out previously and the computational results were found to match very well with the data of the experimental results. Average pressure loss across the cascade for helium is found to be 10.47% and for Air 9.15%. The analysis shows how a hypothetical test rig for helium using air can be run for Reynolds Number similarity or Mach number similarity. If both Reynolds Number similarity and Mach number similarity are required, the diameter of the test rig has to be reduced to 45% for helium. Consequently, significant savings in cost and complexity can be accomplished by using air instead of helium with appropriate scaling of the test facility.

Chapter .9
Conclusions and Recommendations.

9.1 On Performance analysis.

High Temperature Gas Reactors (HTGR) coupled with helium turbines have been considered as a viable option for several power generation issues. However it was always considered as a technology ahead of its time. As we moved into the 21st century, and having technology for almost all engineering challenges, it is the time to give HTGRs the attention it deserves. The economics rather than the technical viability is the main focal point in the argument against this technology. But there will be a time when the engineering companies will be forced to think of HTGR, when they need a less expensive solution for the problem of diminishing fossil fuels and escalating emission.

A detailed performance analysis has been carried out on the conceptual design of a developmental project Pebble Bed Modular Reactor (PBMR) in South Africa. This is a three shaft direct Brayton cycle with nuclear reactor using helium as coolant. The simulation was carried out using a computer code called GTSI developed by a previous research student at Cranfield University. Some alterations and additions were done to adapt it to the PBMR design and also to improve its control characteristics. The performance analysis was focussed on all aspects of the operations such as start-up, load ramping, load rejection shut down etc. The effect of the various control hardware operations on the system performance was also analysed. This included bypass valve, inventory valves, interrupt valves etc. The start-up method using hot gas injection has been studied in detail.

The simulation demonstrated that Closed Cycle Gas Turbine offer unique opportunities for managing the load variation. This is very much significant for Modular High Temperature Reactor Units generating electricity for small grids or as captive power plant where rapid load changes at high magnitude occur. Out of the three options, Bypass control can be used for quick changes whereas and Inventory control is considered as an efficient way but moderate in speed and the Temperature control at heat source is slow in response. The part load efficiency with inventory control is almost constant and this feature makes these units a suitable substitute as peak load and base load units at the same time. Conventional stations do have some difficulty in performing this way. Due to the compactness of the equipment, which use Helium as working medium, the bypass operation can be used for very rapid load changes. Hence the Modular Reactor Units using Helium will be able to handle step changes better than conventional power plants.

Experience shows the clearances in the helium turbomachineries will have serious impact on its performance due to the low molecular size of helium. The magnetic bearings with different type of gaps and clearances, compared to conventional bearings, will have a serious impact on the final performance on the PBMR.

Some of the conclusions, specific to the technical aspects, derived from this exercise are

1. Different loads can be attained without moving from the compressor characteristic design point. This is done by changing the pressure level in the system. The power can be lowered up to 40% of the full load. The efficiency will remain same during this span.

2. The TET is not supposed to go up in the PBMR design. This is due to the negative reactivity, which reduces the release of heat in the event of a temperature rise. This neutronic action is instantaneous. However the fuel particles are coated and surrounded by other low conducting materials like graphite. Hence there will be a time delay in the response to a rise in TET. In the event of rising TET, the power available to the turbine will go up provided the mass flow remains same or higher. The possibility of a rise in temperature can happen only when there is a reduction in the mass flow rate through the reactor. This means, a temperature rise will be accompanied by a fall in mass flow. This may keep the turbine power constant.

3. The only practical possibility of turbine power going up is when the mass flow rate goes up. When the mass flow rate goes up, the reactor will release more heat to keep the temperature constant because the reactivity is a function of temperature and not the total heat. This will give more energy into the turbine, which will increase the speed and can take the compressor to surge. The possibility of high mass flow through the turbine is when the bypass valve closes or when the pressure level in the system increases.

4. The bypass valve operation has to be optimised to keep the shaft speed constant. A slow operating valve will give enough time for the compressor to increase its resistance against the rising turbine power.

9.2 On Start-up and Shutdown

A detailed analysis of various start-up and shutdown methods for a closed cycle multiple shaft arrangement has been carried out. The electrical motor starting will be simple and convenient, but extra hardware will not be useful for normal operation. Cold gas injection is simple but inefficient. Unsuccessful start-ups can increase the inventory, which will have to be pumped back.

A hot gas injection method has been suggested here. In this the gas will be heated before injecting into the HP turbine. This is an efficient way and also obviates the need of any extra hardware on the shaft such as pony turbines. The drawback is to have a heating system for the start-up. If the reactor is not ready for it, a separate heating may not be practical. The starting time depends on the flow rate of valve and the gas temperature. A successful start region is mapped using a specific control valve and it gives certain temperature as the minimum required temperature to attain self-sustaining speed. A procedure is written based on the analysis.

Different mode of shutdown is also analysed. Normal shut down can be done by lowering the inventory level. The turbo-shaft speed can be reduced by overloading it

using the bypass or by using the inventory inlet and exit together. The valve characteristics were derived for various type of shutdown. From the performance analysis it is found that around 30% of the bypass will be sufficient to bring the system to synchronous idling. Synchronous idling using bypass, is not recommended for long duration, as it is not efficient. An emergency shutdown will have to use interrupt valves to stop the Brayton cycle completely.

9.3 Recommendations for further work

1. The high temperature helium turbines developed in the past had more of operational problems rather than any other engineering issues. These were mainly originated from the unexpected flow of helium through the seals, tip gaps etc. PBMR is deploying magnetic bearings, which inherently needs more clearance. This can have a serious impact on all turbomachineries. A detailed analysis has to be done separately based on the change of clearances from conventional bearings to magnetic bearings.
2. The simulation programme can be enhanced further by improving its operation and control logic. This can be done either by incorporating more controllers into it or by linking this with other popular control system simulation software such as Simulink.
3. A more detailed study on the effect of vertical shaft compared to the horizontal shafts on the final performance of the plant is recommended. This coupled with the magnetic bearing axial movement (vertical lifting and landing) will make that study more interesting and valuable.
4. A start-up using hot gas injection has to make use of the heating from the reactor. If heating from the reactor is not available before the starting of the Brayton cycle, an external heating facility has to be considered. A study on the requirements and viability of such a system is suggested for a future work.

9.4 On CFD analysis

A CFD analysis has been carried out on the pressure vessel of the PBMR design. The pressure vessel is one of the massive components in the design with a complex geometry. The flow behaviour of helium in this vessel has to be understood prior to its manufacturing. The CFD analysis focused at two aspects.

One was to identify pockets or locations, where the velocity is high or a location of significant pressure drop. The model has identified two locations with significant pressure losses. The first one was close to the HP compressor discharge. When the gas is flowing from the HP discharge through the narrow concentric gap between the HP compressor and the pressure vessel, in the upward direction, it experiences significant pressure loss. This can be solved by increasing the port diameter and or widening the gap available for the flow. The second one was at the junction between the horizontal part of the pressure vessel and the power turbine. Here the flow was taking a 90^0 turn through a small gap. This can be solved by reducing the angle of turn of flow or by widening the gap as shown in the picture below.

The second objective was to study the flow behaviour during various inventory level. The percentile flow loss with respect to the system pressure was found to be very

much same. The relation between pressure loss and density is quite linear and no sudden increase in the pressure loss was noticed as the density decreased. The reason is that, the system inherently has a very low Mach number and Reynolds number even during full load. This shows that the pressure vessel does not contribute much to the low efficiency during low inventory operation.

A CFD analysis was carried out to compare the flow characteristic of Air and Helium inside an axial flow compressor cascade. This was carried out with the objective of doing some preliminary work for the design and development of a test rig for helium turbomachinery development, which can be run with air.

The CFD analysis was based on an experimental test carried out previously and the computational results were found to match very well with the data of the experimental results. Average pressure loss across the cascade for helium is found to be 10.47% and for Air 9.15%. The analysis shows how a hypothetical test rig for helium using air can be run for Reynolds Number similarity or Mach number similarity. If both Reynolds Number similarity and Mach number similarity are required, the diameter of the test rig has to be reduced to 45% for helium. Consequently, significant savings in cost and complexity can be accomplished by using air instead of helium with appropriate scaling of the test facility.

9.5 Recommendations for further work on CFD analysis.

1. The current exercise carried out with a mesh size of 170mm due to the computational limitations. The dimensional detail of the geometry is taken from a conceptual design. As more details become available, the geometry has to be remodelled with more dimensional details and to be meshed in fine grids to improve the accuracy.

2. An attempt was made to carry out a time dependant, user defined flow condition. However due to the complexity and massiveness of the model and due to the computational limitations, the programme was crashing and the attempt was unsuccessful. This activity is recommended for the future work..

3. The pressure vessel is acting as a pipe connecting HP Compressor and the Recuperator inlet. The Bypass valve will be opening for branching the flow to the pre-cooler inlet where the pressure will be one of the lowest in the system. Hence a sudden opening of the Bypass valve is a source of unsteady flow. This can be modelled in CFD. As a next step, a time dependant, unsteady flow solution can be done. This will give an idea of the response time required by the valves to change the flow through the reactor for load control.

4. The Interrupt valves are for the Emergency shut down. These are stop valves placed between the HP compressor outlet and the pre cooler inlet to stop the flow completely through the reactor. This flow should be modelled to see the possibility of any reverse flow or any other oscillatory flow in the pressure vessel due to the operation of Interrupt valves. This should be done with a time dependant user defined input

Bibliography and References

1. Agazzani, A., Massardo A F., Korakianitis, T., *An assessment of the Performance of closed cycles with and without heat rejection at cryogenic temperatures*. ASME, Journal of Engineering for gas Turbines and Power, Vol121, July 1999 , pp 458-464.
2. Ainley, D G., Barnes J F., *An assessment of the efficiencies and component sizes of nuclear closed – cycle gas turbines of 250MW output, using argon and helium.* Ministry of Aviation, National Gas Turbine Establishment, Pyestock, Hants, NGTE Report No. R 270, Sept 1965.
3. American Nuclear Society Topical Meeting report. *Gas cooled Reactors: HTGR and GCFBR*, May 7 –10, 1974, Gatlinburg, Tennessee, Page 401.
4. Arthur, J G., *Summary of brayton cycle analytical studies for space power systems applications*. Lewis research Centre, Cleveland, Ohio NASA TN D-2487, September 1964.
5. Arthur, J G., *Thermodynamic and turbomachinery concepts for radioisotope and reactor brayton – cycle space power systems*. Lewis research Centre, Cleveland, Ohio NASA TN D-2968, August 1965.
6. Baggenstoss, W.G and Ashe, T.L. *Mission design drivers for closed Brayton cycle space power conversion configuration,* Transactions of the ASME, Journal of Gas Turbines and Power, Vol. 114, October 1992, pp 721-726.
7. Bammert, K and Groschup, G., *Status report on closed cycle power plants in the federal republic of Germany.* Transactions of ASME. Journal of Engineering for Power, Vol 98-99, 1976-77.
8. Bammert, K., *Design and Construction of helium turbines, helium compressors and helium turbine power plants*, NASA / CASI – N7827435.
9. Bammert, K., Groschup, G., *Status Report on closed cycle power plants in the Federal republic of Germany.* ASME, Journal of Engineering for Power, January 1977, pp 37-46.
10. Bammert, K., Krey G., *Dynamic behaviour and control of single shaft closed cycle gas Turbines.* NASA / CASI – N7922095.
11. Bammert, K., Rurik J, Griepentrog H., *Highlights and future development of closed cycle gas turbines.* ASME, Journal of Engineering for Power, October 1974, pp 342-348.
12. Bammert, K., Zehner p., *Back flow in turbines of nuclear closed –cycle gas turbine plants in case of circuit pipe rupture.* ASME, Journal of Engineering for Power., April 1975, pp 185-194.
13. Banerjea, A., Hammeke K., *Thermodynamic properties of helium in the range from 20 to 1500 C and 1 to 100 bar,* Kernforschungsanlage Julich GmbH, December 1978.
14. Bausa, J., Tsatsaronis G., *Dynamic optimisation of startup and load increasing processes in power plants. Part I and II,* ASME, Journal of Engineering for gas Turbines and Power.,vol 123 January 2001 , pp 246-253.
15. Bloch, H P, *A Practical guide to compressor technology*, 1996, McGraw-Hill
16. Bloch, H., *Turboexpanders and Process Applications*, 2001, Gulf professional Publishing. ISBN 0-88415-509-9

17. Brey, H L., *Development history of the gas turbine modular high temperature reactor.* International Atomic Energy Agency Report of the Technical Committee meeting Paulo Alto, United States of America, 14 – 16 November 2000. IAEA August 2001.
18. Britcher, C P., Groom N J., *Computational analysis of static and dynamic behaviour of magnetic Suspensions and magnetic Bearings.* NASA CASI – 96N34254.
19. Brown, D P., Gibbs R J., Schlafke A P., *Operating experiences and test results of six cold helium compressors.* Brookhaven National Laboratory, Associated Universities, Inc. Upton, New York. NASA/CASI – N8810982.
20. Brown, R N, *Compressors-Selection and Sizing.* Gulf Publishing Company, Houston, Texas. ISBN 0-88 415-164-6
21. Cantoni, D A., *A parametric study of motor starting for a 2 to 15 KW Brayton Power system.* Lewis research centre, Cleveland Ohio, NASA TN D –2432.
22. Cantoni, D A., *Gas Injection start and shutdown characteristic of a 2 to 15 KW Brayton Power system.* Lewis research centre, Cleveland Ohio, NASA TN D – 6938.
23. Cohen, H., Rogers G.F.C., Saravanamuttoo, H.I.H., *Gas Turbine Theory.* Longman Scientific and Technical UK. ISBN 0-582-23632-0
24. Crawford, R. A., *Quantitative evaluation of transient heat transfer on axial flow compressor stability.* AIAA paper 85-1352, July 1985, Monterey, California.
25. Cumptsy, NA, *Compressor Aerodynamics.* Longman Scientific and Technical, UK, 1989
26. Decher, R., *Energy Conversion, Systems, Flow physics and Engineering.* Oxford University Press, 1994
27. Dhole, V.R and Zheng, J.P., *Applying combined pinch and exergy analysis to closed cycle gas turbine system design*, Transactions of the ASME, Journal for Gas Turbines and Power, vol 117, January 1995, pp47-52.
28. Dixon, S L., *Fliud Mechanics and Thermodynamics of Turbomachinery.* Butterworth Heinemann, 1998, Oxford.
29. Donald, T K., *A method for predicting the off design performance of closed brayton cycle engines.* NASA / CASI – N7914562
30. Duponchel, J.P., Loisy, J., and Carrillo, R., *Steady and transient performance calculation method for prediction of gas turbine engines.* AGARD series 183, May 1992.
31. El-Masri, M.A., *GASCAN – An interactive code for thermal analysis of gas turbine systems.* Transactions of the ASME, Journal of Engineering for gas Turbines and Power, vol 110, April 1988, pp.233-240.
32. Fielding L., *Turbine Design - The effect on axial flow turbine performance of parameter variation,* 2000, ASME Press, New York.
33. Fluent Inc, *FLUENT User Guides*, Volume 1-4, Fluent Inc, USA, 1999
34. Fraas, A.P., *Engineering evaluation of energy systems,* McGraw-Hill Book company, New York, 1982.
35. Frutschi, H U., *Ensuring stable circuit conditions of direct cycle helium gas turbine system.* ASME, Journal of Engineering for Power., October 1974, pp 435-439.

36. Frutschi, H.U., *The relationship of power and heat production with closed cycle gas turbines.* Transactions of the ASME, Journal of Engineering for the Power, Vol. 102, April 1980, pp 288-291.
37. Gill, A.B., *Power Plant Performance*, Butterworths, 1984.
38. Glass mann, A.J , *Turbine Design and Application.* Vols 1-3, NASA SP-290,1972.
39. Harman, R.T.C, *Gas Turbine Engineering*. The MacMillan Press, 1981.
40. Hosny, W M, Botter, S J and Steenken, W G: *Turbofan Engine Non recoverable Stall Computer Simulation Development and Validation.* AIAA- 85 -1432, AIAA/SAE/ASME/ASEE 21st Joint Propulsion Conference, Monterey California July 1985
41. Hosny, W M., Bitter, S.J., Steenken, W G., *Turbofan engine non-recoverable stall computer simulation development and validation.* AIAA/ SAE/ ASME/ ASEE 21st propulsion conference, July 1985 Monterey, California.
42. Hunter, I., *Design of turbomachinery for closed and semi closed gas turbine cycles*, MSc Thesis, 1993-94, Cranfield University.
43. Innocente, G., Wydler, H., Halzl J., *Helium heaters of the helium turbine unit of the Oberhausen Energy Supply.* NASA / CASI – N7827440.
44. Itoh, M., Ishigaki, T. and Sagiya Y., *Simulation study of transient performance matching of turbofan engine using an analogue computer to evaluate its usefulness as design tool.* Transactions of ASME, Journal of Engineering for power, vol 97, pp369-374, July 1975.
45. Keenan, J.H., Kaye, J., and Chao, J., *Gas Tables: International version 2nd Edition (SI units).* 1983.
46. Keller, C., *Operating experience and design features of closed cycle gas turbine power plants.* Transactions of ASME April 1957, Paper No.56-GTP-15.
47. Kim, J H., Song, T W., Kim, T S ., Ro, S T., *Model development and simulation of transient behaviour of heavy duty gas turbines.* ASME, Journal of Engineering for gas Turbines and Power, July 2001, pp 589-594.
48. Klann, J L., Hettel, J H., *Predictability of brayton electric power system performance.* Lewis research centre, Cleveland Ohio, NASA TN D –6808.
49. Klann, J.L., *Steady state analysis of a brayton space power system*, Lewis Research Centre, NASA TN D –5673.
50. Knauss, DT., *A method for predicting the off-design performance of closed – Brayton cycle engines.* Propulsion and auxiliary systems department, Research and Development Report, September 1978, NASA/ CASI –N7914562.
51. Koch, CC., *Stalling pressure rise capability of axial compressors.* ASME Journal of Engineering power Vol103,1981
52. Korakianitis, T., Svensson, K., *Off –design performance of various gas turbine cycle and shaft configurations*. ASME, Journal of Engineering for gas Turbines and Power., Vol 121 October 1999, pp 649-655.
53. Korakianitis, T., Vlachopoulos, N.E., *Models for the prediction of transients in closed regenerative gas turbine cycles with centrifugal impellers.* ASME paper 94-GT-342.
54. Korakianitis, T., Wilson, D G, *Models for predicting the performance of Brayton- Cycle Engines.* ASME, Journal of Engineering for Gas Turbines and Power., Vol 116 April 1994 , pp 381-388.
55. Kotas, T.J., *The exergy method of Thermal Plant analysis*. Butterworths, 1985.

56. Krey, G., *Utilisation of the cold by LNG vaporisation with closed cycle gas turbine.* Transactions of the ASME, Journal of Engineering for power, Vol102, April 1980, pp225-230.
57. Kunitomi, K., Tachibana, Y., Saikusa, A., Sawa, K., Lidsky, L M., *Conceptual design of a 50 MW severe – accident free HTR and the related test program of the HTTR.* pp-245, Nuclear Technology Sep 1998.
58. Kurzke, J., *Calculation of installation effects within performance computer programs.* AGARD Lecture series 183, Steady and Transient Performance Prediction of Gas Turbine Engines, May 1992.
59. Lee, J.C., Campbell, J.Jr., Wright, D.E., *Closed cycle gas turbine working fluids.* Transactions of ASME, Journal of Engineering for power, vol. 103, 1981.
60. Levine, W S., *Control system applications.* 2000, CRC Press London.
61. Livingood, J.N.B., *1971 NASA Turbine Cooling Research Status Report.* NASA TM-X-2384, Lewis research Centre, Cleveland, Ohio, 1971.
62. Maccallum, N.R.L. and Qi, Q.F., *The transient behaviour of aircraft gas turbines.* University of Glassgow, September 1989.
63. Massardo, A., Arnulfi, G., *Combined closed cycle systems for under water power generation.* ASME Paper 92-GT – 97.
64. Matsuo, E., Tsutsumi, M., Ogata, K., Nomura, S., Conceptual design of helium gas turbine for MHTGR-GT. Proceedings of International Atomic Energy Agency Technical committee meeting, Beijing, 30 October – 2 November 1995, Page95.
65. Matzner, D., *PBMR Technical specification.* Issue 1.0, and PBMR Doc 196-28 issue 3, Thermohydraulic component specification for simulator input 1999. www.pbmr.co.za
66. McDonald, C F., Van Hagan T., Vepa K., *Heat exchanger design considerations for gas turbine HTGR power plant.* ASME, Journal of Engineering for Power, April 1977, pp 237-45.
67. Mohitpour, M., Golshan, H., Murray, A., *Pipeline design and construction- A practical approach. 2000.* ASME press, New York.
68. Murrill, P W., *Fundamentals of Process Control Theory.* 2000, Instrument Society of America.
69. Navaratnam, M., *The investigation of an aero-derivative gas turbine using alternative working fluids in closed/semi closed cycles.* MSc Thesis 1993-94, Cranfield University.
70. Nicholls, D., *Pebble Bed Modular Reactor - Executive Summary.* Doc. No 79/1, May 1999.
71. Perz, E., *A computer method for thermal power cycle calculation.* Transactions of the ASME, Journal for Gas Turbines and Power, Vol 113, April 1991, pp. 184-189
72. Philpot, M.G., *Practical considerations in designing the engine cycle.* AGARD lecture series 183, Steady and Transient Performance Prediction of Gas Turbine Engines, May 1992.
73. Pietsch, A., Rackley, R. A., *Closed brayton cycle system optimisation for undersea, terrestrial and space applications.* NASA / CASI – N7922096.
74. Pilidis. P., *Gas Turbine Performance.* Course Notes, Thermal Power MSc, 1999, Cranfield University

75. Pradeep Kumar K N., Tourlidakis, A., Pilidis P., *Analysis of a 115mw, 3- shaft, helium brayton cycle using nuclear heat source.* Proceedings of ASME Turbo Expo 2001 Land, Sea& Air. June 4-7, 2001. New Orleans, Louisiana USA. Paper Number: 2001-GT-0523
76. Pradeep Kumar K N., Tourlidakis, A., Pilidis, P., *Performance Review: PBMR closed cycle gas turbine power plant.* Proceedings of Technical Committee Meeting on HTGR –Power conversion systems. International Atomic Energy Agency, Paulo Alto, United States of America, 14 – 16 November 2000. IAEA August 2001. pp 99-112.
77. Pradeep Kumar K N., Tourlidakis, A., Pilidis, P., *Design and performance review of PBMR closed cycle gas turbine plant in South Africa.* 2001 International Joint Power Generation Conference. New Orleans, Louisiana, June 4-7, 2001. Paper Number: JPGC2001/NUC-19170
78. Pradeep Kumar K N., Tourlidakis, A., Pilidis, P., *Generation and control of electricity in HTGR helium turbine plant.* Proceedings of ICONE10 .10TH International Conference on Nuclear Engineering. Arlington, VA, USA, April 14-18, 2002, Paper Number: ICONE10-22200.
79. Pradeep Kumar K N., Tourlidakis, A., Pilidis, P., *HTGR closed cycle GT plant analysis: Options and procedures for start-up with hot gas injection.* Proceedings of ASME Turbo Expo 2002, June 3-6, 2002. Amsterdam, Paper Number: GT-2002-30146.
80. Ramsden, K.W., *Axial compressor and Turbine Design and Performance.* Course Notes, Thermal Power MSc, 1999, Cranfield University
81. Rhoden, H. G, and Bennet, M., *Effects of Reynolds number on the flow of air through a cascade of compressor blades.* Aeronautical Research Council, Ministry of Supply, Reports and Memoranda, R & M No 29, 15259, ARC Technical Report, September 1956
82. Saravanamuttoo, H.I.H., Fawke, A.J., *Digital computer methods for prediction of gas turbine dynamic response,* SAE paper 710550, Montreal, Canada, 1971, 1971.
83. Saravanamuttoo, H.I.H., Fawke, A.J., *Simulation of gas turbine dynamic performance.* ASME paper 70-GT-23, Brussels, Belgium, 1970.
84. Sawyer, J.W., *Sawyer's Gas Turbine Engineering Handbook.* Vol I and II, Third edition, 1985.
85. Schobeiri, M.T., Attia, M. and Lippke, C., *GETRAN : A generic, modularly structured computer code for simulation of dynamic behaviour of aero and power generation gas turbine engines.* Transactions of the ASME, Journal of Engineering for Gas Turbines and Power, Vol.116, July 1994, pp.483-494.
86. Singh, R., *Gas Turbine Technology and Applications.* Course Notes, 1999, Thermal Power, Cranfield University, UK
87. Skousen, P L., *Valve Handbook*, Mcgraw-Hill publications.
88. Thring, M W., *Nuclear Propulsion*, 1960, Butterworth &Co, London
89. Tiberini, A., *Operational limits for gas turbine compressors during transient conditions in a helium cooled reactor.* ASME, Journal of Engineering for Power., October 1974, pp 427-434.
90. Tourlidakis A., Elder R L and Tan S C., *Applying computational fluid dynamics to real fluid machinery and pump flow problems*, Proceedings of the 14th BPMA Technical Conference, pp 623-651.

91. Ulizar, I., *A semi-closed cycle gas turbine with carbon dioxide- Argon as working fluid.* Journal of Engineering for Gas Turbines and Power, Vol 119, July 1997, pp612 –616.
92. Ulizar, I., *Design and off design performance study of a variable cycle engine with convergent-divergent nozzle.* MSc Thesis, Cranfield Institute of Technology, UK, 1992.
93. Ulizar, I., *Design of a semiclosed cycle gas turbine with carbon dioxide- argon as working fluid.* ASME Turbo Expo, 1997, Orlando, Florida.
94. Ulizar, I., *Gas Turbine Simulation Programme* – Industrial version
95. Ulizar, I., *Simulation of multi fluid gas turbines.* PhD thesis, Cranfield University. 1998
96. Versteeg, H K., Malalasekera, W., *An introduction to computational Fluid Dynamics*. Addison Wesley Longman Limited, 1998, England.
97. Walsh, P., Fletcher, P., *Gas Turbine Performance.* Blackwell Science. ISBN 0-632-04874-3
98. Weisbrodt I A, *Summary of report on technical experiences from high temperature helium turbomachinery testing in Germany.* Proceedings of International Atomic Energy Agency Technical committee meeting, Beijing, 30 October – 2 November 1995, Page181
99. Weisman, J., Eckart, L.E., *Modern Power Plant engineering.* ISBN 0-08-040502-9
100. Wright T., *Fluid machinery- Performance, Analysis and Design.* 1999, CRC Press, London.
101. Zhu, P., Saravanamuttoo, H.I.H., *Simulation of an advanced twin spool industrial gas turbine.* Transactions of the ASME, Journals for Gas Turbines and Power, Vol 114, April 1992, pp 180-186.

Appendix .I
High Temperature Helium Test Facility-HHV Test Loop [3]

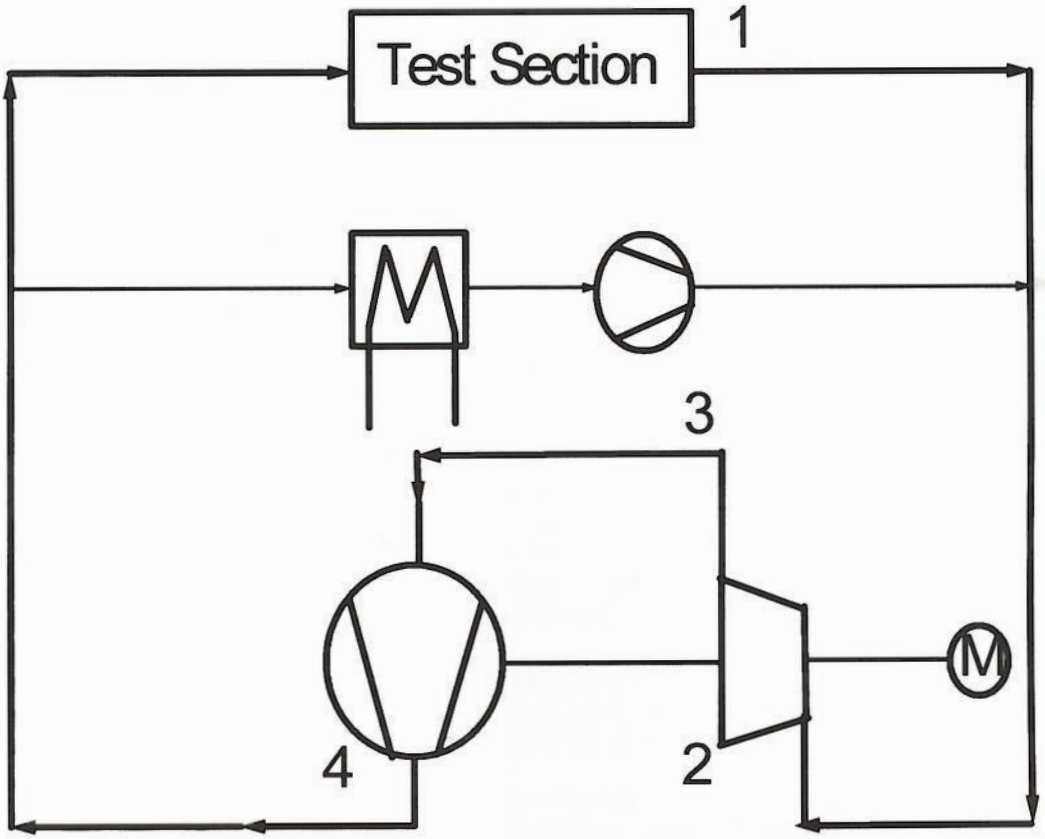

HHV Test Circuit
Legend : 1. Test Section 2. Helium Turbine
3. Duct to Compressor Inlet 4. Compressor

Appendix .II
GTSI- Input File I - DESIGN.DAT

```
&GEOMETRY
 NMAX =          16
 IVARLPC =        1
 IVARHPC =        1
 IVARHPT =        1
 IVARLPT =        1
 IVARFPT =        1
 ILPTCOL =        0
 ILPTCOLP =       0
 IFPTCOL =        0
 IFPTCOLP =       0
 &MOTOR
 W0DS =       121.200000
 BET2 =     7.000000E-01
 XN2 =        1.000000
 DH21 =    400000.000000
 T23 =        300.000000
 BET25 =     7.000000E-01
 XN25 =       1.000000
 T33 =        833.962100
 DH33 =    1760658.000000
 DHQT67 =     2.205140E-01
 XN67 =       1.000000
 DH71 =    563061.100000
 P2 =   2900000.000000
 ANGVS2 =     0.000000E+00
 ANGVS25 =    0.000000E+00
 AQA0_HT =        1.000000
 AQA0_LT =        1.000000
 AQA0_FT =        1.000000
 PSTD =   2900000.000000
 TSTD =       300.000000
 RSTD =       2078.625000
 GAMSTD =         1.667400
 /
&LPCOMP
 P2STD =   2900000.000000
 T2STD =      300.000000
 R2STD =      2078.625000
 GAM2STD =        1.667400
 BET2DS =     7.000000E-01
 DHQT2DS =    3.874890E-01
 SWEFF2 =     0.000000E+00
 E2DS =     8.700000E-01
 EP2DS =      9.000000E-01
 P21Q2DS =        1.660000
 XN2DS =      1.000000
 TH2DS =      9.998794E-01
 SWMAP2 =     0.000000E+00
 DHQT2SF =        1.695683
 E2SF =       1.027947
 P21Q2SF =        1.000000
```

```
&INTERCOL
 WSC22DS =        81.900660
 CDP22DS =    0.000000E+00
 &HPCOMP
 P25STD =   4814006.000000
 T25STD =       300.000000
 R25STD =       2078.625000
 GAM25STD =         1.667400
 BET25DS =     7.000000E-01
 DHQT25DS =     3.874890E-01
 SWEFF25 =     0.000000E+00
 E25DS =     8.700000E-01
 EP25DS =     8.700000E-01
 P3Q25DS =        1.660000
 TH25DS =     9.998794E-01
 XN25DS =         1.000000
 SWMAP25 =     0.000000E+00
 DHQT25SF =         1.695683
 E25SF =        1.027947
 P3Q25SF =         1.000000
 WSC25SF =         7.674235
 SWSUR25 =     0.000000E+00
 SWMAP25V =         1.000000
 TH25TDS =     9.994107E-01
 /
 &REGEN
 EREG =     9.711000E-01
 WSC32DS =        47.462860
 CDP32DS =     2.000000E-02
 WSC7DS =       192.800300
 CDP7DS =     2.000000E-02
 /
 &MAINHEX
 WSC33DS =        71.985820
 CDP33DS =     5.000000E-02
 /
 &HPTURB
 P4STD =   2900000.000000
 T4STD =       300.000000
 R4STD =      2078.625000
 WSC405SF =         91.109200
 XNRT41SF =     2.939995E-02
 DHQT41SF =     2.831988E-03
 E41SF =     8.908908E-01
 CPLOS41 =     5.000000E-03
 DHQT41DS =     2.888658E-04
 SWEFF41 =     0.000000E+00
 E41DS =     8.900000E-01
 EP41DS =     8.600000E-01
 XNRT41DS =     1.699605E-02
 /
 &HPLPDUCT
```

```
 WSC2SF =        7.674235
 SWSUR2 =     0.000000E+00
 SWMAP2V =         1.000000
 TH2TDS =     9.994107E-01
/
 / &LPTURB
 P45STD =   2900000.000000
 T45STD =       300.000000
 R45STD =      2078.625000
 WSC455SF =       110.038000
 XNRT46SF =     3.055298E-02
 DHQT46SF =     2.656688E-03
 E46SF =     8.976181E-01
 CPLOS46 =     2.000000E-03
 DHQT46DS =     2.888658E-04
 SWEFF46 =     0.000000E+00
 E46DS =     8.900000E-01
 EP46DS =     8.800000E-01
 XNRT46DS =     1.699605E-02
  &LPFPDUCT
 WSC48DS =       131.001900
 CDP48DS =     1.000000E-02
  &FPTURB
 P66STD =   2900000.000000
 T66STD =       300.000000
 R66STD =      2078.625000
 WSC665SF =       132.374700
 XNRT67SF =     3.172433E-02
 DHQT67SF =     1.309966E-03
 E67SF =     9.077037E-01
 CPLOS67 =     2.000000E-03
 DHQT67DS =     2.888658E-04
 SWEFF67 =     0.000000E+00
 E67DS =     9.000000E-01
 EP67DS =     8.950000E-01
 XNRT67DS =     1.699605E-02
 XN67DS =         1.000000
&FPRGDUCT
 WSC69DS =       190.872300
 CDP69DS =     1.000000E-02
  &PRECOOL
 WSC71DS =       136.570000
 CDP71DS =     1.000000E-02
 WSC43DS =       108.896900
 CDP43DS =     1.000000E-02
/
 &NOZZLE
 WSC72DS =       118.229100
 CDP72DS =     5.000000E-03
 A8DS =     1.647857E-01
/
 &COOLFPT1
 SW203 =     0.000000E+00
 CH203 =     7.500000E-01
 DEP203 =    -5.000000E-03
 P203SEG =         5.000000
 P203LOSS =        10.000000
 CWS203 =     1.000000E-04
 SW253 =     0.000000E+00
 CH253 =     7.500000E-01
 DEP253 =    -5.000000E-03
 P253SEG =         5.000000
 P253LOSS =        10.000000
 CWS253 =     1.000000E-04
 PCWB1 =     0.000000E+00
 PCWB2 =     0.000000E+00
 PCWB3 =     0.000000E+00
&TRANSITO
 OMEGA2 =      1570.800000
 OMEGA25 =      1570.800000
 OMEGA67 =       314.160000
 XINER2 =        30.000000
 XINER25 =        22.000000
 XINER67 =       125.000000
 VOL21 =     2.000000E-02
 VOL23 =     5.000000E-02
 VOL3 =     2.000000E-02
 VOL33 =     5.000000E-02
 VOL4 =     1.000000E-01
 VOL43 =     2.000000E-02
 VOL45 =     3.000000E-02
 VOL48 =     3.000000E-02
 VOL5 =     2.000000E-02
 VOL69 =     2.000000E-02
 VOL7 =     8.000000E-02
 VOL71 =     5.000000E-02
 VOL72 =     4.000000E-02
 &VARGLPC1
 N_VS2_E =           9
 X_VS2_E =       -30.000000      -20.000000      -10.000000       -5.000000
   0.000000E+00        5.000000       10.000000       20.000000
      30.000000    0.000000E+00    0.000000E+00    0.000000E+00
   0.000000E+00    0.000000E+00    0.000000E+00    0.000000E+00
   0.000000E+00    0.000000E+00    0.000000E+00    0.000000E+00
 Y_VS2_E =    -1.000000E-01   -6.000000E-02   -2.500000E-02   -1.000000E-02
   0.000000E+00   -1.000000E-02   -2.500000E-02   -6.000000E-02
  -1.000000E-01    0.000000E+00    0.000000E+00    0.000000E+00
   0.000000E+00    0.000000E+00    0.000000E+00    0.000000E+00
   0.000000E+00    0.000000E+00    0.000000E+00    0.000000E+00
/
```

Appendix .III GTSI-Input File II
CONTROL.DAT

```
&CONTROL
 SWDES =        0.000000
 ITRANS =             0
 ENGINE = 'indumap.dat        '
 SENGINE = 'indumaps.dat       '
 DESIGN = 'designt6.dat       '
 OUTDES = 'outdes.dat         '
 OUTDAT = 'out03.dat          '
 OUTRES1 = 'result1.dat       '
 OUTRES2 = 'result2.dat       '
 ISALIDA =            0
 I_INP1 =             1
 I_INP2 =             2
 I_INP3 =             3
 I_OUT1 =             4
 LOOPERH =         2000
 CDVAR =     5.000000E-01
 CDVARH =        10.000000
 TOLALL =     1.000000E-03
 DTTRANS =     1.000000E-01
 TTRANS =        150.00000
 RATCOOL1 =     0.000000E+00
 CT23 =       300.000000
 CPWX22 =    800000.000000
 RATCOD =         0.000000
 CT41 =      1640.000000
 CT4 =       1183.000000
 CXN2 =          1.000000
 CXN25 =         1.000000
 CXNRT2 =        1.050000
 CXNRT25 =       1.100000
 CP_21 =    1000000.000000
 CP_3 =     4000000.000000
 CT3 =       890.000000
 CP8QAMB =       1.020000
 CPWX33 =    1000000.000000
 CPWX67 =    2500000.000000
 CSM2 =         10.000000
 CSM25 =        15.000000
 CT46 =      1240.000000
 CT67 =      1000.000000
 CWSC2 =       100.000000
 CWSC25 =      100.000000
 CT69 =       890.000000
 CBET2 =     6.000000E-01
 CBET25 =    6.000000E-01
 RATFRE =    0.000000E+00
 CXN67 =         1.000000
CT2 =        300.000000
 RATCLOS =    0.000000E+00
 CP_2 =    2900000.000000
 RATLPC =    0.000000E+00
 CANGVS2 =    0.000000E+00
 RATHPC =    0.000000E+00
 CANGVS25 =    0.000000E+00
 RATHPT =    0.000000E+00
 CAQA0_HT =    1.000000E+00
 RATLPT =    0.000000E+00
 CAQA0_LT =    1.000000E+00
 RATFPT =    0.000000E+00
 CAQA0_FT =    1.000000E+00
 PCWB22 =    0.000000E+00
 PCWB31 =    0.000000E+00
 PWX67H =    2.000000E+08
 T3H =        900.000000
 T4H =       1350.000000
 T41H =       1300.000000
 T46H =       1150.000000
 T67H =       1050.000000
 T69H =        950.000000
 XN2H =          1.300000
 XN25H =         1.300000
 XN67H =         1.400000
 XNRT2H =        1.300000
 XNRT25H =       1.300000
 SM2L =         10.000000
 SM25L =        10.000000
 P21H =    8000000.000000
 P3H =    16000000.000000
 P69H =    4000000.000000
 PWX41AUX =    0.000000E+00
 PWX46AUX =    0.000000E+00
 SA8 =          1.000000
 DA8 =     0.000000E+00

TTPWX22 =    0.000000E+00    100.000000    1000.000000  0.000000E+00
   0.000000E+00   0.000000E+00   0.000000E+00   0.000000E+00
   0.000000E+00   0.000000E+00   0.000000E+00   0.000000E+00
   0.000000E+00   0.000000E+00   0.000000E+00   0.000000E+00
   0.000000E+00   0.000000E+00   0.000000E+00   0.000000E+00
 PWX22T =    4.877736E+07   4.877736E+07   4.877736E+07   0.000000E+00
   0.000000E+00   0.000000E+00   0.000000E+00   0.000000E+00
   0.000000E+00   0.000000E+00   0.000000E+00   0.000000E+00
```

```
  0.000000E+00   0.000000E+00   0.000000E+00   0.000000E+00
  0.000000E+00   0.000000E+00   0.000000E+00   0.000000E+00
NPWX22T =          3
TTPWX33 =    0.000000E+00     10.000000    1000.000000   0.000000E+00
  0.000000E+00   0.000000E+00   0.000000E+00   0.000000E+00
  0.000000E+00   0.000000E+00   0.000000E+00   0.000000E+00
  0.000000E+00   0.000000E+00   0.000000E+00   0.000000E+00
  0.000000E+00   0.000000E+00   0.000000E+00   0.000000E+00
PWX33T =    2.094526E+08   1.841990E+08   1.841990E+08   0.000000E+00
  0.000000E+00   0.000000E+00   0.000000E+00   0.000000E+00
  0.000000E+00   0.000000E+00   0.000000E+00   0.000000E+00
  0.000000E+00   0.000000E+00   0.000000E+00   0.000000E+00
  0.000000E+00   0.000000E+00   0.000000E+00   0.000000E+00
NPWX33T =          3
TTPWX71 =    0.000000E+00     100.000000    1000.000000   0.000000E+00
  0.000000E+00   0.000000E+00   0.000000E+00   0.000000E+00
  0.000000E+00   0.000000E+00   0.000000E+00   0.000000E+00
  0.000000E+00   0.000000E+00   0.000000E+00   0.000000E+00
  0.000000E+00   0.000000E+00   0.000000E+00   0.000000E+00
PWX71T =    6.838511E+07   6.331817E+07   6.331817E+07   0.000000E+00
  0.000000E+00   0.000000E+00   0.000000E+00   0.000000E+00
  0.000000E+00   0.000000E+00   0.000000E+00   0.000000E+00
  0.000000E+00   0.000000E+00   0.000000E+00   0.000000E+00
  0.000000E+00   0.000000E+00   0.000000E+00   0.000000E+00
NPWX71T =          3
TTPWX67 =    0.000000E+00     100.000000    1000.000000   0.000000E+00
  0.000000E+00   0.000000E+00   0.000000E+00   0.000000E+00
  0.000000E+00   0.000000E+00   0.000000E+00   0.000000E+00
  0.000000E+00   0.000000E+00   0.000000E+00   0.000000E+00
  0.000000E+00   0.000000E+00   0.000000E+00   0.000000E+00
PWX67T =    9.176434E+07   7.572687E+07   7.572687E+07   0.000000E+00
  0.000000E+00   0.000000E+00   0.000000E+00   0.000000E+00
  0.000000E+00   0.000000E+00   0.000000E+00   0.000000E+00
  0.000000E+00   0.000000E+00   0.000000E+00   0.000000E+00
  0.000000E+00   0.000000E+00   0.000000E+00   0.000000E+00
NPWX67T =          3
XN2T =    4.000000E-01   4.500000E-01   5.000000E-01   5.500000E-01
  6.000000E-01   6.500000E-01   7.000000E-01   7.500000E-01
  8.000000E-01     1.500000   0.000000E+00   0.000000E+00
  0.000000E+00   0.000000E+00   0.000000E+00   0.000000E+00
  0.000000E+00   0.000000E+00   0.000000E+00   0.000000E+00
N_ANGVS2 =         10
ANGVS2XNT =       40.000000      35.000000      30.000000      25.000000
     20.000000      15.000000      10.000000       5.000000
  0.000000E+00   0.000000E+00   0.000000E+00   0.000000E+00
  0.000000E+00   0.000000E+00   0.000000E+00   0.000000E+00
  0.000000E+00   0.000000E+00   0.000000E+00   0.000000E+00
```

```
NQDOT72T =         3
 ILPBREAK =        0
 IHPBREAK =        0
 IFPBREAK =        0
 XINER2B =       5.000000
 XINER25B =      5.000000
 XINER41B =      5.000000
 XINER46B =      7.000000
 XINER67B =     75.000000
```

```
STOP =    0.000000E+00
 /
 &CONTROL
  CT4 =     1173.000000
 /
  &CONTROL
 STOP =    1.000000E+00
 /
```

Appendix .IV Input File III- Addition to the Programme
VALVE INPUT DATA

```
1. COMPONENT
   NAME                          'PEBBLE BED'
   TYPE                          '1D REACTOR'
   LOCATED AT                        'PEBBLE_BED_ELEMENT'
   REACTOR STEADY STATE POWER        265.0E+06
   FUELLED ZONE WEIGHTING FACTOR     1.0
   CENTRAL ZONE WEIGHTING FACTOR     1.0


    INITIAL CONDITION DATA
     ENTITY NAME       'CORE_INLET'
     PRESSURE          70.00E+05
     TEMPERATURE         809.0

   INITIAL CONDITION
     ENTITY NAME       'CORE_OUTLET'
     PRESSURE          70.0E+05
     TEMPERATURE         1173.0

   INITIAL CONDITION
     ENTITY NAME       'REAC_OUT1_PLENUM'
     PRESSURE          70.00E+05
     TEMPERATURE         1173.0

   INITIAL CONDITION
     ENTITY NAME       'REAC_OUT2_PLENUM'
     PRESSURE          70.00E+05
     TEMPERATURE         1173.0

2. COMPONENT
   NAME                          'BYPASS VALVE'
   TYPE                          'CONTROL VALVE'
   LOCATED AT                        'BYPASS_VALVE_ELEMENT'
   CONTROL MODE                      'STATIC'
   CHARACTERISTIC                    1
   CONTROL POSITION                    0.0
```

Appendix .V

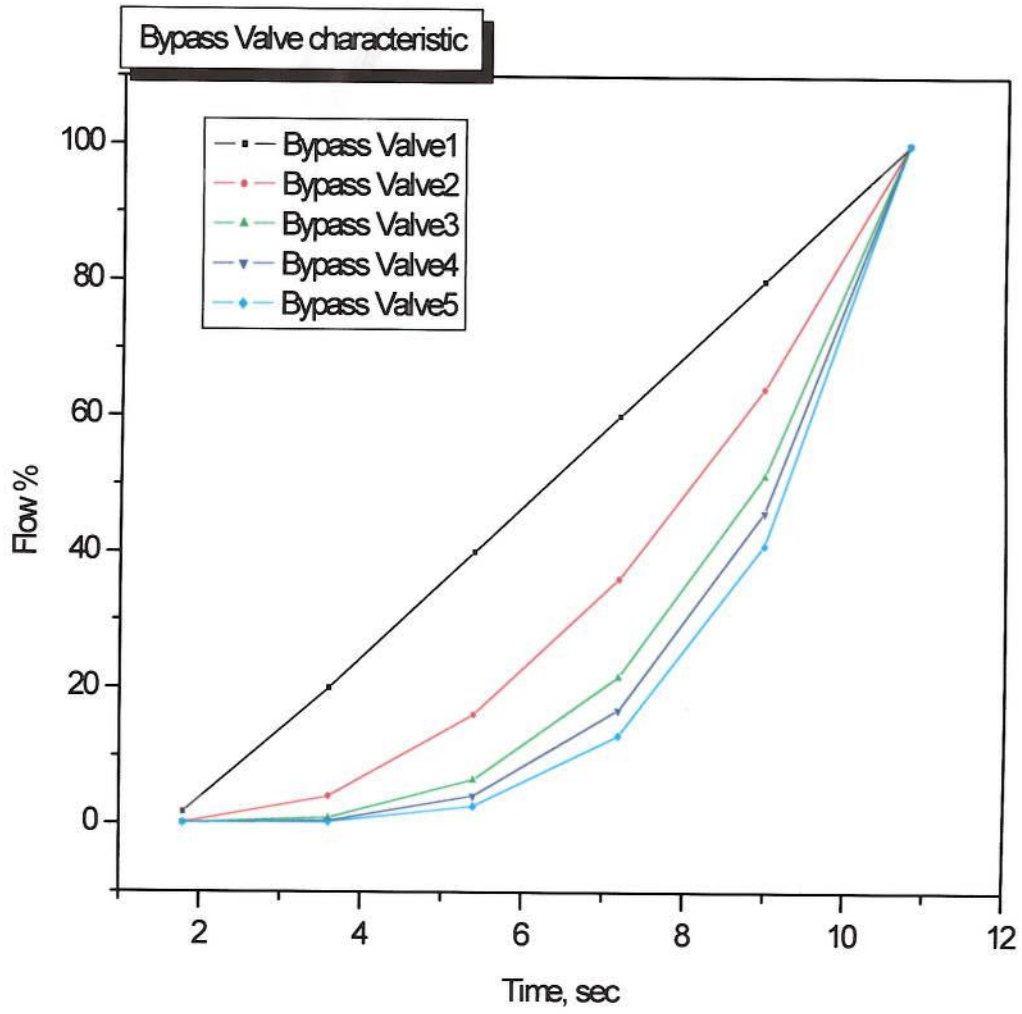

Different type of Bypass Valve characteristic

Appendix .VI

Contours of Different Parameters in the vertical section of the Pressure Vessel

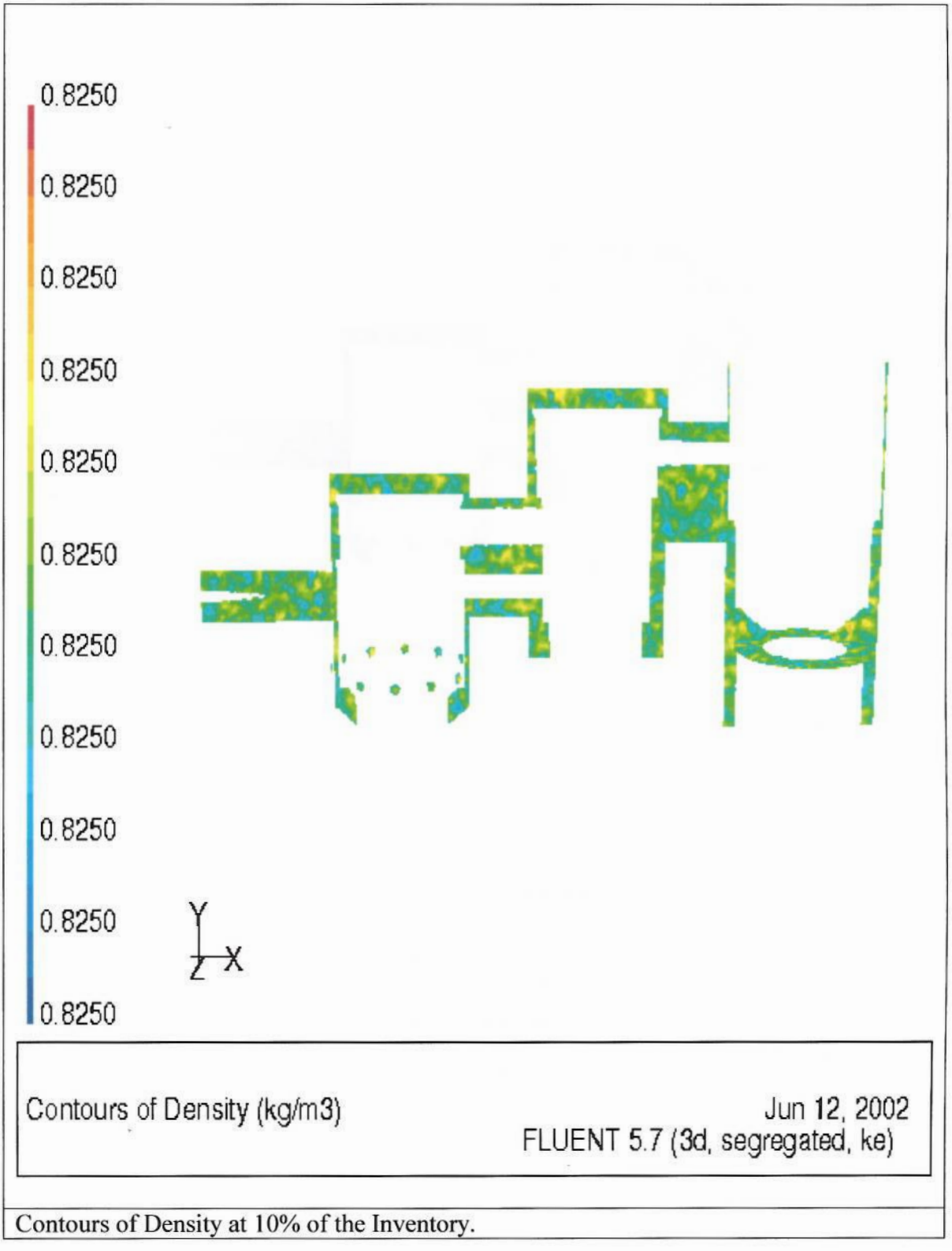

Contours of Density at 10% of the Inventory.

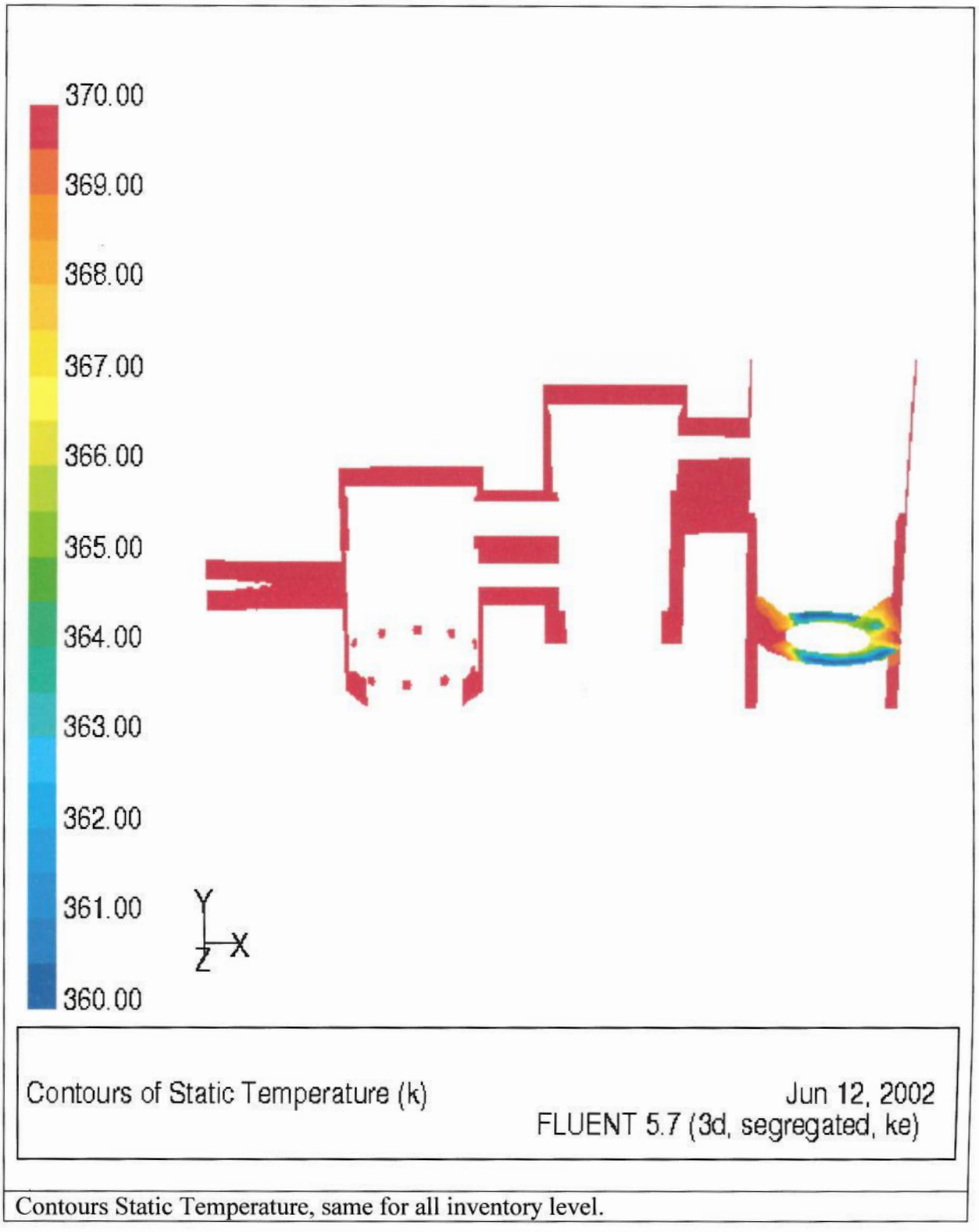

Contours Static Temperature, same for all inventory level.

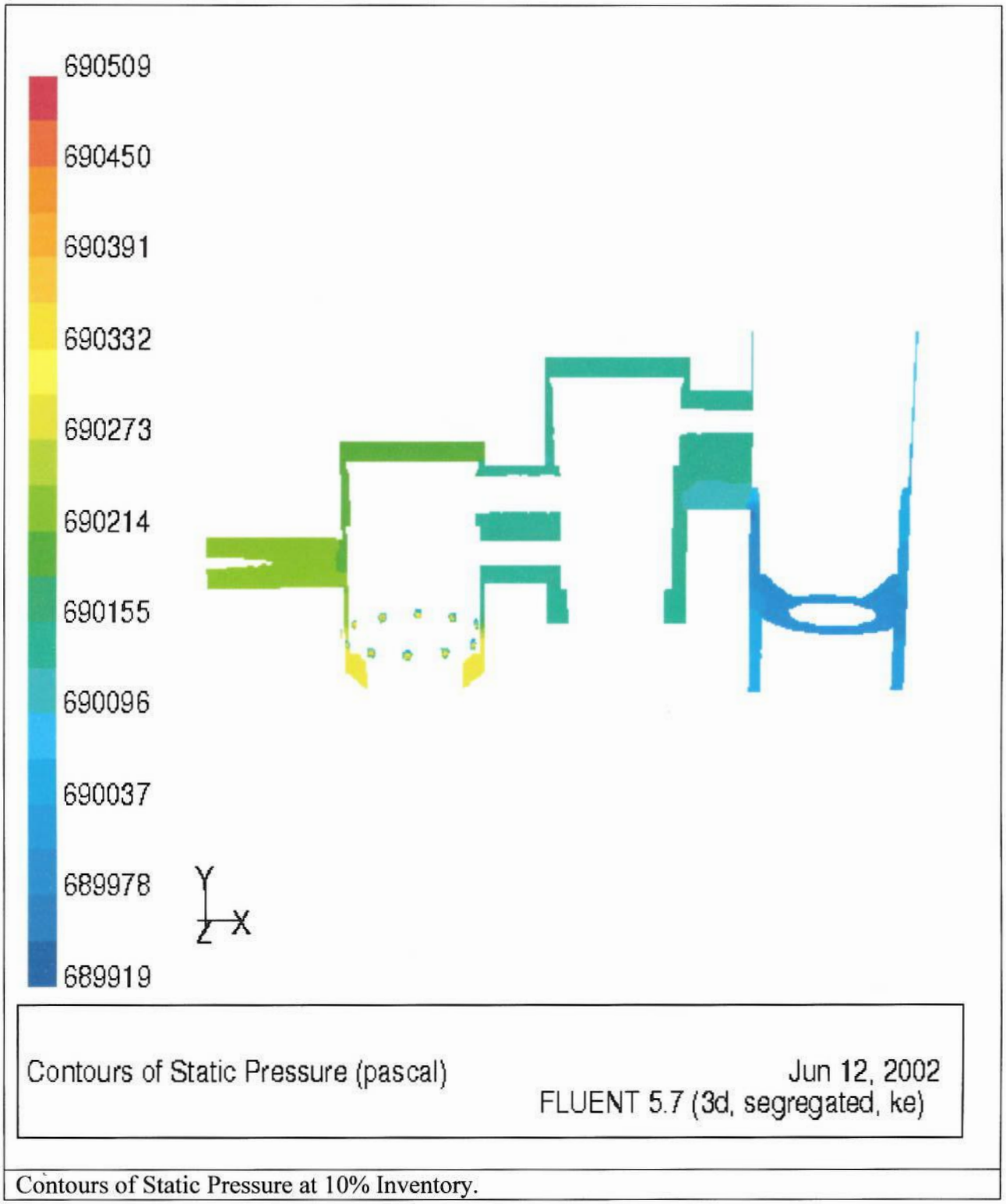

Contours of Static Pressure at 10% Inventory.

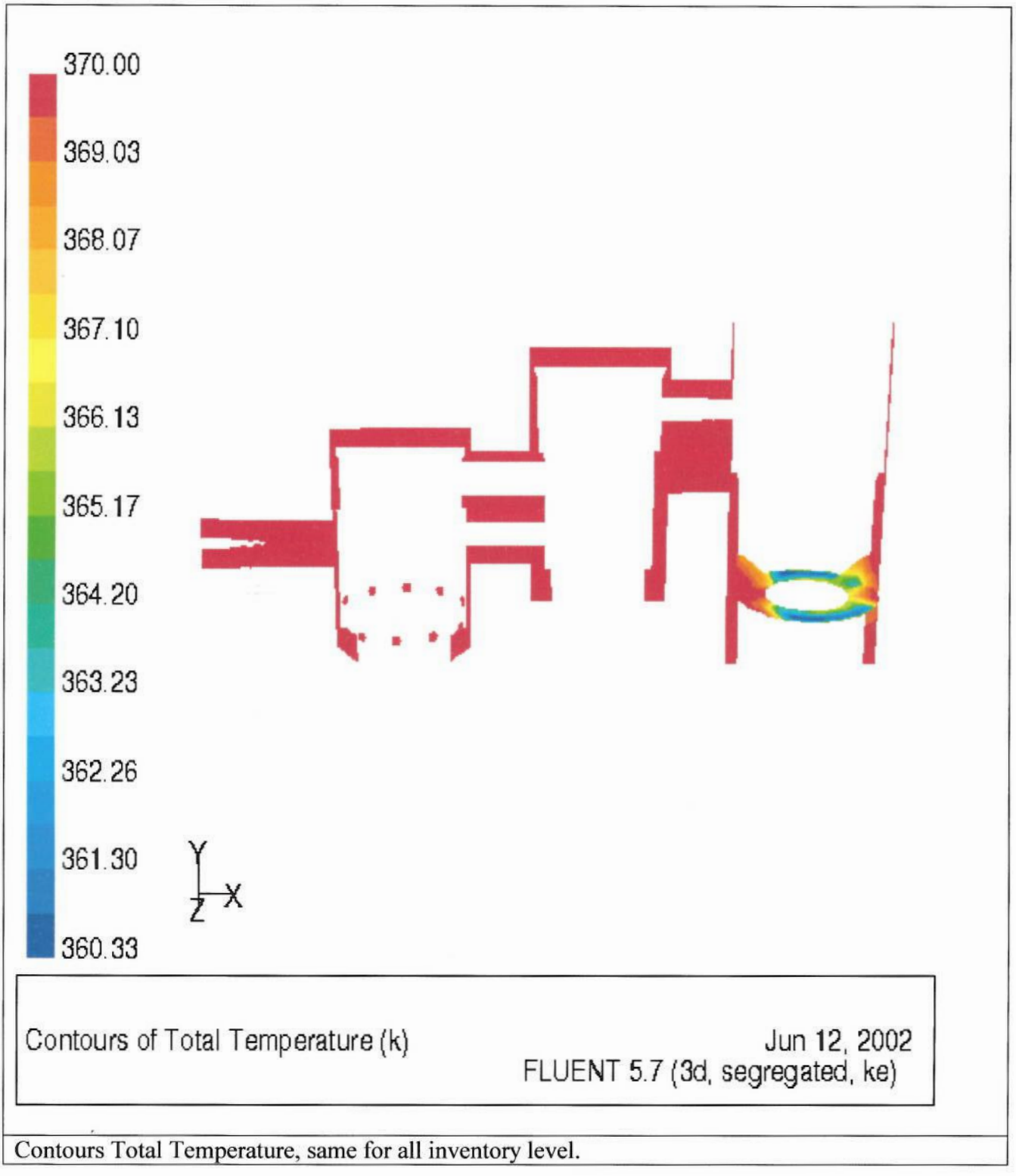

Contours Total Temperature, same for all inventory level.

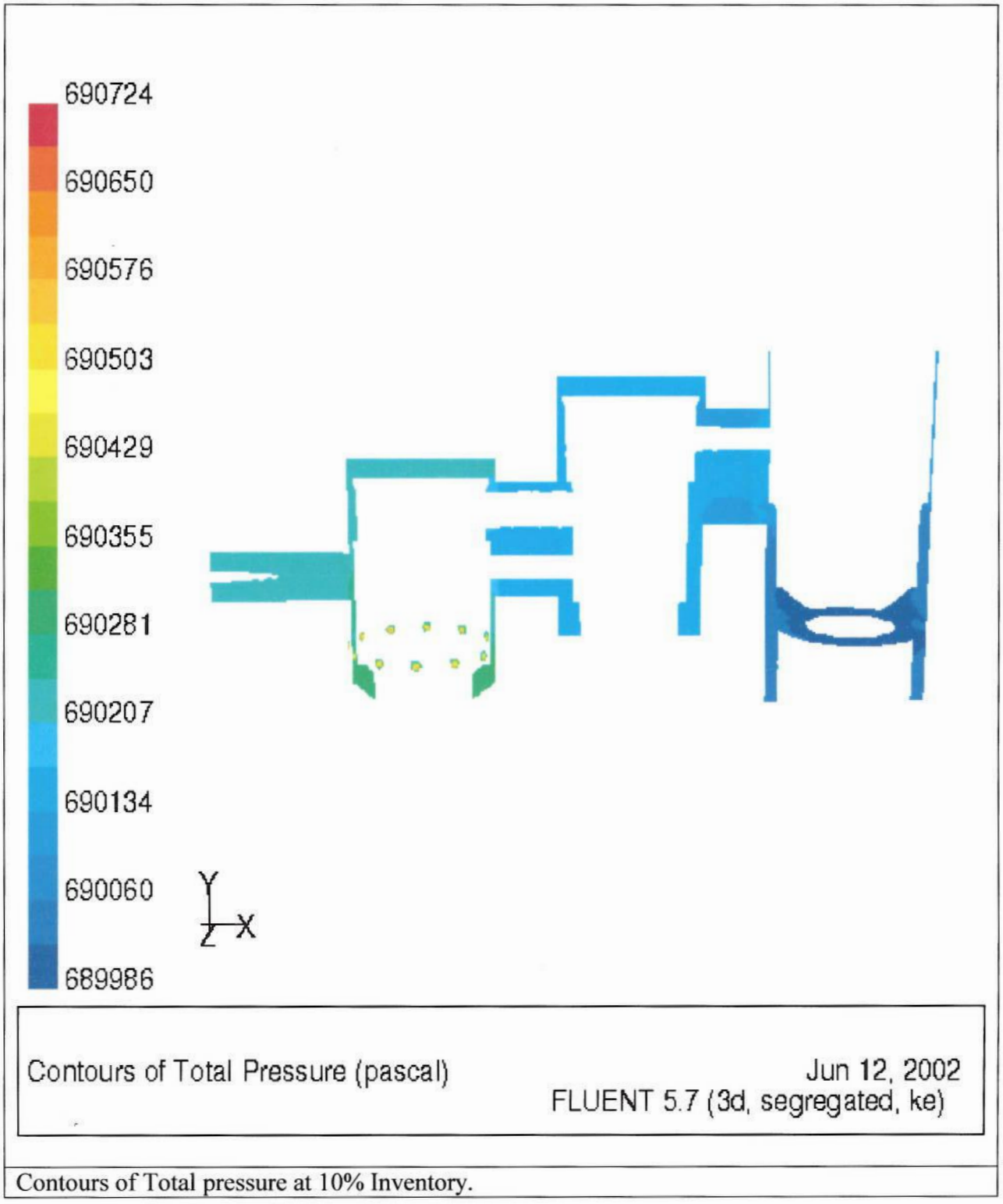

Contours of Total pressure at 10% Inventory.

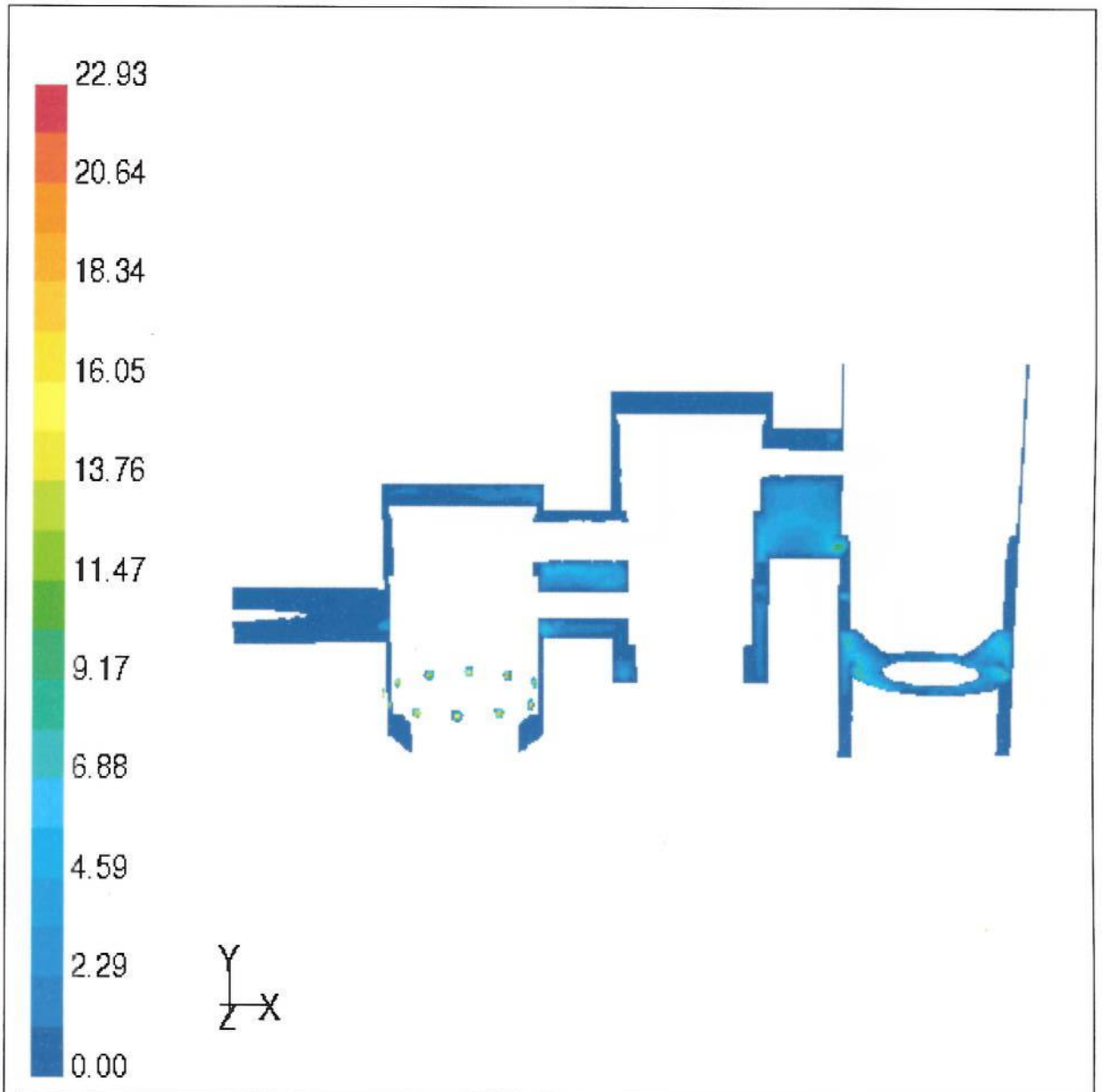

Contours of Velocity Magnitude at 10% Inventory.

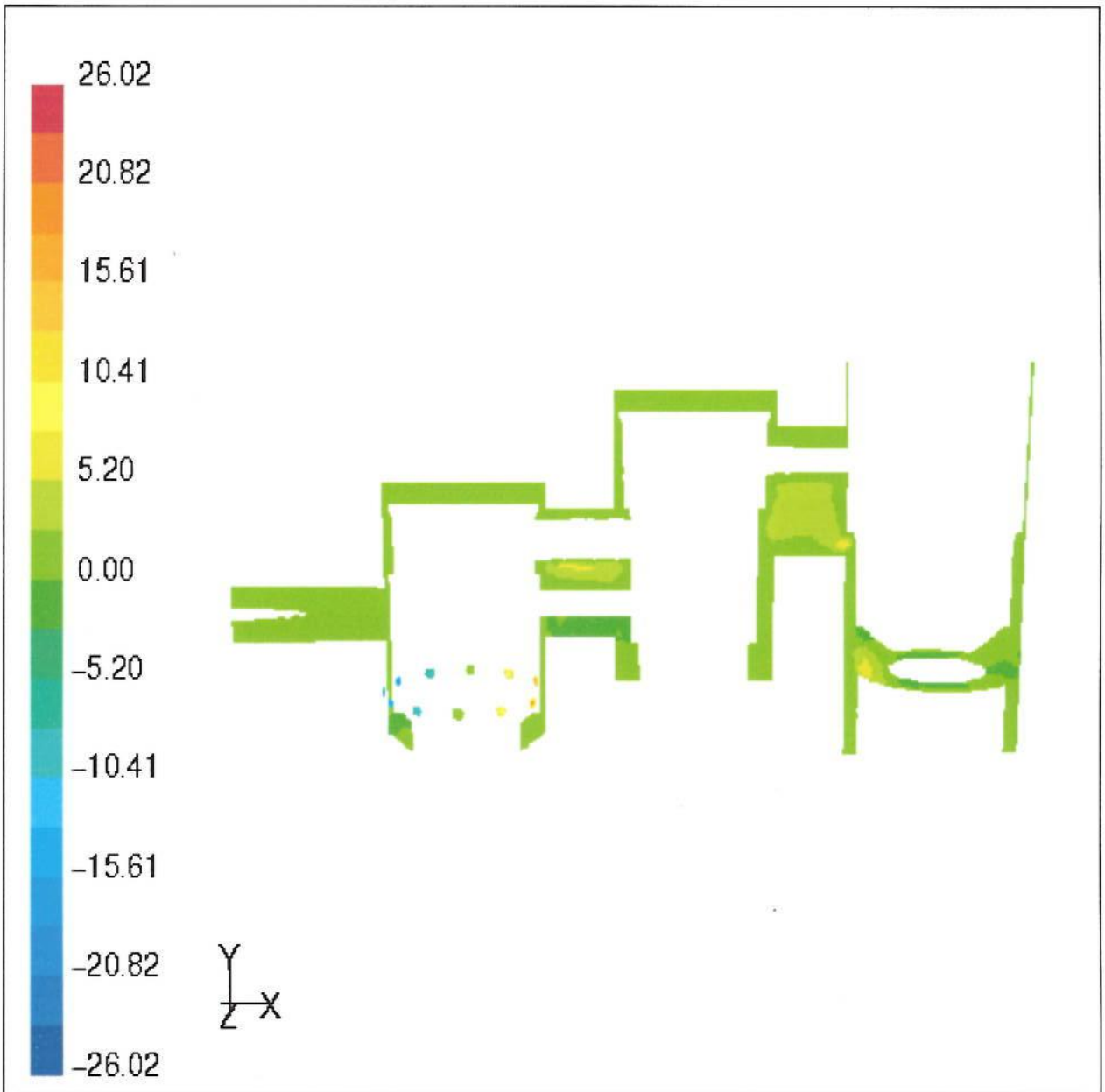

Contours of Velocity Magnitude in X direction at 10% Inventory

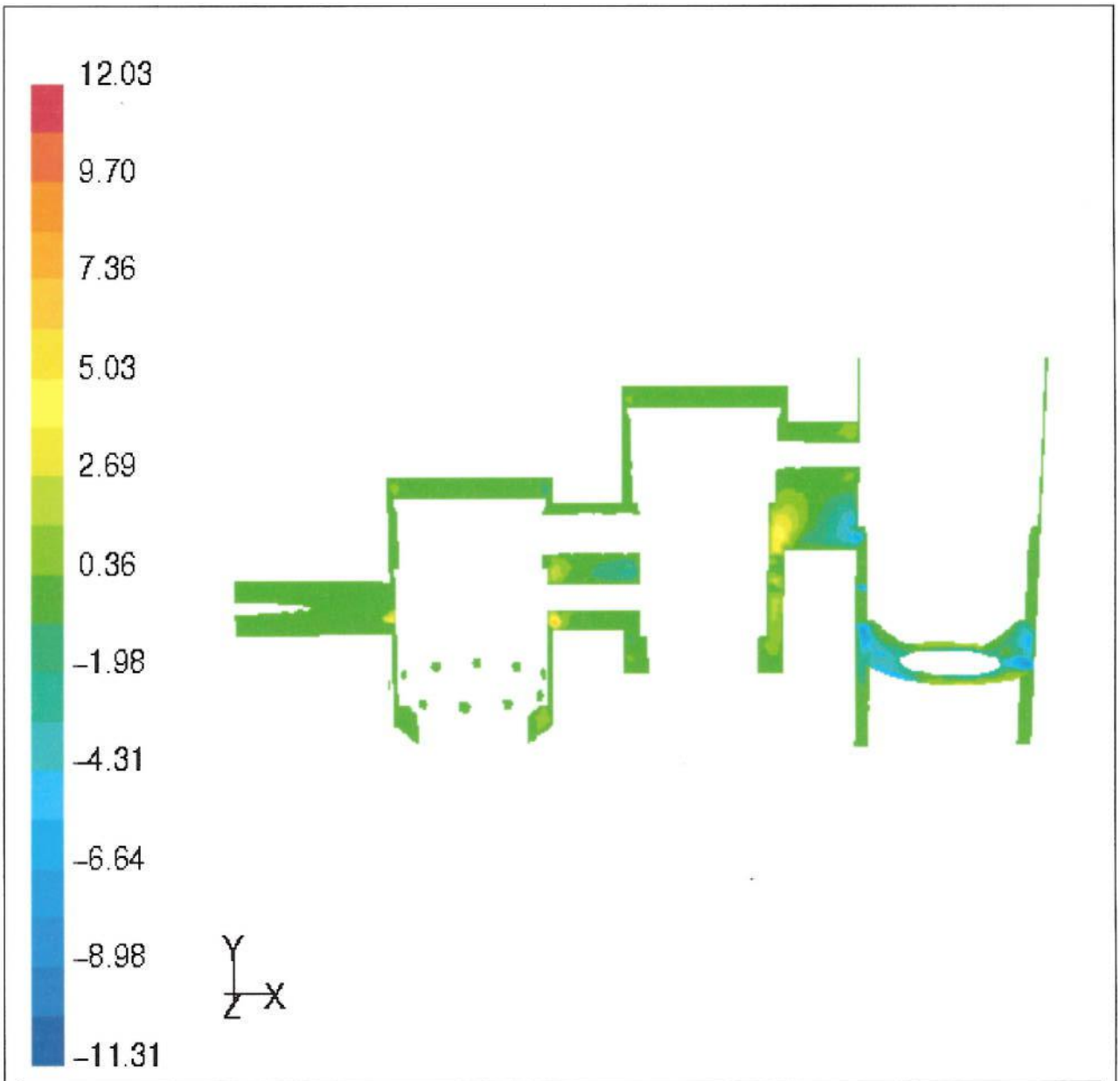

Contours of Velocity Magnitude in Y direction at 10% Inventory

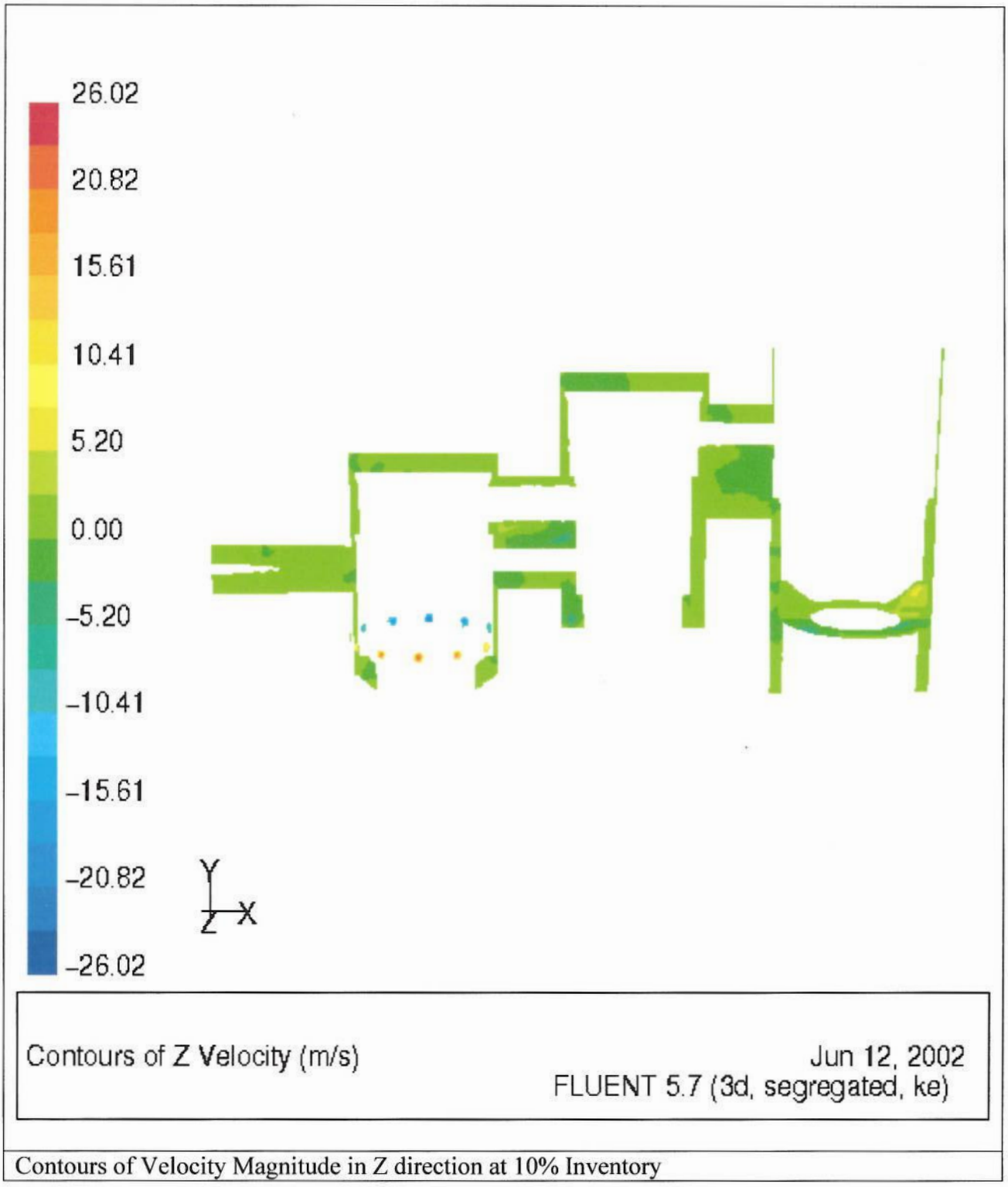

Contours of Velocity Magnitude in Z direction at 10% Inventory